

# Sheffield Hallam University

*Fundamental studies of the applications of atomic fluorescence spectroscopy to steel analysis.*

MICHEL, Robert G.

Available from the Sheffield Hallam University Research Archive (SHURA) at:

<http://shura.shu.ac.uk/20061/>

## A Sheffield Hallam University thesis

This thesis is protected by copyright which belongs to the author.

The content must not be changed in any way or sold commercially in any format or medium without the formal permission of the author.

When referring to this work, full bibliographic details including the author, title, awarding institution and date of the thesis must be given.

Please visit <http://shura.shu.ac.uk/20061/> and <http://shura.shu.ac.uk/information.html> for further details about copyright and re-use permissions.

7009

COUNCIL FOR NATIONAL ACADEMIC AWARDS

3 DEVONSHIRE STREET, LONDON, W1N 2BA

Telephone: 01-580 3141

MR. D. THACKER

Thesis returned as stated in letter of  
the 18th September, 1974.

*With Compliments*

BAR CODE .

100 250 757 X

**Sheffield City Polytechnic Library**

**REFERENCE ONLY**

~~13 JUL 75~~

~~9 APR 76~~

Books must be returned promptly, or renewed, on  
or before the last date stamped above.

**FAILURE TO DO SO WILL INCUR FINES**

PL/17

ProQuest Number: 10697368

All rights reserved

INFORMATION TO ALL USERS

The quality of this reproduction is dependent upon the quality of the copy submitted.

In the unlikely event that the author did not send a complete manuscript and there are missing pages, these will be noted. Also, if material had to be removed, a note will indicate the deletion.



ProQuest 10697368

Published by ProQuest LLC (2017). Copyright of the Dissertation is held by the Author.

All rights reserved.

This work is protected against unauthorized copying under Title 17, United States Code  
Microform Edition © ProQuest LLC.

ProQuest LLC.  
789 East Eisenhower Parkway  
P.O. Box 1346  
Ann Arbor, MI 48106 – 1346

A thesis entitled

FUNDAMENTAL STUDIES OF THE APPLICATIONS OF  
ATOMIC FLUORESCENCE SPECTROSCOPY TO STEEL ANALYSIS

presented by

ROBERT GEORGE MICHEL B.Sc., A.R.I.C., F.C.S.

in part fulfilment of the requirement for the degree of

DOCTOR OF PHILOSOPHY

of the

COUNCIL FOR NATIONAL ACADEMIC AWARDS

Department of Chemistry and Biology,  
Sheffield Polytechnic,  
Pond Street,  
Sheffield, S1 1WB.

SEPTEMBER, 1974.



~~74-03752~~

## SUMMARY

This thesis describes the adaptation of a Jarrell-Ash 82-529 atomic absorption/atomic emission spectrometer to obtain the maximum atomic fluorescence signal-to-noise ratio at the instrument readout that was possible within a relatively small budget. A detailed study of the interference effects of matrix elements on the determination of tin, arsenic and aluminium in steel is reported.

The work has shown that the technique of atomic fluorescence flame spectroscopy can be successfully applied to steel analysis in the same way that flame atomic absorption can be utilised. However atomic fluorescence can be more sensitive than atomic absorption when proper attention is given to the improvement of signal-to-noise ratios.

ACKNOWLEDGEMENTS

I should like to express my sincere thanks to both Dr. D. P. Hubbard and Dr. L. Ebdon for their excellent guidance and friendship. Also, my thanks go to Mr. P. H. Scholes of BISRA, with whom I have had many valuable discussions over the past three years.

I acknowledge with thanks the Science Research Council for the provision of an S.R.C (CAPS) Studentship and BISRA for the loan of equipment.

Acknowledgements are also due to the Polytechnic workshops, Metallurgy Department, for the construction of various items for the instrumentation and to the Physics Department for the use of facilities during the electronics work.

I should like to give my thanks to the Chemistry and Biology Department for providing the facilities and in particular to the staff for making the department such a congenial place in which to work.

Finally, I should like to thank Mrs. L. A. Ruddiforth for typing chapters one and three and appendix one and Mrs. J. Ebdon for typing the rest of the thesis.

## POSTGRADUATE STUDIES

1. A series of lectures on electronics given by Dr. N. C. Hilyard and Mr. M. Boyle at the Physics Department, Sheffield Polytechnic.
2. Departmental research colloquia, relevant lectures on the final year degree and M.Sc. courses and invited lectures on the M.Sc. course.
3. Meetings of the Society for Analytical Chemistry (SAC), Analytical Division, Chemical Society.
4. SRC Graduate School, Sept. 16-23, 1973, at the University of Liverpool. A course aimed at providing research students with some knowledge of challenges and problems that exist in industry. The course was organised by Mr. J. Blears of Liverpool University.
5. A three month period during the summer of 1972 at BISRA, The Intergroup Laboratories of the British Steel Corporation, Sheffield. This work was carried out in the Chemical Analysis Section, of which Mr. P. H. Scholes was Head, and included work with Energy Dispersion X-ray Analysis using a silicon semiconductor detector and with gas analysis using a quadrupole mass spectrometer.
6. The author gave lectures at departmental research colloquia and also gave a paper at the 'Research and Development Topics' meeting of the SAC at Jesus College, The University of Cambridge on 26th March, 1974. This latter paper was entitled "The Determination of Tin in Steels by Atomic Fluorescence Spectroscopy".

CONTENTS

## ONE - GENERAL INTRODUCTION

1.1. The flame spectroscopic techniques	1
1.2. The potential of atomic fluorescence	3
1.3. Matrix effects in atomic fluorescence	5

## TWO - ATOMIC FLUORESCENCE INSTRUMENTATION

2.1. Introduction	7
2.2. Signal-to-noise ratio theory	10
2.2.1. The Signal	11
2.2.2. The noise	12
A. Noise type: source noise	12
flame noise	
detector noise	
amplifier-readout noise	
B. Noise amplitude	13
C. The relative contributions of the various noise sources to the total noise.	14
2.2.3. The signal-to-noise ratio	16
2.2.4. Detection limit	16
A. Standard deviation	16
B. Relative standard deviation	17
C. Detection Limit	17
2.2.5. Analytical curves	18
2.3. Optimisation of experimental parameters that affect the atomic fluorescence signal-to-noise ratio at the readout.	19
2.3.1. Signal processing (Electronics)	20
A. D.C. amplifiers	22
B. Noise, modulation and a.c. tuned amplifiers	24
C. The lock-in amplifier	28
D. Building of the lock-in amplifier	32
The power supply	34
The preamplifier	35
The input amplifier	41
Low pass filter, high pass filter and filter output amplifier to p.s.d.	43
Reference input amplifier	46
Phase shifting and squaring stages	46
Phase sensitive detector p.s.d.	48
Output amplifier (Differential output low pass filter)	48
The performance of the lock-in amplifier	51

## CONTENTS

v

2.3.2. The source (Electrodeless discharge lamps)	52
A. Electronic modulation of electrodeless discharge lamps.	55
The application of high frequency modulation.	60
Signal-to-noise ratios obtained with variation in modulation frequency	60
a. Tin	
b. Aluminium	
B. Temperature control of electrodeless discharge lamps.	66
The application of temperature control.	69
C. Two further observations on the operation of EDL's	74
D. Some conclusions concerning the operation of EDL's.	75
2.3.3. The Flame	76
A. The gas handling arrangements, premix chamber and burner	79
B. Flame separation	81
The application of flame separation	85
2.3.4. The optical arrangement	88
The application of an optical arrangement	92
The effect of mirrors on analytical curves	97
2.3.5. Two further considerations of atomic fluorescence	98
a. Scatter	
b. Spectral bandwidth	
2.3.6. Conclusion	100
 THREE - THE APPLICATION OF ATOMIC FLUORESCENCE SPECTROMETRY TO THE DETERMINATION OF TIN IN STEELS	
3.1. Introduction	102
3.2. Optimisation of conditions for measurement of tin fluorescence.	106
<hr/>	
3.2.1. Stability of trace levels of tin in aqueous solution	107
3.2.2. Choice of gas flow rates, flame separation and flame height	107
3.2.3. Operating conditions for the tin electrodeless discharge lamp as source	112
3.2.4. Atomic fluorescence spectra of tin excited in four flames. Sensitivities in the different flames.	113
3.3. Interferences affecting the determination of tin in aqueous solution	116
3.3.1. The effect of acids	117
3.3.2. The effect of elements	118

## CONTENTS

3.3.3. The effect of iron on the interferences from other elements	124
3.3.4. The effect of iron, on the interference from acids	126
3.3.5. The effect of organic solvents	128
3.3.6. Mechanism of interference elimination	130
3.3.7. Analytical curves	134
3.3.8. Detection limits	137
3.4. The determination of tin in steel samples	139
3.5. Conclusion	149
FOUR - THE APPLICATION OF ATOMIC FLUORESCENCE SPECTROMETRY TO THE DETERMINATION OF ARSENIC IN STEEL	
4.1. Introduction	151
4.2. Optimisation of conditions for measurements of arsenic fluorescence	154
4.2.1. Choice of gas flow rates, flame separation and flame height	155
4.2.2. Operating conditions for the arsenic electrodeless discharge lamp used as source	157
4.2.3. Improvements in sensitivity obtained by flushing the monochromator with nitrogen	158
4.2.4. Atomic fluorescence spectra of arsenic excited in four flames - choice of flame	159
4.3. Interferences affecting the determination of arsenic	162
4.3.1. The effect of acids	163
4.3.2. The effect of elements	165
4.3.3. The effect of iron on the arsenic fluorescence and on the interferences from other elements	173
4.3.4. The effect of organic solvents	175
4.4. Analytical curves and detection limits	
4.4.1. Analytical curves	177
4.4.2. Detection limits	179
4.5. The determination of arsenic in steel samples	182
4.6. Conclusion	184
FIVE - THE APPLICATION OF ATOMIC FLUORESCENCE SPECTROMETRY TO THE DETERMINATION OF ALUMINIUM IN STEELS	
5.1. Introduction	186
5.2. Optimisation of conditions for measurements of aluminium fluorescence	190

5.2.1. Choice of gas flow rates, flame separation and flame height	190
5.2.2. Operating conditions for the aluminium electrodeless discharge lamp used as source	191
5.2.3. Atomic fluorescence spectrum of aluminium in the argon-separated nitrous oxide-acetylene flame.	192
5.3. Interferences affecting the determination of aluminium	193
5.3.1. The effect of acids	197
5.3.2. The effect of elements	198
5.3.3. The effect of iron and of easily ionisable elements	202
5.3.4. The effect of organic solvents	204
5.4. Analytical curves and detection limit	205
5.4.1. Analytical curves	205
5.4.2. Detection limit	206
5.5. The determination of aluminium in steel samples	207
5.6. Conclusion	210
SIX - CONCLUSIONS	212
APPENDIX I -	
THEORY OF ATOMIC FLUORESCENCE	A1.1
Derivation of the radiance (intensity) of atomic fluorescence	A1.2
Summary	A1.2
Derivation	A1.3
Final fluorescence radiance expressions	A1.10
Generalisations made from radiance expressions	A1.11
APPENDIX 2 -	
EXPERIMENTAL	
A.2.1. Apparatus	A2.1
A.2.2. Reagents	A2.3
A.2.3. Measurement procedure	A2.6
Detection limit measurement procedure	
A.2.4. Some practical considerations	A2.7
Use of the lock-in amplifier	
a. Use of the output low pass filters	
b. Continuous use of the oscilloscope	
Choice of photomultiplier tube	
Optics	

## CONTENTS

A.2.5. Significance of the magnitude of quoted results for interference effects	A2.5
--	------

## APPENDIX 3 - DATA FOR ELECTRONIC COMPONENTS

Power supply	A3.1
SN72741 ( $\mu$ A741)	A3.2
SN72702 ( $\mu$ A702)	A3.4
SN72710 ( $\mu$ A710)	A3.6
3N138	A3.7
$\mu$ A727	A3.8

## REFERENCES

## PUBLICATIONS

## CHAPTER ONE

### GENERAL INTRODUCTION

#### 1.1. The flame spectroscopic techniques

Of the three flame spectroscopic techniques for the determination of traces of elements atomic fluorescence flame spectrometry is the youngest and least developed as an analytical tool. The first atomic fluorescence papers appeared in 1964<sup>1,2,3</sup>. The use of atomic emission flame spectrometry dates back to the classical period in science while atomic absorption was proposed as an analytical method in 1955<sup>4</sup>. With the introduction of atomic absorption the analytical applications of atomic emission declined, mainly because atomic absorption suffers less from interference problems.

In all three techniques a solution of the element is sprayed into the flame as a fine mist. The high temperature of the flame (2000 to 3000°C) causes the solvent to evaporate and the metal compounds to dissociate, mainly into ground state atoms. In atomic emission the flame then has sufficient thermal energy to enable a small proportion of the ground state atoms to absorb heat energy. This extra energy, by promoting electrons to a higher energy level, produces a population of excited state atoms. Each atom then reverts to the ground state by loss of a photon of light of wavelength corresponding to the energy difference between the ground state and the excited state of the element concerned. The intensity of the light emitted is proportional to the concentration of element in the original solution. Therefore, by

measuring the intensity of light emitted from the flame when aspirating solutions of known concentration, a calibration curve can be constructed and quantitative measurements on unknown solutions can be made. The wavelength of the light emitted can enable qualitative information to be obtained.

In atomic absorption and atomic fluorescence the excitation energy is not the thermal energy of the flame, instead energy of the appropriate wavelength is absorbed from a light source. In atomic absorption the detection system views the source directly and the amount of light absorbed from the light beam by the atoms in the flame can therefore be measured in terms of absorbance.

Where absorbance,  $A = \lg \frac{100}{100 - \% \text{ absorption}}$  the absorbance is proportional to the concentration of ground state atoms present in the flame.

In atomic fluorescence the light from the source is focused onto the flame at  $90^\circ$  to the flame-detector axis. The source light is not therefore viewed by the detection system. The same absorption process takes place as in atomic absorption but the reduction in light intensity is not measured. Instead the intensity of the emitted light is measured. This emitted radiation, called fluorescence, is a result of the excited state atoms reverting to the lower ground state, i.e. essentially the same process as in atomic emission except that the source of excitation energy is different.

The three techniques are roughly complementary in the range of elements to which they can be applied. For instance atomic emission has a high sensitivity for sodium and potassium while

atomic fluorescence is more sensitive for cadmium and zinc. Atomic absorption and atomic fluorescence are both virtually free of spectral interferences whereas atomic emission is limited by this type of interference. The range of application of the absorption and fluorescence techniques is very wide but any possible advantages of either one over the other have not yet been proven conclusively.

### 1.2 The potential of atomic fluorescence

Atomic fluorescence spectrometry has some potential advantages over atomic absorption spectrometry. One such advantage is the possibility of increased sensitivity owing to the direct proportionality of the intensity of fluorescence radiation to the intensity of the light source. Another advantage is the greater linear range of fluorescence intensity vs concentration curves shown by some elements. Winefordner and Elser<sup>5</sup> and Kirkbright and West<sup>6</sup> have discussed these and other considerations. The long linear range and high sensitivity in atomic fluorescence depends on the optimisation of two basic factors, the fluorescence signal and the noise associated with that signal. The signal-to-noise ratio must be maximised.

Winefordner et al<sup>7</sup> develop in detail the theory of atomic fluorescence and produce a series of generalizations based on expressions for the intensity or radiance of the atomic fluorescence signal from the flame. Those generalizations applying to conventional flame atomic fluorescence are reproduced in

appendix I. The radiance expressions indicate that the intensity of the atomic fluorescence signal depends on the concentration of the element, intensity of the source, the solid angle of radiation collected from the source to focus on the flame, the power yield of fluorescence, i.e. the ratio ( $Y_p$ ) of fluoresced radiant flux to absorbed radiant flux, and the solid angle of fluorescence radiation collected by the detection system. To maximise these factors a well-designed optical arrangement around the flame is necessary and the flame itself must be chosen to give a maximum value for  $Y_p$ .

The noise associated with the fluorescence signal is primarily due to flame gas reactions which produce random fluctuations in the light emitted from the flame. Other factors that contribute to the noise are: fluctuations in the intensity of the light source, and electronic noise which is due mainly to the thermal motions of electrons in the detection system, i.e. the photomultiplier tube and electronic amplification stages.

Assuming that the signal has been maximised using the appropriate optics and flame, the signal to noise ratio can be further improved by choosing a detection system which is capable of amplifying the signal more than the noise, i.e. the amplifier must be able to discriminate between the signal and the noise and then amplify the signal preferentially, thus improving the signal to noise ratio.

This thesis describes the adaptation of a Jarrell-Ash atomic absorption/atomic emission flame spectrometer to obtain the

maximum fluorescence signal-to-noise ratio that was possible within a relatively small budget. The instrument that resulted was then used to evaluate atomic fluorescence as a technique for the analysis of trace concentrations of various metals in steels.

### 1.3 Matrix effects in atomic fluorescence

Scholes<sup>8</sup> has reviewed the analysis of a number of metals in steel by atomic absorption. He has shown that most metals which occur in amounts above 0.1% are, in general, readily determinable by the technique. However, the difficulty in achieving adequate sensitivity has rendered the technique unsatisfactory for trace element analysis below 0.1%, without a prior concentration stage being incorporated into the procedure. The aim of the work described in this thesis was to determine whether or not flame atomic fluorescence, with a microwave electrodeless discharge tube as source, does in practice have any real advantages over atomic absorption. The two main areas of interest were the sensitivity of the atomic fluorescence method and the effect of the steel matrix on the atomic fluorescence signals.

The interference effects encountered in atomic fluorescence have not yet been studied in detail for many particular matrices, although most of the early work on the atomic fluorescence of the elements was accompanied by preliminary investigations of the effect of a range of trace metals on the fluorescence

signals. Some examples of such studies are: Tin<sup>9</sup>; Molybdenum, Titanium, Vanadium and Zirconium<sup>10</sup>; Arsenic<sup>11</sup>; Manganese<sup>12</sup>; Bismuth<sup>13</sup>; Lead<sup>14</sup>; Beryllium<sup>15</sup>; Silicon<sup>16</sup> and Gold<sup>17</sup>. The best reported detection limits have usually been obtained using the relatively cool air-hydrogen, argon-hydrogen and argon-oxygen-hydrogen flames where the power yield of fluorescence is high. However, Browner and Manning<sup>18</sup> have pointed out that practical analyses may require the use of higher temperature flames (e.g. Air-Acetylene) which often give more efficient atomization and fewer interferences. Note also that the large number of interelement effects found in cool flames also occur in atomic absorption<sup>19</sup>. These considerations of interferences and choice of flame are highlighted by the work described in this thesis.

## Instrumentation

2.1. Introduction

The basic components of an instrument for making atomic spectroscopic measurements are an atom cell, a monochromator, and a photographic detection system or photomultiplier tube and amplifier with chart readout. In atomic absorption and fluorescence there is the additional requirement of a source of radiation which can either be a line source or a continuum source. Over the past ten to fifteen years the most widely used form of instrumentation in atomic emission, absorption and fluorescence has been composed of a flame as the atom cell, a monochromator and a photomultiplier tube and amplifier. The hollow cathode discharge lamp has been the best line source for atomic absorption and the microwave excited electrodeless discharge lamp has been the most used line source for atomic fluorescence.

Continuum sources have given limits of detection by atomic fluorescence which are at least one order of magnitude inferior to those obtained with line sources especially in the ultraviolet region of the spectrum<sup>20-22</sup>. The principle type of continuum source has been the 150 or 450 watt high-pressure xenon arc lamp although more recently<sup>23</sup> a 900 watt xenon arc has been used in conjunction with double modulation atomic fluorescence spectrometry. Double modulation has been used in atomic absorption with a continuum source<sup>24</sup>. Wavelength modulation together with a continuum source has also been employed in atomic absorption<sup>25</sup>. A variable wavelength line source has been obtained by using a xenon arc lamp and a grating monochromator in series with a piezoelectric scanning

interferometer<sup>26</sup>. The dye laser, a quasi-continuum source, is able to give atomic fluorescence detection limits equal to or better than those obtained with electrodeless discharge lamps both with flame<sup>27,28</sup> and non-flame cells.<sup>29</sup> A laser has also been used in atomic absorption<sup>30</sup>.

Hollow cathode lamps as well as being used extensively in atomic absorption have also been employed for atomic fluorescence measurements. The types of high intensity lamps available are the hollow cathode with pulsed<sup>31 - 38</sup> or intermittent<sup>39-41</sup> operation and the hollow cathode with direct current<sup>42-44</sup> or high frequency<sup>45,46</sup> (i.e. microwave) boosted output. A further improvement in the use of hollow cathode lamps has been the development of the demountable cathode<sup>47-50</sup>. A number of workers have used pulsed and/or boosted hollow cathode lamps for atomic fluorescence measurements<sup>14,51-58</sup>.

In atomic fluorescence there is the possibility of dispensing with the monochromator because atoms in the atom cell act as their own monochromator<sup>6,59</sup>, i.e. unwanted radiation from the source e.g. non-resonance line emission, at wavelengths close to that of the fluorescence emission, is transmitted by the atom cell and not detected.

In contrast, in atomic absorption in order to provide for high sensitivity and linear calibration curves, it is necessary to exclude this unwanted radiation from the detector by use of a narrow spectral band-pass monochromator or sophisticated selective modulation techniques. Simultaneous multi-element analyses have been performed on non-dispersive instruments by fluorescence<sup>27,60-68</sup>. Such instruments can be successfully applied to those elements which can be determined in the air-acetylene<sup>61</sup> or nitrous oxide-acetylene<sup>62</sup> flames and which have their sensitive wavelengths

below 300 nm. The wavelength limitation is due to the use of the Hamamatsu R166 solar blind photomultiplier tube which has its peak response between 200 and 300 nm. This tube is used to improve signal-to-noise ratios because its low response in the visible region reduces flame noise originating above 300 nm. Multi-channel systems have also been built for atomic absorption measurements<sup>67</sup>. These instruments use either resonance monochromators<sup>67,69</sup> and/or selective modulation techniques<sup>67</sup> rather than an optical monochromator. The absorption and fluorescence multichannel instruments have all used hollow cathode lamps in one form or other although some non-dispersive fluorescence instruments have employed single or multi-element electrodeless discharge lamps (A further discussion concerning multielement analysis is given in Chapter Six).

Non flame devices are rapidly becoming accepted as atom cells which are convenient alternatives to the flame. Among these devices are the carbon rod<sup>70</sup> - 94, Massmann furnace<sup>95</sup>, L'vov furnace<sup>96,97</sup>, tantalum strip<sup>98-100</sup>, platinum loop<sup>101</sup>, various other variations of the heated graphite rod or tube<sup>102-106</sup>, hollow cathode excitation<sup>107,108</sup>, and various special methods for particular elements.<sup>155-157</sup> Kirkbright<sup>109</sup> has reviewed the application of non-flame atom cells in atomic absorption and atomic fluorescence spectroscopy. Aldous et al<sup>110</sup> describe a computer-controlled instrument for the measurement of transient atom populations such as those produced by non-flame atomization systems. The development of non-flame atom cells has shown them to possess capabilities complementary to those of flame cells, High absolute sensitivity is attainable which permits very small solid or liquid samples to be examined by atomic absorption and fluorescence. The low background emission obtainable in non-

flame cells is particularly useful for utilising the advantages of atomic fluorescence. The results for precision obtained with many non-flame devices are not as satisfactory as those obtainable with flame systems, however, it is the reproducibility of the sample transfer to the cell that may at present limit the precision attainable.

The instrument described in this chapter was designed to bring together a number of features reported in the literature which have been said to improve the signal-to-noise ratio and hence the precision and detection limits of atomic fluorescence measurements. This work was restricted to the use of the flame as atom cell and the microwave excited electrodeless discharge lamp as source because the limited budget available ruled out the possibility of a non-flame cell or the use of other sources such as the boosted hollow cathode lamps. A Jarrell-Ash Maximum Versatility atomic absorption/atomic emission spectrometer (model 82-529) was available. This is a fairly typical flame spectrometer and the optical bench,  $\frac{1}{2}$ -m Ebert grating monochromator, photomultiplier tube and associated power supply and the gas handling arrangements were all retained for use in atomic fluorescence. This chapter firstly gives a brief review of signal-to-noise ratio theory. This reveals the parameters which affect the signal-to-noise ratio at the instrument readout. Secondly a description is given of that experimental work which was aimed at optimising those important parameters which are under the investigator's control.

## 2.2. Signal-to-noise ratio theory

The importance of maximising the signal-to-noise ratio, SNR, rather than just the signal has been emphasised in the

literature of atomic fluorescence a large number of times<sup>7,59,111-114</sup>

Jenkins<sup>59</sup> and Winefordner et al.<sup>111</sup> have derived expressions for calculating limits of detection using signal-to-noise ratio theory. Similar derivations have been reported for atomic emission<sup>115</sup> and absorption.<sup>116</sup>

### 2.2.1. The Signal

The average photodetector signal current  $i_F$  due to atomic fluorescence of the analyte (assuming the atomic fluorescence line half width is considerably less than the spectral bandpass of the monochromator) is given by<sup>111</sup>:

$$i_F = mWK \delta B_F \quad (1)$$

where  $m$  is a factor that accounts for the light loss when a mechanical chopper is used ( $m$  equals 0.5 for most choppers and 1.0 if no chopper is used),  $W$  is the monochromator slit width (cm),  $K$  is the optics factor (cm sr) ( $K = HT_f \Omega_F$  where  $H$  = illuminated height of the slit,  $T_f$  = transmission factor of the optical system and  $\Omega_F$  = effective solid angle of light collected by the monochromator),  $\delta$  is the radiant sensitivity of the photodetector ( $A \text{ watt}^{-1}$ ) and  $B_F$  is the radiance ( $\text{watt cm}^{-2} \text{sr}^{-1}$ ) of fluorescence.

The magnitude of  $B_F$  is related to the atomic absorption coefficient  $K_0$  (continuum source) or the average absorption coefficient  $\bar{K}$  (line source) in the manner shown in appendix I.

These absorption coefficients are linearly related to the atomic concentration of  $N_0$  atoms in the flame gases by fundamental equations that are quoted and discussed in most textbooks on flame atomic absorption and atomic fluorescence spectroscopy<sup>7,97,117</sup>

$N_0$  is related to the sample solution concentration,  $C_0$ , mole  $\text{cm}^{-3}$ ,

$$N_0 = (6 \times 10^{23}) \frac{F \epsilon \beta C_0 \rho_0}{Q_t e_f Z_t} \text{ cm}^3 \text{ sec}^{-1} \quad (2)$$

where  $F$  is the solution transport rate,  $\epsilon$  is the aspiration efficiency

$\beta$  is the atomisation efficiency,  $Z_t$  is the electronic partition function,  $e_f$  is the flame expansion factor and  $Q_t$  is the flow rate of gases into the flame ( $\text{cm}^3 \text{sec}^{-1}$ ).  $Q_t e_f$  is the burnt gas flow rate in  $\text{cm}^3 \text{sec}^{-1}$ .  $Z_t$  is defined by:

$$Z_t = \sum_i g_i \exp \frac{E_i}{kT}, \text{ where the } g\text{'s are the statistical}$$

weights of the ground (o) and excited (i) state,  $E_i$  is the excitation energy for state i, k is the Boltzmann constant, and T is the flame temperature (K).

### 2.2.2. The noise

#### A. Noise type

Noise is defined as any undesirable fluctuation in the readout signal of an instrumental system such as drift and random noises. The components that constitute the total noise of the readout (chart recorder, meter etc.) of a flame atomic fluorescence instrument fall into four main categories.

#### Source Noise

Drift and random fluctuations in source radiance may be due to power supply instability lamp ageing, etc.

#### Flame Noise

This depends upon the flame and burner type, the spectral region observed and the position in the flame observed. Laminar premixed flames are less noisy than turbulent flames produced on total consumption burners. The principle causes of flame noise are convection turbulence of the flame gases, scattering of light from solvent droplets or unevaporated solute particles, fluctuations in the aspiration process and variations in flame background emission.

#### Detector Noise

Photodetector noise, mainly dark current shot noise, is

attributable to the fundamental quantum nature of electrons and photons and is often the fundamental limiting noise when other noise sources have been reduced or eliminated. The rms shot noise current of a photomultiplier tube is given by <sup>59,112</sup>;

$$\overline{\Delta i_D} = (2eBM\Delta_f i_a)^{\frac{1}{2}} \quad (3)$$

where  $e$  is the charge on the electron,  $M$  is the total multiplication factor of the tube,  $B$  is a constant ( $\approx 1.3$  for most tubes),  $\Delta_f$  is the noise bandwidth of the system and  $i_a$  is the total phototube anode current due to photoemission and thermal emission (dark current). It can be seen from equation (3) that shot noise increases as the square root of the detector current.

#### Amplifier-readout noise

Electronic noise in modern instrumentation is usually insignificant compared to other noise sources. Possible sources of noise include Johnson noise (also called Nyquist or thermal noise) in the phototube load resistor and flicker noise in the transistors. Electronic noise is independent of any variable before the electronics.

#### B. Noise Amplitude

The amplitude of noise is not always constant over the full frequency range from very low to very high frequencies. The frequency distribution is usually characterized by a noise-power spectrum (watt Hz<sup>-1</sup>) rather than in terms of wave forms (e.g. d.c., sine wave etc.) because, being inherently random, noise has no periodic character so that a noise waveform is meaningless. Two basic types of noise are each characterized by the appearance of the power spectrum. For WHITE noise a flat power spectrum is found (Fig. 2.1.). The power density is independent of frequency. Examples of white noise are shot noise in photomultiplier tubes and Johnson noise caused by the random movements of electrons in a resistor. Johnson noise is governed by the

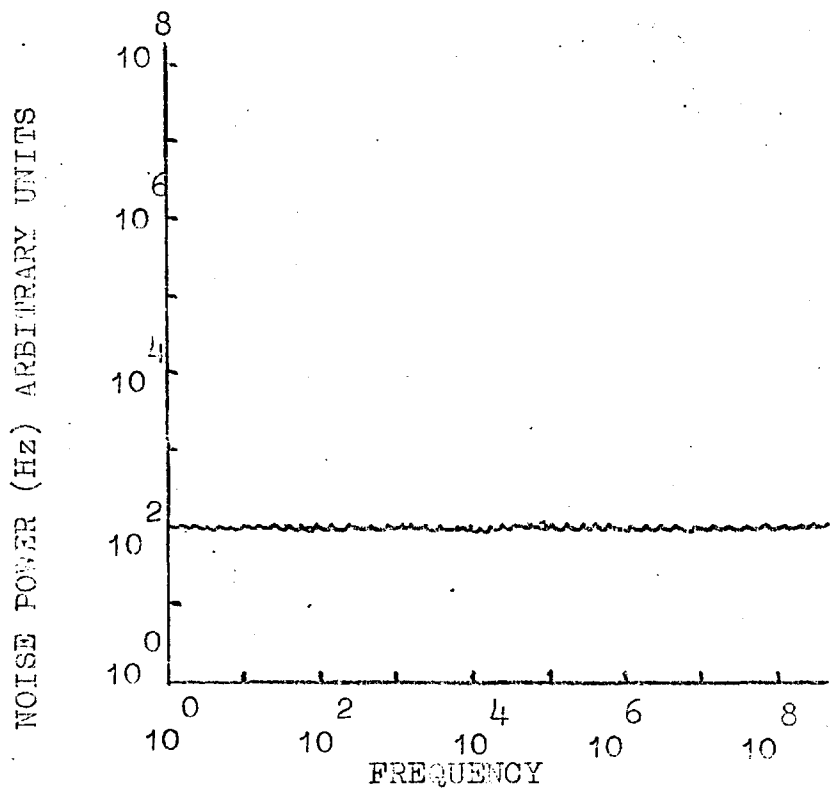


Fig.2.1 White noise power spectrum

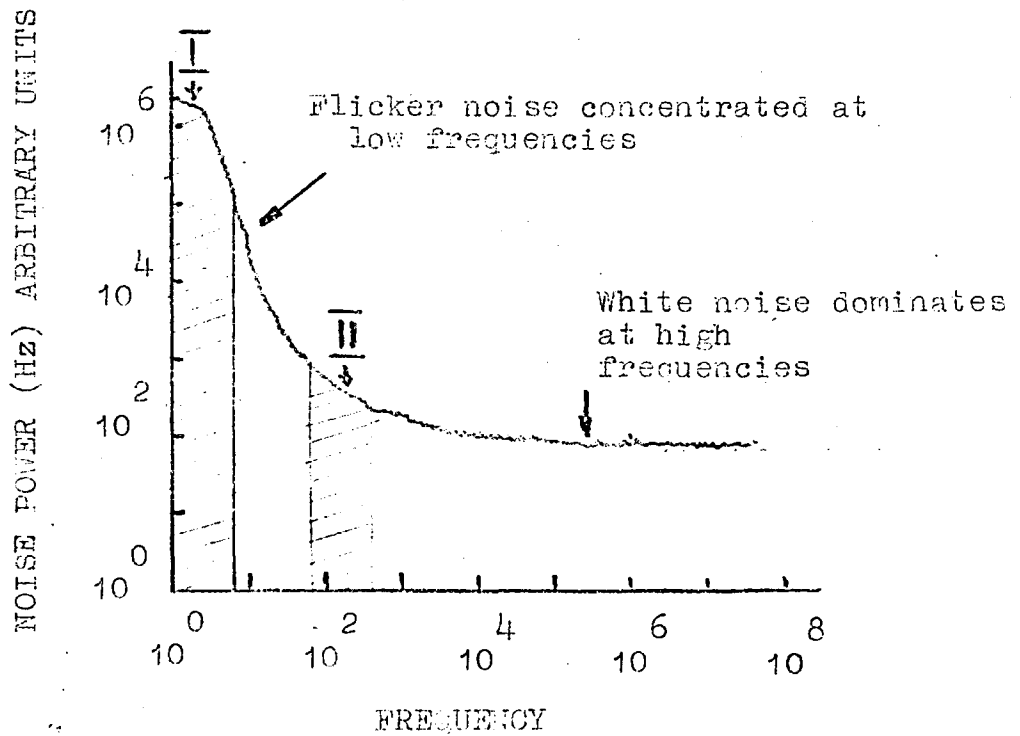


Fig. 2.2 Flicker noise power spectrum

relationship:

$$E = (4RkT\Delta_f)^{\frac{1}{2}} \quad (4)$$

where E is the rms noise voltage contained in a bandwidth  $\Delta_f$  produced in a resistance R,  $k$  is the Boltzmann constant and T is the resistor temperature (K). The noise power, which is proportional to rms voltage, increases as the square root of both the observed bandwidth and magnitude of the resistance.

FLICKER noise has a spectrum in which the power is approximately proportional to the reciprocal of the frequency. It is often called 1/f (one-over f) noise and has the power spectrum shown in Fig. 2.2. Source noise and flame noise exhibit strong 1/f noise. Noise expressions for flame background have been given in relative terms <sup>111, 115, 116</sup> where the rms noise current due to a flame,  $\bar{\Delta} i_f = \xi (\Delta_f i_B)^{\frac{1}{2}}$  (5)

where  $i_B$  = photoanodic current due to flame background.

$\Delta f$  = bandwidth of amplifier-readout system.  $\xi$  = the relative flame flicker factor in  $(\text{sec})^{\frac{1}{2}}$  i.e. the ratio of the rms noise fluctuation signal, due to the flame background intensity, to the signal due to the flame background at a 1 Hz bandwidth. A similar expression is usually applied to source intensity fluctuations. This type of equation is then used when theoretical estimations of signal-to-noise ratio are made <sup>111</sup>.

C. The relative contribution of the various noise sources to the total noise

The noise at the readout is a result of the total effect of the various noises discussed above. The different types of noise combine in two ways: offsets and drifts add linearly and algebraically; Independent random noises add quadratically <sup>7, 111</sup> i.e.

$$\bar{\Delta} i_t = (\sum_n \bar{\Delta} i_n^2)^{\frac{1}{2}} \quad (6)$$

where  $\bar{\Delta} i_t$  is the total rms current noise and the  $\bar{\Delta} i_n$  are the

individual rms current noises due to each of the various noise sources.

The relative contribution of the various noise sources can be evaluated by varying monochromator slit width or height to change the radiant flux reaching the detector. Source noise is a constant fraction of the total source radiance and thus its noise contribution to the output noise increases linearly with the radiant flux reaching <sup>the</sup> detector. However the signal-to-noise ratio increases with source radiance and finally levels off when scattering noise becomes dominant (cf the laser studies carried out by Winefordner and co-workers which are discussed in appendix I).

The monochromator slit width exhibits an optimum value <sup>7,111</sup>. The signal-to-noise ratio is reduced at small slit widths by the dominance of detector noise and electronics noise and at large slit widths by flame background flicker noise.

It is noteworthy that in flame atomic fluorescence the major source of noise is from the flame <sup>59</sup> while in flame atomic absorption the major source of noise is source flicker noise <sup>20,116,118</sup> with a contribution from shot and flame noise.

This fundamental difference arises because the source is observed directly in atomic absorption and not in atomic fluorescence. Thus, provided that high radiance sources are used, near the limit of detection the ratio of atomic absorption noise to atomic fluorescence noise may exceed the same ratio of their signals\*. Consequently atomic fluorescence detection limits can be superior particularly where the fluorescence can be collected over a large solid angle. Detection limits in atomic emission are also often superior to atomic absorption for the same reason although of course there is no contribution from source noise in this case.

\* It has been predicted <sup>7,20,118</sup> that atomic absorption will always give greater signals than either atomic fluorescence or atomic emission.

### 2.2.3. The signal-to-noise ratio

If analytical expressions for  $i_F$  (equation 1) and  $\overline{\Delta i_t}$  (equation 6) could be obtained, then the optimal value of any experimental parameter could be found. No theoretical analytical expressions are known for source and flame flicker noise. Therefore it is not possible to predict theoretically the conditions for maximisation of SNR without first having to estimate the magnitude of a large number of parameters. However some calculations of this nature have been reported<sup>59, 111, 114-116, 119</sup>

The effect of each important experimental parameter on the SNR is usually determined empirically. This optimisation of parameters was the main object of the work presented in this chapter (Section 2.3.).

### 2.2.4. Detection Limit

The precision of analytical flame fluorescence measurements is limited by random noise particularly when measuring signals near the limit of detection. Statistical methods may be used to evaluate the effect of random noise on analytical precision in the following ways:

#### A Standard deviation

The rms noise  $\sigma_R$  is the standard deviation of the difference between the two noisy signals  $i_s$  (sample) and  $i_b$  (blank) where  $S$  is the analytical signal:  $S = i_s - i_b$ .

$\sigma_S$  can be shown to be:

$$\sigma_S = (\overline{\Delta i_s^2}/N_s + \overline{\Delta i_b^2}/N_b)^{1/2} \quad (7)$$

where  $\overline{\Delta i_s}$  and  $\overline{\Delta i_b}$  are the rms noises on the two signals and  $N_s$  and  $N_b$  are the number of measurements of  $i_s$  and  $i_b$  respectively. Normally  $N_s = N_b = N$ , and therefore

$$\sigma_S = \left[ (\overline{\Delta i_s^2} + \overline{\Delta i_b^2})/N \right]^{1/2} \quad (8)$$

## B Relative standard deviation

The Relative Standard Deviation, RSD, of a series of successive readings of  $S$  is given by:

$$\text{RSD} = \frac{100 \sigma_s}{S} \quad (9)$$

For large sample concentrations  $i_s \gg i_b$  also, in atomic fluorescence, the most important sources of noise increase in amplitude with the analytical signal and thus  $\Delta i_s \gg \Delta i_b$  at large sample concentrations, therefore:

$$\text{RSD} = \frac{100 \Delta i_s}{\sqrt{N} S} \quad (10)$$

At low sample concentrations  $i_s \approx i_b$  and  $\Delta i_s = \Delta i_b = \Delta i$  therefore:

$$\text{RSD} = \frac{100 \sqrt{2} \Delta i}{\sqrt{N} S} = \frac{141 \Delta i}{\sqrt{N} S} \quad (11)$$

The smallest analytical signal,  $S_1$  that can be measured with a given maximum RSD can be found from equation (9) or in two special cases (equations 10 and 11):

$$S_1 = \frac{100}{\text{RSD}} \left[ (\Delta i_s^2 + \Delta i_b^2) / N \right]^{1/2} \quad (12)$$

## C Detection Limit

The smallest detectable signal that can be measured with a given level of confidence is derived from small sample statistical theory by the use of the 'student t' statistic. This statistic is defined as the ratio of the smallest detectable difference between two means to the standard deviation of those differences, i.e.

$$t = \frac{(i_s - i_b)_m}{\sigma_s} = \frac{S_m}{\sigma_s} \quad (13)$$

where  $S_m$  is the minimum detectable  $S$ . The value of  $t$  is available in tables and is a function of the number of degrees of freedom (equal to  $2N - 2$ ) and the required confidence level.

Combining equations 8 and 13 then:

$$S_m = t \sigma_s = \frac{t (\overline{\Delta i_s}^2 + \overline{\Delta i_b}^2)^{\frac{1}{2}}}{N^{\frac{1}{2}}} \quad (14)$$

In general  $S_m$  is small so that  $i_s \approx i_b$  and  $\overline{\Delta i_s} = \overline{\Delta i_b} = \overline{\Delta i}$  so that

$$S_m = \frac{\sqrt{2t} \overline{\Delta i}}{\sqrt{N}} \quad (15)$$

The sample concentration giving a signal equal to  $S_m$  is called the Detection limit.

Once the various experimental parameters have been optimized the limiting detectable atomic concentration can be estimated theoretically<sup>111</sup> by combining equations (14) and (1). Equation 2 will give the sample concentration at the limit of detection.

A confidence level of 99.5% and a value of  $N$  of 6 results in a signal-to-noise ratio of 2 at the detection limit<sup>120</sup>. This was the experimental criterion most used in this thesis. The criterion of that concentration which corresponds to twice the standard deviation on a measurement near the detection limit was found experimentally to give equivalent results (see chapter five section 5.4.2.)

#### 2.2.5. Analytical Curves

The practice of analytical atomic spectroscopy relies entirely on obtaining experimental curves of analytical signal vs element concentration or  $I_g$  (signal) vs  $A_g$  (concentration) using standard samples. From these analytical curves the concentrations of unknown samples are interpolated. It is clear that the same parameters which have been discussed in section 2.2.1. also govern the shape of analytical curves. The lack of detailed theoretical expressions concerning a number of these parameters restricts the prediction of the shape of analytical curves to a semiquantitative level. Svoboda, Browner and Winefordner<sup>121</sup> give a definitive

treatment of the theoretical prediction of the shapes of analytical curves. There are a number of other publications on the same subject<sup>122-125</sup>. In this thesis the theoretical basis of the shape of analytical curves is summarised in appendix I.

Referring to equation (2), if the aspiration efficiency  $\xi$  and the atomization efficiency  $\beta$  do not vary with sample concentration,  $C_0$ ,  $N_0$  will vary directly with  $C_0$ . In that case the experimental analytical curve should be the same shape as the theoretical curve shown in Fig. A1.1 (appendix I). Unfortunately  $\xi\beta$  decreases significantly both at very low concentrations (because of changes in degree of ionization) and at high concentrations (because of reduced solution transport rate, increased solute vaporization interference and decreased aspirator yield.)

### 2.3. Optimisation of experimental parameters that affect the atomic fluorescence signal-to-noise ratio at the readout

The signal-to-noise ratio theory highlights the important experimental parameters that can be optimised in order that atomic fluorescence measurements can be made with maximal precision and sensitivity. The detected signal can be optimised by

- a) maximising the source radiance incident on the flame;
- b) choosing optimal flame parameters to minimise quenching and maximise the atomic population in the flame;
- c) maximising fluorescence radiance collected by the detection system.

The noise at the instrument readout can be reduced by minimising

- a) source intensity flicker variations and
- b) flame flicker

and by employing signal processing techniques that will distinguish between the wanted signal and the noise, i.e. sophisticated electronics need to be considered. All these considerations are discussed here under four main headings: 2.3.1. Signal Processing

(Electronics), 2.3.2. The Source (Electrodeless discharge lamps),

2.3.3. The Flame and 2.3.4. The Optical Arrangement.

### 2.3.1. Signal Processing (Electronics)

Hieftje<sup>113</sup> has reviewed the electronic techniques available for improving signal-to-noise ratios including filtering, narrow-band amplifiers, lock-in amplifiers, signal averaging, boxcar integration and correlation techniques. Correlation techniques<sup>126</sup>, and the lock-in amplifier<sup>127</sup> have both been discussed in more detail. The textbook by Winefordner et al.<sup>7</sup> gives a similar review but also looks at photon counting, Fourier transform and Hadamard spectrometry. Flint<sup>128</sup> gives an account of the detection and measurement of very low light levels. Photon counting for spectrometry has been discussed by Halmstat et al.<sup>129</sup> and other workers<sup>130-132</sup> and comparisons between photon counting and lock-in<sup>133</sup> or direct current<sup>134</sup> amplification have been made. Photon counting instruments have been described for spectroscopic applications<sup>130, 135-137</sup>. The photomultiplier tube (P.M.) still possesses a definite signal-to-noise ratio advantage over other transducers e.g. photodiodes<sup>138-140</sup> especially when the dark current is reduced by controlled cooling<sup>128, 141</sup>, biasing techniques and other precautions<sup>128</sup>.

Circuits and discussions have been presented for various phase-sensitive detectors (p.s.d.) both analog<sup>142, 143</sup> and digital<sup>144</sup> and for various forms of electronic integrator<sup>145-148</sup>. In particular a design for a lock-in amplifier (effectively an amplifier incorporating a p.s.d.) has been published by Caplan and Stern<sup>142</sup>.

In the initial stages of the project described here some experiments were carried out with the atomic fluorescence of tin

in turbulent argon-hydrogen and air-hydrogen flames. Poor signal-to-noise ratios (detection limits  $\approx 10$  ppm) were obtained which were partly attributable to the amplifier on the Jarrell-Ash instrument not being able to discriminate sufficiently between the very weak fluorescence signals and their associated noise. When mirrors were placed around the flame to increase the light incident upon the entrance slit of the monochromator no improvement in signal-to-noise ratio was observed. Hofton and Hubbard<sup>150,151</sup>, using the same instrumentation, also found that the use of mirrors and a lens did not improve the signal-to-noise ratio of bismuth atomic fluorescence. Other criticisms of the experimental arrangement were that the use of a total consumption burner increases the risk of scattered source radiation<sup>149</sup> (section 2.3.3. A premix flame is usually preferred for atomic fluorescence studies) and the Jarrell-Ash a.c. tuned amplifier is designed to accept modulation frequencies around 50 Hz and therefore very susceptible to mains borne noise.

Further experiments showed that the Jarrell-Ash a.c. amplifier gave an output when observing the radiation from a d.c. source such as a d.c. operated electrodeless discharge lamp or the d.c. background emission from the flame. This output was in magnitude about 10% of the value obtained when measuring the same d.c. signals using the d.c. emission amplifier of the instrument. It is clear that the amplifier would therefore also be susceptible to respond to emission signals due to the possible presence of strongly emitting matrix elements such as sodium. Moreover, although this d.c. background could be considered to be a blank signal, it was found by Hofton and Hubbard<sup>150</sup> that the zero control on the Jarrell-Ash amplifier was not capable of completely backing off the background,

blank signal. A  $10\text{K}\Omega$  variable resistor was incorporated into the zero control circuit<sup>150,151</sup> to enable this 'backing off' to be effectively carried out at high P.M. voltages.

However this solution to the problem, whilst enabling measurements to be made at high P.M. gains, was not satisfactory because any drift in the d.c. background would give drift in the wanted output thus leading to decreased measurement precision and inferior detection limits. More sophisticated signal processing techniques were necessary to overcome these problems.

The only real alternative was to build a lock-in amplifier to the design by Caplan and Stern<sup>142</sup>. The other alternatives (Photon counting, signal averaging, etc.) were far too expensive to consider. Particularly attractive features of the Caplan and Stern design were that such an amplifier was inexpensive to build ( $\sim$  £100) and could be tuned to any signal frequency from d.c. to 5 MHz. This latter facility gives the investigator the option on a modulation frequency which avoids the regions of the frequency spectrum where most flame noise is found. Moreover a lock-in amplifier is specifically designed to give an output due only to a.c. signals at the input which are a result of the frequency of modulation. Background d.c. signals are blocked completely and a.c. noise signals can be effectively filtered to reduce their magnitude.

A discussion is given here concerning amplifiers, electrical bandwidth, filtering and narrow-band, tuned amplifiers. These subjects are integral with the qualitative understanding of the operation of a lock-in amplifier.

#### A D.C. Amplifiers

An amplifier can be represented (Fig. 2.3a) by a triangle with an input and an output. All amplifiers as such will amplify

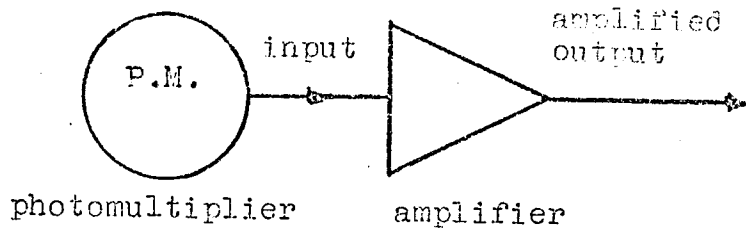
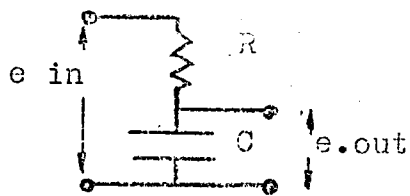
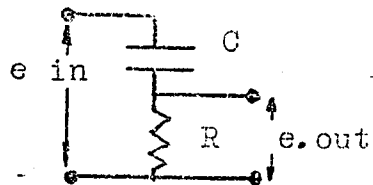


Fig 2.3a



low pass filter



high pass filter

Fig 2.3b

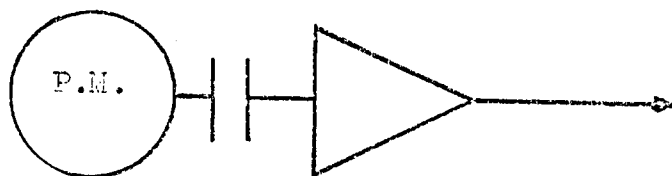


Fig 2.3c

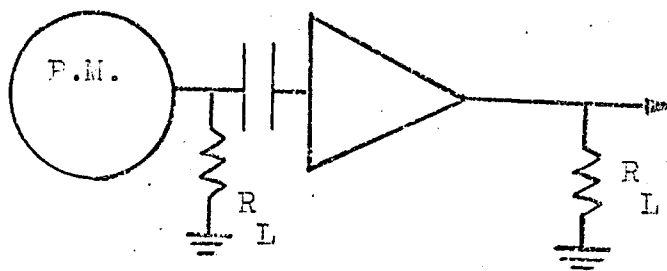


Fig 2.3d

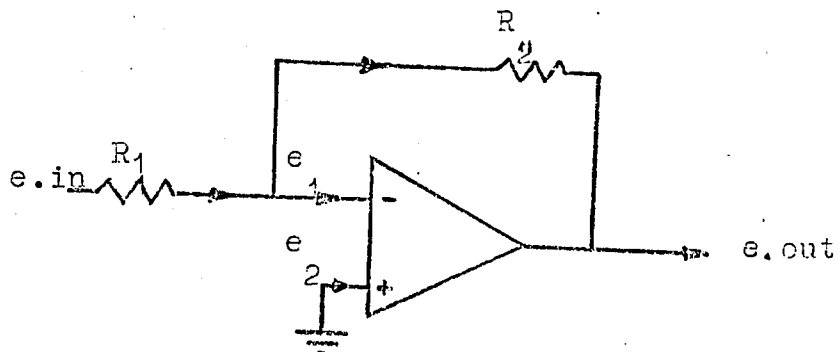


Fig 2.3e

any signal whether a.c. or d.c. A d.c. signal would be the emission of resonance radiation by a thermally or radiationally excited atomic population in a flame or the absorption signal in a flame observed when monitoring the output from a d.c. operated hollow cathode lamp. With a d.c. amplifier the d.c. signal would be fed into the input, amplified and the d.c. output fed to a readout device such as a meter or potentiometric recorder. However, there are two problems. Firstly, there is drift due to low frequency variations in the output which are a result of slow change in the flame conditions (usually caused by temperature variations) and temperature dependent drifts in the electronics, monochromator etc. Secondly there is noise the sources of which have been discussed in section 2.2.2. Thus a d.c. amplifier gives a signal associated with drift and noise. Normally the output of the amplifier is filtered to remove a.c. noise components.

Consider the resistance-capacitance (R.C.) combinations shown in Fig. 2.3b. For the low pass filter,  $e_{out}$ , the voltage across the capacitor, decreases as the frequency increases i.e. only low frequencies are passed. It can be shown that the upper cut-off frequency  $f_{upper}$  is given by:

$$f_{upper} = \frac{1}{2\pi RC} \quad (16)$$

This is simply the frequency at which the capacitors impedance (i.e. a.c. resistance) is equal to R. Low pass filters are used to filter out a.c. noise components. The degree to which the output low-pass filter attenuates a.c. signals is a function of the time constant  $T = RC$  (secs.) calculated in ohms x farads. The significance of the time constant is discussed later in relation to the output low pass filter used with the lock-in amplifier (section 2.3.1. C).

For the high pass filter (Fig. 2.3b) the voltage across the resistor decreases as frequency decreases. This is because as the frequency decreases, the capacitors impedance increases and the fraction of  $e_{in}$  found across R decreases. Therefore, only high frequency signals will pass unattenuated. Again, when the impedance of C = R this is the lower cut off frequency and

$$f_{lower} = \frac{1}{2\pi RC} \quad (17)$$

Hence with a high pass filter any d.c. component in the signal will not be passed by C and thus will not appear across R.

This type of filter is used in a.c. tuned amplifiers.

### B Noise, modulation and a.c. tuned amplifiers

With a D.C. amplifier it is difficult to have more than one amplification stage because one stage would simply amplify the drift of the previous stage. An improvement in this situation can be brought about by coupling the amplifier to the photo-multiplier tube (P.M.) via a capacitor (Fig. 2.3c). D.C. signals and drift signals are thus prevented from entering the amplifier. However the wanted signal must now be converted into an a.c. signal in order to pass the capacitor and be amplified. This is done by modulating the light producing the signal or by modulating the incoming d.c. signal. In atomic absorption and atomic fluorescence the former method is used (chopping of the source radiation) while in flame emission the latter method is employed (chopping the radiation coming from the flame or electronically chopping the d.c. signal at the P.M. output). This type of amplifier is called an a.c. coupled amplifier. Normally the output of the amplifier being a.c. is rectified, i.e. converted back to d.c., and filtered to remove noise components.

Thus with an a.c. amplifier one can obtain a d.c. output proportional to the input voltage or current whether it

is initially a.c. or d.c., the latter being subsequently chopped to produce an a.c. signal. The anode current from the P.M. a.c. or d.c., will develop a voltage, a.c. or d.c. across the P.M. load resistor  $R_L$  (Fig. 2.3d). If the signal is a.c. it will pass the capacitor, if it is d.c. it has to be electronically chopped before the capacitor. The a.c. signal is then amplified and the output voltage is measured across the amplifier load resistor  $R_L'$  (Fig. 2.3d).

The amplifier represented by the triangle in Fig. 2.3d could be any operational amplifier which uses valves, transistors or an integrated circuit\*. The main requirements for amplifiers are gain stability and low noise. The amplification of valves and transistors is not stable with age or environment (e.g. temperature). Gain stability is obtained by the use of feedback. With feedback the gain of a particular amplification stage is lowered and the loss in gain pays for the stability. The feedback concerned here is called negative feedback and consists in feeding part of the signal from the output back to the input through the resistor  $R_2$  in Fig. 2.3e. Operational amplifiers and integrated circuit amplifiers are usually differential amplifiers with two inputs (marked + and - in Fig. 2.3e, the non-inverting and inverting input respectively). The term differential indicates that the amplifier amplifies the difference between the voltages

\* The properties of semiconductors make it possible to produce an entire electronic circuit within one single crystal. Such an integrated circuit miniaturizes electronic networks and also reduces the number of individual components in complex electronic circuits. This is so because an entire integrated circuit can contain the equivalent of tens or hundreds of transistors, resistors and capacitors but still represents only one component.

at its two inputs. The output voltage can be written as (Fig. 2.3e):

$$e_{\text{out}} = A(e_2 - e_1) \quad (18)$$

The value of  $A$ , the gain without feedback (also called the open loop gain) is typically in the range 2000  $\rightarrow$  50,000. In the above circuit the non-inverting input is earthed i.e. no signal is applied to it and therefore  $e_2 = 0$ . It can be shown<sup>152</sup> that because  $A$  is large:

$$\frac{e_{\text{out}}}{e_{\text{in}}} = \frac{R_2}{R_1} \quad (19)$$

i.e. the voltage gain with feedback (in this case shunt, negative feedback) depends entirely on the two resistors  $R_1$  and  $R_2$ . The required gain or amplification equals  $R_2/R_1$ . The values of  $R_1$  and  $R_2$  can be extremely stable if good quality components are used and hence the stability of the amplifier will also be high. Even if the amplifier itself is not linear the feedback amplifier will have good linearity, provided  $A$  is large, because fluctuations in  $A$  do not affect the resulting gain. Noise which is part of the signal at the amplifier input is amplified by the same amount as the signal. Noise which is internally generated in the amplifier and appears at the output is reduced, by applying feedback, by the same amount that the gain is reduced. Thus feedback does not improve the SNR. However electronic noise in modern amplifiers is usually very small and moreover the property of feedback can be used to reduce noise, present with the signal, at the input.

As indicated in section 2.2.2. the dominating noise source in flame spectroscopy is due to flicker variations in the radiation from the flame. It was also indicated that the noise spectrum shows the  $1/f$  distribution which is shown in Fig. 2.2.

Looking at this figure, firstly it is clear why d.c. measurements are to be avoided whenever flame noise dominates other noise, such as photomultiplier shot noise and electronic noise. Most of the flicker noise is concentrated at the low frequency end of the plot i.e. around d.c. Secondly, by modulating the source radiation the signal channel can be shifted to any favourable position in the frequency spectrum. For instance the band of frequencies at II ( $\sim 100$  Hz) in the  $1/f$  plot is obviously in a more favourable position than I as far as SNR is concerned. However if modulation was carried out at 100 Hz and the a.c. amplifier responded to a wide band of frequencies, noise would still appear at the readout. The response of the amplifier, ideally, must be reduced at all frequencies except the signal frequency. The frequency response bandwidth,  $\Delta f$ , of the amplifier must be made less wide.

The two types of filter discussed in section 2.3.1. (A) can be put into the feedback loop of an a.c. amplifier such that the amplifiers response is modified. The filters when combined have a maximum impedance at a particular frequency,  $f_0$ . Thus, in effect, the resistor  $R_2$  (Fig. 2.3e) has a high value at a particular frequency, thus giving less feedback and therefore more gain. At other frequencies the resistor  $R_2$  has a low value, giving more feedback and less gain. Thus a fairly sharply tuned a.c. amplifier is obtained which responds to a narrow band of frequencies around  $f_0$  (i.e. bandwidth,  $\Delta f$  is small). It is possible to make tuned a.c. amplifiers with several stages and with a  $\Delta f$  of only a few Hertz. However any slight drift in the signal frequency (i.e. the modulation frequency in flame spectroscopy) will cause a serious change in the signal level. There is therefore a limit to how narrow one can make  $\Delta f$ .

### C The lock-in amplifier

Figure 2.4 is a block diagram based on the various parts of the lock-in amplifier which was built during this work.

This home made amplifier, based on the design by Caplan and Stern<sup>142</sup> uses integrated circuits throughout the circuit except in the phase sensitive detector.

The signal, taken from the output of a preamplifier (which converts the anode current from the photomultiplier to a voltage at an acceptable level for the lock-in amplifier - see later) is amplified initially by a d.c. coupled input amplifier. The signal is then fed into a low pass filter and then a high pass filter the combination of which constitutes a tuned a.c. amplifier. Lock-in amplifiers in general may or may not be tuned before the phase-detection stage but it is usually desirable to eliminate much of the noise at frequencies far removed from the chopping frequency. These low and high pass filters are each incorporated into the feedback loop of an integrated circuit operational amplifier and therefore the filtering effect is associated with a certain amount of gain (see section 2.3.1.B and equation 21). After passing through a further amplification stage, the filter output amplifier, the signal is then fed into the phase-sensitive detector, p.s.d. (variously called a mixer, synchronous detector, chopper etc.).

The reference signal, derived from the source power supply (or mechanical chopper) can be of any waveform provided that it has two zero crossing points per cycle. The phase of the reference can be adjusted to that of the signal by means of the phase shift control. This is necessary if there is anything causing a phase shift in the signal somewhere before the p.s.d. The output from the reference and phase-shifting circuits consists

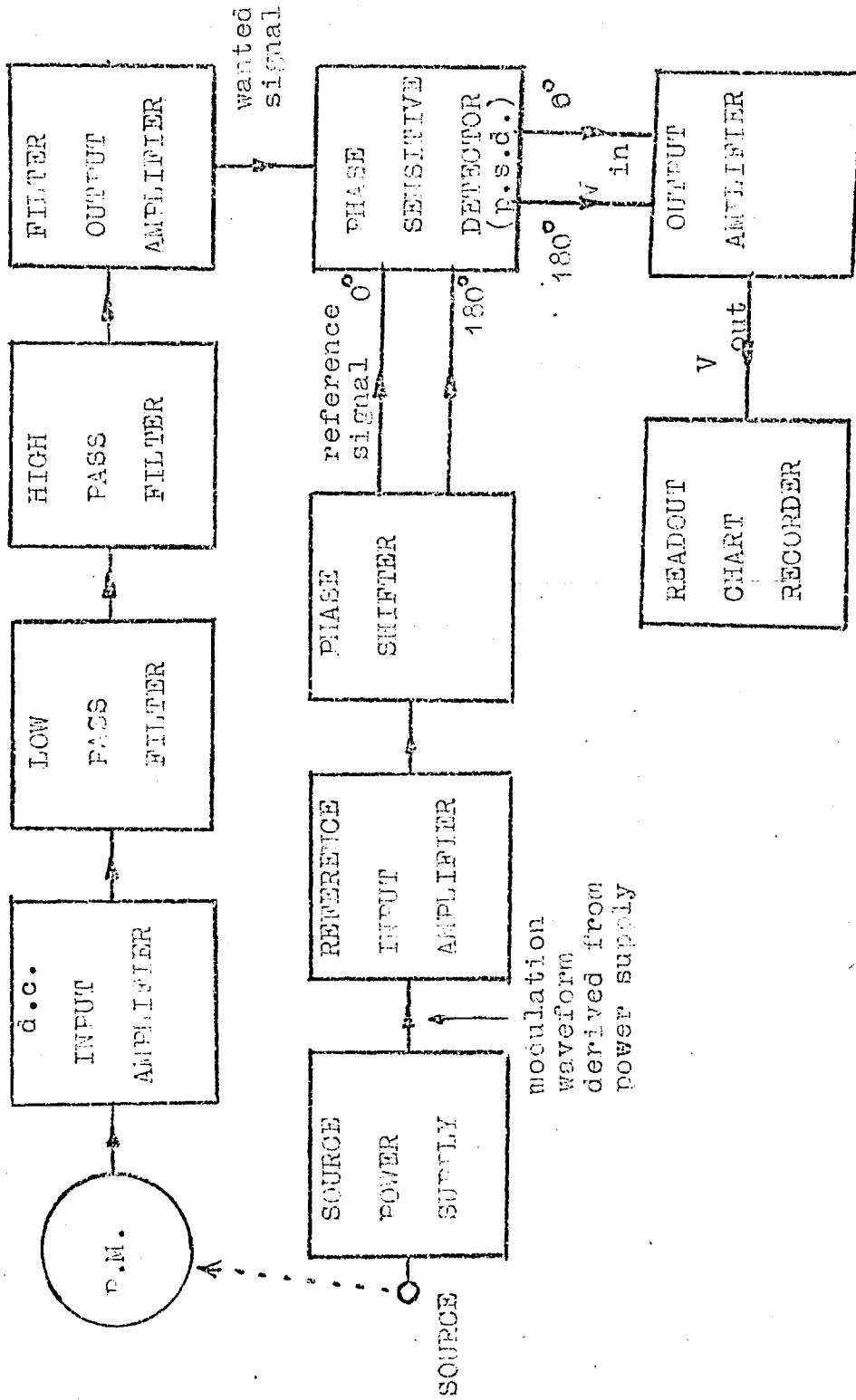


Fig. 2.4. Block diagram of the lock-in amplifier

consists of two square waves. The first output is  $180^\circ$  out of phase with the input while the second output is in phase with the input. These two complementary reference outputs are then fed into the p.s.d. where they switch complementary half-wave portions of the detected signal via two sets of chopper switches. The resulting two chopper outputs are then applied to the differential inputs of the output amplifier (differential low-pass filter) which then acts as a half-wave rectifier\*. When the signal and reference are in phase the output is a mean direct voltage proportional to the amplitude of the signal voltage. When the signal and reference are in antiphase the d.c. output is reversed. When the signal and reference are in quadrature the mean output is zero (Fig. 2.5). These results may be summarised by:

$$V_{\text{out}} = V_s \cos \alpha \quad (20)$$

where  $V_{\text{out}}$  is the average output voltage,  $V_s$  is the signal voltage and  $\alpha$  is the phase angle between the signal and reference. A.C. asynchronous signals are not rectified by the output amplifier. The signal is then fed into some readout device such as a potentiometric recorder.

The output amplifier as well as acting as the rectifier

\* The difference between the complementary half-wave portions of the signal is amplified. The inverting input in fact gives an output which is  $180^\circ$  out of phase with its input while the non-inverting input does not change the phase of the signal. As the two inputs are already  $180^\circ$  out of phase with each other the net result is a rectified signal.

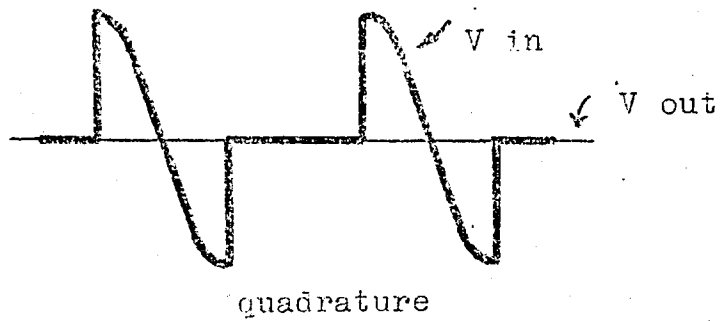
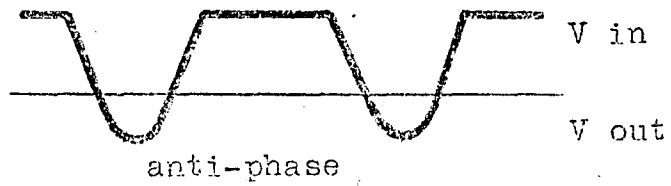
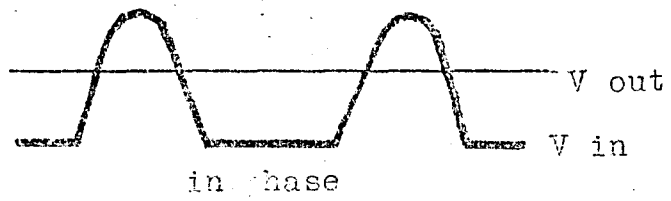


Fig. 2.5 Output signals

V in = Waveforms at output of p.s.d.  
 V out = Output of low pass filter

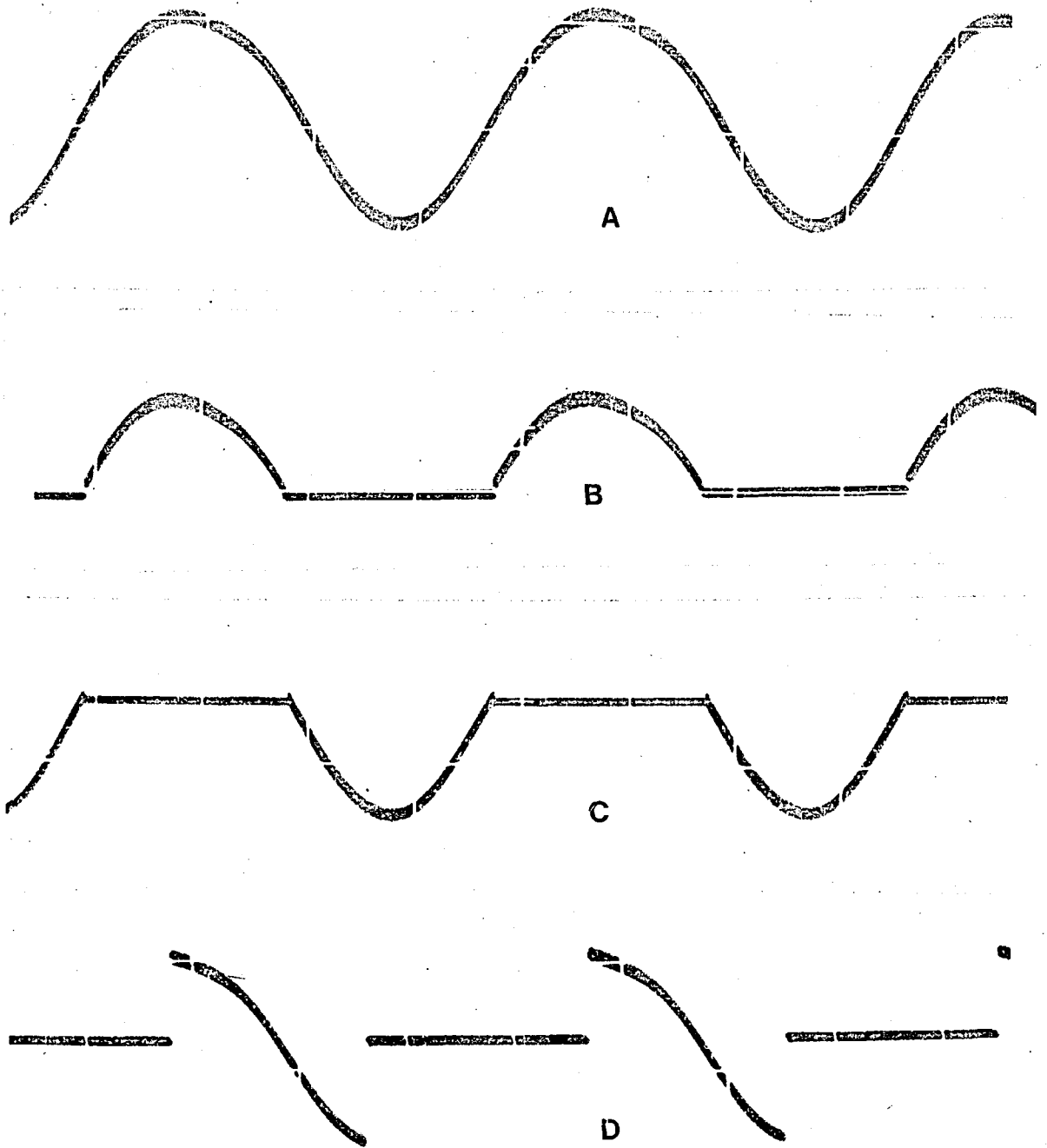


Fig. 2.5 (cont.)

Photographs of the oscilloscope traces at Test Point 4 which illustrate, A - The original signal as seen at Test Point 1; B - The signal in phase with the reference as seen at Test Point 4. C - The signal in antiphase. D - The signal in quadrature. The signal source was a 10 KHz modulated tin EDL observed directly by the detection system at 303.4 nm.

also has a low pass filter in its feedback loop which attenuates the a.c. asynchronous signals.

The degree to which the output low-pass filter attenuates a.c. asynchronous signals depends on the time constant of the filter and the output resistance of the amplifier. When an R.C. filter is on the negative feedback loop of a high gain operational amplifier the output of the filter is given by<sup>147,152</sup>

$$V_{dc\ out} = -\frac{1}{RC} \int_0^t V_{in} dt. \quad (21)$$

where  $V_{out}$  is the net output d.c. voltage after application of the in phase signals ( $V_{in}$ ) from the p.s.d. for  $t_{sec}$  with the time constant  $T = RC$  calculated in ohms x farads. The time constant thus determines the net gain of the filter. The signal bandwidth of the operational amplifier with an RC filter in the feedback loop is the same as the simple R.C. low pass filter (Fig. 2.3b) i.e. where  $f_{upper} = \frac{1}{2\pi RC}$  (equation 16). This value is a result of defining<sup>152</sup> the bandwidth,  $\Delta f$ , as equal to that sinusoidal frequency at which the circuits response is  $1/\sqrt{2}$  of its maximum value ( $\Delta f$  and  $f_{upper}$  are therefore the same value). However consider a white noise source generating a noise voltage per unit bandwidth which gives an rms voltage at the output of the filter and refer to equation 6.

It can be seen that to find the noise output of the RC filter, the square of the noise voltage must be integrated over the range of frequencies of interest. The result<sup>152</sup> is an equivalent noise bandwidth of:

$$f_{upper} = \frac{1}{4RC} \quad (22)$$

This is significantly different from the signal bandwidth  $\frac{1}{2\pi RC}$ .

It actually corresponds to a wider bandwidth which is why  $\sqrt{\Delta f}$

appears in the equations for shot and Johnson noise. This argument is true for white noise. If the noise is not white, the relation between noise and bandwidth is different but in general reducing  $\Delta f$  reduces the noise at the output.

Not only is the bandwidth of the system determined by the time constant but also the response time is affected. The response time  $T_R$  is defined as the time it takes for the output signal to reach 99% of its final value. It may be shown that

$$T_R = 4.6RC \quad (23)$$

Combining equations (22 and (23):

$$T_R = \frac{1.15}{\Delta f} \approx \frac{1}{\Delta f} \quad (24)$$

If the electrical bandwidth is reduced in an attempt to reduce random noise the response time increases (equation 24).

Unfortunately not only does this extra time required cause difficulties but also the trade of time for noise is not linear. The noise only decreases as the  $(\text{time})^{\frac{1}{2}}$  a consequence of equivalent noise bandwidth. (i.e. equations (3) to (5) where the magnitude of the various noise sources are proportional to the square root of the bandwidth). To illustrate this point consider that going from a time constant of 1 second to one of 100 seconds narrows  $\Delta f$  by a factor of 100, but this only decreases the noise by  $(100)^{\frac{1}{2}}$  i.e. 10. Thus it is necessary to wait 100 times larger to improve this signal-to-noise ratio by a factor of 10. Moreover the increase in response time will introduce errors and inconveniences which effectively limit the extent by which  $\Delta f$  may be profitably reduced. These difficulties are outlined below:

(1) Analysis time - the extra time necessary for the amplifier to give a readout becomes inconvenient when carrying out multiple

readings such as statistical checks on a large number of samples and standards.

(2) Sample consumption - A longer analysis time will mean more sample solution consumed which may be a disadvantage for some applications.

(3) Drift Errors - Instrumental drifts resulting from source spectral radiance drift, amplifier drift etc. have a greater effect on analytical accuracy the longer it takes to complete a measurement.

(4) Spectrum-scanning - For recording line spectra, the monochromator scan speed  $r$  (non  $\text{sec}^{-1}$ ) should be approximately<sup>7</sup> :

$$r \leq \frac{S}{T_R} = S (\Delta f) \quad (25)$$

where  $S$  is the spectral bandpass of the monochromator. In the present work  $S$  was 0.25 nm and in fact a scan speed of 0.03 nm  $\text{sec}^{-1}$  was used routinely whereas the optimum should have been  $\approx .008$  nm  $\text{sec}^{-1}$  ( $\Delta f = 0.032 \text{ sec}^{-1}$ ). However the Jarrell-Ash monochromator is capable of a scan speed of 0.003 nm  $\text{sec}^{-1}$  if greater scan accuracy is required.

The ideal lock-in amplifier is inherently linear, the main result of this being that unwanted signals are a.c. and consequently give random fluctuations about the d.c. level given by the wanted signal. By contrast the noise passed by a tuned amplifier into a conventional polarity sensitive rectifier gives an a.c. output superimposed on a d.c. offset. This d.c. output is an error which depends in magnitude upon the mean value of the noise and is subject to changes which do not depend on the signal level.

#### D. Building of the lock-in amplifier

The basic principles of the lock-in amplifier circuit have already been outlined in section 2.3.1.C. The circuit

was taken from the design by Caplan and Stern <sup>142</sup>. This design was specifically titled 'An Inexpensive Lock-In Amplifier' and so it has proved to be. All the components were inexpensive although it was necessary to build a twin power supply (£17) to power the amplifier. The total cost of the electronics (including the preamplifier) was less than £100. The design for the power supply was taken from the R.S. Components Ltd. catalogue <sup>‡</sup> and R.S. voltage regulators were used.

Two relatively minor modifications were made to the lock-in amplifier circuitry. Firstly a modification to the input amplifier. This amplifier as designed had too low an input impedance to be compatible with the photomultiplier tube or the preamplifier which was subsequently built. Secondly a new output amplifier (differential low-pass filter) was built to be used as supplementary to the design output amplifier. This new differential low-pass filter was temperature stabilised to give minimum drift with ambient temperature, thus permitting longer time constants to be used at the output.

The main problem encountered during the building of the lock-in amplifier was with high frequency oscillation caused by instability of the integrated circuit operational amplifiers. (This is a common problem with such amplifiers and there are standard remedies based usually on trial and error with different values of circuit components <sup>153</sup>). In this section the circuitry in its final form is reproduced in sections as the description of its features continues. Any differences between the Caplan and Stern design and this circuitry are pointed out where necessary. The preamplifier, described below, was not part of the original design but was necessary to match the lock-in amplifier to the photomultiplier tube.

<sup>‡</sup> The relevant part of the catalogue is given in appendix 3

### The power supply

The lock-in amplifier requires a twin d.c. power supply giving -7.5 volts and +14.5 volts. A power supply for use in solid state electronics usually has to be stabilised (regulated) i.e. any variations in the value of the voltage given say by a transformer-rectifier arrangement is compensated for by some sort of regulation circuitry to give a constant output voltage which varies by less than about  $\pm 4\text{mV}$  in say 7.5 volts. Variations which are not compensated for by regulation would show themselves as noise at the output of the amplifier.

Integrated circuit operational amplifiers are frequently used as reference amplifiers in voltage regulated power supplies. The purpose of the amplifier is to isolate the voltage reference (a zener or temperature compensated reference diode) from changes in loading at the supply output. Figure 2.6 is a typical example of a small voltage regulator circuit. (The amplifier in this example is an SN72741 monolithic integrated circuit operational amplifier. This is the same integrated circuit as used in the preamplifier, described later, and the output amplifier of the lock-in amplifier.) Because of the high gain of the SN72741 amplifier the voltage applied to the inverting input from the output voltage divider ( $R_2$ ,  $R_3$  and  $R_4$ ) is always maintained to within a few millivolts of the reference voltage provided by the zener diode  $Z_1$ . The output voltage can be adjusted by changing the division ratio of the divider. The transistor (BFY56A is a typical example) provides the power necessary to give the output of 0-100 mA.

Because of the large number of components in the lock-in amplifier rather more power than 100 mA is necessary to drive

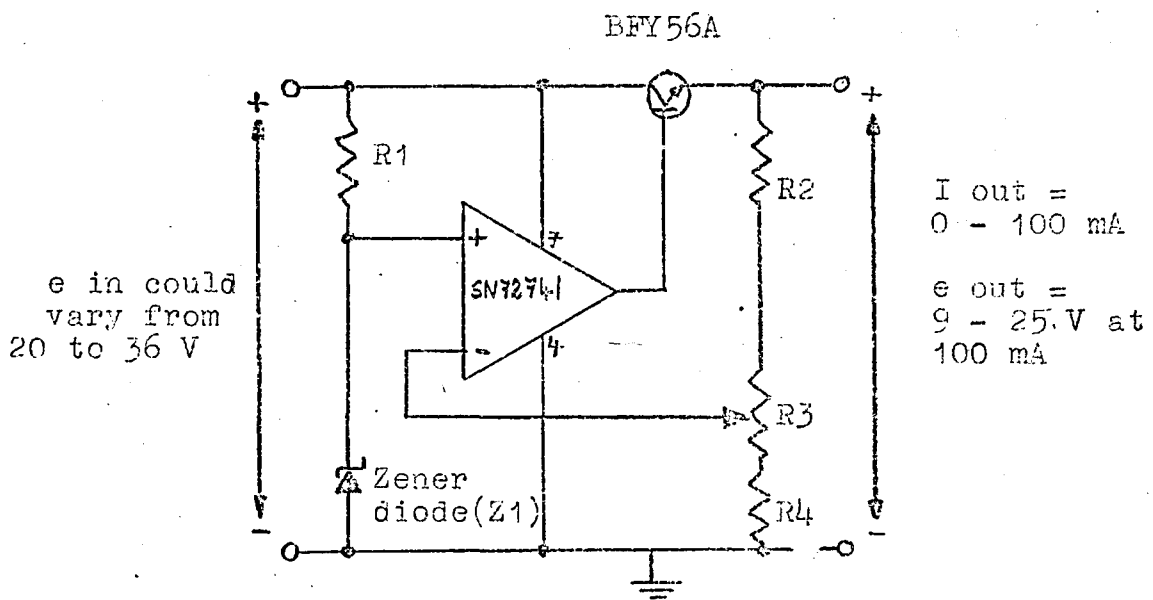


Fig.2.6. Typical voltage regulator

its circuits. (Caplan and Stern specify power supplies of +14.5 and -7.5V with 250 mA minimum from each supply). The regulator chosen for the circuit that was built (Fig. 2.7) was the RS components 2-30V regulator which has an external transistor encapsulated with the monolithic integrated circuit regulator amplifier. With the additions of a further, power, transistor (2N3055) ample power was available to cope with the demands from the lock-in amplifier and the preamplifier.

The data for the transformer and regulator are given in Appendix 3. The circuit shown in Fig. 2.7 was based on the information given with the regulator data. The main points about the circuit are: The transformer giving two outputs one for each of the bridge rectifiers (REC 41A) which supply the -7.5V and +14.5V circuits respectively. The large 2500 $\mu$ F smoothing capacitors ( $C_1$  &  $C_2$ ) which remove most of the ripple components present after rectification. The 8.2V regulating zener diodes ( $Z_1$  &  $Z_2$ ). The RS regulators. The 2N3055 transistors providing the power output. The output voltages can be set by altering the present potentiometers ( $V_1$  &  $V_2$ ) which are located on the power supply circuit board. The power supply is capable of giving at least one amp. from each output (-7.5 and +14.5V set by  $V_1$  &  $V_2$ ).

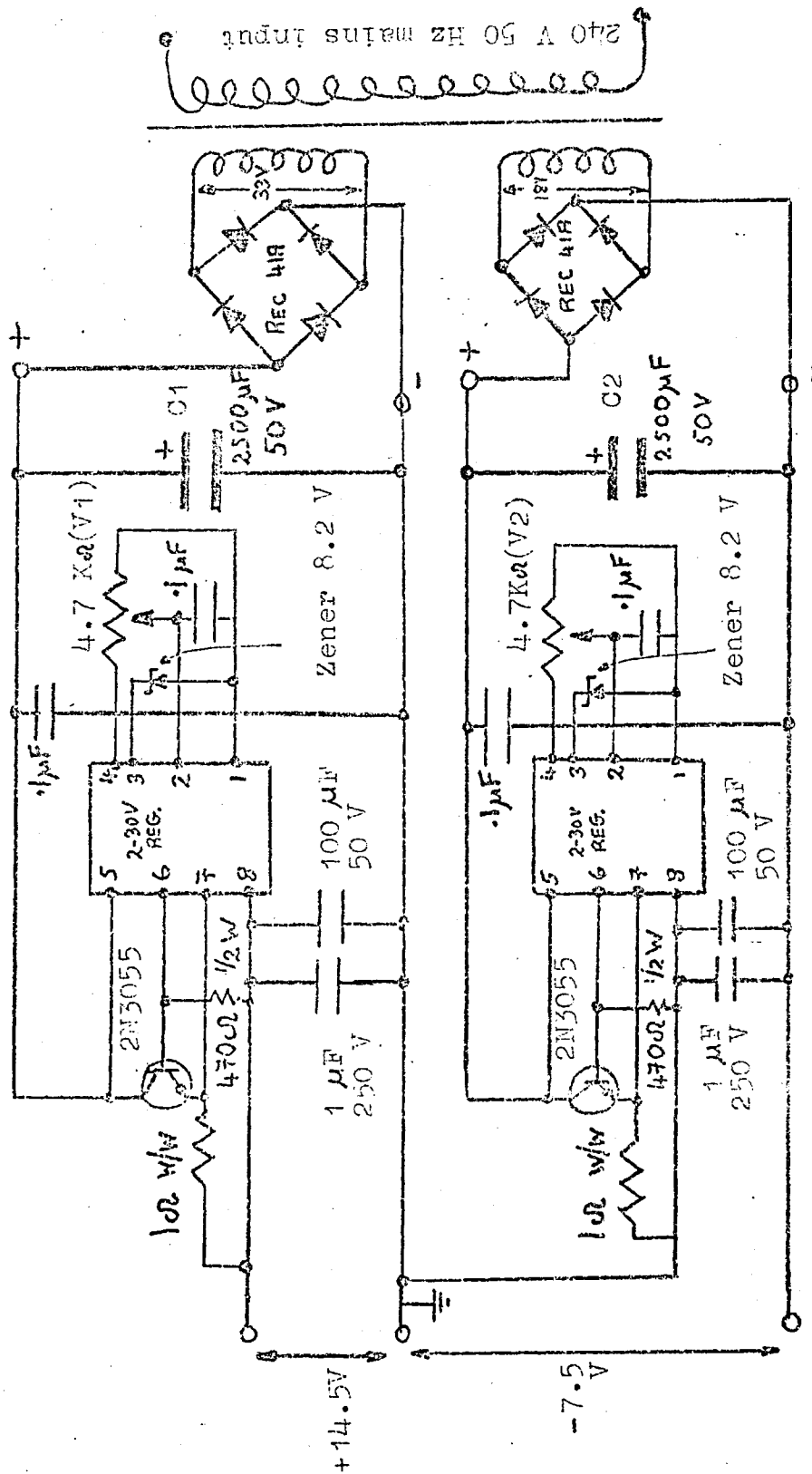
### The Preamplifier

There are usually two basic functions of a preamplifier:

1. To create the correct impedance matching from the source to the main amplifier and
2. To provide some initial amplification before the main amplifier with as little introduction of noise as possible.

When connecting the output of a photomultiplier tube to the input of an amplifier care must be taken that the relative

The first part of the document discusses the importance of maintaining accurate records of all transactions. It emphasizes that every entry should be supported by a valid receipt or invoice. This ensures transparency and allows for easy verification of the data. The second part of the document provides a detailed breakdown of the financial data for the quarter. It includes a table showing the revenue generated from various sources, as well as the associated costs and expenses. The final part of the document concludes with a summary of the overall financial performance and offers recommendations for future improvements. It suggests that by implementing more rigorous controls and regular audits, the organization can further enhance its financial stability and growth.



REGULATED  
 OUTPUT +14.5 V  
 and -7.5 V  
 relative to earth

FIG. 2.7 LOOK-IN AMPLIFIER POWER SUPPLY

For data on the 2-30 V regulator see appendix III

impedances are compatible. Referring to Fig. 2.3d, the anode current from the photomultiplier produces a corresponding voltage drop across the load resistor  $R_L$  which is measured by the following amplifier. This load resistor may be part of the photomultiplier circuit or simply the input impedance of the amplifier. The P.M. itself (i.e. without  $R_L$ ) has an extremely high output resistance due to the resistance between the anode and the last dynode. With this high output resistance  $R_L$  can be very large which is an important advantage. Thermal noise generated in  $R_L$  is amplified by the following electronics and therefore the larger the voltage drop across  $R_L$  the larger the resulting signal-to-noise ratio. This is because the noise will increase as  $\sqrt{R_L}$  while the signal increases as  $R_L$ . Any noise generated in the lock-in amplifier is then negligible compared to the amplified noise generated in  $R_L$  and shot noise generated in the P.M. will dominate thermal noise in  $R_L$ . Also the P.M. can be operated at lower gains due to the larger signal available. High gains on photomultiplier tubes can often lead to deterioration in signal-to-noise ratio caused by a relatively large increase in shot noise and in the extreme to internal breakdown which destroys the tube.

To be able to use a very high value of  $R_L$ , the input impedance of the preamplifier must be larger than  $R_L$ , otherwise voltage division will occur. For example if  $R_L$  is  $10^7 \Omega$  and the input impedance of the amplifier ( $R_n$ ) is only  $10^6 \Omega$ , the resulting parallel resistance has a net value of only  $R_n$ , given by:

$$\frac{1}{R_n} = \frac{1}{10^6} + \frac{1}{10^7} \quad \text{i.e. } R_n = 9.1 \times 10^5 \Omega$$

Therefore the net load resistance is essentially that of the amplifiers input. Higher values of  $R_L$  will not appreciably increase the measured signal.

Preamplifiers usually have an input impedance at least 100 times greater than the output impedance of the photomultiplier. Such amplifiers are voltage amplifiers\* (i.e. they measure the voltage drop across  $R_L$ ) and can be either a buffer amplifier with a gain of unity or they can have a fixed or variable gain greater than unity.

When the lock-in amplifier was first built and connected to the P.M. various circuit configurations of the input amplifier were tried in an attempt to raise the input impedance. However the characteristics of the SN72702 integrated circuit used in the input amplifier were such that the input impedance could not be raised above about  $40K\Omega$ . (see data for this integrated circuit, appendix 3 and further discussion concerning the input amplifier in a later section).

The SN72741 integrated circuit operational amplifier is a more advanced component with an input resistance of  $400M\Omega$  when the gain with feedback is between 0 and 20 dB. The table

\* Instead of using a voltage amplifier measurements can be made with a field effect transistor-input operational amplifier acting as a current amplifier. As well as reducing problems associated with the capacitance of the lead from the P.M. output the current amplifier can also be used to obtain very high sensitivities. The voltage amplifiers described in this section were a compromise between high sensitivity and cost of components.

below summarises the variation of input resistance of this amplifier with bandwidth and gain. (See data for the SN72741, appendix 3)

Gain	Typical bandwidth	Input resistance $Z$ (impedance)		
		Inverting amplifier	Non-inverting amplifier	
1	0	1 MHz	10 K	400 M
10	20	100 KHz	1 K	400 M
100	40	10 KHz	1 K	230 M
100	60	1 KHz	100	80 M

✱

Gain in dB = 20 lg (voltage gain)

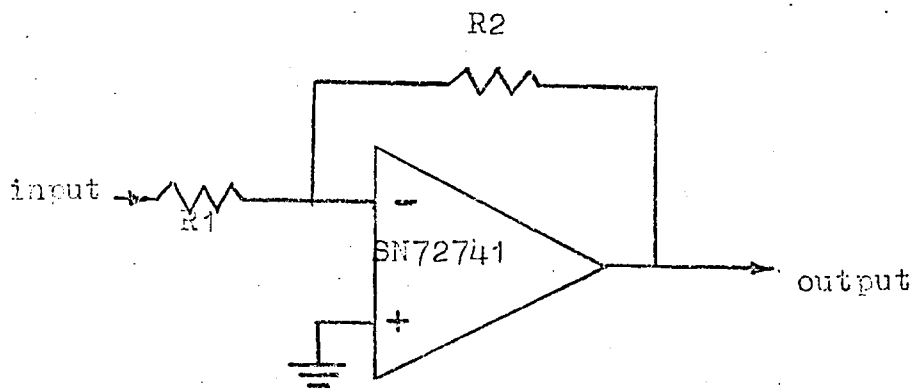
Whether an integrated circuit operational amplifier is being used as an inverting amplifier or a non-inverting amplifier depends upon whether the signal is being fed into the inverting input (Fig. 2.8a) or the non-inverting input (Fig. 2.8b) respectively.

It can be seen from the above table that in order to obtain the required high input impedance for the preamplifier using the SN72741 it is necessary to use the non-inverting input.

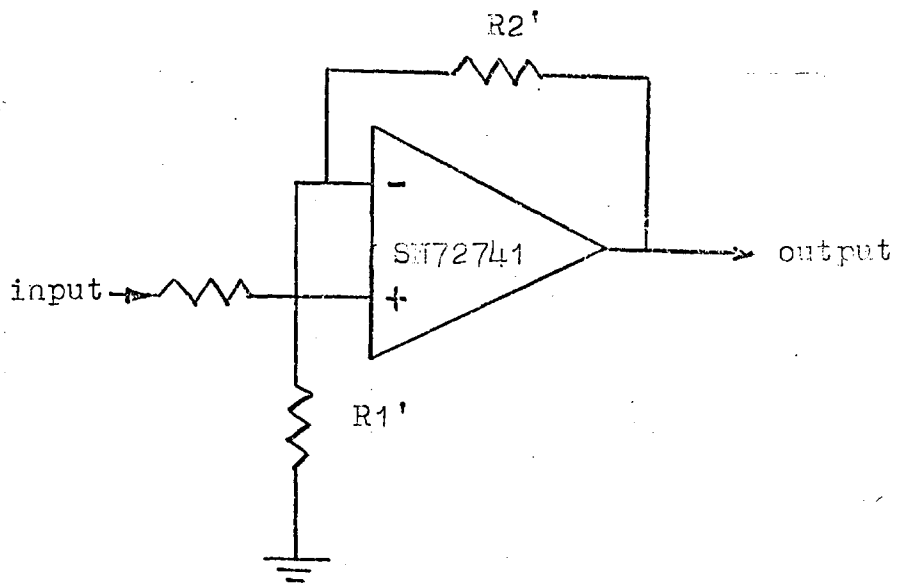
Fig. 2.8a is identical to Fig. 2.3e for which it can be shown (equation 19) that the voltage gain =  $-\frac{R_2}{R_1}$  when the non-inverting input is used the voltage gain is calculated by:

$$\text{Gain} = \frac{R_2' + R_1'}{R_1'} \quad (\text{Fig. 2.8b}) \quad (26)$$

In this work two simple preamplifiers were built using the SN72741 integrated circuit. The first (Fig. 2.9) is a voltage follower or buffer amplifier. This has no gain (i.e. 0 dB)



a) input at inverting input



b) input at non-inverting input

Fig. 2.8. Choice of input configuration for an operational amplifier.

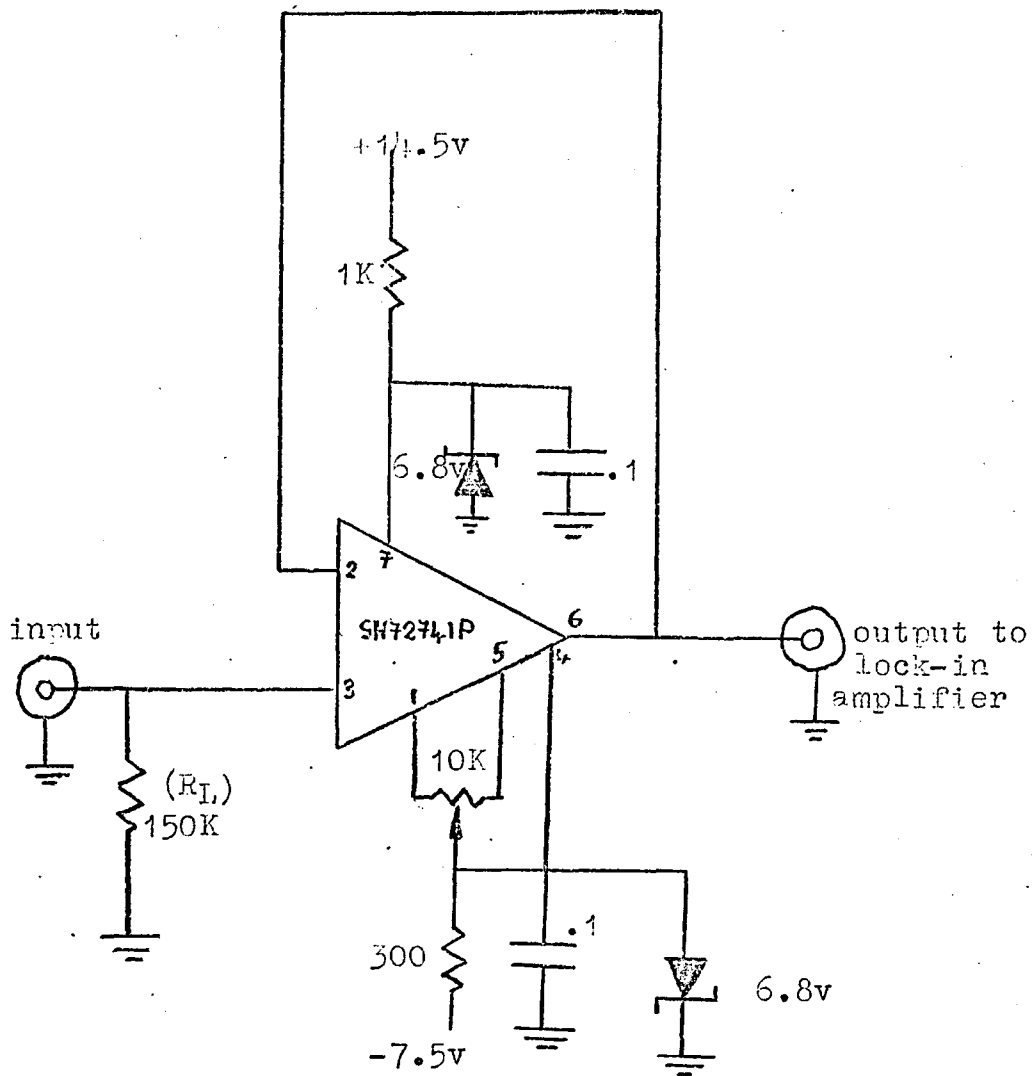


Fig. 2.9 Buffer amplifier. Resistance in ohms, capacitance in microfarads. (2)-inverting input; (3)-non-inverting input. For device data see appendix 3.

associated with it because the output is fed directly back to the input, i.e. maximum amount of negative feedback. The high input impedance of the SN72741 at 0 dB gain (see above Table) isolates the high impedance of the photomultiplier while the output voltage duplicates or follows the input voltage, hence the name voltage follower. When a signal from the P.M. was fed through the buffer amplifier into the lock-in amplifier the output signals were larger than when feeding the P.M. signal directly into the input amplifier of the lock-in amplifier. However no further improvement in signal could be obtained by increasing  $R_L$  (Fig. 2.9) above 150 K $\Omega$ . This was because attenuation was occurring in the lead between the P.M. and the buffer amplifier.

In view of the initial success of the buffer amplifier it was considered that a similar amplifier but with some gain could be useful. This alternative preamplifier is shown in Fig. 2.10a. Again the non-inverting input of the SN72741 was used to take advantage of the high-input impedance of this configuration. Referring to Fig. 2.8b and comparing with Fig. 2.10a,  $R_2 = 9.1K\Omega$  and  $R_1$  is the combination of the 1K $\Omega$  preset potentiometer A and the 1K $\Omega$  resistor in parallel with it. From equation 26 it can be seen that when the 1K $\Omega$  preset potentiometer (A) is varied, the closed loop gain varies between some high value and a value around 20. However, this is accompanied by a variation in input impedance, which falls from just less than 400 M $\Omega$  at gain 20 to lower values as the gain is increased, and by a decrease in bandwidth. If it is assumed that initially the input impedance of the amplifier is high enough, at 400 M $\Omega$ , to prevent signal loss, any increase in gain would give an increased signal at the pre-amplifier output only as long as the input impedance remains high. As soon as the

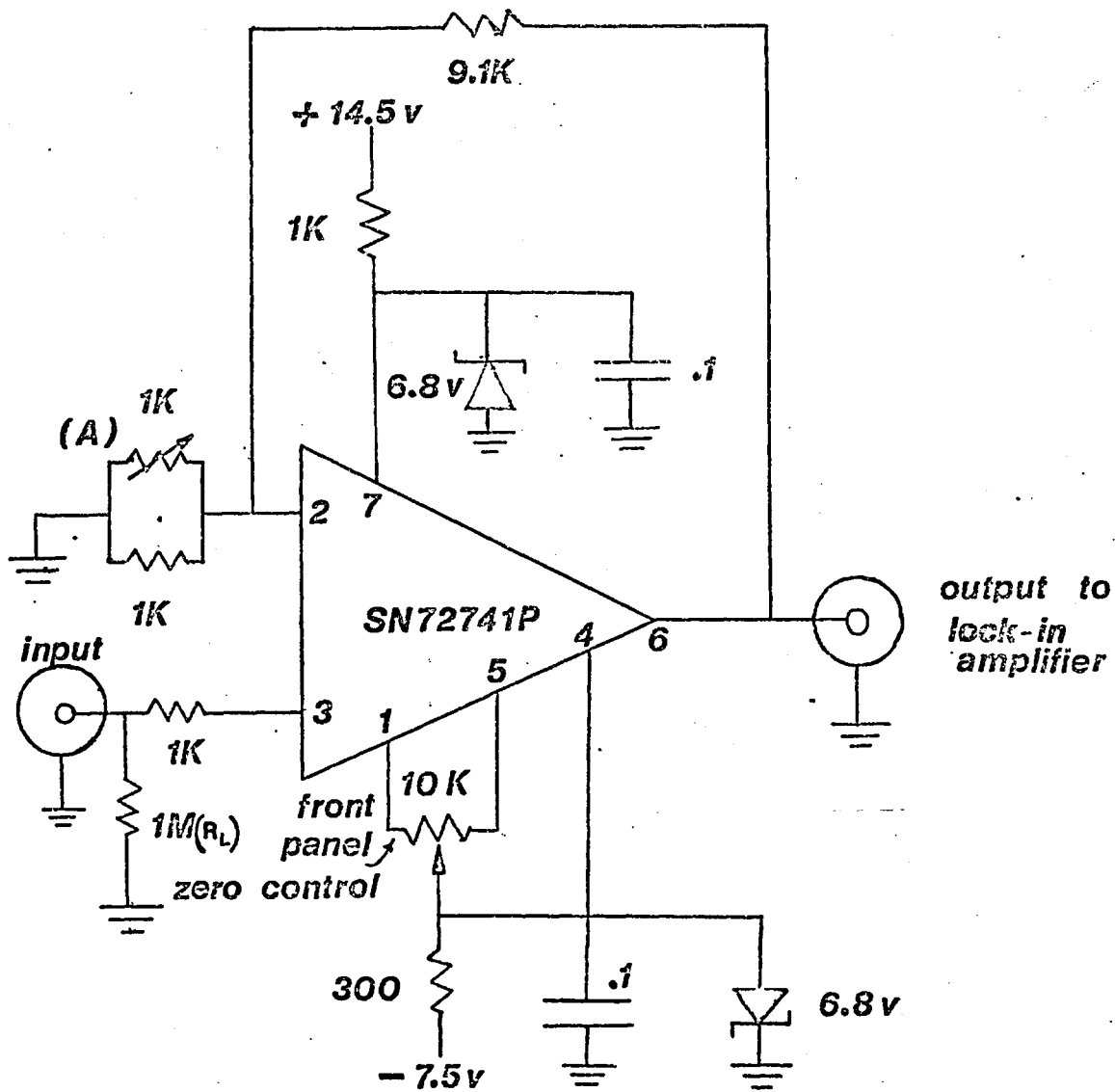


Fig. 2.10a The pre-amplifier. Resistance in ohms, capacitance in microfarads. Input via 100 mm,  $50\ \Omega$  coaxial cable from photomultiplier tube. Load resistor ( $R_L$ ) variable, as shown in Fig. 2.10b. (2) inverting input; (3) non-inverting input. For device data see appendix 3.

impedance drops sufficiently to attenuate the signal, further increase in gain will result in overall signal decrease. Thus the pre-amplifier can be connected to the photomultiplier and the gain optimized by varying the preset potentiometer (A) until a maximum in the output signal has been obtained.

Unfortunately there still remains the inherent capacitance (between the inner and outer conductors) of the 1-m long 50 coaxial cable between the P.M. and the preamplifier. This capacitance in conjunction with the resistance of the cable, can attenuate high-frequency signals. As the relatively high frequency of 10 KHz was being used (see section 2.3.2) attenuation was suspected, and therefore the cable was cut in half to reduce its resistance and capacitance. This resulted in an increase in output of 40%. The length of the lead was finally reduced to 100 mm to minimise the signal loss. The P.M. load resistor was then set at a maximum of  $1\text{ M}\Omega$  and the preset pot. (A) varied for maximum output signal. (Values of  $R_L$  above about  $2.2\text{ M}\Omega$  did not appreciably alter the output signals obtainable.)

Although the preamplifier in Fig. 2.10a was very sensitive the situation often arises that if the signals from the flame are too large the amplifier is saturated, i.e. the swing of the signal voltage about the earth point becomes greater than that allowed by the value of the power supply voltage (for the pre-amplifier  $\pm 6.8\text{ Vdc}$ ). The signals can become too large if at the wavelength of interest there is a large amount of noise. This only occurred once in this study. The noise at 396.2 nm, the wavelength used for measuring aluminium fluorescence, was far greater than the noise at 189.0 nm (arsenic) and 303.4 nm (tin). In order to reduce the sensitivity of the preamplifier in these noise limited situations a variety of values of  $R_L$  were provided at the preamplifier input. The switching arrangement for this

is shown in Fig. 2.10b. Thus, at high light levels, one can use lower values of  $R_L$  to prevent saturation, and at low light levels (particularly at low wavelengths, e.g. 189.0 nm) increase  $R_L$  to increase the measured signal level. This effectively increases the dynamic range over which the signals can be measured.

From a practical point of view it was possible to tell whether or not saturation of the preamplifier was occurring by observing the signal at a point in the lock-in amplifier circuit (Test point 1, see Fig. 2.12) using an oscilloscope. The symmetrical power supply for the preamplifier was derived from the supply built for the lock-in amplifier. The pre-amplifier circuit board was built into a diecast metal box to provide electrical shielding and to allow placing of the lock-in amplifier remote from the photomultiplier.

#### The input amplifier

Similar impedance matching problems occurred between the output of the pre-amplifier and the input amplifier as were encountered in the P.M. - preamplifier situation. The SN72702 integrated circuit used in the input amplifier behaves in a similar way to the SN72741 amplifier insofar as the consequences of changing the feedback configuration are concerned. However using the non-inverting input does not give the same high input impedance as would be obtained with an SN72741 amplifier (see data for SN72702 amplifier in appendix 3). The impedance matching of preamplifier to input amplifier was not as serious as the P.M. to preamplifier situation because the output impedance of the preamplifier was low (an inherent advantage of the output of most integrated circuit amplifiers is a low output impedance). The non-inverting input of the SN72702 input amplifier was therefore used rather than the lower impedance inverting input

Input from anode  
of photomultiplier

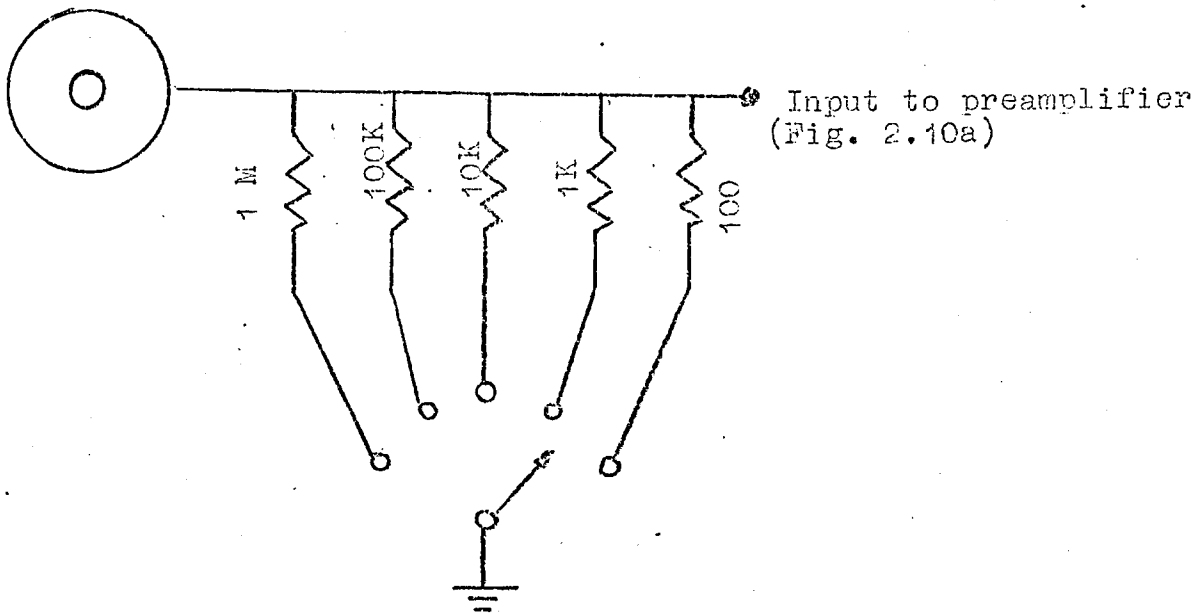


Fig. 2.10b. Switching arrangement for alternative values of load resistor, ( $R_L$ ).

Resistance in ohms.

L

which is used in the original design. The resulting circuit is shown in Fig. 2.11. A switch was used to change the gain of the input amplifier from 20 to 40 dB rather than the two separate BNC connectors used by Caplan and Stern.

Use of the non-inverting input of the input amplifier decreased the stability of the SN72702 sufficiently to cause it to go into self-oscillation. In order to prevent these high-frequency oscillations the response of the amplifier at high frequencies was reduced by altering the frequency compensation components<sup>\*</sup> R and C, Fig. 2.11. However reducing the amplifier's response in this way effectively reduces the bandwidth of the input amplifier. The bandwidth of the lock-in amplifier as designed by Caplan and Stern was from d.c. to 5 MHz. The resulting bandwidth of the preamplifier and lock-in amplifier combination in this work was found, experimentally, to be wide enough to accept signals at frequencies between 10 and 20 KHz without significant attenuation (the attenuation was -3dB at 17 KHz). This bandwidth was satisfactory for measuring the 10-20 KHz signals routinely obtained during the atomic fluorescence measurement.

<sup>\*</sup>The high frequency oscillation problem is caused by the inter-relationship of the phase shift of the amplifier with the amount of feedback applied and with the input impedance. This problem is dealt with in most basic electronics textbooks, for example Brophy<sup>154</sup> and in the particular case of the SN72702 amplifier the subject is discussed extremely clearly in a booklet produced by one of the manufacturers of integrated circuits<sup>153</sup>. The phase-shift and bandwidth of the SN72702 amplifier can be tailored to remove high frequency instabilities in the amplifier by altering the values of the frequency compensation components.

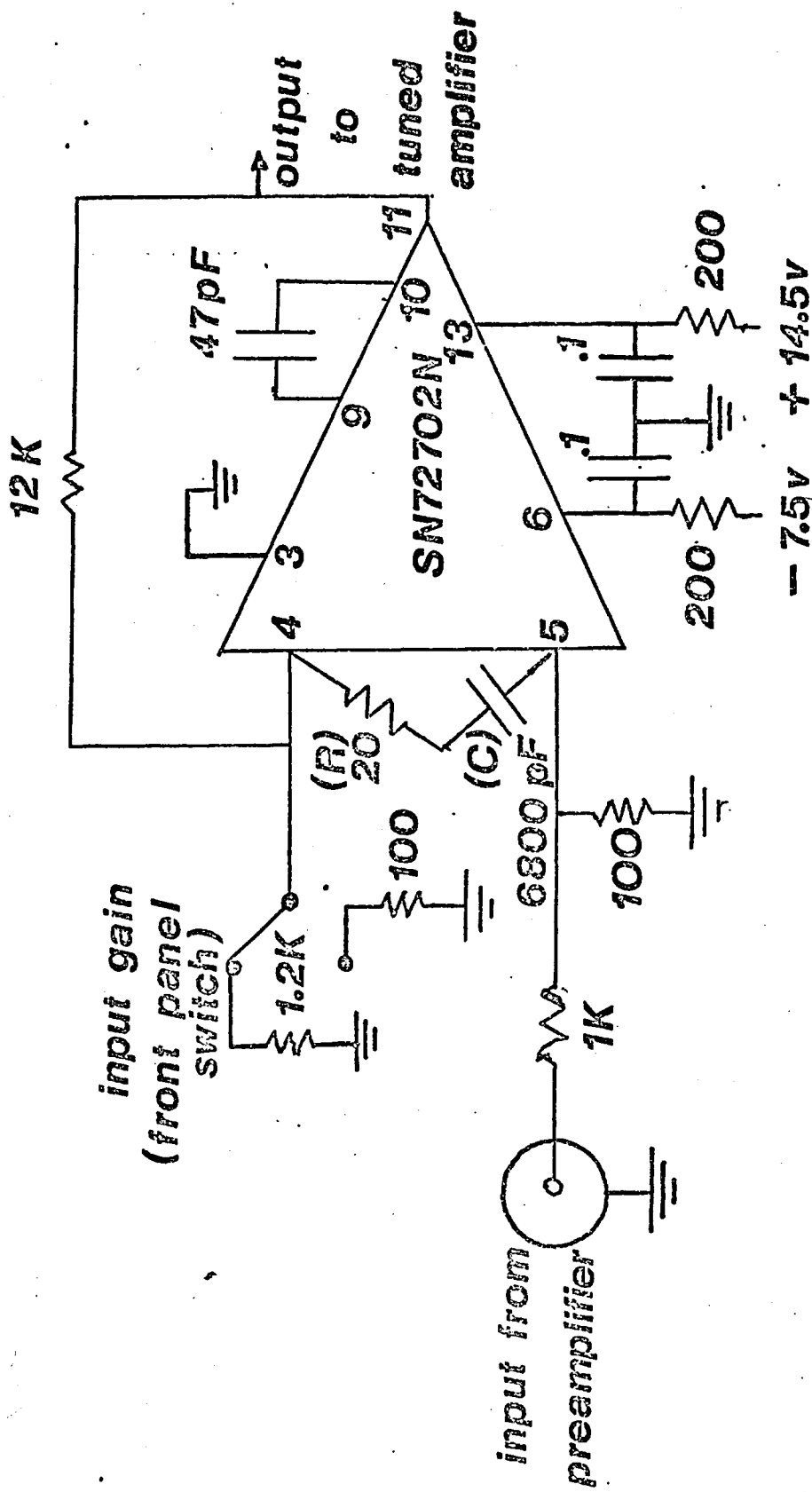


Fig. 2.11 Modified input amplifier. The SN72702N device is equivalent to the  $\mu A702$  used by Caplan and Stern. (4) -inverting input; (5) -non-inverting input. For device data see appendix 3.

Low pass filter, high pass filter and filter output amplifier

The complete circuit for these sections of the lock-in amplifier is shown in Fig. 2.12. This figure also includes the input amplifier to facilitate direct comparison with the same circuit diagram in the published circuit by Caplan and Stern<sup>142</sup>.

The main points about the complete circuit in Fig. 2.12 are as follows<sup>142</sup>. The filtering is performed by the SN72702 operational amplifiers as described in section 2.3.1c. The cut-off frequencies of the low and high pass filters can be moved independently by two 12-position switches on the front panel. In this way the operator can select the centre frequency and bandwidth while maintaining relatively constant gain. Table 2.1 lists the component values of C2 and C5 being switched in the low pass filter and the respective cut off frequencies. Table 2.2 lists the component values of C1 and C3 being switched in the high pass filter and the associated cut off frequencies. Some of these capacitor values are slightly different from the ones used by Caplan and Stern due to the non-availability of specific values.

The filter amplifier again uses the SN72702 operational amplifier. The gain of this stage may be switched by a front panel control between 0dB (unity) and 20dB. Additionally a front panel control potentiometer is available for manual balance of the output from this stage allowing the signal channel to provide a signal to the mixer with zero bias. It was found by Caplan and Stern that the presence of a direct voltage could cause errors when measuring low level signals.

The whole of the circuitry of Fig. 2.12 is identical to the circuitry as designed by Caplan and Stern with the exception of the input amplifier and the frequency compensation components.

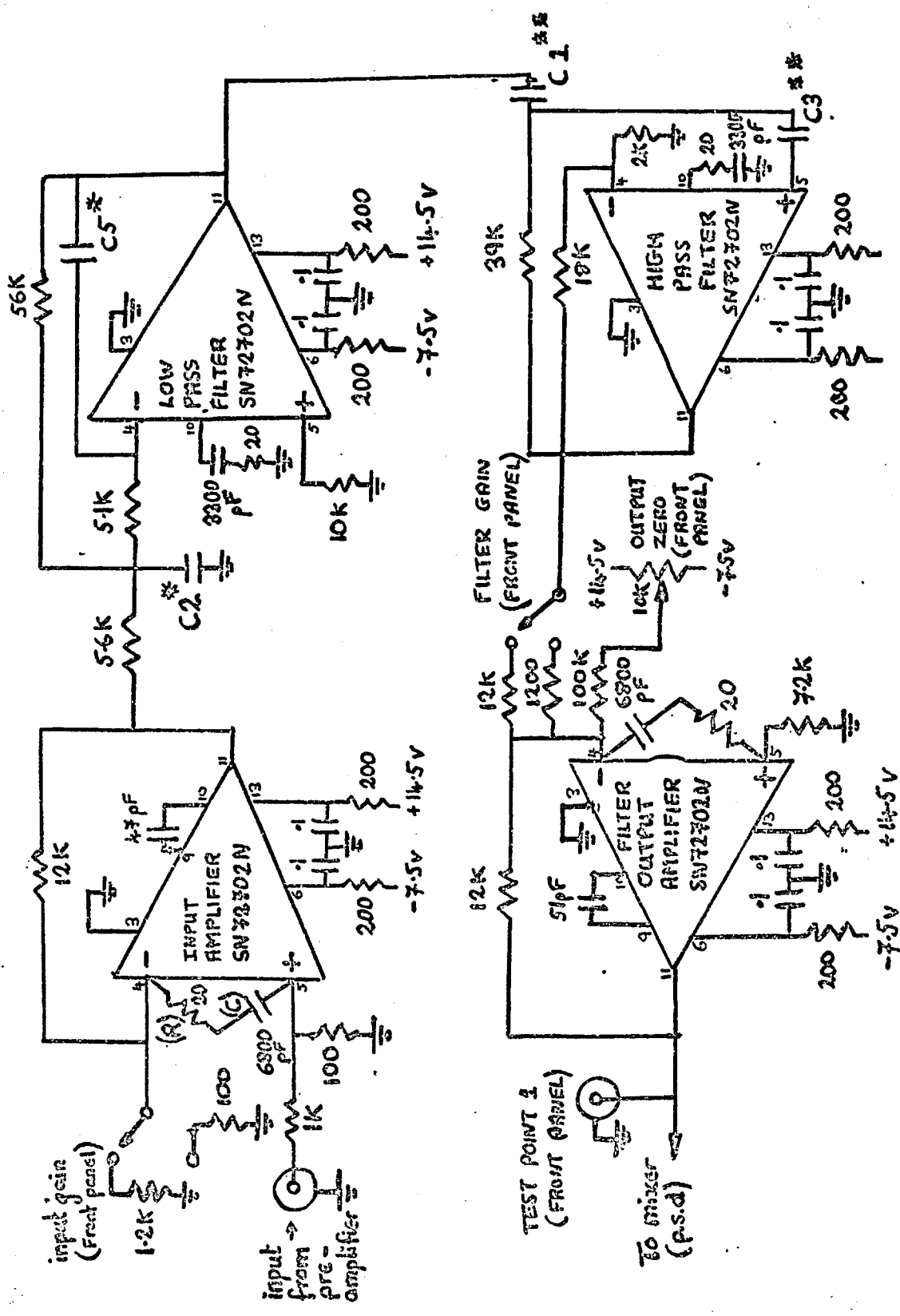


FIG. 2.12 Input amplifier, low pass filter, high pass filter and filter output amplifier. The complete circuit is effectively a tuned amplifier. Unless otherwise specified, resistance in ohms, capacitance in microfarads. (x) see Table 2.1 (x x) see Table 2.2 Input amplifier is identical to Fig. 2.11. (4)-(4)-inverting inputs; (5)-non-inverting inputs. The SN72702N device is equivalent to the  $\mu$ A702 used by Caplan and Stern. For device data see appendix 3.

TABLE 2.1.

## LOW PASS FILTER SWITCHING VALUES

Switch position	Cut off frequency	C2	C5
1	37.5 Hz	1 $\mu$ F	0.047 $\mu$ F
2	100 Hz	0.047 $\mu$ F	0.022 $\mu$ F
3	250 Hz	0.22 $\mu$ F	6800 pF
4	625 Hz	0.068 $\mu$ F	3.3 nF
5	1500 Hz	0.033 $\mu$ F	1400 pF
6	3750 Hz	0.015 $\mu$ F	560 pF
7	10 KHz	4700 pF	200 pF
8	25 KHz	1500 pF	68 pF
9	62.5KHz	680 pF	47 pF
10	10 KHz	3000 pF	200 pF
11a	150 KHz	250 pF	10 pF
12a	375 KHz	100 pF	5 pF

a - Capacitor values added for experimental purposes. The capacitance of C2 and C5 can be varied using front panel controls. In this way bandwidth can be varied. These were found to be of little use.

TABLE 2.2

## HIGH PASS FILTER SWITCHING VALUES

Switch position	Cut off frequency	C1 = C3
1	37.5 Hz	0.33 $\mu$ F
2	100 Hz	0.10 $\mu$ F
3	250 Hz	0.033 $\mu$ F
4	625 Hz	0.015 $\mu$ F
5	1500 Hz	6800 pF
6	3750 Hz	4700 pF
7	10 KHz	1000 pF
8	25 KHz	470 pF
9 <sup>a</sup>	ca. 8 KHz	1500 pF
10 <sup>a</sup>	62 KHz	200 pF
11 <sup>a</sup>	150 KHz	50 pF
12 <sup>b</sup>	0	32 F

a - Capacitor values added for experimental purposes (see footnote Table 2.1)

b - C1 and C3 were short circuit in the design of Caplan and Stern but in our amplifier this lead to instability.

C1=C3=32  $\mu$ F enabled low frequency signals to be measured but not as low as 1 Hz.

Oscillation of all the SN72702 operational amplifiers was encountered at some stage in the building of the lock-in amplifier. The phenomenon was cured each time by altering the frequency compensation components at pins 4 and 5 or pin 10 on each amplifier. (see footnote page 42). The output from the filter section can be monitored using an oscilloscope at testpoint 1, Fig. 2.12.

#### Reference Input Amplifier

The whole of the circuitry in Fig. 2.13 is identical to the circuitry as designed by Caplan and Stern. The reference input amplifier stage (Fig. 2.13) again uses the SN72702 operational amplifier. The input resistance of this amplifier can be varied by a front panel 10 K $\Omega$  potentiometer which allows for a continuous gain variation from unity to fifty. Because the output of this amplifier is passed through the phase shift stages (Fig. 2.13) each of which have a gain less than unity, the reference amplifier output is monitored (Test point 2) and the gain adjusted until maximum undistorted output is achieved. In this way the maximum signal amplitude reaches the comparator resulting in the most accurate square wave output (Test point 3).

#### Phase shifting and squaring stages

The capacitors  $C'$  are changed in the phase shift stages by a single front panel six position switch. This is necessary so that the stage can cope with any frequency that is being detected. The values of  $C'$  and the frequencies of operation are given in Table 2.3. Two phase shift stages are connected together by the front panel phase shift control to give a maximum phase control of  $340^\circ$ . To give an additional  $180^\circ$  of phase variation a front panel controlled inversion switch is provided which switches the necessary complementary outputs

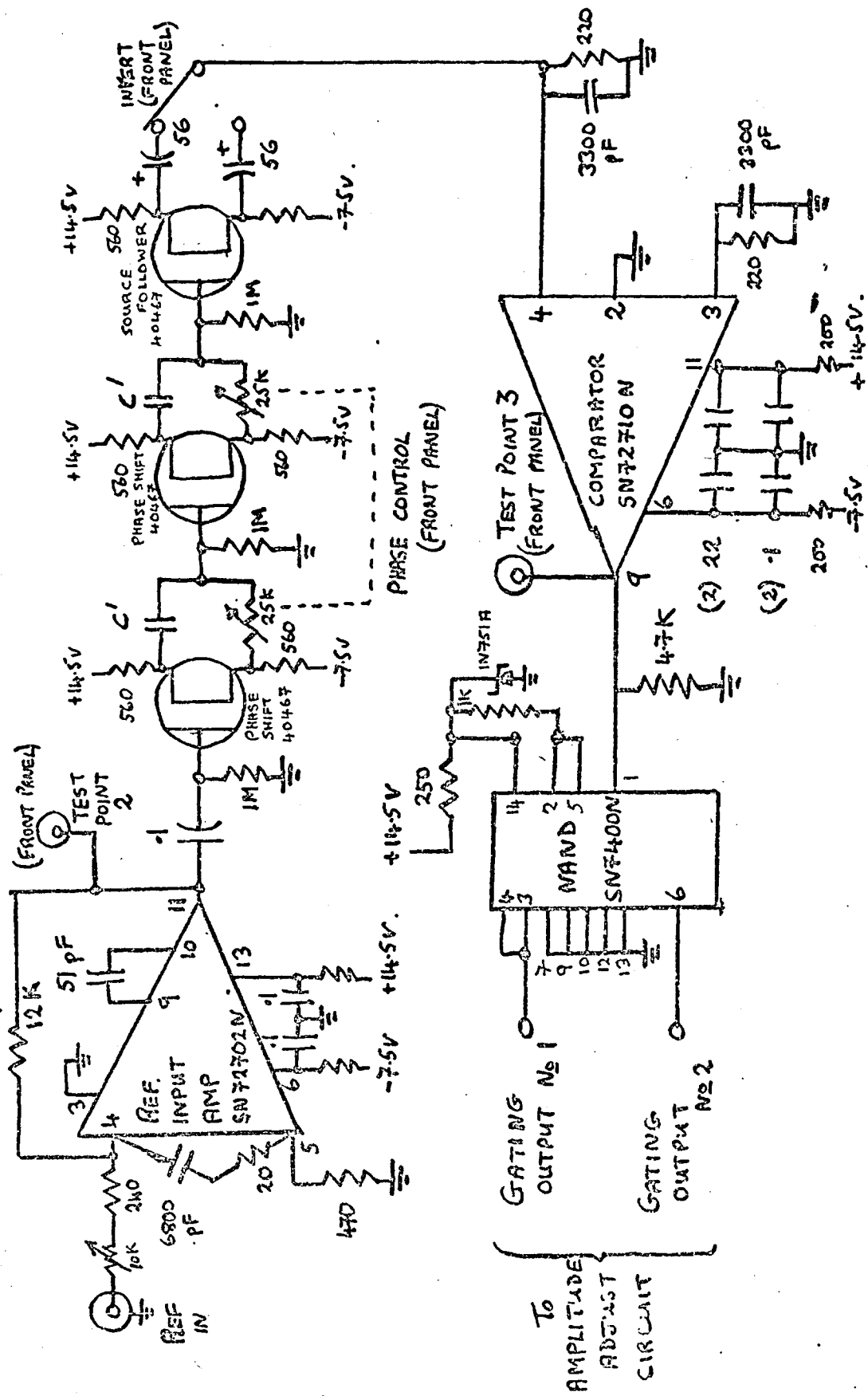


Fig. 2.13 Reference input amplifier, phase shift and squaring. Unless otherwise specified resistance in ohms, capacitance in microfarads; (C') see Table 2.3. For device data, SN72702N and SN72710N, see appendix 5.

TABLE 2.3

## PHASE SHIFT SWITCHING

Switch position	Lowest operating frequency	Highest operating frequency	Capacitor value (C')
1	32 Hz	100 Hz	0.47 $\mu$ F
2	100 Hz	250 Hz	0.22 $\mu$ F
3	250 Hz	800 Hz	0.08 $\mu$ F
4	800 Hz	5 KHz	0.022 $\mu$ F
5	5 KHz	50 KHz	2200 pF
6	50 KHz	500 KHz	200 pF

from the source follower stage.

The comparator is used here as a zero crossing detector. As long as the sinusoidal input from the source follower stage is larger than 10-20 mV peak-to-peak the output waveform at Test point 3 is square with rise and fall times of less than 20 nsec. (Data for the comparator  $\mu$ A 710 is given in Appendix 3).

The square wave output from the comparator is fed into the NAND gate which, in the circuit configuration used, gives at the output the two complementary square waves discussed in section 2.3.1.C. The rise and fall times of these two output square waves from the NAND gate were the best obtainable at the time Caplan and Stern wrote their paper.

#### Phase Sensitive Detector p.s.d.

This circuit (Fig. 2.14) was again built exactly to the design by Caplan and Stern and no circuit changes were necessary.

Each amplitude adjust circuit is used to process the complementary outputs from the NAND gate section and consists of a 2N2369 switching transistor which is used to amplify the NAND gate output waveform.

The chopper switching discussed in section 2.3.1.C is realized by using two pairs of 3N138 MOSFET's, each pair switching one of the complementary half-wave portions of the detected signal. Some further discussion of the circuitry of the p.s.d. is given in the paper by Caplan and Stern<sup>142</sup> (Data for 3N138 given in appendix 3).

#### Output amplifier (Differential output low pass filter)

The rectifying action of the output amplifier was described in section 2.3.1.C.

The output amplifier also acts as a low pass filter.

SERIES SHUNT CHOPPERS

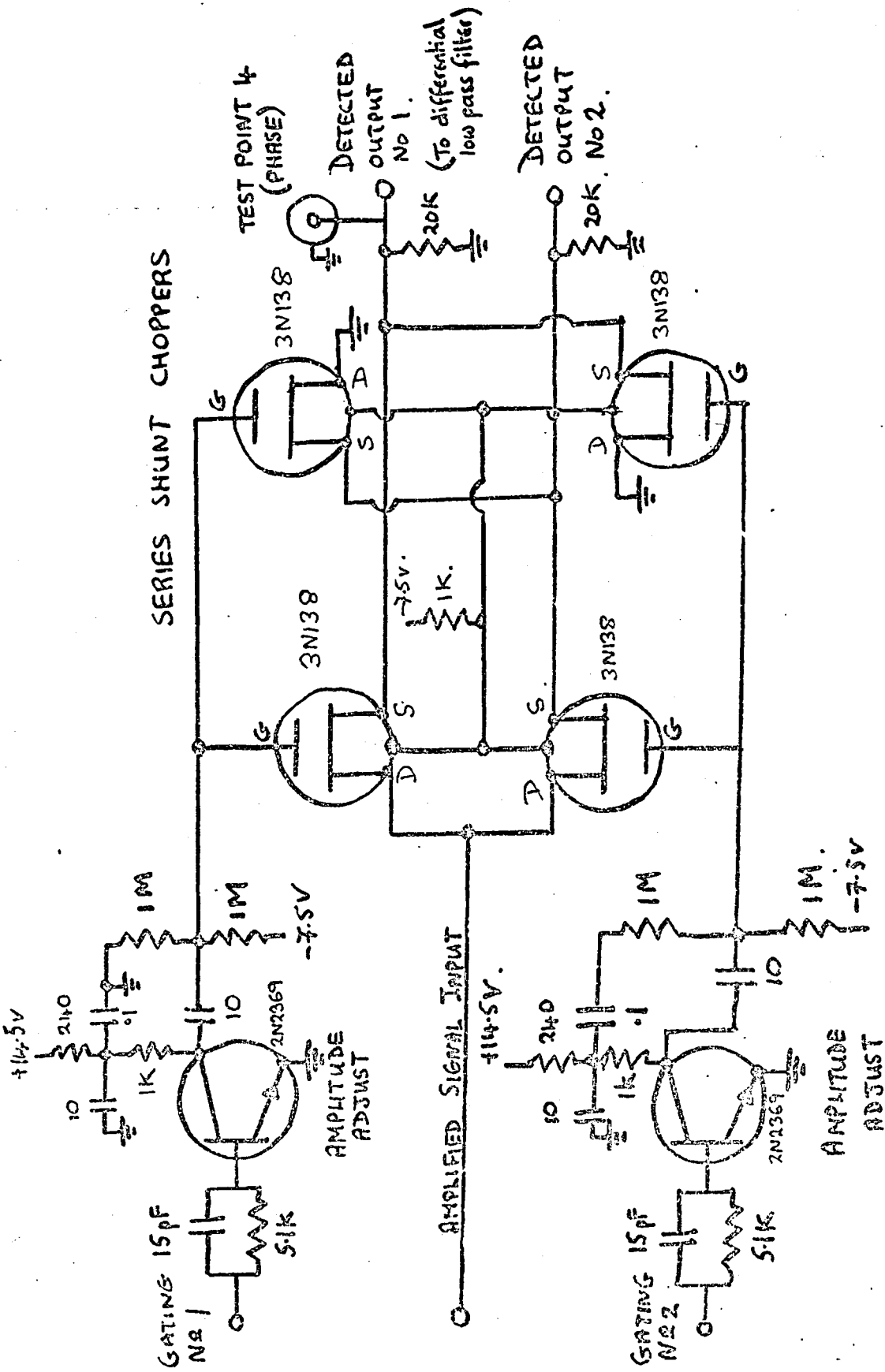


Fig. 2.14 Mixer (p.s.d) Unless otherwise specified, resistance in ohms, capacitance in microfarads. For device data, 3N138, see appendix 3.

This filter as designed by Caplan and Stern used the same SN72741 operational amplifier as used in the pre-amplifier described earlier. When this filter was built, the d.c. output stability of the lock-in amplifier with an output filter bandwidth of 0.034 Hz and a time constant of 4.7s was satisfactory at  $0.02\%V^{-1}$ . However, a change to a bandwidth of 0.0031Hz and a time constant of 51.7s resulted in a stability of only  $3\%V^{-1}$ . This was likely to degrade the detection limits for atomic fluorescence. To improve this situation, a second output filter was built (Fig. 2.15). This circuit uses a  $\mu$ A-727B, SGS-Fairchild amplifier which is kept at a constant temperature by active regulator circuitry incorporated into the same monolithic integrated circuit chip as the amplifier<sup>153</sup>. (Some data and information on this operational amplifier is given in appendix 3 ). Drift in d.c. amplifiers is caused predominantly by changes in ambient temperature, hence the advantages of an amplifier which is held at constant temperature. The  $\mu$ A-727B is a pre-amplifier designed to drive a standard linear integrated circuit amplifier, in this case an SN72741.

The output stability of the lock-in amplifier with the second filter (output 2) with a bandwidth of 0.0031 Hz and a time constant of 51.7s was  $0.02\%V^{-1}$ . This large improvement was sufficient to allow the use of an even longer time constant of 103.4s without further significant loss in stability of the electronics. The circuitry associated with the 51.7s time constant of the original filter was removed. The resulting circuit is shown in Fig. 2.16. The output (output 1) was provided with a separate BNC connector.

The time constant and bandwidth details of both filter circuits are given in Table 2.4 together with the relative

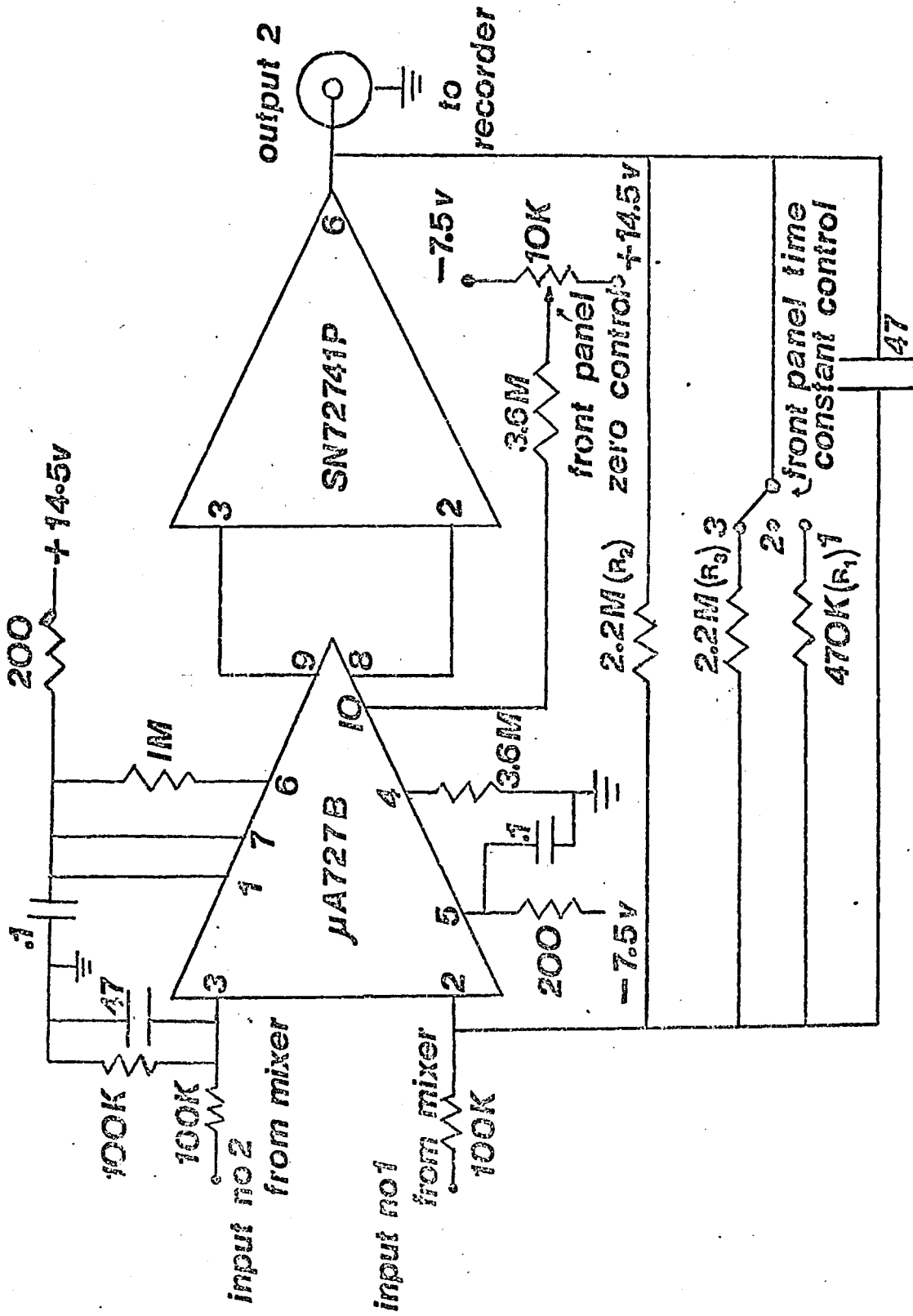


FIG. 2.15 Output filter 2. Switch positions give time constants of (1) 18.2s, (2) 103.4s, and (3) 51.7s. Connections to pins 1, 4, 5, and 7 of the SN7241P device are identical to those in Fig. 2.16.

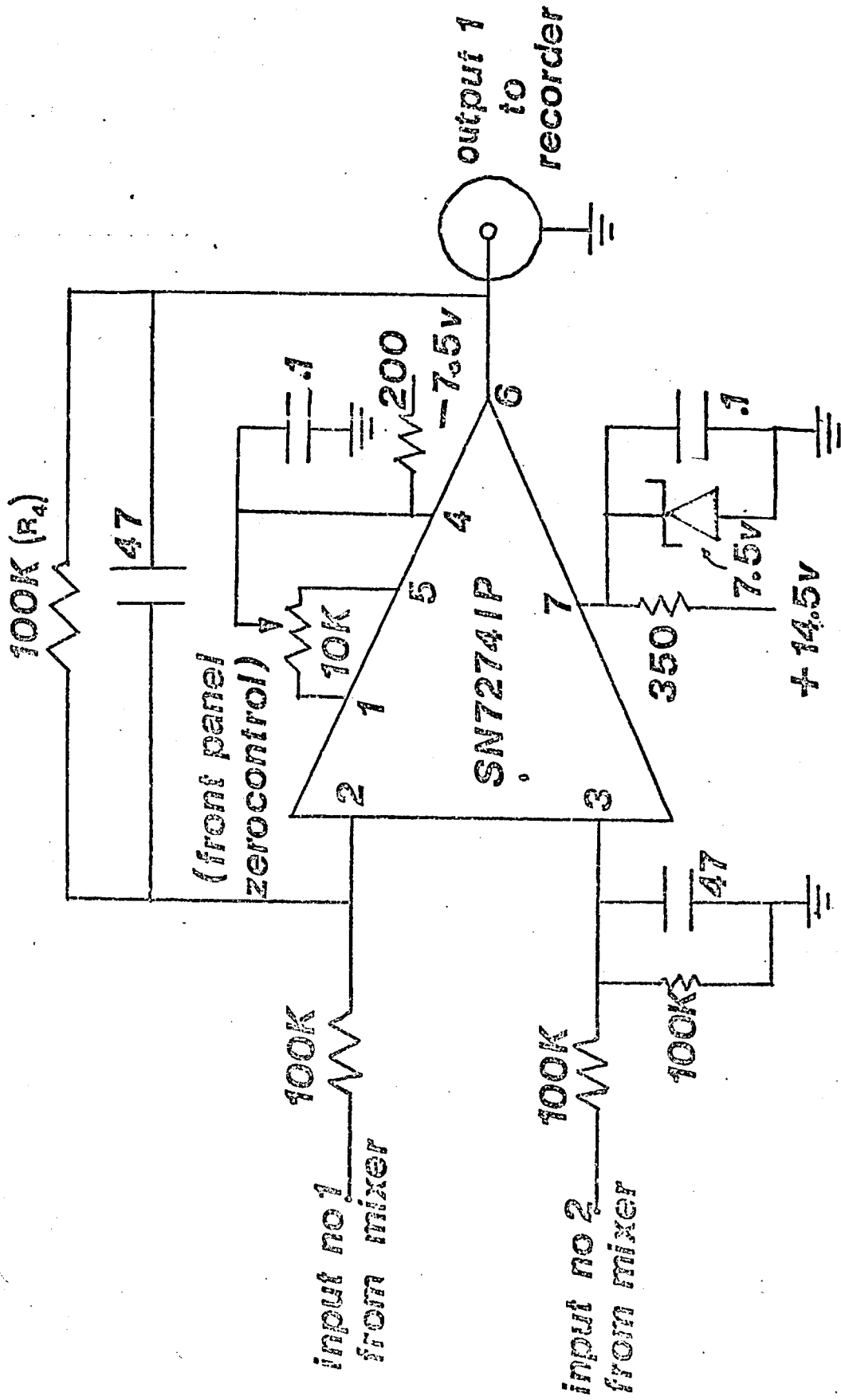


Fig. 2.16 Modified output filter 1. The SN72741P device is equivalent to the  $\mu A-741$  device used by Caplan and Stern. Time constant fixed at 4.7s.

TABLE 2.4

PERFORMANCE OF THE OUTPUT LOW PASS FILTERS AND  
ATOMIC FLUORESCENCE DETECTION LIMITS FOR TIN

A 1 ppm aqueous tin solution nebulized into an argon-separated air-acetylene flame and the fluorescence measured at 303.4 nm. Optical system A (Section 2.3.4.) 10 KHz modulation. EDL cooled in  $\frac{3}{4}$  cavity. Acetylene flow  $0.9 \text{ l min}^{-1}$ , air flow  $3.7 \text{ l min}^{-1}$ . Time constant 4.7s.

output filter	Time constant T (s)	Band- width f(Hz) <sup>a</sup>	Signal (arbitrary units)	Noise	Signal- to-noise ratio	Detection Limit (p.p.m.) <sup>b</sup>
1	4.7	0.034	8.0	1.5	5.3	0.38
2	18.2	0.0056	24.0	2.5	10.0	0.20
2	51.7	0.0031	61.5	4.5	13.6	0.15
2	103.4	0.0015	92.0	3.0	30.6	0.065

a  $f = 1/2\pi T$  (signal bandwidth)

b Signal-to-noise ratio of 2.

improvements in signal-to-noise ratio which are obtained with increasingly long time constants. The time constant is easily calculated by  $R \times C$  where  $R = R_1, R_2, R_3$  or  $R_4$  in Figs. 2.15 or 2.16 respectively and  $C$  is  $47 \mu F$  in both figures. The  $R$ 's and  $C$ 's are both in the feedback loops of the operational amplifiers concerned and are acting as low pass filters as described in sections 2.3.1.B and 2.3.1.C.

Referring to Table 2.4 it can be seen that the improvement in the detection limit for tin fluorescence in the argon-separated air-acetylene flame in going from a 4.7s time constant to a 103.4s time constant is nearly an order of ten. However the 51.7s and 103.4s time constants are impractical (see section 2.3.1.C) because the signal takes far too long to appear at the readout. Consequently in all the fluorescence work reported here a 4.7s time constant was used routinely and the 18.2s time constant was used for measuring detection limits. It was a perfectly practical proposition to carry out analyses using the 18.2s time constant, although it is clear that this is only necessary if one is measuring solution concentrations fairly near the detection limit.

#### The performance of the lock-in amplifier

The detection limits reported in chapters three to five for arsenic, tin and aluminium are eminently satisfactory. However the lock-in amplifier was only one of the contributing factors which led to the performance of the atomic fluorescence instrument as a whole. The discussion in the following sections of this chapter indicates that the improvement in SNR due to high frequency modulation of electrodeless discharge lamps and the optical arrangement could not have been made but for the extra versatility of the lock-in amplifier relative to the Jarrell-Ash a.c. tuned amplifier. Moreover the large number of

variables involved make the improvement due to the lock-in amplifier itself difficult to evaluate except in terms of the performance of the complete instrument.

Some practical comments on the use of the lock-in amplifier and some other incidental information is given in appendix 2.

### 2.3.2. The Source (Electrodeless discharge lamps)

In order to obtain optimal signal-to-noise ratios in atomic fluorescence the source needs to have a high radiant output over the absorption line and exhibit minimal short term noise and long term instability or drift. The high radiant output is necessary because this leads to high fluorescence radiant output. A direct result of the proportional relationship between source radiance and fluorescence radiance (appendix I). Microwave excited electrodeless discharge lamps (EDL'S) have been the most successful type of high intensity line source for atomic fluorescence as demonstrated by the low detection limits that have been reported<sup>5,6,158-162</sup>. EDL's have been shown to give radiant outputs 10-100 times greater than hollow cathode lamps<sup>163</sup> (HC DL's) and to have narrow line emission profiles<sup>97,164</sup>. The application of these lamps to atomic absorption<sup>163</sup> has also been successful, for example for the determination of a number of the more volatile elements (e.g. As<sup>165</sup>). These elements have their main resonance lines in the ultraviolet and generally provide short-lived or less satisfactory hollow-cathode lamps.

EDL's can be made for a large number of elements although the range of elements covered by HC DL's is a little wider. However, although a large percentage of the literature on EDL's is devoted to describing basic detailed preparation

of EDL's is devoted to describing their detailed preparation\* a number of workers<sup>166</sup> have found that it is difficult to reproduce preparative procedures sufficiently well to obtain lamps with all the desirable properties of high stability, intensity and long life.

EDL's consist of a sealed, quartz tube about 3 cm in length and a little less than 1 cm in diameter and containing a few mg or  $\mu$ g of a metal or volatile metal salt. The tube is filled with an inert gas at a few torr pressure. The lamp is placed in a microwave field by means of a resonant cavity ( $\frac{3}{4}$  wave Broda cavity<sup>167-169</sup> or  $\frac{1}{4}$  wave Evenson cavity<sup>167,170</sup>) or an 'A' type antenna<sup>120</sup>. A tesla coil is used to initiate the discharge by ionizing some of the inert gas atoms. The resulting electrons are accelerated by the microwave field and their energy is then sufficient to cause further ionization. Metal vapour is then excited to give the required line spectrum. The metal vapour itself is obtained by a combination of the heating effect of both the accelerated electrons and the microwave field.

Comparatively recently Winefordner and his co-workers<sup>171</sup> have indicated that the most likely cause of the difficulties encountered in the past with these lamps was that work on the optimisation of preparative and operational conditions relied upon the microwave field to achieve both lamp heating and

\* An excellent recent review<sup>166</sup> by Haarsma, De Jong and Agterdenbos can act as a convenient source for the literature concerning the whole field of EDL's particularly the preparative aspects.

excitation. These workers therefore provided for a heated air-stream to pass around the EDL operated in either a  $\frac{3}{4}$  wave cavity or an 'A' antenna <sup>171 -174</sup> thus giving controlled supplementary heating. The results of detailed studies <sup>171</sup> using this temperature control indicated that lamp temperature is the most important variable in controlling the radiant output of an EDL.

West and his co-workers <sup>163, 168, 169, 175-178</sup> and other workers <sup>179-183</sup> have looked at the use of electronic modulation of the light output from these lamps. Previously a mechanical chopper was placed between the source and flame or flame and monochromator entrance slit to give the required modulation for detection by a.c. amplifiers. The modulation frequencies used for both mechanical and electrical modulation were in the range 50-400 Hz depending upon the particular instrumentation used. The higher frequencies near 400 Hz were usually used in conjunction with a lock-in amplifier and were chosen to avoid  $1/f$  and mains bourn noise.

West and co-workers developed a qualitative view of electronic modulation <sup>175, 177, 184</sup> and were able to electronically modulate their lamps at frequencies up to 20 KHz. The lamps used were mainly those containing the more volatile elements, i.e. Cd, Hg, Zn, Sb, Se, As and Pb. The modulation frequency that gave the optimal fluorescence signal-to-noise ratio was found to be 10 KHz <sup>175</sup> for all these lamps. Winefordner and his co-workers used mechanical modulation with their temperature controlled EDL's probably in order to be able to isolate more easily some of the variables which affect lamp radiance and stability.

## A Electronic modulation of electrodeless discharge lamps

Modulation is necessary in all the flame techniques because the predominance of noise at the low frequency end of the noise spectrum makes d.c. measurements undesirable. Using modulation the signal channel can be shifted to another portion of the spectrum where noise levels are smaller. Background noise levels in a shielded nitrogen-oxygen-hydrogen flame have been determined by Alkamade et al.<sup>185</sup> over a wide frequency range ( $10-10^5$  Hz). The typical  $1/f$  pattern Fig. 2.2 was observed. Other workers<sup>186</sup> have obtained similar results using a premixed acetylene-nitrous oxide total consumption flame (PANT). Alkamade et al. concluded that in their case the optimal modulation frequency for fluorescence measurements was in the region 2 to 5 KHz where the noise spectrum attains a minimum.

In atomic fluorescence modulation of the source output before the flame prevents the d.c. output due to the flame background level from appearing at the readout. No backing off is then necessary and drifts due to changes in the background level are not observed. Hence precision and detection limits are improved. Most work has been carried out using modulation frequencies below 600 Hz i.e. just sufficient to avoid serious  $1/f$  noise.

Mechanical choppers have disadvantages. Firstly, it is difficult to design a chopper to operate at high frequencies above 1 to 2 KHz although some manufacturers do now make such units. Secondly, it is necessary to move the source away from the flame so as to be able to fit the chopper between the two which reduces the light intensity reaching the flame according to the inverse square law. Thirdly, operation of the chopper

close to the flame can lead to atmospheric turbulence and flame instability.

Various methods of electronically modulating EDL's have been described. Thompson and Wildy<sup>179,180</sup> transformer-coupled a small a.c. voltage into the anode circuit of the magnetron which is the source of the microwave power in the microwave generator (Electro-Medical Supplies Ltd., EMS Ltd., Microtron 200 instrument).

Fig. 2.17 is the circuit diagram for the modulator unit which EMS Ltd. supply to modulate the microwave output from their generator. The circuit designed by Thompson and Wildy<sup>180</sup> was essentially a simplified version of Fig. 2.17 and gave a range of modulation frequencies from 180 to 330 Hz. The latter authors in fact could not use the EMS modulator because it was not compatible with their Southern Analytical A3000 atomic absorption instrument. Referring to Fig. 2.17, the circuitry within the dotted square is an oscillator which provides the small ( $\sim 3V$ ) a.c. signal. The rest of the circuit is a power amplifier which amplifies the oscillator signal to a high level. This amplified signal is placed across the transformer T which is coupled into the anode circuit of the magnetron. The amplified oscillator voltage swings the anode voltage to give the required modulation. The depth of modulation is controlled by the potentiometer, P, which acts as a voltage divide on the output of the transformer.

EMS Ltd. supply different versions of their modulator which only differ according to the components of the small signal oscillator. With one set of components the oscillator gives a spot output frequency of 400 Hz variable by  $\pm 10\%$  using VRI. This variation enables the modulation of the EDL's to be phase adjusted to any lock-in amplifier which may be part of the particular



instrument in use. The reference frequency for the lock-in amplifier can be taken from the sync. output point (Fig. 2.17). Different values of the oscillator components can be selected to give a variety of spot frequencies.

Thompson and Wildy came to the conclusion that it was possible to operate EDL's in the modulated mode in a similar manner to hollow cathode lamps but the conditions for successful results were much more stringent and close attention needed to be paid to operating conditions. They had problems with shifting of material within the lamp and sometimes found that volatile element tubes were much easier to initiate without modulation, the modulation being switched on when the tube had warmed up. This sort of behaviour was also typical of the work carried out on electronic modulation of EDL's, up to 1970, by West and his co-workers who also used modulation frequencies in the low hundred hertz region. The problems encountered were probably as much a result of the dependence on microwave heating to achieve satisfactory output radiance as it was on the effect of modulation or of preparative methods.

In 1970 West and co-workers<sup>175,177,184</sup> pointed out that transformer coupled modulation has certain disadvantages. Because the secondary of the transformer is in the anode circuit, the high d.c. current may cause saturation of the core material and the modulation waveform applied to the primary of the transformer via the amplified oscillator signal may not be faithfully reproduced at the microwave output. Also the frequency and waveform that can be used are limited by the use of a transformer which in general is most efficient at low frequency sinusoidal waveforms. West et al. point out that these difficulties can be overcome for particular cases by

careful design but for a flexible system which can be used over a range of frequencies and waveforms an alternative method of modulation is preferable.

West and his co-workers<sup>175,184</sup> used a microwave generator (Evans Electroselenium Ltd.) which was current stabilised\* and the modulation of the magnetron output was provided by injecting the modulation waveform at the error-sensing point of the stabilising circuitry of the magnetron power supply (current modulation). A range of modulation frequencies and waveforms were studied by West et al. in order to determine the effect on the output from EDL's and consequently the effect on atomic fluorescence signal to noise ratios.

The percentage modulation obtainable with current modulation is greater than that obtainable by transformer coupled modulation but West et al. found that this was of little advantage because the lamp became more noisy at the high modulation levels. The best signal-to-noise ratio was obtained at 63% modulation.

Of the different waveforms tried by West et al.<sup>175,184</sup> including pulses, the square wave with equal mark-to-space ratio always gave the most intense lamp output. The effect of the modulation frequency on the radiance of the resonance lines from Cd, Hg, Zn, Sb, Se, As and Pb EDL's was determined. All the sources gave a maximal modulated output at a frequency of ca. 20 KHz

187

\* There is a circuit published for the current stabilisation of a Raytheon PGM-10 generator. The circuit was not adequate to control the amount of power available from our EMS generator.

but a frequency of about 10 KHz gave the optimal signal-to-noise ratio for use in atomic fluorescence spectroscopy.<sup>175</sup>

Other researchers<sup>181, 182</sup> have developed means of high frequency modulation of EDL's but have not used these sources for atomic fluorescence. Their circuits employed valves to inject modulation directly into the anode circuit rather than through a transformer.

West and co-workers<sup>176</sup> have also developed switched resistor modulation which depends on the value of the magnetron anode load resistor being repetitively changed at the modulation frequency. The microwave generator modified by these workers, an Evans Electro Selenium Model 245, has its anode load resistor in the d.c. side of the power supply. It was therefore possible, by means of a power transistor which can withstand a large collector-to emitter voltage, to switch, at the modulation frequency, a second resistor in parallel with the anode load resistor. This resistor controls the power to the magnetron and hence the microwave power output. Changing the anode resistors value by switching another resistor in parallel to it therefore has the effect of modulating the microwave output.

The switched resistor method cannot be applied to the EMS Microtron 200 generator because it has its power control in the a.c. side of its power supply. A transistor, therefore, cannot be used to achieve switched resistor modulation, the alternative being the more complicated thyristor or triac control of the power. Current modulation is not easy to apply<sup>176</sup> because both a current stabilised microwave generator and a voltage amplifier to amplify the injected modulation waveform are necessary.

### The application of high frequency modulation

In view of the above difficulties in modifying the EMS generator it was decided to retain transformer-coupled modulation. An EMS 400-Hz modulator was available for use with the EMS generator. The internal oscillator circuit which provides the small a.c. voltage at 400 Hz was disconnected by breaking the circuit at points A and B (Fig. 2.17). An oscillator (Sine-square oscillator Type LFM2, Farnell Instruments Ltd.) variable in frequency between 1 Hz and 1 MHz, was placed across A and B. Point B is the earth and A takes the injected signal at about 3.25 volts. The square-wave output of the Farnell oscillator was used because West et al. demonstrated that this waveform gave optimal lamp radiant output. This was experimentally confirmed in the present work. The reference for the lock-in amplifier was taken from the synchronisation socket on the Farnell oscillator.

The above simple modification allowed the modulation frequency to be varied from 200 Hz to 40 KHz. Modulation at 50 Hz and 100 Hz was obtained using another EMS modulator. Incidentally, this 50/100 Hz modulator takes the modulation signal from the mains a.c. and does not therefore incorporate the boosting circuitry necessary for the 400 Hz modulator. Suitable modification for modulation over a large range of frequencies is therefore more difficult to apply.

A block diagram of the complete atomic fluorescence instrument is given at this point in the discussion (Fig. 2.18) in order that it can be seen clearly how the lock-in amplifier and modulation system are interconnected.

### Signal-to-noise ratios obtained with variation in modulation frequency

The atomic fluorescence of three elements was investigated in this work. viz. arsenic, tin and aluminium (chapters three to

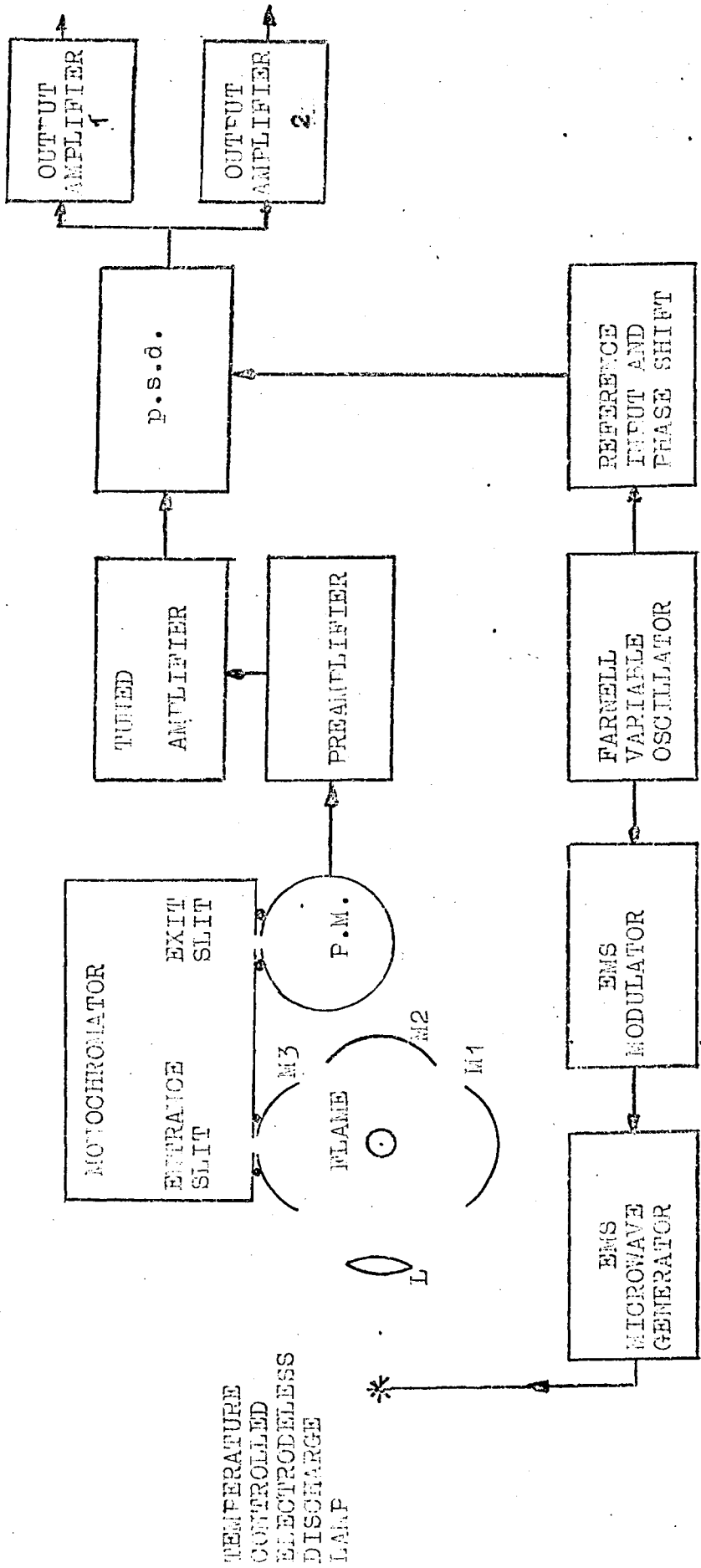


Fig. 2.18. Block Diagram of the atomic fluorescence system. M1, M2, M3 and L are the components of the optical system (Fig. 2.27) Either one or other of the outputs 1 and 2 taken to the chart recorder.

five). Observations concerning variation of modulation frequency were made for tin and aluminium lamps. For the arsenic lamp it was noted that West et al.<sup>175,184</sup> found that 10 KHz was the optimal modulation frequency and therefore 10 KHz was used in this study.

a) Tin<sup>\*1</sup>

The atomic fluorescence of tin in an air-acetylene flame was observed while varying the modulation frequency. The results, obtained with an aqueous 10 ppm tin solution and an output time constant of 4.7s are plotted in Fig. 2.19. The lamp was cooled with a flow of air from a compressor not temperature controlled. The  $\frac{3}{4}$  wave cavity and an incident microwave power of 40 watts were used (Reflected power 25 watts). It can be seen that the optimal modulation frequency is 10 KHz. This frequency gave the best signal-to-noise ratio. At higher frequencies, up to 20 KHz, the fluorescence radiance did increase further but short term noise increased and degraded the signal-to-noise ratio to below that at 10 KHz. (The same results tabulated in table 2.5 show this more clearly). The minimum at 3.5 KHz in the plot of Fig. 2.19 probably appears because the bandwidth of the tuned section of the lock-in amplifier was wide around this frequency compared to the bandwidths at all the other chosen frequencies. Consequently, noise was not being reduced as effectively and the signal-to-noise ratio was relatively poor.

b) Aluminium<sup>\*2</sup>

The atomic fluorescence of aluminium in the argon-separated nitrous oxide-acetylene flame was observed while varying

\*1 The tin and arsenic lamps were obtained from EDT supplies Ltd., London.

\*2 The aluminium lamp was obtained from EMI Ltd., Hayes, Middlesex.

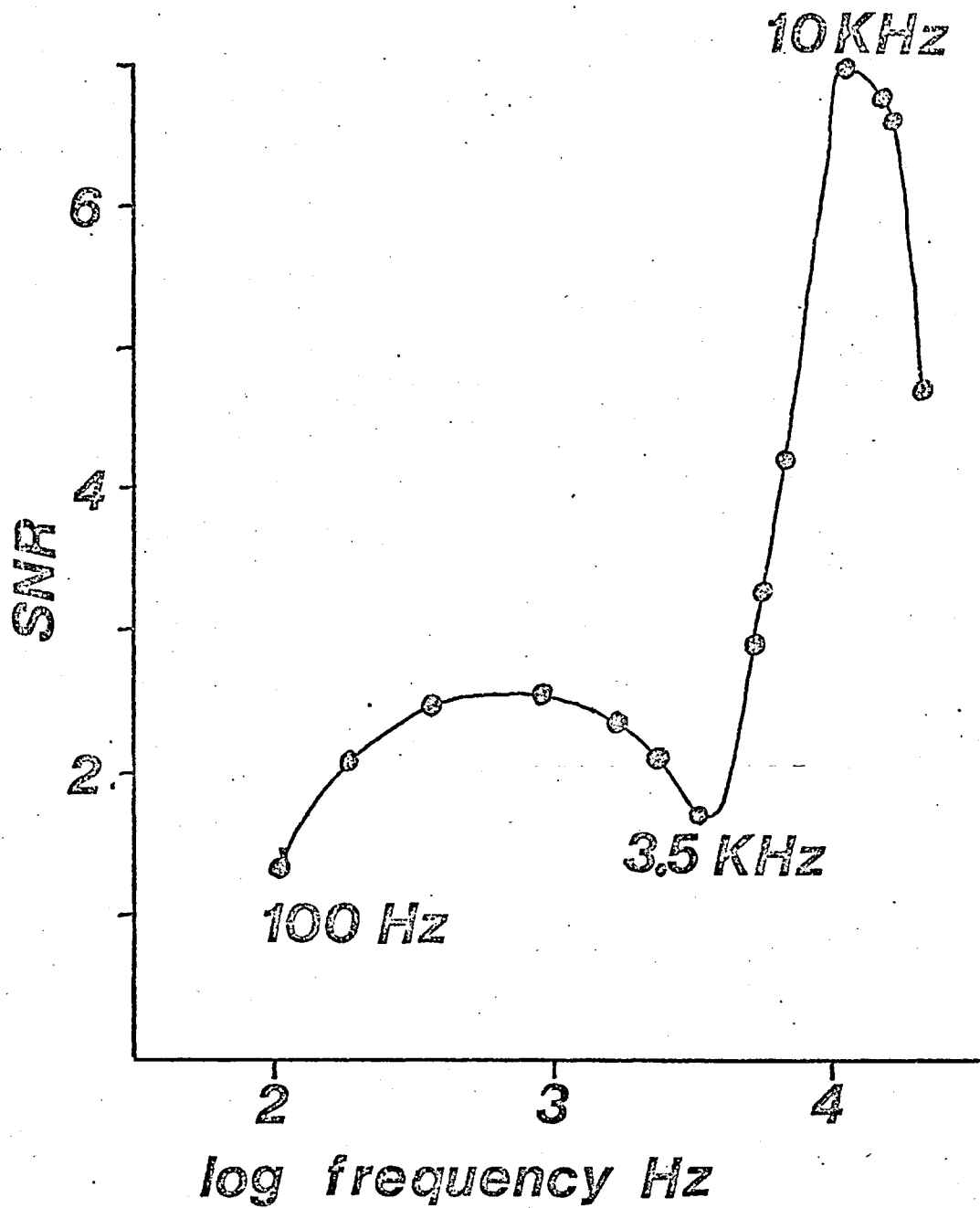


Fig. 2.19 Plot of frequency of modulation applied to a TIN EDL vs. the fluorescence signal-to-noise ratio obtained at 303.4nm. No flame separation or mirrors were used. Air-acetylene flame

TABLE 2.5

FLUORESCENCE SIGNAL AND NOISE LEVELS OBSERVED  
WHILE VARYING MODULATION FREQUENCY OF A TIN EDL

Fluorescence of 10 ppm tin measured at 303.4 nm in an unseparated air-acetylene flame. Fuel flows,  $1 \text{ min}^{-1}$ , acetylene - 0.9, air - 3.7, EDL cooled in  $\frac{3}{4} \lambda$  cavity, optical system A (Section 2.3.4)

Relative amplifier response <sup>a</sup> Arbitrary units	Modulation frequency	SIGNAL (corrected for amplifier response) Arbitrary units	NOISE Arbitrary units	Signal-to-noise ratio Time constant 4.7s
60	18.5 KHz	337	71	4.77
50	15.4 KHz	497	75	6.62
46	14.5 KHz	575	82	6.8
20	14.0 KHz	910	134	6.8
20	13.0 KHz	910	134	6.8
20	12.0 KHz	910	134	6.8
20	11.0 KHz	910	132	6.9
20	10.0 KHz	875	125	7.0
50	7.0 KHz	575	135	4.26
80	6.0 KHz	478	144	3.33
160	5.0 KHz	545	183	2.94
100	3.5 KHz	447	262	1.70
40	2.3 KHz	679	300	2.23
13	1.6 KHz	500	212	2.36
60	900 Hz	605	242	2.59
60	340 Hz	700	279	2.52
50	195 Hz	375	175	2.14
50	100 Hz	275	200	1.38
50	50 Hz	375	350	1.0

a At each frequency the amplifier had a different response depending upon the bandwidth of the filter section of the lock-in amplifier. The response at each frequency was measured using a 1.0 mV input signal (square wave) from a variable frequency oscillator. The signal and noise levels were then corrected for amplifier response.

the modulation frequency. The results, obtained with an aqueous 10 ppm aluminium solution and output time constant of 4.7s are plotted in Fig. 2.20. The lamp was temperature controlled at 565K in the Broida  $\frac{3}{4}$  wave cavity with an incident microwave power of 40 watts. (Reflected power ca. 10 watts). It can be seen that the optimal modulation frequency is not as critical as for tin and can lie between 11.0 and 14.0 KHz. The results are tabulated, Table 2.6, to show the effect of modulation frequency on just the fluorescence signal.

Some general observations can be made concerning the choice of modulation frequency. Firstly the two plots Fig. 2.19 and 2.20 indicate that high modulation frequencies give definite improvements in the signal-to-noise ratio of the atomic fluorescence measurements. Secondly Tables 2.5 and 2.6 indicate that this improvement is due to an increase in the fluorescence radiance as well as a decrease in noise. Thirdly, in the case of tin a slight increase in noise degrades the signal-to-noise ratio at frequencies between 10 and 14 KHz while in the case of aluminium the noise levels are not affected by increasing the modulation frequency between 10 and 14 KHz. For both element lamps the signal continues to increase with modulation frequency up to 14 KHz.

These observations are in general agreement with the work of West et al.<sup>175,184</sup> who studied a number of volatile element lamps including arsenic but not tin or aluminium. These workers noted an increase in lamp radiance with modulation frequency. They did not however make any quantitative observations on the change in fluorescence readout noise levels with modulation frequency. They did indicate that less source noise and drift was achieved and that phase-sensitive detection could increase the analytical signal-to-noise ratio.

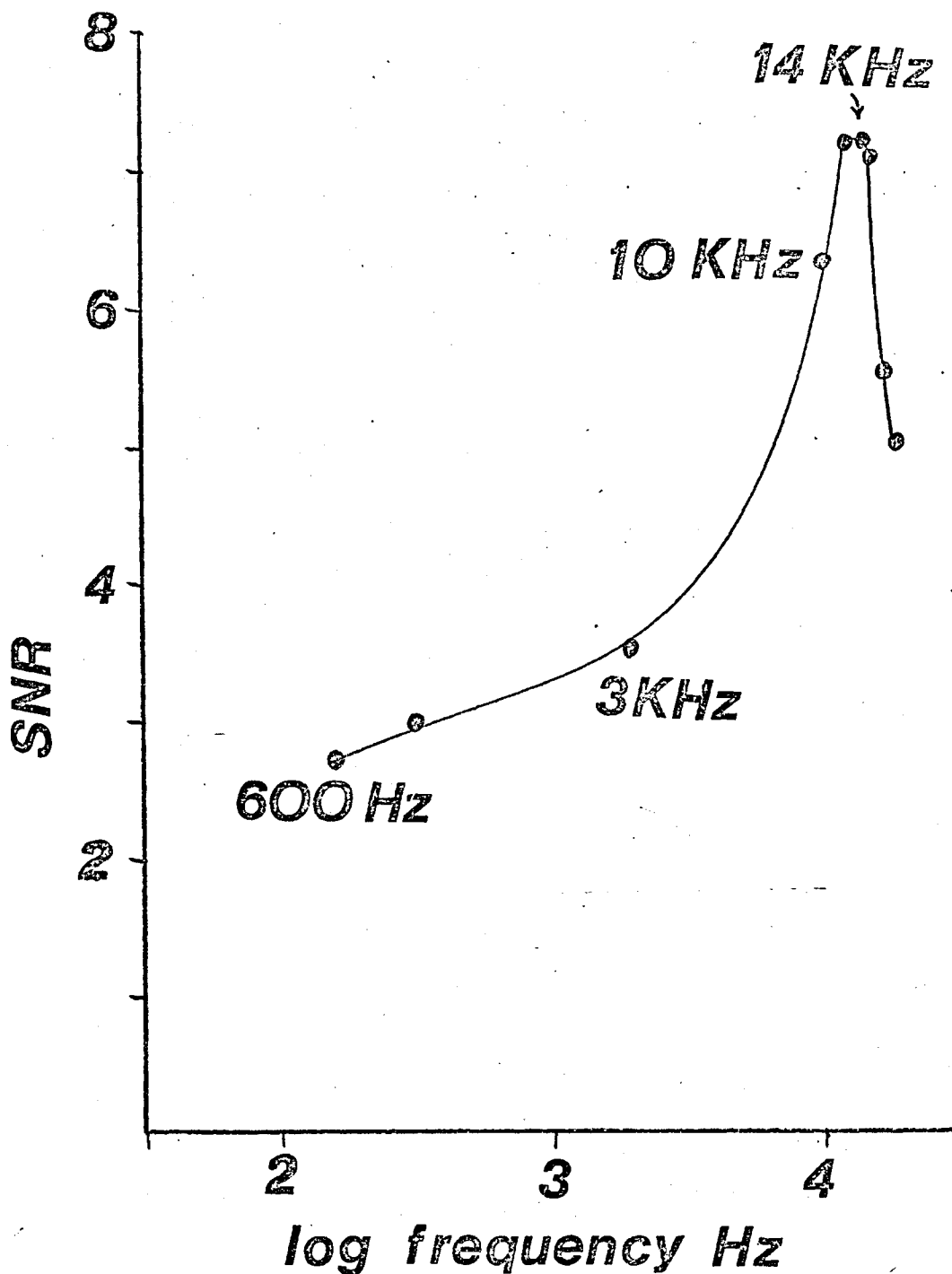


Fig. 2.20 Plot of frequency of modulation applied to an ALUMINIUM EDL vs. the fluorescence signal-to-noise ratio obtained at 396.2 nm. Argon-separated nitrous oxide-acetylene flame. The mirror system was used.

TABLE 2.6

FLUORESCENCE SIGNAL AND NOISE LEVELS OBSERVED WHILE  
VARYING MODULATION FREQUENCY OF AN ALUMINIUM EDL

Fluorescence of 1.0 ppm aluminium measured at 396.2 nm in an argon-separated nitrous oxide-acetylene flame. Fuel flow, 1 min<sup>-1</sup>, acetylene - 3.25, nitrous oxide - 4.8. EDL temperature controlled at 565 K in the  $\frac{3}{4}$  wave cavity. Optical system B (Section 2.3.4.)

Modulation frequency  kHz	Signal (corrected for amplifier response) <sup>a</sup> Arbitrary units	Noise	Signal - to - Noise ratio Time constant 4.7s
18.5	75	15	5.0
17.0	110	20	5.5
15.4	200	28	7.1
14.0	215	30	7.2
13.0	215	30	7.2
12.0	215	30	7.2
11.0	215	30	7.2
10.0	190	30	6.3
3.0	80	24	3.3
1.0	100	40	2.5
0.6	120	55	2.2

a - See table 2.5

An explanation for the increased signal behaviour of the EDL's was not postulated by West et al. However this behaviour could be explained in the following way: Under modulation there is a short period when the lamp is switched off and an equal period when the lamp is switched on corresponding to the square wave modulation frequency. At the low modulation frequencies ca. 100 Hz the off time is relatively long and some d.c. discharge is required to keep the lamp alight during the off time and thus prevent it extinguishing altogether. This is achieved by optimising the percentage modulation. The a.c. component i.e. 100 Hz modulation component, is therefore superimposed on a relatively high d.c. component. This d.c. will excite fluorescence but the a.c. amplifier tuned to 100 Hz will only detect the 100 Hz signal. As the modulation frequencies are made progressively higher the 'on' and 'off' times become proportionately shorter. Consequently the lamp is less likely to extinguish during the off period and the d.c. level required to keep the lamp alight need not be so large. The percentage modulation can be increased. The a.c. component of the radiation from the lamp will therefore be larger at the higher modulation frequencies than at 100 Hz. The fluorescence signals detected by the a.c. amplifier will be proportionately improved.

The percentage modulation was optimised at each of the frequencies used. It was found that for frequencies above about 6-10 KHz it was possible to apply the maximal percentage modulation that the equipment could deliver (ca. 50 to 60%). The response of the lock-in amplifier begins to fall off at 10 KHz and the fall becomes significant (-3dB) at ca. 17 KHz. Accordingly the modulation frequency giving maximal detected a.c. component must lie between 10 and 17 KHz from the point of view of both the maximal percentage modulation available and the response of the

amplifier. Moreover in view of the increase in noise, observed by West et al., as a result of ca. 75% modulation, this frequency range is probably the optimum.

The different optimal modulation frequency for the two lamps is probably a result of the use of the two different flames. For tin the slight increase in noise that was observed above 10 KHz could probably be a function of the noise spectrum of the air-acetylene flame. For aluminium the nitrous oxide-acetylene flame is far noisier than the air-acetylene flame throughout the noise spectrum and apart from the preponderance of noise at low frequencies ( $1/f$  noise) there are probably very few regions of low noise. However the changes in the levels of noise in the regions above 10 KHz are small, difficult to measure and therefore the results are rather subjective. The important basic trends are, the increase in the detected a.c. component, which is due to a greater depth of modulation, and the decrease in noise in going from 50 Hz to 10 KHz, which is due to moving well away from the low frequency ( $1/f$ ) region of the flame noise spectrum. If any changes in source noise were achieved with increased modulation frequency they were not evident because of the predominance of flame noise at all frequencies. Subjectively, however, the 10 KHz modulated lamp did seem more stable and reliable in operation.

#### B. Temperature control of electrodeless discharge lamps

The importance of allowing the temperature of a lamp in its cavity to stabilise before a stable output could be expected was well recognised throughout the early literature of EDL's.

However direct control of the temperature has only been pioneered recently by a few workers viz. T. C. Rains et al.,<sup>188,189</sup>

J. J. Ball<sup>190</sup> and Winefordner and co-workers<sup>171-174</sup>

The system described by J. J. Ball and also used by

T. C. Rains et al. consists of a small heater coil wound inside a piece of glass tubing. The glass tubing was placed inside a  $\frac{3}{4}$  wave cavity. With the application of a small voltage to the heater wire, to dissipate 15-18 watts, a convection current of warm air passing up through the glass and around the lamp was sufficient to maintain the lamp at constant temperature. No forced air was used. The main effect of this arrangement was to stabilise lamp output to within 2% for hours. Rains et al.<sup>188,189</sup> found that the intensity of a cadmium lamp increased with increase in temperature (relative intensities 1 at 20°C and 671 at 232°C) although it was not clear exactly which type of cavity ( $\frac{3}{4}$  or  $\frac{1}{4}$  wave) or heating was used (Ball or Winefordner systems).

Winefordner and co-workers<sup>173</sup> used the 'A' type antenna to couple the microwave power to the lamp. Air from a small fan was heated by passage over a nichrome heater coil and then passed over the EDL. The heating unit was rigidly fixed with respect to the antenna and wrapped with asbestos insulation. A chromel/alumel thermocouple placed in the air stream was connected to a temperature control system which precisely regulated the current to the heater coil. These workers used this system to operate multiple-element EDL's<sup>172</sup> as well as single element EDL's.<sup>173</sup> At constant microwave power (40W), all the EDL's studied (Hg, Cd, Tl, Zn, Fe and Cu) exhibited a peak in spectral radiant output at one temperature specific to each element lamp. A compromise temperature was chosen to give acceptable outputs from each element within a particular multi-element lamp.

Browner and Winefordner<sup>171</sup> have reported a detailed study on the use of temperature controlled (thermostatted) EDL's. Both thermostatted and unthermostatted EDL's operated in either

an A-antenna or a  $\frac{3}{4}$  wave Broida cavity were studied with respect to the effect of preparative conditions, lamp temperature and microwave power upon source radiant output, atomic absorption and atomic fluorescence signals of Zn, Pb, Mn, Hg and Tl. The main observations of these workers is best illustrated by the plots shown in Fig. 2.21. These plots represent the behaviour of a zinc lamp. Fig. 2.21a shows the relationship between lamp temperature and source radiant output. A constant 50 W incident power was used. The curve is extremely steep over the linear range. A change in temperature of 150<sup>o</sup>K gave a change in radiant output of approximately 1000 times. The optimal operating temperature was the same whether the  $\frac{3}{4}$  wave cavity or the 'A' antenna was used. The shape of the plot was the same for both means of excitation. A change in the absorbed microwave power from 6 W (using a 6dB attenuator) to 25 W and 50 W did not change the shapes of the curves or the peak temperature.

Fig. 2.21b shows the relationship between microwave power and radiant output with the EDL both thermostatted at its optimal temperature and unthermostatted in the  $\frac{3}{4}$  wave cavity. When thermostatted absorbed microwave powers above approximately 40 W produce very little further increase in radiant output. Comparing Figs. 2.21a and 2.21b it can be seen that there is a similarity between Fig. 2.21a and the curve showing the effect of microwave power on radiant output in the unthermostatted system. This demonstrates that the microwave power is mainly controlling the temperature of the lamp and hence the vapour pressure of zinc in the unthermostatted cavity. Similar observations and conclusions were made for the 'A' antenna and for other element EDL's.

With the 'A' antenna most lamps gave peak atomic fluorescence signals when thermostatting at temperatures identical

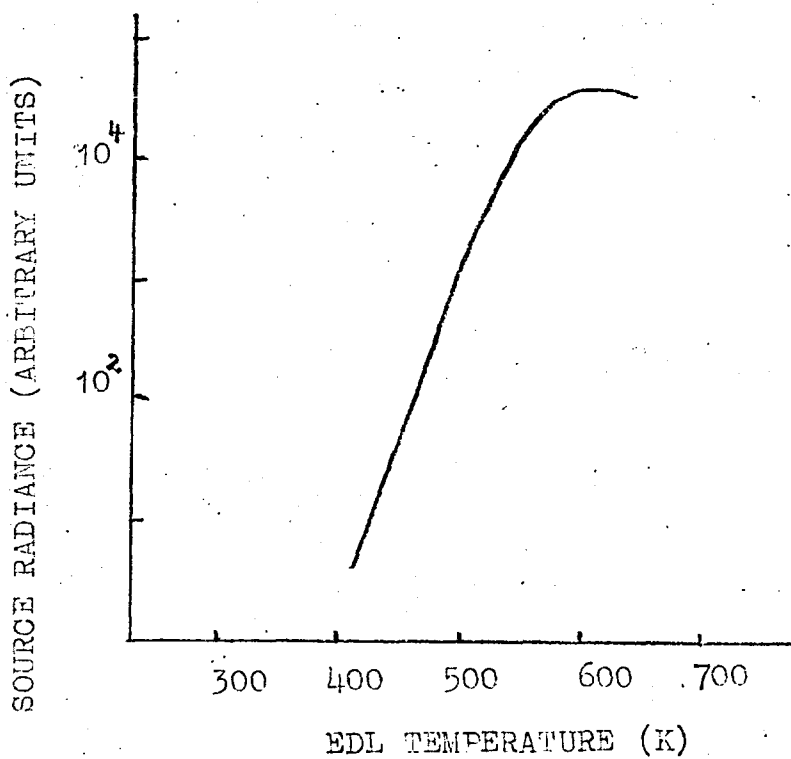


Fig. 2.21a Dependence of zinc EDL radiance on lamp temperature in thermostatted antenna. 50 W incident power 213.8nm. (Ref.171)

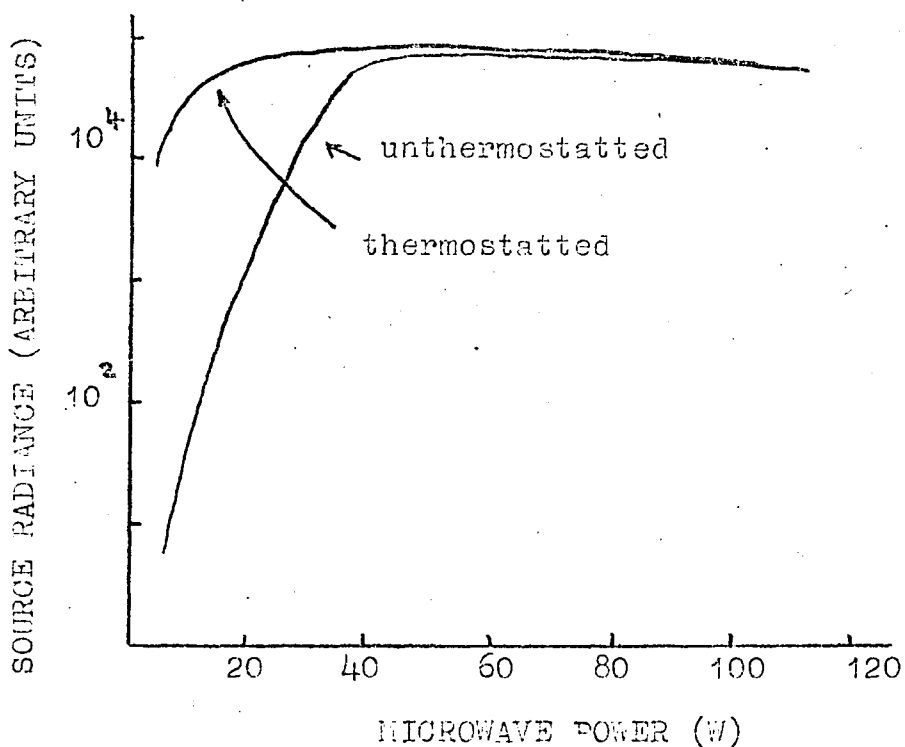
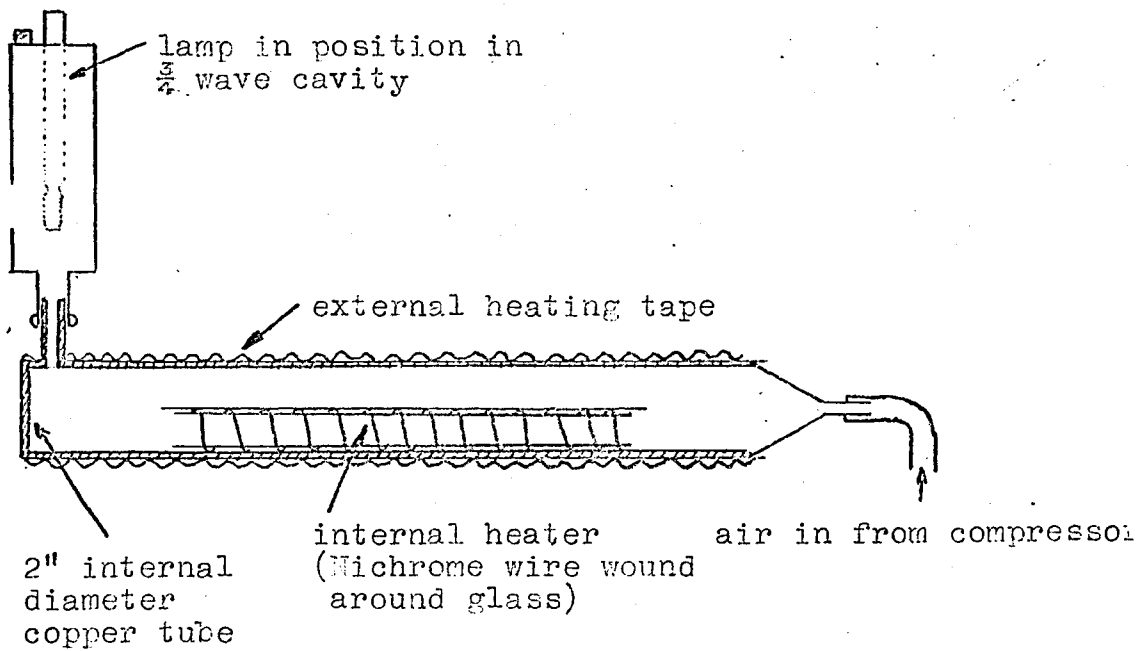


Fig. 2.21b Variation of zinc EDL radiance with microwave power in thermostatted and unthermostatted  $\frac{3}{4}$  wave cavity 213.8 nm. (Ref.171)

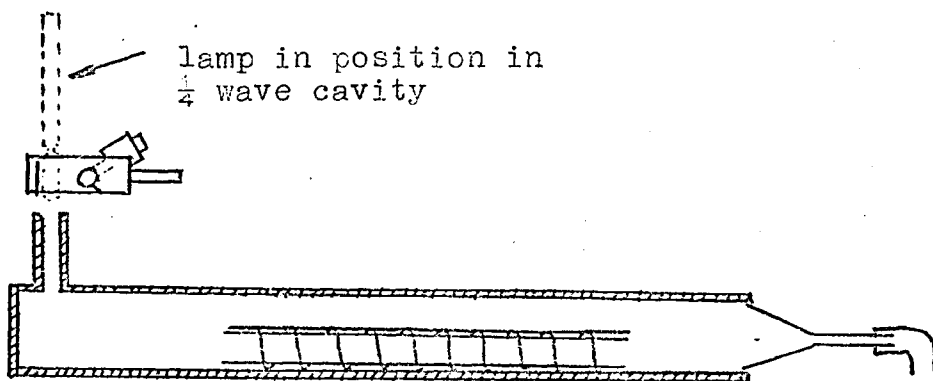
to those for peak source radiant output. However Zn and Cd lamps gave a peak fluorescence output at ca. 30K lower than the peak source emission temperature. Browner and Winefordner studied the effect of microwave power on the fluorescence signals using EDL's in an unthermostatted  $\frac{3}{4}$  wave cavity. Thus relying on microwave heating to achieve optimal source radiant output rather than thermostating. The general conclusions regarding the fluorescence signals as a function of temperature in the 'A' antenna also applied to the unthermostatted cavity as a function of microwave power. However very high microwave powers were required to obtain the best operating temperature which, for some lamps, was never reached or caused other difficulties.

#### The application of temperature control

Temperature control of the EDL's was achieved in the present work by passing air from an air-compressor through a heated tube and around the lamp in either a  $\frac{1}{4}$  wave or  $\frac{3}{4}$  wave cavity (Fig. 2.22). The tube was heated externally using heating tape and internally using a nichrome heating coil wound around glass tubing (appendix 2). In order to control the current through the heating elements each heater was connected to a variac. No precise regulation of the power to the heaters was attempted because the necessary equipment was not available. However measurements of the air temperature after the air had passed through the heating tube indicated that variations were not greater than  $\pm 2$  K over a period of 1 hour. The stability of the heating effect depended upon the stability of the mains supply which was connected directly to the two variacs. The maximum temperature of the air-stream that was attainable at the EDL position was about 620 K in the  $\frac{3}{4}$  wave cavity and about 560 K in the  $\frac{1}{4}$  wave cavity. Draughts in the laboratory cooled the air-stream in the  $\frac{1}{4}$  wave cavity thus limiting the temperature.



a. System with  $\frac{3}{4}$  wave cavity in position



b. System with  $\frac{1}{4}$  wave cavity in position

Fig. 2.22. Schematic representation of air-heating system for temperature control of EDL's.

For particulars of heaters see appendix two.

The procedure used to measure lamp temperature was the same as that used by Browner and Winefordner<sup>171</sup> i.e. the temperature of the lamp was measured with a chromel-alumel thermocouple placed against the cooler, lower, front portion of the lamp. Spectroscopic measurements were not made while the thermocouple was in position because the thermocouple disturbs the microwave field. Browner and Winefordner did not correct temperature measurements for the effect of microwave heating of the thermocouple which they found was 5 K for the maximum microwave power setting.

In this work at 40 W incident power the microwave heating of the thermocouple was less than 8K in the  $\frac{3}{4}$  wave cavity and no heating effect was observed for the  $\frac{1}{4}$  wave cavity. This difference arises because the lower front portion of the lamp is probably almost out of the microwave field of the  $\frac{1}{4}$  wave cavity. These measurements were made with the lamp in position but not alight and with no hot air passing over the lamp.

Plots of the radiant output of the Tin (Fig. 3.6), arsenic (Fig. 4.6) and aluminium (Fig. 5.2) EDL's vs. the temperature of the lamps are given in the appropriate chapters. The temperatures that gave the maximal lamp outputs were 385 K (tin), 340 K (Arsenic) and 565 K (aluminium). The tin and arsenic lamps were operated in the  $\frac{1}{4}$  wave cavity and the aluminium lamp was operated in the  $\frac{3}{4}$  wave cavity. Temperature measurements were easier for the  $\frac{1}{4}$  wave cavity than for the  $\frac{3}{4}$  wave cavity because the lamp is relatively inaccessible in the latter cavity.

Plots of the radiant output of the tin (Fig. 3.7) and arsenic (Fig. 4.7) EDL's vs incident microwave power were also obtained while the lamps were temperature controlled. The aluminium lamp behaved similarly to the arsenic lamp. No attempt was made to keep the temperature of the lamps constant while varying the microwave power, i.e. no correction was made for the

heating effect of the microwaves. It is probable that the constant stream of hot air around the lamp maintained the temperature within the limits set by the precision and accuracy of the measurements. (The accuracy was probably about 5 to 10 K due to the low surface area of contact between the thermocouple and lamp and the precision was not better than 5 K). These assumptions would only be true when varying the microwave power over a small range, say 20-50 W.

The main features of the temperature-radiant output plots are firstly, a change in temperature of 15 K results in a change in radiant output of approximately 10 times for all three lamps. This is an order of ten less sensitive to temperature than the lamps studied by Browner and Winefordner<sup>171</sup>. Secondly all the plots exhibit a plateau where the lamp becomes relatively insensitive to temperature although this plateau is only 10 K in the case of tin.

A change in microwave power from 40 W to lower powers caused the radiant output to drop for all three lamps. A change to higher powers made little difference to the aluminium and arsenic lamps but caused a drop in output from the tin lamp.

The aluminium lamp gave no significant output when operated at 40 W without heating. Switching on the temperature control resulted in an immediate rise in output. No attempt was made to try and duplicate this rise in output by putting more microwave power into the lamp and thus raising the temperature.

No significant net increase in radiant output was achieved by thermostating the tin lamp because the equilibrium temperature of the lamp in the unthermostatted  $\frac{1}{4}$  wave cavity (380 K) is close to the operating temperature of the lamp which gives maximal output (385 K). This was also the case with arsenic except that normally the arsenic lamp would need to be slightly

cooled to give the most intense output.

From a practical point of view the most significant effect of temperature control was that the radiant output could be reproduced to within 20%, everyday, with little more than twenty minutes stabilisation time. In the case of aluminium however a little longer was required before the air-stream attained the correct operating temperature. This was a function of the high thermal capacity of the heating equipment not the operating characteristics of the lamp. If the lamp was switched off, cooled under running water and replaced it took under ten minutes to restabilise.

Long term drift was improved from about 10% per hour to about 2% per hour for the arsenic and tin lamps. The aluminium lamp gave slightly worse drift figures of 4% per hour. A typical warm up period and drift observation for the aluminium lamp is shown in Fig. 2.23.

Any improvements or otherwise in the short term noise of the three lamps was not observable at the instrument readout (4.7s). Moreover observations of the noise from the lamp using an oscilloscope monitoring after the filter section of the amplifier (Test point 1 fig. 2.12) also showed no change in short term noise with the use of temperature control. Most noise from EDL's would be expected to be  $1/f$  noise (section 2.2.2.B) and this would be significantly reduced by the 10 KHz modulation.

Observation of the atomic fluorescence signals of the three elements indicated that maximum fluorescence radiance was obtained while running each lamp at the temperature that gave optimal radiance.

#### Electronic modulation and temperature control combined

Browner and Winefordner used a mechanical chopper to provide the a.c. signal for the detection system rather than

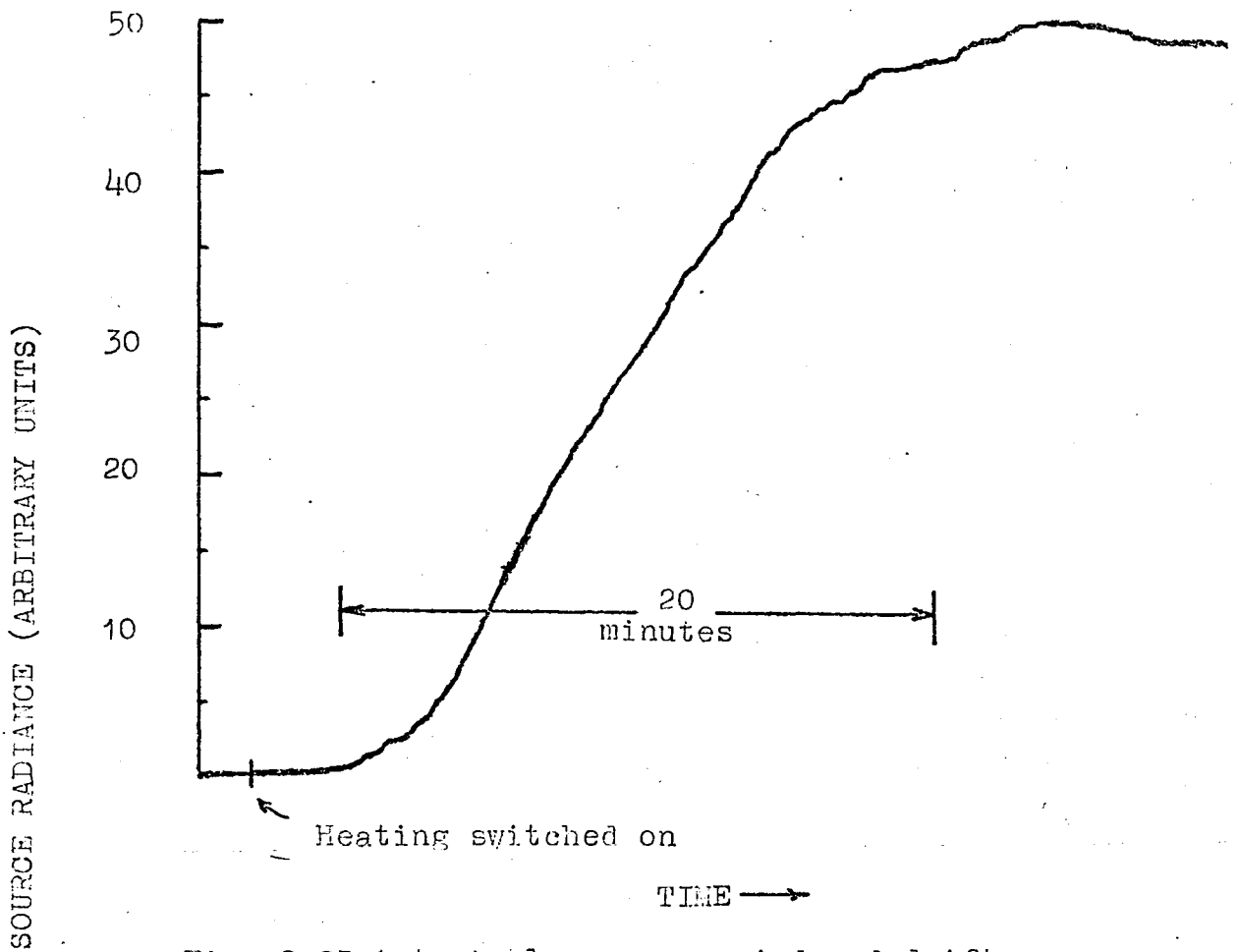


Fig. 2.23 A typical warmup period and drift observation for the aluminium EDL.

electrical modulation. Some discussion is therefore necessary to postulate a mechanism by which a temperature controlled lamp can be electronically modulated.

Fig. 2.25 is a plot of radiant output vs microwave power for a temperature controlled EDL as operated in the d.c. mode and as shown by Browner and Winefordner for a number of EDL's (for example Hg). Fig. 2.24 is a similar plot but of a different shape that is characteristic of an unthermostatted EDL. The mechanism of modulation shown in Fig. 2.24 is that postulated by West et al.<sup>184</sup> in their paper on high frequency modulation. The triangular modulation waveform produces an a.c. component of the emitted radiation from a modulated EDL. If the EDL had been optimised for d.c. operation (i.e. a microwave power setting of 70-80 W) and then modulated then no signal would be observed at the p.s.d., for two reasons: the amplitude of the a.c. component of the radiation is very small as a result of the shallow gradient of the plot and the frequency of the a.c. component of the emitted radiation is twice that of the modulation frequency. If the EDL had been optimised for a.c. operation the optimal operating power would be about 30 W where the gradient of the plot is greatest (Fig. 2.24). In fact West et al.<sup>184</sup> were able to demonstrate experimentally some of the points illustrated by Fig. 2.24, i.e. they were able to observe frequency doubling at the optimal d.c. operating power and a  $180^\circ$  phase-shift at higher microwave powers and optimal a.c. modulated operating powers were found to be lower than optimal d.c. operating powers.

The argument applied here is demonstrated by Fig. 2.25. The operating power which gives the optimal a.c. component will again be along the steepest part of the curve. This is essentially the same argument as put forward by West et al. and thus can easily be applied to temperature controlled lamps without modification.

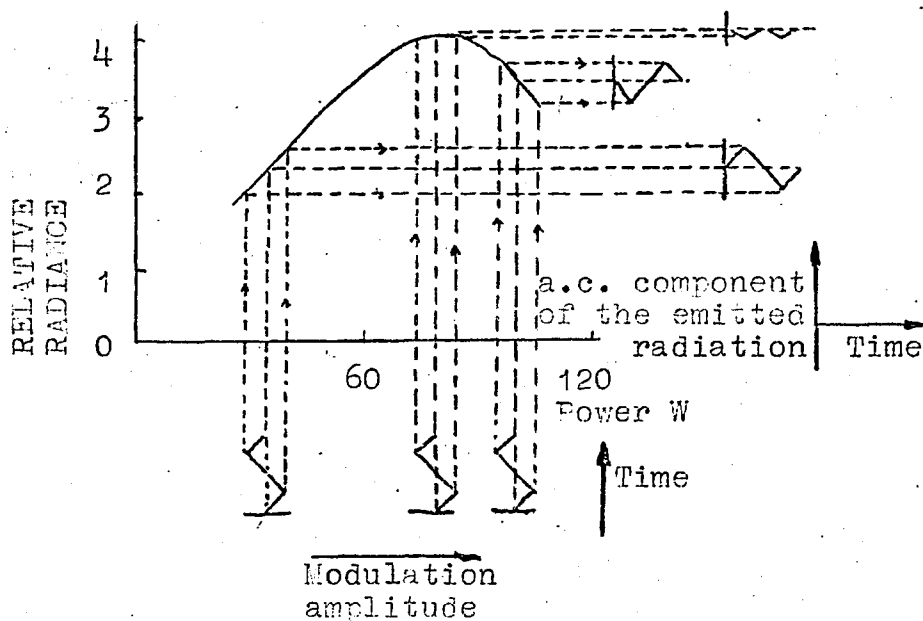


Fig. 2.24 Schematic representation of modulation of microwave power and its effect on radiant output. A triangular waveform modulating an unthermostatted lamp at different microwave power levels. (Ref. 184)

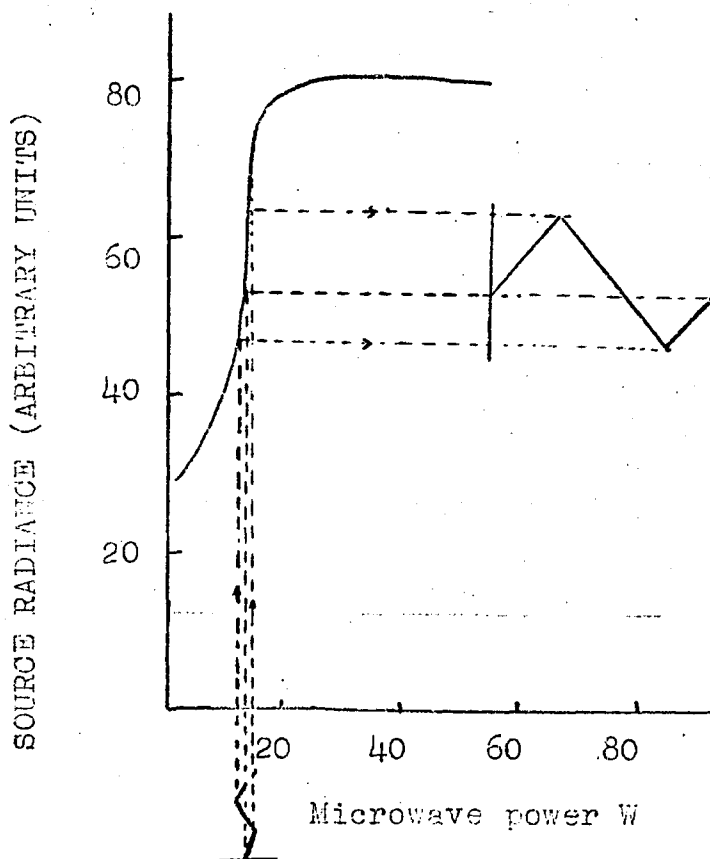


Fig. 2.25 Schematic representation of the same situation as in Fig 2.24 but showing in this case the possible result of modulating a thermostatted lamp.

A plot of power vs radiant output will be of the form demonstrated by arsenic and aluminium Fig. 4.7. The depressed plateau in this plot reflects the plateau in the equivalent d.c. plot, Fig. 2.25. In the case of tin (Fig. 3.7) there is probably a peak in the d.c. plot which would give a faster decrease in signal at relatively high microwave powers. Plots of radiance vs power have been shown to give a peak as reported by Browner and Winefordner for d.c. operated thermostatted lamps. In fact, for the unthermostatted situation in Fig. 2.24, once the lamp has reached its proper operating temperature by microwave heating, the effective radiance vs power plot would be Fig. 2.25. Consequently the a.c. component of the radiation around the optimal power would be the same in both cases.

Finally the temperature effect is similar to that observed by Browner and Winefordner<sup>171</sup>. However the gradients of the radiant output vs temperature plots are smaller than the gradients observed by the latter workers (see Figs. 3.6, 4.6 and 5.2). This is probably a function of the amount of material in the lamps. The discharge in all three lamps pinched near the optimal temperature and in the case of tin and aluminium the discharge extinguished itself and could not be relit at higher temperatures. Collisional quenching of the discharge due to the presence of excess material would cause this effect. The result would be that the attainable radiant output would be progressively reduced with increase in temperature hence reducing the gradient of the radiant output vs. temperature plot.

#### C. Two further observations on the operation of EDL's

The heater used by J. J. Ball<sup>190</sup> and T. C. Rains<sup>188,189</sup> was tried in this work. The construction was similar to that described in their paper and a 12v d.c. power supply was used to heat the nichrome wire to give a 20 W heater. The maximum

equilibrium temperature of the air, which rises by convection into the microwave cavity, was found to be 390 K. This was just sufficient to maintain the tin lamp at its optimal operating temperature (385 K) and the resulting increase in radiant output was about 5%. i.e. essentially the same results as the more sophisticated system described above. This heater was not suitable for powering the arsenic and aluminium lamps.

Dagnall and Silvester<sup>191</sup> have evaluated a microwave attenuator which was said to improve by about one third the short term noise on the output of those EDL's which operate at very low powers ca. 25 watts, e.g. Cd, Zn, Hg etc. A 3dB attenuator was tried, in the work reported here, using the tin lamp without temperature control. No significant effect was found except that the lamp took a long time to warm up. However such a small improvement as one third is hardly worthwhile and certainly difficult to detect.

#### D Some conclusions concerning the operation of EDL's

The benefits which arose from the use of high frequency modulation and temperature control were very significant both from the point of view of ease of operation as a result of temperature control and improvements in signal-to-noise ratio due to both modifications. High frequency modulation is however a compromise when compared to mechanical modulation. This is because a mechanical chopper while introducing different noise problems has an effective depth of modulation of 100% which gives the maximum possible a.c. signal. This is not possible with electronic modulation. High frequency modulation simply improves the efficiency of electronic modulation nearer the ultimate 100% modulation. There is no evidence either in the literature or in this work which has indicated that high-frequency

modulation enables pulsing of the EDL to give high instantaneous radiant outputs similar to those found when pulsing hollow cathode lamps. Moreover from the point of view of flame noise it is not necessary to go to 10 KHz modulation to avoid the worst part of the flame noise spectra. i.e. the low frequency end.

Despite these arguments in favour of mechanical choppers it is clear that the high-frequency electronic modulation is a convenient alternative and can be used with temperature control of the EDL radiant output. The EDL's that were used in this study were all obtained from commercial sources and all three appeared to contain too much material. This may have been the limiting factor in obtaining high radiant outputs. It is to be hoped that because the development of temperature control has separated some of the many variables that affect lamp operation more reliable EDL preparative methods will be developed.

The ability of temperature control to create the correct conditions for maximal radiance and minimal drift of EDL emission is a significant contribution to the attainment of high signal-to-noise ratios in atomic fluorescence.

### 2.3.3. The Flame

The basic aspects of the use of flames in atomic emission, absorption and fluorescence are discussed in most textbooks concerned with the three techniques<sup>7, 97, 117, 192-194</sup>. Therefore a detailed discussion of the processes occurring when a sample solution is nebulized into the flame and of atomization efficiency is not necessary here.

The flame chosen for the analysis of a particular element or group of elements should be sufficiently hot and reducing and of low burning velocity to provide optimal atomization efficiency. This is the primary requirement for all three techniques. However the flame must also be cool enough to

minimize ionisation and flame background. Unfortunately these requirements cannot all be met with a single flame.

The nitrous oxide-acetylene flame is hot, has a low burning velocity and some unique reducing properties which minimize interference effects and help maintain high atomization efficiencies. However it has a high, noisy background level in most spectral regions particularly above 300 nm. The cool hydrogen-argon, hydrogen-oxygen-argon and air-hydrogen flames have very low background and noise levels throughout the spectrum and give minimal ionization. The air-acetylene flame in most respects lies midway between the two extremes represented by the cool flames and the hot nitrous oxide-acetylene flame. The oxy-acetylene flame, although slightly hotter than the nitrous oxide-acetylene flame, does not possess the same reducing properties.

In addition to the above aspects, which are relevant to all three atomic spectroscopic techniques, atomic fluorescence has the additional requirement of a low quenching flame. This is a result of the fact that not all of the radiationally excited atoms return to the ground state by fluorescence emission. The fraction that does return to the ground state by fluorescence is quantified by  $Y_p$ , the fluorescence spectral power yield (appendix I). The remaining excited atoms are deactivated by other species in the flame, for example by molecular collisions and other radiationless deactivation processes. Both nitrogen and hydrocarbons give rise to relatively high quenching, and therefore flames that do not contain these gases give better fluorescence power yields<sup>149,195</sup>. For example the cool hydrogen flames, particularly those containing argon, are poor quenching media<sup>149</sup>. However these flames, although optimal for easily atomized elements (e.g. arsenic, bismuth, thallium etc.), are

of little use for refractory oxide forming elements and for analyses of solutions containing complex matrices.

There are two basic types of flames - premixed and turbulent. A premixed flame is produced by mixing the flame gases, in a chamber, before introduction to the burner head on top of which the flame burns. A turbulent flame is produced by allowing the gases to mix only within the flame, i.e. by passing the gases separately to the burner head and burning the mixing gases. The turbulent flames result in considerable turbulence, audible noise and air entrainment and associated nebulisation procedures produce relatively large solvent droplets in the flame which may cause scatter.<sup>149</sup> The premixed flames are less audibly noisy, the flame burns smoothly with little turbulence, have less flame flicker and associated nebulisation procedures produce smaller solvent droplets than turbulent flames<sup>149, 195</sup>.

Turbulent hydrogen flames were used extensively in early atomic fluorescence work<sup>2, 196, 197</sup> but it is now more usual to use a premixed flame<sup>149, 198, 199</sup> and the gas mixture which gives the best compromise between all the factors mentioned above. For example although the nitrous-oxide-acetylene flame has the disadvantages of high quenching ability, high background noise etc. it does have high atomization efficiency for Al, Mo, V, Si, Ge, and Be. For these elements atomic fluorescence studies have been carried out in the nitrous oxide flame<sup>10, 15, 16, 200</sup>.

Other elements may have better sensitivity in cooler flames but interferences may be greater. In such cases either the air-acetylene or nitrous-oxide-acetylene flame is chosen or the matrix is separated from the analyte by suitable solvent extraction techniques.

Once a flame has been chosen according to the above criteria there is little else that can be done to improve the

fundamental sensitivity of the method insofar as the flame is concerned. However the signal-to-noise ratio can be optimised by proper design of the gas handling arrangements, premix chamber and burner and by use of flame separation. In particular flame separation is discussed in this section. Discussions on the choice of flame for the atomic fluorescence determination of tin, arsenic and aluminium are included in chapters three to five respectively.

A. The gas handling arrangements, premix chamber and burner

There are two kinds of fluctuation in the flame which will produce noise at the photomultiplier output. Firstly, there are random fluctuations in the concentration of element in the flame, due to uneven spray delivery by the nebulizer, which will give fluctuations of the fluorescence and of the thermal emission from the element. Secondly, there are variations in flame temperature due to turbulence and air entrainment, which will give fluctuations in the intensity of thermal emission from the element and of the background emission. The magnitudes of these fluctuations depend upon the design of burner and spray chamber and on the flow rates of the flame gases. In designing a burner a detailed knowledge of the principles of fluid flow as well as the properties of the burning gases is required. It is not necessary here to go into the details of the fundamental parameters involved. However such factors as the burning velocity, the streaming velocity and the quenching effect of the burner walls are taken into account when designing a new burner<sup>201,202</sup>. A few burners designed for atomic fluorescence spectroscopy have been reported<sup>199,203</sup> but in general it has been usual to use a meker-type burner<sup>199</sup> as originally used for atomic emission measurements. Slot burners are now more generally used in both atomic absorption and emission

but give no advantage in atomic fluorescence because the whole length of the flame needs to be illuminated by the source. This is not easy to arrange with presently available sources.

The burner used in the present study was a Beckman RIIC model with two interchangeable heads. One head (Meker-type) had 13 holes arranged in a square and was used for supporting all the flames except for the nitrous oxide-acetylene flame. This flame was supported on the second head which had a circular slot of the critical dimensions required. The assembly had provision for inert gas shielding via a water cooled jacket surrounding the burner head.

Pneumatic nebulization is one of the most common methods of spray generation probably because other techniques produce only very limited concentrations of aerosol. The only real alternative seems to be the more expensive ultrasonic generation which is also capable of generating relatively high density aerosols<sup>204-208</sup>. A number of heated<sup>209</sup> or improved spray chambers<sup>210</sup> have been reported but the majority of researchers use equipment obtained from instrument manufacturers.

The nebulizer and premix spray chamber used in the present study was a Pye-Unicam (Cambridge) model as used on that manufacturer's SP90 atomic absorption/emission instrument. The nebulizer was fitted with an impact bead assembly which effectively breaks up the spray produced by the nebulizer, into a finer aerosol. The impact bead gave an 80% improvement in fluorescence signals compared to using the system without the bead in place. The Beckman burner was modified slightly so that it could be connected to the Unicam spray chamber.

The gas handling arrangements that were used in this study were basically those belonging to the Jarrell-Ash instrument. Calibrated manometric flowmeters (Gallenkamp type FL-420) with

interchangeable jets were used to control flow rates and replaced the Jarrell-Ash rotameters which were calibrated in SCFH units.

### B. Flame separation

Three types of separated flame have been reported in the literature. These are 1. The flame is separated from the atmosphere by another flame (usually hydrogen) burning around its perimeter. This is called flame shielding 2. The flame is separated from the atmosphere by a cylindrical silica tube. 3. A flow of inert gas is passed upwards and around the perimeter of the flame to fulfill the function of separation from the atmosphere.

All three methods of separation have essentially one major effect viz. the exclusion of air from the analytical flame and consequent increase in fluorescence yield due to reduced quenching. However there are a number of secondary effects which are important. For example the absolute magnitudes of background emission can be reduced by up to two orders of ten. This is because the flame background emission originates primarily from the secondary diffusion zone which is removed, upon separation, to higher regions of the flame where analytical measurements are not usually made. There is also a reduction in noise levels because the noise associated with the secondary diffusion zone is out of the field of view of the detection system.

In the 310 nm region the unseparated flame emits a strong OH band system. Separation therefore gives reductions in noise and background level which are particularly great in this region<sup>18,222</sup>.

The flame sheath method<sup>184,185,195,211,212,222,223</sup> is less widely used in analytical flame spectroscopy although theoretical studies often use a flame protected in this way. Jenkins<sup>195</sup> has demonstrated that a sheath significantly reduces the concentration

of quenchers in the flame. He not only had a flame sheath but also the entire flame was further protected from air entrainment by a shield of an inert gas. Slevin et al.<sup>199</sup> used a similar doubled sheathed air-acetylene flame supported on a burner specially designed for atomic fluorescence. It was concluded that from the point of view of both analytical sensitivity and minimisation of interferences this burner was markedly better than standard meker burners. The sheathed burner gives a more uniform atomic distribution in the control flame<sup>199</sup> due to the more uniform temperature obtained. For those elements which form oxides in the flame a reduction in the entrainment of atmospheric oxygen is a further advantage. A more uniform atomic distribution makes the choice of viewing region less critical and the larger region of high temperature and low oxygen content can give increased atomic concentrations.

However the greatest number of studies have been carried out on inert gas separated flames. The separated flame was studied extensively by West and his co-workers in London. They started by looking at air-acetylene and nitrous oxide-acetylene flames separated using the silica tube method<sup>213-215</sup>. The tube however could not be used for fuel-rich flames because of sooting up of the glass. Attention was then turned to the nitrogen and argon separated flames<sup>13,18,203,216-221</sup> for which essentially the same effects were observed as with the silica tube but without the disadvantages.

The main observations and conclusions concerning the published work on inert gas separation are set out here:

In the separated air-acetylene flame a drop in temperature has been indicated to occur upon separation<sup>216</sup>. When atomic emission signals have been observed this drop in temperature has led to a decrease in emission signal<sup>216-218</sup>. However

because the drop in analytical signal is not great in regions close to the primary cones this effect can be minimised and advantage taken of the decreased noise levels to give a net, greater signal-to-noise ratio. In atomic absorption the slight temperature drop has not led to decrease in analytical signal<sup>216</sup> as would be expected.

In atomic fluorescence, increases in fluorescence emission have been observed<sup>222</sup> and attributed<sup>13</sup> to reduced absorption of source radiation and reduced quenching due to the presence of the inert gas. When nitrogen is used for shielding the reduction in quenching is small<sup>12,13</sup> although noise is still reduced. It is usually emphasised<sup>18,216-218</sup> that the effect of separation of the air-acetylene flame reduces noise levels. Often it is not clear what effect on the signal itself was observed upon separation<sup>14,17,18,218</sup>. In general however, whatever the source of the improvement (signal or noise or both), argon separation usually gives greater improvements in detection limit than nitrogen separation<sup>222</sup> especially in atomic fluorescence<sup>18</sup>

Separation of the nitrous oxide-acetylene flame has been shown to lead to a drop in temperature<sup>221</sup> which is minimal just above the primary cone. Published information<sup>200,220-222</sup> shows clearly that separation gives increases in signal, in atomic emission, atomic absorption and atomic fluorescence, as well as a decrease in noise. It is postulated that an increase in atomic population of refractory oxide forming elements occurs on separation of the nitrous oxide flame. The most significant evidence for the increase in atomic population is said to be<sup>220</sup> the increase in atomic emission<sup>219</sup> from several elements on separation of the flame, even though it was shown that separation leads to decreased flame temperature<sup>221</sup>. The results of experiments with controlled apertures indicated<sup>220</sup> that the increase in

emission was not due to the observed increase in volume of the red interconal zone of the fuel-rich flame. Moreover the prevention of the diffusion of atmospheric oxygen into the flame upon separation is thought to be the important factor for refractory oxide forming elements which are more efficiently atomized under reducing conditions<sup>222</sup>. Indeed the improvements obtained on separation in all three flame techniques tend to support these conclusions particularly well in the case of Al<sup>10,219,220</sup> and Si<sup>16,219,220</sup> and several other of the refractory oxide forming elements<sup>10,15,200,219,220</sup>.

Hydrogen flames, particularly argon-oxygen-hydrogen, have been separated and improvements in detection limit obtained although again this has only been attributed to reduction in noise where nitrogen separation was used<sup>9</sup>. In fact the present author was not able to find a significant number of reports of separation of cool flames except where flame sheathing was used.

In summary it can be said that flame separation increases emission and fluorescence signals in most instances probably by reduced quenching of emitted radiation. In the case of emission the magnitude of the effect will be dependent on the opposing effects of reduced quenching and the drop in temperature. Argon as separating gas gives a smaller cooling effect than nitrogen and is a less effective quencher. It is therefore optimal for emission and fluorescence work. In the case of refractory oxide forming elements increases in signal are also observed in atomic absorption using the nitrous-oxide-acetylene flame. These increases are thought to be due to an increase in atomic population. Noise levels and flame background emission levels are always reduced. This is particularly useful in atomic emission where the background cannot be reduced by using an a.c. detection system.

### The application of flame separation

The Beckman RIIIC burner had provision for separation. The inert gas was directed upwards around the flame using coiled, corrugated steel strip packed into a water cooled jacket as used by West et al.<sup>218</sup>. However this method uses 10-13 l min<sup>-1</sup> of the inert gas to give efficient separation. A more recent form of separator<sup>18,203</sup> uses stainless steel capillary tubing to direct the gas flow. A very even, stiff gas flow is established and only ca. 6 l min<sup>-1</sup> flow is required for efficient separation (It is interesting to note that the researchers who built this separator<sup>203</sup> also built a capillary burner. This type of burner gives a very laminar flame and its advantages have led to it being used a great deal in recent atomic fluorescence studies<sup>18,28,</sup>)

In the present work a capillary separator was constructed by packing a ring of hypodermic needles around the centre of the Beckman RIIIC water cooled jacket. The corrugated strip was removed. Araldite was the adhesive used. This separator gave efficient separation of both the air-acetylene and the nitrous oxide-acetylene flames and used only ca. 6 l min<sup>-1</sup> of gas.

The effects of argon flame separation on the three elements studied are detailed in chapters three to five. As expected separation gave increases in fluorescence signals for all three elements in both the air-acetylene and nitrous oxide-acetylene flames. No success was achieved when separating the argon-oxygen-hydrogen flame probably because this flame 'lifted off' before it could be efficiently separated. This is a result of its relatively low burning velocity and the situation could only have been improved by use of a better burner e.g. a capillary burner. This was particularly disappointing for the determination of tin whose most sensitive wavelength 303.4 nm lies very close to the OH band system<sup>9</sup>.

The increases in fluorescence signal that were obtained in the acetylene flames were always significant, their magnitude usually being a factor of 2 or 3 times. As expected an increase in the atomic emission signal from aluminium was observed in the nitrous oxide-acetylene flame. This increase was about the same magnitude as that found in atomic fluorescence. This supports the idea that for aluminium the drop in temperature (usually 10-100 K) obtained upon separation is more than compensated for by an increase in atomic population and a decrease in quenching. Both the latter effects would be expected to affect atomic emission and fluorescence roughly equally.

Browner and Manning<sup>18</sup> indicated that flame separation would not be expected to reduce noise, with a high frequency modulated and synchronously detected system, quite as well as with a d.c. readout. This is because most flame (i.e.  $1/f$ ) noise is concentrated at the low frequency end of the noise spectrum<sup>185,186</sup> and therefore flame separation is most beneficial at those frequencies. An a.c. modulated system is most beneficial at the same frequencies. However Browner and Manning reported that flame separation does reduce noise at the readout of an a.c. system apparently because of a reduction in shot noise.

In the present study noise in both flames was reduced at the readout by about 30% in the atomic fluorescence of tin, arsenic and aluminium. These small reductions in readout noise were expected because of the use of a high frequency modulated system where the frequency bandpass is well away from the low  $1/f$  end of the spectrum. For the atomic emission of aluminium, using the 50 Hz modulated Jarrell-Ash amplifier and the nitrous oxide-acetylene flame, again only a slight decrease in noise was observed on separation. This indicates that there is relatively little background at the aluminium wavelength, 396.2 nm, because

any reduction in  $1/f$  noise would have been relatively large with the 50Hz modulated detection system. West<sup>222</sup> reported an improvement in emission detection limit of only two times for aluminium. This also must have been mainly due to an increase in signal. Large reductions in noise can only be expected when measuring in a region of relatively high background, for example the OH band emission at 310 nm. In the case of the atomic fluorescence of tin, at 303.4 nm, noise levels are very high and flame separation would be more effective<sup>9</sup>. However in this work the use of 10 KHz modulation and the lock-in amplifier made the effect of separation on noise levels appear small. This can be seen from Table 2.5 (tin fluorescence in the unseparated air-acetylene flame) when in going from 50 Hz modulation\* to 10 KHz modulation there was a factor of nearly 3 times decrease in noise. Published<sup>222</sup> examples of the effect of separation in the 310 nm region when using low frequency modulation are noteworthy: Bismuth emission 306.8 nm, 50 Hz modulation, 10 times improvement in detection limit on nitrogen separation of the air-acetylene flame. Molybdenum fluorescence 313.3 nm, 13.6 times improvement on nitrogen separation of the nitrous oxide-acetylene flame. In the case of molybdenum this improvement probably included a signal increase. In view of the work reported here this signal increase may have been about two times.

\* Here the signal-to-noise ratio performance is comparable to the 50 Hz modulated Jarrell-Ash amplifier.

It was found therefore that the most significant effect of flame separation in improving signal-to-noise ratios was due to an increased signal as a result of reduced quenching or, in the case of aluminium, increased atomic population. Although flame separation has been shown to reduce low frequency  $1/f$  noise this factor was not important here because of the use of the lock-in amplifier at 10 KHz modulation. However there was a slight decrease in noise upon separation which was probably due to a reduction in the white, shot noise from the flame.

#### 2.3.4. The Optical Arrangement

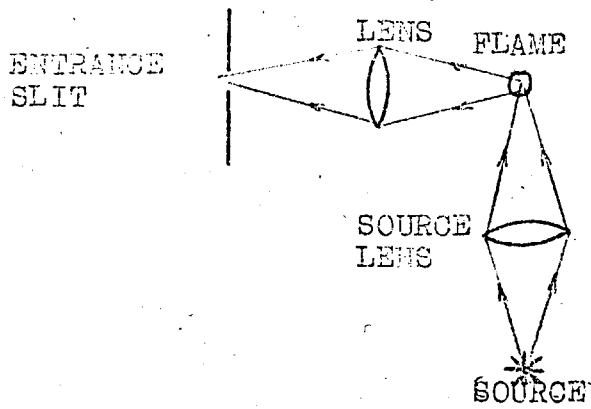
Two important variables appear in the equations that govern the magnitude of the fluorescence signal at the readout. These are the solid angles of a) collection of source radiation to focus on the flame i.e.  $\Omega_E$  in appendix I and b) collection of fluorescence radiation to focus on the monochromator entrance slit i.e.  $\Omega_F$  where  $K = HT_F \Omega_F$  equation (1) section 2.2.1. These angles  $\Omega_E$  and  $\Omega_F$  can be maximised using a suitable arrangement of mirrors and/or lenses. The importance of the proper choice of optics was emphasised when atomic fluorescence was first proposed as an analytical method<sup>1</sup> and since that time quite a large number of optical arrangements have been reported. These are adequately described by Winefordner and Elsor<sup>5</sup> in their review of atomic fluorescence.

Early work in atomic fluorescence was often carried out simply by placing the source as close to the flame as possible thereby allowing the maximum amount of light onto the flame<sup>2,3</sup> However this arrangement prevents the development of the rest of the optical system because mirrors designed to collect fluorescence radiation can easily pick up light from the source and focus this into the monochromator entrance slit thus creating a large,

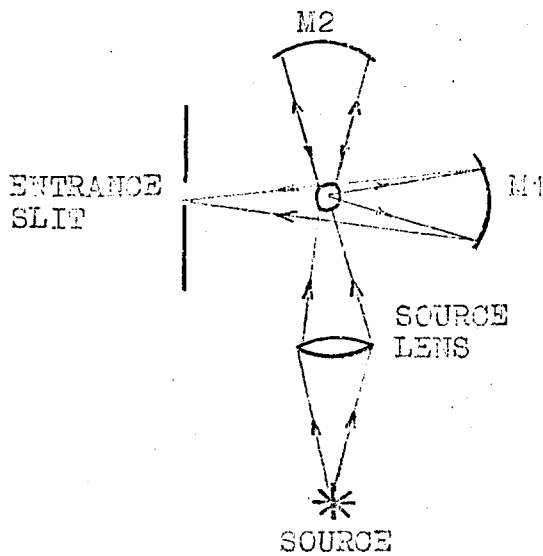
noisy background signal. Baffles were usually constructed around the monochromator entrance slit to prevent light from the source being viewed directly.

The two most popular optical arrangements which have been reported are illustrated in Fig. 2.2.6. In (a) the amount of light collected from both the source and flame is limited by the size and focal length of the lenses used (Appendix I page A12). Moreover lenses have a number of disadvantages. Firstly they become more expensive as size increases and focal length decreases. Secondly a lens gives more aberrations and more light is lost by absorption and reflection than when using equivalent and less costly mirrors. Thirdly the use of lenses does not give the same versatility that is obtained with mirrors<sup>224</sup> This latter point is best illustrated by the optical arrangement in Fig. 2.26b. The source lens is still necessary to focus radiation onto the flame. Although some alternatives to this lens are available<sup>5</sup> these are limited by the geometry of the source itself. In cases where the lens is not used the source must be set slightly back from the flame and/or baffles constructed to minimise stray light entering the slit. However lenses cannot perform the functions of mirrors M1 and M2.

Mirror M2 gives a second pass of the source radiation through the flame thus increasing the effective source radiance. Mirror M1 is able to collect radiation travelling away from the detector and focus it back onto the entrance slit. Omenetto and Rossi<sup>224</sup> observed an increase in fluorescence intensity of 168% using a mirror in the M1 position. Other researchers have obtained similar increases<sup>17</sup>. However the physical characteristics of mirrors (size, focal length etc.) are not always given and it is therefore difficult to compare the improvements



a) All lens system



b) Mirror system with a source lens

Fig. 2.26 Two popular optical systems for atomic fluorescence.

in fluorescence signals that have been reported.

Sychra and Matoušek<sup>V</sup> <sup>14,17</sup> used a combination of 2.26 (a) and (b) but without the source lens (The source was set 55 mm back from the flame and baffles were used). These researchers in common with a number of others found that the mirror M1 was not always advantageous because it increased the background emission and hence noise from the flame. This is important; any optical system designed to collect the fluorescence radiation will collect the flame background and noise equally efficiently. Hence the desirability of a detection system that can distinguish between signal and noise.

With the optical arrangement in Fig. 2.26b it is desirable to have the flame as close as possible to the entrance slit. To this end Omenetto and Rossi<sup>224</sup> moved the flame position from the normal atomic absorption position on a Jarrell-Ash spectrometer to within 12 cm of the slit. In a later paper<sup>225</sup> the same authors reported some measurements on sodium emission which indicated that there is no difference in the signals obtained by using a condensing spherical lens between the flame and the entrance slit and those observed when the flame is placed about 12 cm from the slit. Omenetto et al.<sup>225</sup> also designed and built a sophisticated optical arrangement based on the flame being close to the entrance slit. This optical arrangement can be discussed here in conjunction with Fig. 2.27. (Fig. 2.27 represents the arrangement used in our study. However the mirror M1 was a spherical concave mirror while Omenetto used an ellipsoidal mirror at the M1 position, otherwise the two optical systems are identical). The mirror M1 can most efficiently collect radiation from the flame and focus it onto the slit if it has two foci. This requirement is met by an

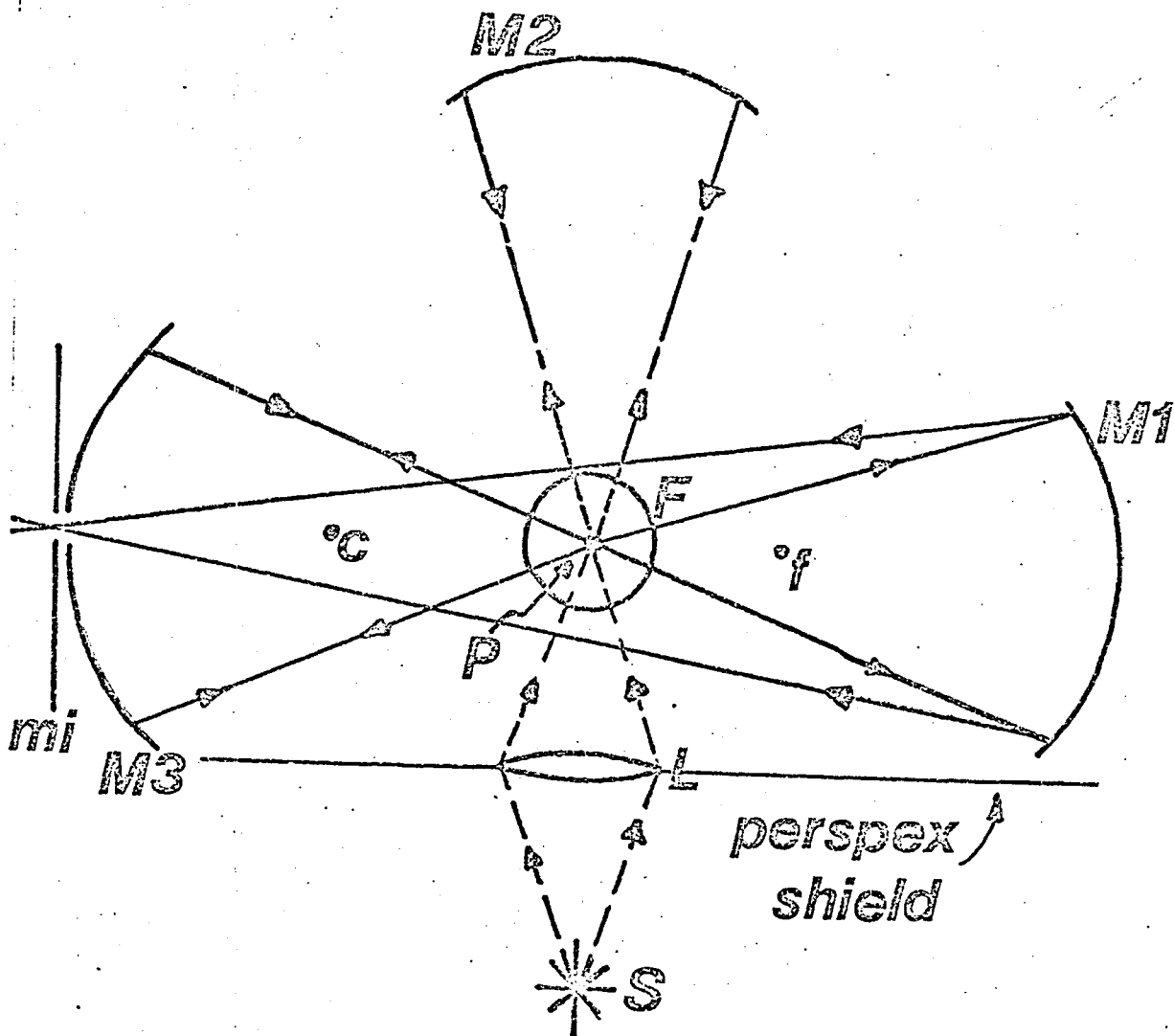


Fig. 2.27 (F) Flame; (S) source; (mi) monochromator entrance slit; (c and f) centre of curvature and focal point of mirror M1; (P) centre of curvature of mirror M3 at flame position.

Details of mirror dimensions and mirror to flame distances are given on the next page.

Fig. 2.27 Details of mirror dimensions and mirror to flame  
( cont. ) distances.

Mirror System A

M1 - Concave, rectangular, front-silvered,  
48 x 87mm, focal length 69mm.

M2 - Concave, spherical, front-silvered,  
diameter 62mm , focal length 60mm.

M3 - Concave, spherical, front-silvered,  
diameter 90mm, focal length 57.5mm  
with a rectangular slit in the vertex  
(5 x 20mm)

L - Lens, silica, 30 mm diameter, focal  
length 50mm.

Mirror to flame distances - (M1-F) 145mm;  
(M2-F) 120mm; (M3-F) 115mm. Source and lens  
positioned to give maximal fluorescence  
signal, the lens being ca. 50mm from the flame

Mirror System B

All mirrors front-silvered, spherical, concave  
and 90mm in diameter.

M1 and M2 each have a focal length of 50mm.

L & M3 identical to mirror system A.

Mirror to flame distances - (M1-F) 85mm;  
(M2-F) 100mm; (M3-F) 115mm.

ellipsoidal mirror. By placing the flame in the first focus its image will be formed at the second focus with a 1:1 magnification. The entrance slit can be placed at the second focus. However consider fluorescence radiation travelling in a direction towards the slit. The solid angle of this radiation viewed by the slit is limited by the finite slit dimensions, the collimator diameter and the source-slit distance. Therefore, any radiation falling out of the slit area will be lost. Omenetto et al. minimized this effect by using the mirror M3. This is a spherical mirror at the slit position with a rectangular window (5 x 20 mm) in the vertex for the passage of light. This mirror has a centre of curvature equal to the source slit distance. The net result of the mirrors M1 and M3 is that radiations normally lost are focused back on the source by the mirror at the slit position and consequently on the slit by the ellipsoidal mirror. The lens and mirror M2 fulfill the same function as discussed for fig. 2.26b.

The optics described (Fig. 2.27) were built by Omenetto et al. and they found that a total increase of 17 times in the radiance reaching the monochromator could be obtained when a tungsten filament lamp was at the flame position. However they pointed out that the same improvement could not be expected when measuring flame signals because a) there is a large difference in size between the flame and tungsten filament b) reflected light passing through the flame would be partially absorbed and c) the flame background will be increased to the same extent as the wanted signals. Further evaluation of their optics using the atomic fluorescence and atomic emission of thallium revealed improvements in detection limits of approximately 10 and 5 times respectively. They were using a home-built lock-in

amplifier tuned to 375 Hz and a Jarrell-Ash 0.5 m Ebert monochromator equipped with variable slits.

### The application of an optical arrangement

The Omenetto system was the most promising optical arrangement that the present author could find in the literature. Moreover it was accurately described and evaluated. Unfortunately a manufacturer could not be found who would make an ellipsoidal mirror for less than £150. Consequently a compromise was made and a simple spherical concave mirror substituted in the M1 position, Fig. 2.27. This mirror still collects radiation from the flame and focuses it onto the slit but not as efficiently as the ellipsoidal mirror.

A mirror was supplied by Optiglass Ltd. (Walthamstow, London) with the same specifications as detailed by Omenetto et al. for M3 (5.75 cm focal length, 9 cm diameter, slit in vertex 5 x 20 mm). Two further concave, spherical mirrors were obtained to use in the M2 and M1 positions. The caption to Fig. 2.27 gives details of the dimensions of these mirrors and the mirror to flame distances used, (optical system A). These distances depend on the focal lengths of the individual mirrors. The mirror M3 has its radius of curvature equal to the mirror-flame distance (11.5 cm); radiation from the flame is therefore collected by this mirror and the image formed is focused back onto the flame. The mirror M1 had a focal length of 6.9 cm and knowing that the flame to slit distance was set by the radius of curvature of M3 then with M1 forming an image of the flame at the slit position the M1 to flame distance was calculated to be 14.5 cm (standard optical formula relating object and image distances from the mirror with focal length). The mirror M2 has its radius of curvature equal to the mirror-flame distance

so that the image of the source formed by the lens on the flame is reflected by M2 and focused back on the flame.

In practice the various optical components were placed in their calculated positions and a tungsten filament lamp placed as accurately as possible in the centre of the flame position. The two images formed by M1 and M3, one from each mirror, could then be seen separately at the slit position. Fine adjustments were then made to bring both images into focus onto the slit. It was found that if this was done carefully no further adjustments were necessary when making fluorescence measurements. In the case of mirror M2 and the lens it was possible to obtain an image of the source at the flame position with 1:1 magnification using the lens, and obtain a similar image due to M2. However the lens was only 3 cm diameter and therefore its light gathering power from a source about 3 cm tall was not optimal. Consequently better fluorescence signals were obtained by placing the EDL as close to the lens as possible, the lens as close to the flame as possible and similarly for M2. This resulted in EDL-lens, flame-lens and flame-M2 distances of ca. 2 cm, 10 cm and 10 cm respectively. These dimensions were set by the physical size of the various components and stands.

For the atomic fluorescence of tin in the argon-separated air-acetylene flame, the above optical arrangement gave a factor of 4.4 times improvement in signal-to-noise ratio made up of the factors detailed in Table 2.7.

When the work with these mirrors was carried out the results seemed disappointing in view of the factor of 10 times obtained by Omenetto et al. for their system with the ellipsoidal mirror. However the mirrors M1 and M2 were second hand and in a rather poor condition. Accordingly two new mirrors were

TABLE 2.7

## IMPROVEMENT IN SNR DUE TO OPTICAL SYSTEM 'A'

A 10 ppm aqueous tin solution nebulized into an argon-separated air-acetylene flame. Fluorescence measured at 303.4 nm using a 4.7 s. output time constant. EDL modulated at 10 kHz

Mirrors in use	Signal (arbitrary units)	Noise	SNR	Improvement factor due to individual mirrors	
				Mirror	Factor (times)
None	14.0	2.0	7.0	M1	1.79
M1	25.0	2.0	12.5	M2	1.12
M1 & M2	28.0	2.0	14.0	M3	2.21
M1, M2 & M3	62.0	2.0	31.0	All 3	4.43

obtained from Optiglass Ltd. each with a focal length of 5 cm and a diameter of 9 cm. These front silvered mirrors were larger than the old ones and obviously of superior reflectance. They were substituted into the optical arrangement. The various intercomponent distances are given in the caption to Fig. 2.27 (optical system B).

With the new mirrors a factor of 6 times improvement in the signal-to-noise ratio was obtained under the same conditions as before. This improvement included not only a total increase in the tin fluorescence signal of 12 but also a 2 times increase in noise (Table 2.8). An increase in noise was not observed with the original mirrors (Table 2.7). Further evaluation of the optical system with the new mirrors was carried out by looking at the improvement in the fluorescence of tin in the argon-oxygen-hydrogen and argon-hydrogen flames. (Table 2.8) Here a factor of 29 times enhancement in signal was obtained. Again a two fold increase in noise was observed giving the net increase in signal-to-noise ratio of a factor of 14.5.

Two main observations can be made concerning the effect of the optical system on fluorescence signals. Firstly, compared to the air-acetylene flame the effect of the mirrors when using the argon flames is larger probably because there is less absorption and quenching of the fluorescence radiation, by the flame gases, as it is passed through the flame. Secondly the increase in noise of only two times convincingly demonstrates the effect of modulating at 10 KHz. The signal increases were detected by the p.s.d. tuned to 10 KHz, and the increases in noise rejected because they originated at the low frequency ( $1/f$ ) end of the flame noise spectrum.

To further demonstrate the effect of modulating at

TABLE 2.8

IMPROVEMENT IN SIGNAL-TO-NOISE RATIO CAUSED BY MODIFIED OPTICAL  
SYSTEM 'B'

(A 10 ppm tin solution, 0.4M in hydrochloric acid, was nebulized into three flames. Fluorescence was measured at 303.4 nm in all but the argon-hydrogen flame when the wavelength used was 317.5 nm (Chapter three). Time constant 4.7s, EDL modulated at 10 KHz and temperature controlled at 385 K.

Mirrors in use	Signal (arbitrary units)	Noise	Signal-to-noise ratio	Improvement factor due to use of mirrors (times)
A) Argon-separated air-acetylene flame				
None	6	2	3	
M1	14	-		
M1 and M3	20	-		
M1, M2 & M3	72	4	18	6
B) Argon-hydrogen or argon-oxygen-hydrogen flames				
None	10	2	5	
M1	37	-		
M1 and M3	73	-		
M1, M2 & M3	292	4	73	14.5

10 KHz, the atomic emission of aluminium was detected using the 50 Hz modulated Jarrell-Ash amplifier. No improvement in signal-to-noise ratio was observed although the same large increases in signal occurred. Hofton and Hubbard<sup>151</sup> were also unable to observe improvements in the signal-to-noise ratio of Bismuth fluorescence using the Jarrell-Ash amplifier and a small mirror in the M1 position.

#### The effect of mirrors on analytical curves

Browner et al.<sup>226</sup> were apparently the first researchers to determine the effect of mirrors M1 and M2 (Fig. 2.27) on analytical curves. They demonstrated that both M1 and M2 are each able to advance the incidence of curvature of the lead analytical curves. In the case of the source mirror M2 at low concentrations, light reflected by M2 will not be significantly depleted of resonance radiation by the atomic population in the flame. Therefore an increase in fluorescence will occur because of the double pass of source radiation. However at high concentrations the depletion of source resonance radiation after passing through the flame will be significant and the effect of the mirrors smaller. The improvement will therefore tend to reduce with increasing concentration. The effect will occur for both resonance and non-resonance fluorescence. In the case of mirror M1 the resonance fluorescence radiation which is passed back through the flame by M1 will be partially absorbed by the atomic population in the flame. This self-absorption will increase with the concentrations of metal atoms in the flame and cause the premature bending of the analytical curves obtained with mirrors in place. The self-absorption effects of mirror M1 would not be expected with for example, direct-line fluorescence where the fluorescence line is not a resonance line. In the

present work the effect of self-absorption of the arsenic resonance line at 189.0 nm with and without mirrors M1 and M3 was determined. The results are shown in Fig 4.18. The expected advanced incidence of curvature was observed with the mirrors in place.

### 2.3.5. Two further considerations of atomic fluorescence

#### a) Scatter

Light scattering of incident radiation by solvent droplets and unvaporized solute particles in the flame is a well recognised interference in atomic fluorescence spectroscopy. The theoretical aspects of light scattering have been studied by Omenetto et al.<sup>227</sup> To correct for incident light scattering<sup>149</sup> a continuum source or a line source can be used. With a line source, a non-fluorescent line of equal or higher intensity is selected to correct for scatter. The non-fluorescent line should be within 10 nm of the analyte line. Rains et al.<sup>189</sup> have reported the use of an instrument which automatically corrects for light scatter using a xenon lamp and a lock-in amplifier. Blank solutions which simulate the sample matrix but without the analyte are also used to correct for scatter<sup>7.149</sup>. This latter method is the one that was used throughout the thesis. Scatter was never a serious problem here because all blanks for steel analysis contained 10,000 ppm iron. If any scatter was occurring it would be expected to be far greater from 10,000 ppm iron than from the analyte or any other minor concomitant. For tin, arsenic and aluminium at the analytical wavelengths and at the instrument sensitivity for 10 ppm full scale deflection significant (more than twice the standard deviation) signals were not observed when aspirating 2500 ppm sodium tungstate, 10,000 ppm iron or distilled water. When measuring detection limits

i.e. at maximum sensitivity, signals were observed for 10,000 ppm iron relative to water. These signals differed in magnitude depending upon which flame was being used. In general the argon-hydrogen flame gave a scatter signal which was far larger than the scatter signals in the argon-oxygen-hydrogen, air-acetylene and nitrous oxide-acetylene flames. Incomplete vaporization of the iron solution is more likely in the cooler flames consequently the relative magnitudes of the scatter signals observed showed decreased scatter with increase in flame temperature. The nitrous oxide-acetylene flame gave an 10,000 ppm iron scatter signal at the analytical wavelength of all three elements studied but its magnitude was only equivalent to that concentration of analyte which represented the detection limit. For tin and arsenic non fluorescent source lines were available (tin 285.0 nm and arsenic 188.2 nm) which were used to obtain some indication of whether analyte signals were scatter or fluorescence. Fluorescence was always confirmed.

b) Spectral bandpass

Spectral interference occurs when another element emits fluorescence radiation simultaneously with the test element and both wavelengths fall within the spectral bandpass of the monochromator. With line sources such interferences are rare, hence the usefulness of nondispersive fluorescence (section 2.1).

The spectral bandpass ( $s$ ) of a monochromator also influences the fluorescence signal through equation (1), section 2.2.1. and the signal-to-noise ratio as discussed in section 2.2.1 (c). With variable slits it is possible to find an optimal slit width ( $W$ ). However in the work reported here only fixed slits (100 mm entrance and 150  $\mu$ m exit) were available. The 150  $\mu$ m exit slit determined the effective spectral bandpass

which is given by <sup>7</sup> :

$$s = R_d W$$

where  $R_d$  is the reciprocal linear dispersion of the monochromator in the first order and is given by <sup>7</sup> :

$$R = \frac{10^3}{\xi F}$$

where  $\xi$  is the number of lines per cm ruled on the grating, and  $F$  is the monochromator focal length. For the Jarrell-Ash monochromator used  $F$  was 50 cm and  $\xi$  was  $1.8 \times 10^4$ .  $s$  was therefore 0.25 nm.

### 2.3.6. Conclusion

The improvements in instrumentation described in the preceding sections all resulted in significant improvements in signal-to-noise ratio. The lock-in amplifier formed the basis for almost all the improvements. Its particular versatility, the ability to be tuned to any frequency from 50 Hz to 20 KHz, resulted in an optimal modulation frequency of 10 KHz. This modulation frequency allowed the EDL's to be modulated to a greater depth than is possible at 50 Hz modulation. Taking the signal channel from the  $1/f$  noise dominated 50 Hz region of the noise spectrum to 10 KHz resulted in a significant decrease in noise.

The optical system increased the fluorescence signal-to-noise ratio to a greater extent than is normally expected. This was because the noise increase due to the mirrors takes place at low frequencies where flame noise is greatest and where the lock-in amplifier, when modulated at 10 KHz, has little response.

Flame separation was effective in decreasing fluorescence quenching by preventing air entrainment. This led to significant increases in signal. A slight decrease in shot noise from the

flame was also observed. However the large decreases in noise levels observed by many workers in the past, were not observed because these take place at low frequencies.

Temperature control greatly simplified the use of EDL's particularly in the case of aluminium where high microwave powers would have been necessary to obtain sufficient output radiance. The EDL output was also considerably improved in terms of stability and reproducibility.

Finally the lock-in amplifier did not give a d.c. output due to strong background emission from the flame or from strongly emitting elements in the flame. This meant that the baseline was particularly stable and interferences from the emission of elements minimised.

## CHAPTER THREE

The application of atomic fluorescence spectrometry to the determination of tin in steels3.1 Introduction

Atomic fluorescence spectrometry has been used for the determination of Lead<sup>228</sup>, Silicon<sup>229</sup>, Bismuth<sup>150</sup>, Chromium and Manganese<sup>230</sup> and Cobalt and Nickel<sup>231</sup> in steels. The present author has not been able to find any published methods for the determination of tin in steels using this technique. Tin can have a detrimental effect on the hot-workability of carbon steels<sup>232</sup> and temper-brittleness can be caused by the presence of trace amounts of tin in alloy steels<sup>233</sup>. For these reasons the concentration of tin in steels is frequently determined. This concentration is usually within the range 0.005 to 0.1 per cent.

Browner et al<sup>9</sup> describe the determination of tin by atomic fluorescence and quote a detection limit of 0.1 ppm using the nitrogen-separated argon-oxygen-hydrogen flame. Several severe interferences were found using flame conditions that gave optimum sensitivity. However, the use of a leaner flame minimised these interferences.

In the atomic absorption determination of tin the nitrous oxide-acetylene flame has usually been chosen because the sensitivity has been adequate for many published applications<sup>234,238,239</sup> and because interferences are small compared to the large number of interferences found in the cooler hydrogen flames<sup>234-237,242,243,249</sup>. The

1947

1. The first part of the document discusses the general situation of the country and the progress of the revolution. It mentions the achievements of the revolution and the challenges it faces. The document also discusses the role of the people in the revolution and the need for a united front.

2. The second part of the document discusses the economic situation of the country and the need for economic reforms. It mentions the need for a new economic policy and the need to mobilize the resources of the country. The document also discusses the need for a new economic system and the need to improve the living standards of the people.

3. The third part of the document discusses the political situation of the country and the need for a new political system. It mentions the need for a new political party and the need to improve the political system. The document also discusses the need for a new political system and the need to improve the living standards of the people.

4. The fourth part of the document discusses the cultural situation of the country and the need for a new cultural system. It mentions the need for a new cultural policy and the need to mobilize the resources of the country. The document also discusses the need for a new cultural system and the need to improve the living standards of the people.

5. The fifth part of the document discusses the military situation of the country and the need for a new military system. It mentions the need for a new military policy and the need to mobilize the resources of the country. The document also discusses the need for a new military system and the need to improve the living standards of the people.

6. The sixth part of the document discusses the international situation of the country and the need for a new international system. It mentions the need for a new international policy and the need to mobilize the resources of the country. The document also discusses the need for a new international system and the need to improve the living standards of the people.

7. The seventh part of the document discusses the future of the country and the need for a new future system. It mentions the need for a new future policy and the need to mobilize the resources of the country. The document also discusses the need for a new future system and the need to improve the living standards of the people.

sensitivity in the nitrous oxide-acetylene flame is intermediate between the less sensitive air-acetylene flame and the more sensitive cool flames<sup>234</sup>. Where absorption sensitivity was not adequate the traditional method of concentration using solvent extraction techniques has been used<sup>240,241</sup>. However, Nakahara et al<sup>242</sup> have described an investigation of the large number of interferences with tin determinations using atomic absorption in the nitrogen-hydrogen, argon-hydrogen and air-hydrogen flames. Iron III chloride was found to be very effective in eliminating interferences from other elements with only a few exceptions. Six acids were also found to interfere seriously with the atomic absorption determination but the effect of iron III chloride on the acid interferences was not reported. The use of iron III chloride was satisfactorily applied to a direct method for the determination of tin in copper-base alloys and steel. The sensitivity for 1% absorption, 0.12 ppm in the argon-hydrogen flame, was similar to that obtained by solvent extraction methods<sup>240,241</sup> and up to an order of magnitude better than the various other direct methods that employ the nitrous oxide-acetylene flame<sup>234,238</sup>.

Juliano and Harrison<sup>243</sup> studied the interferences of various metals and inorganic acids on tin determinations using atomic absorption in a premix air-hydrogen flame over a wide range of flame conditions. Comparative studies made in the air-acetylene and nitrogen-hydrogen flames showed that although tin has a better sensitivity in the hydrogen flames, it is also

1. The first part of the document discusses the importance of maintaining accurate records of all transactions and activities. It emphasizes that proper record-keeping is essential for transparency and accountability, particularly in financial matters. The text suggests that organizations should implement robust systems to track and report on their operations, ensuring that all data is up-to-date and easily accessible.

2. In the second section, the author addresses the challenges of data security and privacy. With the increasing reliance on digital technologies, the risk of data breaches and unauthorized access has become a significant concern. The document recommends that organizations should invest in strong cybersecurity measures, including encryption, firewalls, and regular security audits, to protect sensitive information and maintain the trust of their stakeholders.

3. The third part of the document focuses on the role of leadership in driving organizational success. It argues that effective leaders are those who can inspire and motivate their teams, set clear goals, and foster a culture of innovation and collaboration. The text provides several key strategies for leadership, such as active listening, open communication, and the ability to adapt to changing circumstances. It also highlights the importance of ethical leadership and the need for leaders to act with integrity and fairness.

4. The final section of the document discusses the impact of external factors on organizational performance. It notes that organizations must be aware of their operating environment, including market trends, regulatory changes, and global events. The text suggests that organizations should develop a strategic vision and a flexible business plan that can respond to these external challenges. It also emphasizes the importance of building strong relationships with key stakeholders, such as customers, suppliers, and regulatory bodies, to ensure long-term success and sustainability.

much more subject to interferences than in the air-acetylene flame. Levine et al<sup>244</sup> deal specifically with the effect of potassium on the determination of tin in technical grade potassium stannate using atomic absorption. This enhancing interference was compensated for by adding potassium to the standard solutions.

Smith<sup>245</sup> used atomic absorption spectrometry to determine trace levels of tin in aqueous solution in order to investigate the effect of pH upon the stability, solubility and ease of absorption during storage of tin solutions.

Engberg<sup>246</sup> compared a spectrophotometric (Quercetin) method and an atomic absorption method for the determination of tin in canned foods (range 10 to 1000 ppm) and organotin residues (range 0.01 to 1 ppm). It was concluded that the Quercetin method was to be preferred for the low tin concentrations but both methods were equally useful for the determination of tin in concentrations normally found in canned foods. These conclusions were based on the accuracy, precision and sensitivity of the two methods. Atomic absorption was not sensitive enough for determining organotin residues using the Perkin-Elmer 403 instrument available to Engberg.

The best sensitivity for 1% absorption, 0.12 ppm, was reported by Nakahara et al<sup>242</sup> Winefordner and Elser<sup>5</sup> quote atomic absorption detection limits (0.03 ppm) taken from two sources<sup>247,248</sup> which are unfortunately difficult to compare with atomic fluorescence because of some confusion over the defini-

tion of detection limit. In atomic fluorescence Browner et al.<sup>9</sup> have reported the best detection limit for tin using a Perkin-Elmer 290 modified for fluorescence work. In their work a 0.1 ppm solution gave a signal which was as great as the background noise fluctuations; i.e. a detection limit of 0.2 ppm (detection limits in this thesis are defined as that concentration resulting in a signal-to-noise ratio of two).

The work described in this chapter demonstrates that the atomic fluorescence determination of tin is affected by interferences very similar to those found in atomic absorption by Nakahara et al.<sup>242</sup> and Juliano and Harrison<sup>243,249</sup>. This work also demonstrates that the use of more sophisticated instrumentation improves the detection limit for the atomic fluorescence determination of tin to the point where the full range of tin concentrations in steels can be measured without recourse to the solvent extraction techniques that are necessary in atomic absorption<sup>241</sup>. Moreover, this is achieved using the popular air-acetylene flame rather than the cooler hydrogen flames. If necessary, further improvements in sensitivity can be obtained using the argon-oxygen-hydrogen flame. The argon separated nitrous oxide-acetylene flame was found to be the least sensitive flame for the atomic fluorescence determination of tin.

The work on the determination of tin in steels revealed that iron has a depressing effect on tin fluorescence in the

hydrogen flames investigated. This depressing effect does not occur when iron is present at a concentration of less than 2000 ppm. The effect of iron was compensated for by the addition of iron III chloride to the calibration standards.

Silicon present in the steel samples also interfered with the tin determination. The silicon was therefore removed by filtration or volatilization with hydrofluoric acid, the latter being the preferred method of removal.

### 3.2 Optimisation of conditions for measurement of tin fluorescence

When building the instrument and optimising for atomic fluorescence measurements the atomic fluorescence of tin was used. Consequently the optimisation of flame conditions for tin and the choice of the most sensitive wavelengths were done at an early stage on an incompletely optimised instrument. These parameters were assumed to remain unchanged irrespective of the sensitivity of the measurements. The work on the interferences affecting the determination of tin in aqueous solutions and the determination of tin in solutions of steels was carried out using an unthermostated electrodeless discharge lamp. Detection limits were measured, on completion of the interference work, using a thermostated lamp.

The reagents and measurement procedures used for all the work described in this thesis are given in appendix 2.

### 3.2.1 Stability of trace levels of tin in aqueous solution

Smith<sup>245,250</sup> has examined the relationship between stability and pH for a variety of trace metal solutions including tin solutions. It was found that, with the exception of lithium, none of the metal solutions investigated is stable over the pH range 1.5 to 11 at the 1 or 10 ppm level. To ensure stability of solutions containing the metal ions it was found necessary to acidify them to pH 1.5 or less with hydrochloric acid immediately after sampling or preparation.

In this work, except where otherwise stated, all tin solutions were made up in 0.4M hydrochloric acid to keep the pH less than 1.5. Solutions made up in this way were stable for at least two weeks whereas solutions made up in deionised water were stable for less than an hour.

### 3.2.2 Choice of gas flow rates, flame separation and flame height

The gas flow rates in the premixed air-acetylene, argon-hydrogen, argon-oxygen-hydrogen and nitrous oxide-acetylene flames were optimised by observing the atomic fluorescence signal from 10 ppm tin solutions, except for the nitrous oxide supported flame, a 1000 ppm tin solution was used. The fluorescence was measured at 303.4 nm. The optimal flow rates for each of the four flames both separated and unseparated are listed in Table 3.1. The variations in the tin atomic fluorescence signal with gas flows in three of the

TABLE 3.1

## GAS FLOW RATES

flow rates giving optimal sensitivity for the determination of tin  
by atomic fluorescence using various flames)

flame		Gas flow rates (l min <sup>-1</sup> )	
		unseparated flame	argon separated flame (argon flow 6.0 l min <sup>-1</sup> )
air-acetylene	Air	3.7	3.7
	Acetylene	1.25	0.9
argon-hydrogen	Argon	3.7	-
	Hydrogen	1.0	-
argon-oxygen- hydrogen	Argon	3.7	3.7
	Hydrogen	1.0	1.0
	Oxygen	0.5	0.5
nitrous oxide- acetylene	Nitrous oxide	3.7	3.7
	acetylene	3.2	3.2

flames are given in Figs 3.1 to 3.5. These figures also show the effect of flame separation on the fluorescence signals.

In the unseparated air-acetylene and nitrous oxide-acetylene flames the highest signal intensities occur in the fuel-rich flames. This is also the case in atomic absorption. The reasons for this, in atomic absorption, have been discussed by Ramirez-Munoz<sup>117</sup>, Menis and Rains<sup>251</sup> and Gilbert<sup>252</sup>. These authors discuss the exceptional excitation observed for many elements in fuel-rich flames and use the terms over-excitation or chemiluminescence to describe the phenomenon. Not only are there various kinds of overexcitation but tin is often considered a special case<sup>252</sup> because it exhibits an abnormally high population of free atoms in the cooler hydrogen flames. Apparently the overexcitation of tin is not yet understood<sup>252,253</sup>. Various general hypotheses explaining the reactions taking place in fuel-rich flames which favour production of free atoms are discussed by Mavrodineanu and Boiteux<sup>193</sup> and Gilbert<sup>252</sup>.

The oxygen flow in the argon-oxygen-hydrogen flame (Fig.3.4) is critical as reported by Browner et al<sup>9</sup> for the atomic fluorescence of tin in this flame. However the maximum in the signal obtained by these workers when varying the hydrogen flow could not be reproduced on our instrument. The optimal hydrogen flow in both the argon-

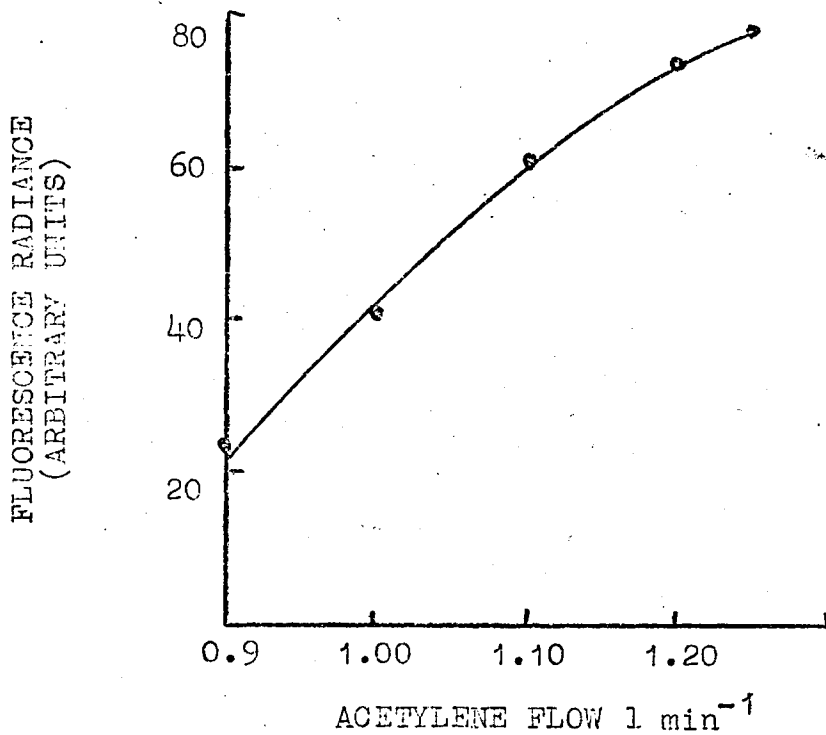


Fig. 3.1 Variation of tin fluorescence with fuel flow in the air-acetylene flame.  
Air flow 3.7 l min<sup>-1</sup>

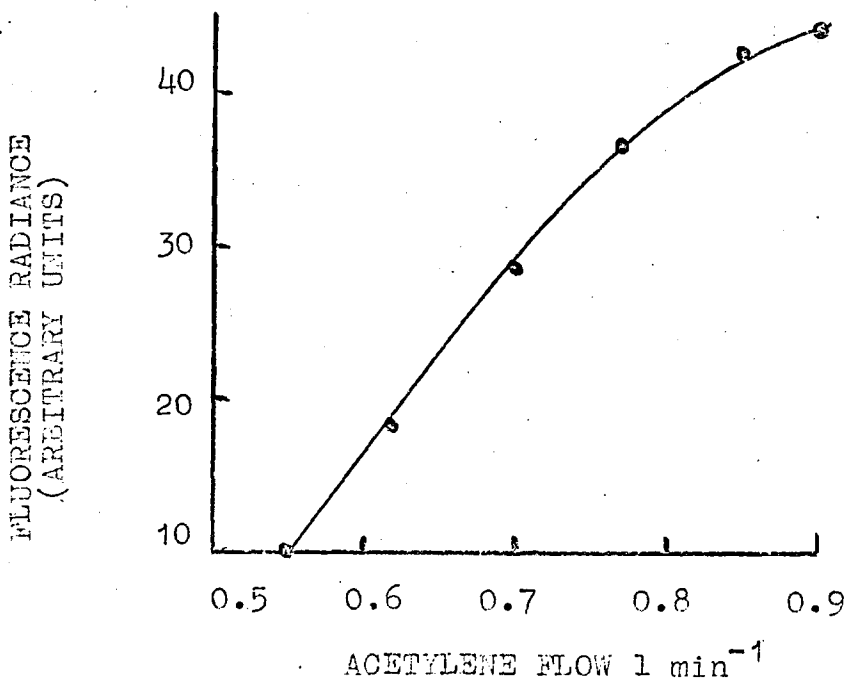


Fig. 3.2. Variation of tin fluorescence with fuel flow in the argon-separated air-acetylene flame.  
Air flow 3.7 l min<sup>-1</sup>

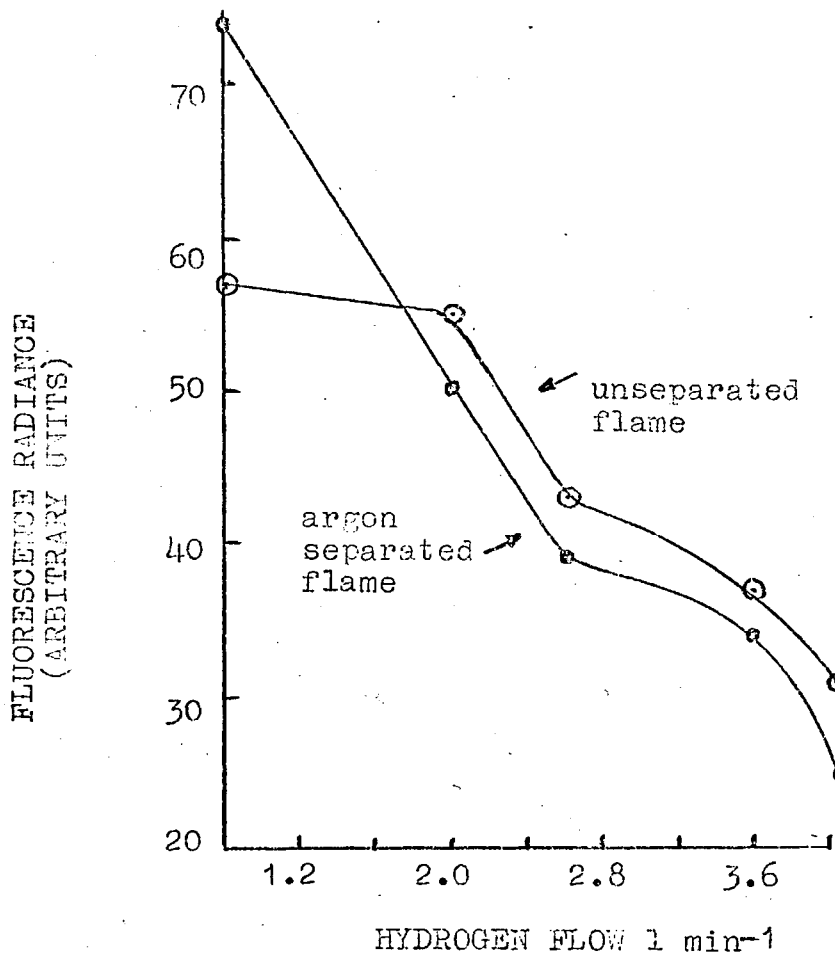


Fig. 3.3 Variation of tin fluorescence with fuel flow in the argon-oxygen-hydrogen flame.  
 Argon flow -  $3.7 \text{ l min}^{-1}$   
 Oxygen flow -  $0.5 \text{ l min}^{-1}$

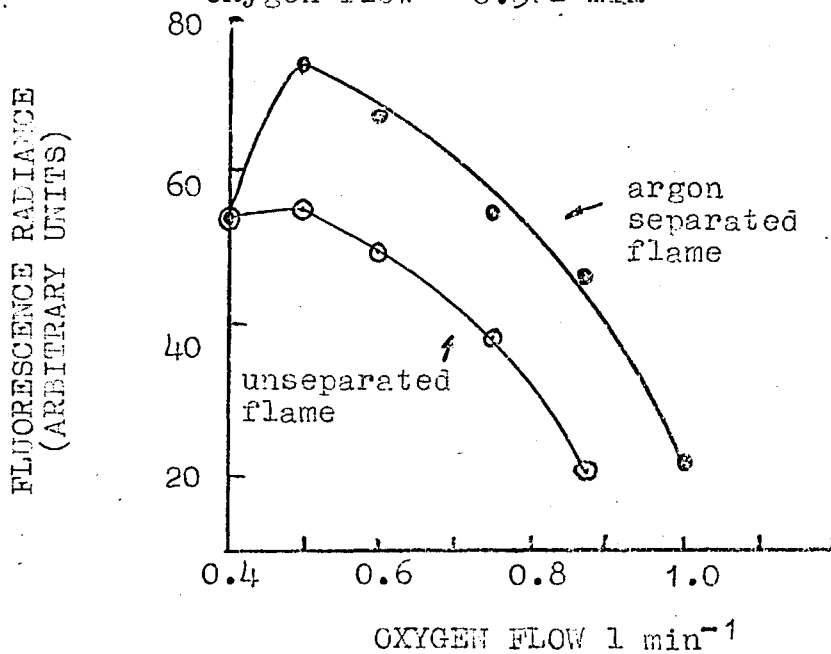


Fig. 3.4 Variation of tin fluorescence with oxygen flow in the argon-oxygen-hydrogen flame.  
 Argon flow -  $3.7 \text{ l min}^{-1}$   
 Hydrogen flow -  $0.8 \text{ l min}^{-1}$

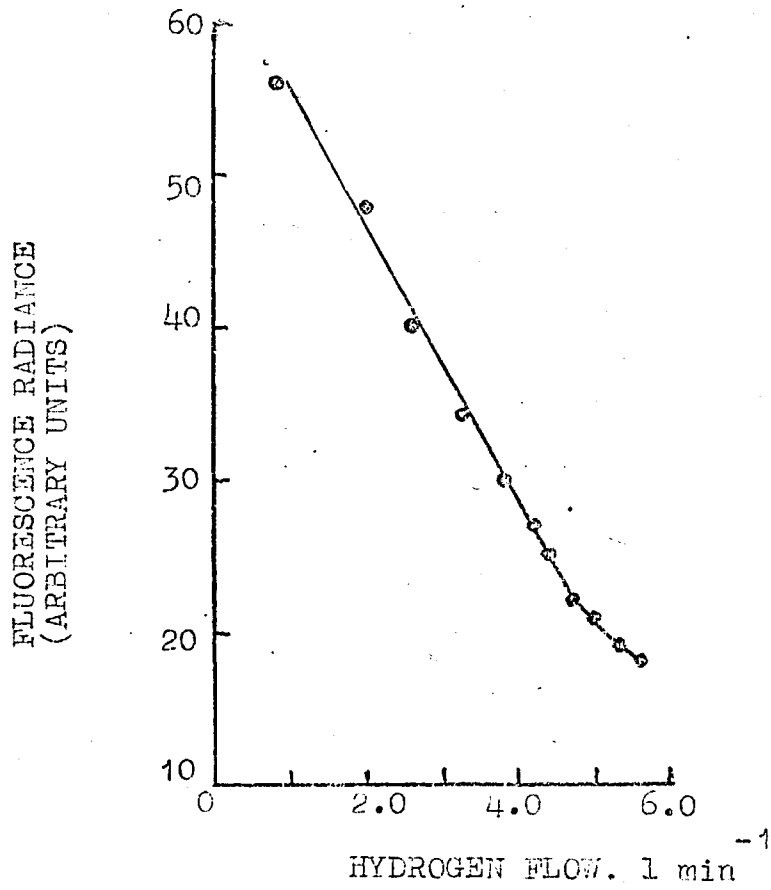


Fig. 3.5. Variation of tin fluorescence with hydrogen flow in the argon-hydrogen flame. Argon flow -  $3.7 \text{ l min}^{-1}$

hydrogen and argon-oxygen-hydrogen flames (Fig.3.5 and Fig.3.3 respectively) was found to be the same.

Neither the air-acetylene nor the nitrous oxide-acetylene flames can be separated when fuel-rich. However the most sensitive conditions in the argon-separated air-acetylene flame gave a factor of 3.8 improvement over the optimal conditions in the unseparated fuel-rich flame. This factor of 3.8 was due not only to a reduction in noise by about 1/3 but also to an increase in fluorescence emission (Table 3.2). Browner and Manning<sup>18</sup> quote a factor of 4.0 improvement in the detection limit for tin fluorescence upon a separation of the air-acetylene flame.

In our work a factor of ten improvement in detection limit was obtained upon argon separation of the nitrous oxide-acetylene flame. This was due to an increase in fluorescence signal of a factor of 3 and an increase in the photomultiplier tube operating voltage from 700 to 850 volts. Without separation the noise from the flame saturated the input to the lock-in-amplifier at ca 700 volts. After separation there was a reduction in noise and it was therefore possible to improve the signal-to-noise ratio by operating the photomultiplier at the higher voltage. The nitrous-oxide flame was always operated under stoichiometric conditions both when separated and unseparated because the Beckman RIIC circular slot burner used easily "sooted up" if the more sensitive fuel-rich conditions were used.

TABLE 3.2

## IMPROVEMENT IN SNR DUE TO FLAME SEPARATION

(A 10 ppm aqueous tin solution nebulized into an air-acetylene flame. Fluorescence measured at 303.4 nm using a 4.7s. output time constant. The optical system was not fully optimised, EDT modulated at 10 kHz)

Fuel flow $l\ min^{-1}$	Air flow $l\ min^{-1}$	Signal (arbitrary units)	Noise	SNR	
1.25 <sup>a</sup>	3.7	24.0	3.0	8.0	unseparated
0.90	3.7	9.0	3.0	3.0	unseparated
0.90 <sup>b</sup>	3.7	60.5	2.0	30.3	argon- separated

a) Fuel-rich flame giving most sensitive conditions for Tin determinations.

b) Fuel flow maximum possible consistent with preventing the argon from extinguishing the flame.

The effect of argon separation on the atomic fluorescence signal from the argon-oxygen-hydrogen flame (Fig.3.3) was to increase the signal by 30% when using the optimal gas flows but there was no attendant decrease in noise levels from the flame. The separation of this flame was therefore considered unjustified, especially in view of the large amount of argon required ( $6 \text{ l min}^{-1}$ ).

Variation in flame height with respect to the monochromator entrance slit gave very little variation in tin fluorescence detected. This was expected because it has been pointed out by Benetti et al<sup>225</sup> that the optical arrangement used in their study does not allow a specific flame zone to be observed or excluded. The optical system on our instrument is similar to the one used by Benetti et al.

### 3.2.3 Operating conditions for the tin electrodeless discharge lamp used as source

Three different tin electrodeless discharge lamps were used in this work. All of these, when new, gave approximately the same output radiance and the resulting atomic fluorescence detection limits were also approximately the same. The characteristics peculiar to these lamps are discussed in chapter two together with the reasons for the choice of operating conditions.

The source was modulated at a frequency of 10kHz and was best operated in a 1/4 wave cavity although a 3/4 wave cavity was used for one lamp. The maximal percentage modulation that the equipment could deliver was used for both cavities.

When the lamps were temperature controlled the operating temperature giving the maximal radiant output was 385 K (Fig.3.6). This rather low temperature reflects the high volatility of the tin iodide in the lamp. Whether the lamp was temperature controlled or not the incident microwave power that gave the maximum lamp radiance (Fig.3.7) was 40 watts (with ca 10 watts reflected power)

#### 3.2.4 Atomic fluorescence spectra of tin excited in four flames. Sensitivities in the different flames

The atomic fluorescence spectra of tin excited in each of the four flames listed in Table 3.1 were obtained (Figs.3.8 to 3.11 and Table 3.3) and all showed similar characteristics to the fluorescence spectrum of tin in the argon-oxygen-hydrogen flame reported by Browner<sup>9</sup> et al.

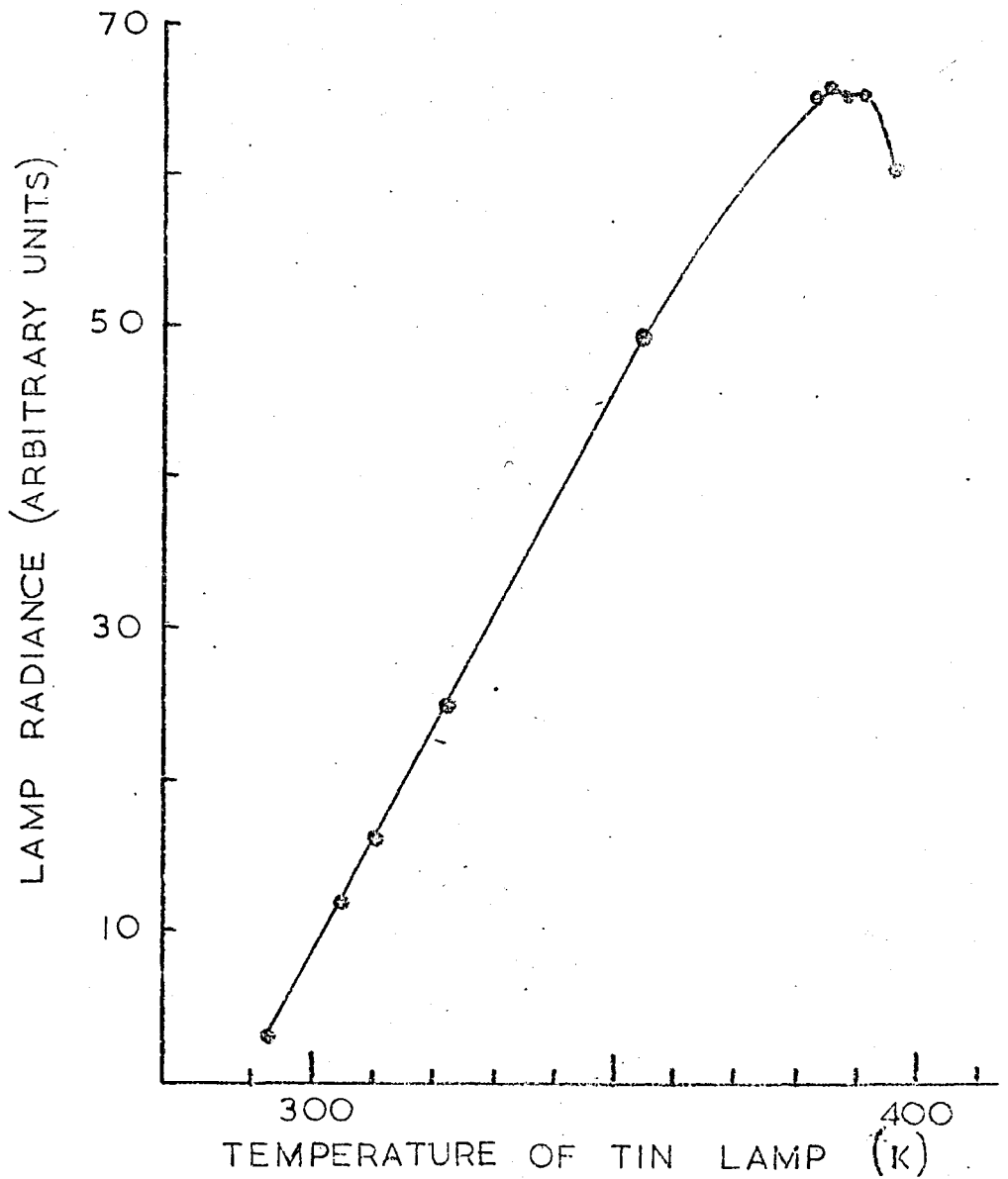


Fig. 3.6. Plot of radiant output of the tin EDL at 303.4nm vs. temperature of the lamp. Lamp operated at 40W incident microwave power in the  $\pi$  wave cavity and modulated at 10KHz.

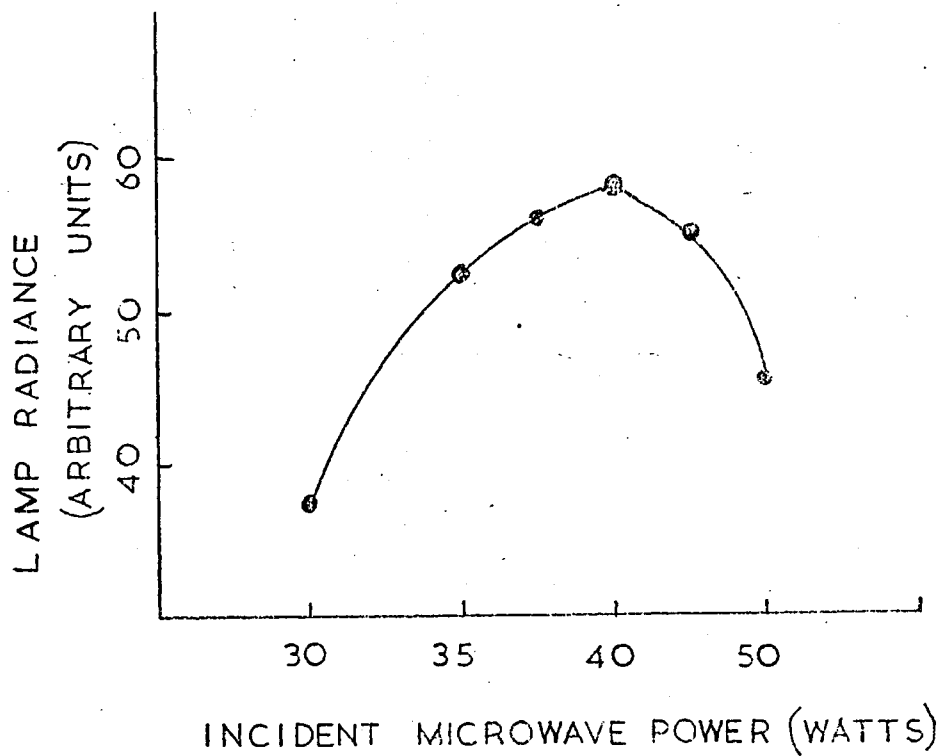


Fig. 3.7. Plot of radiant output of the tin EDL at 303.4nm vs. incident microwave power. (Reflected power ca 7W) Lamp temperature controlled at 385 K although no compensation was made for the effect of microwave heating. Lamp operated in a wave cavity and modulated at 10 kHz.

Fig. 3.8. The atomic fluorescence spectrum of tin excited in the argon-separated air-acetylene flame.

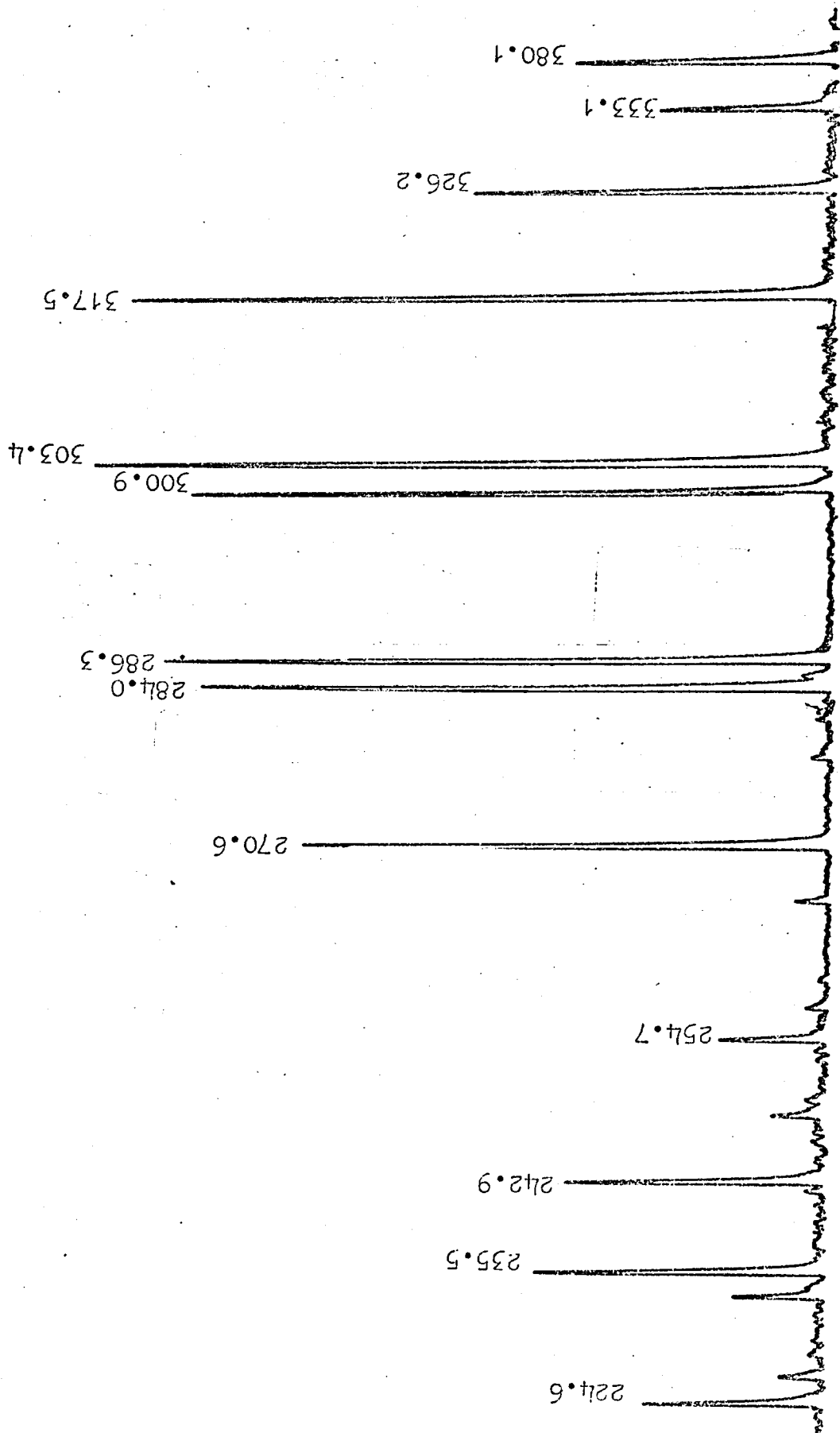


Fig. 3.9 The atomic fluorescence spectrum of tin excited in the argon-separated nitrous oxide-acetylene flame.

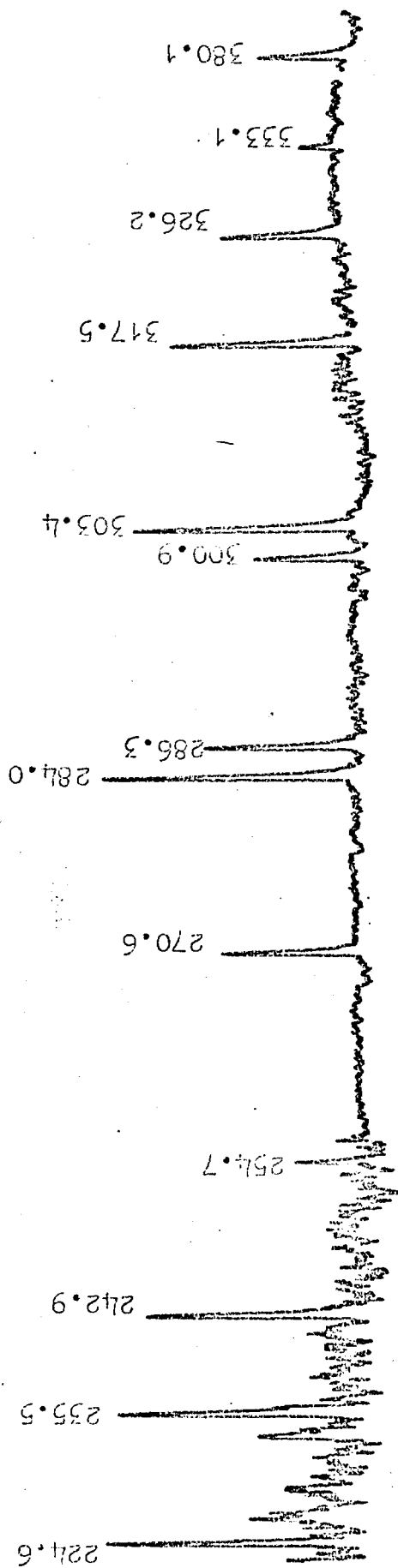


Fig. 3.10 The atomic fluorescence spectrum of tin excited in the argon-oxygen-hydrogen flame.

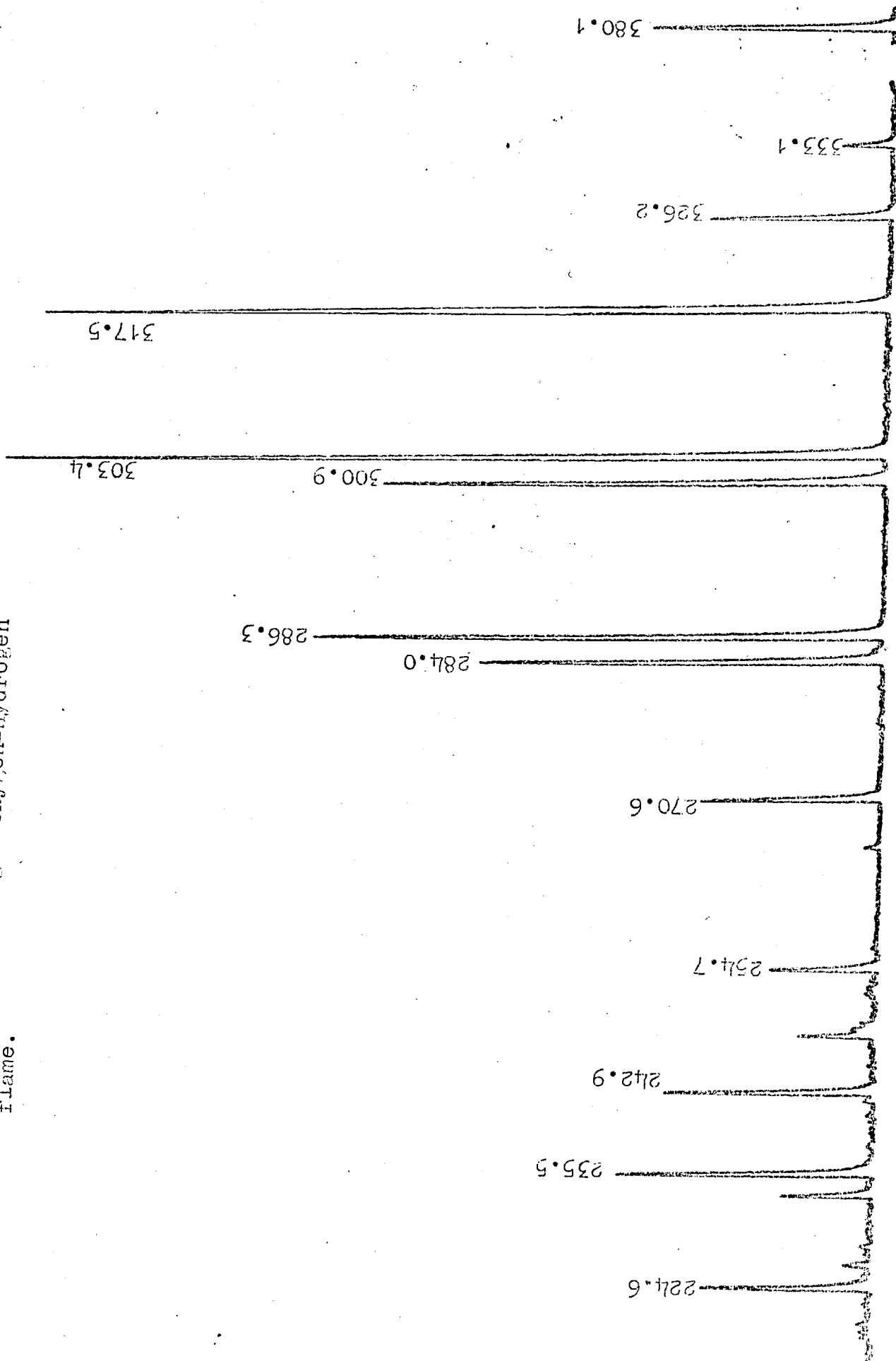
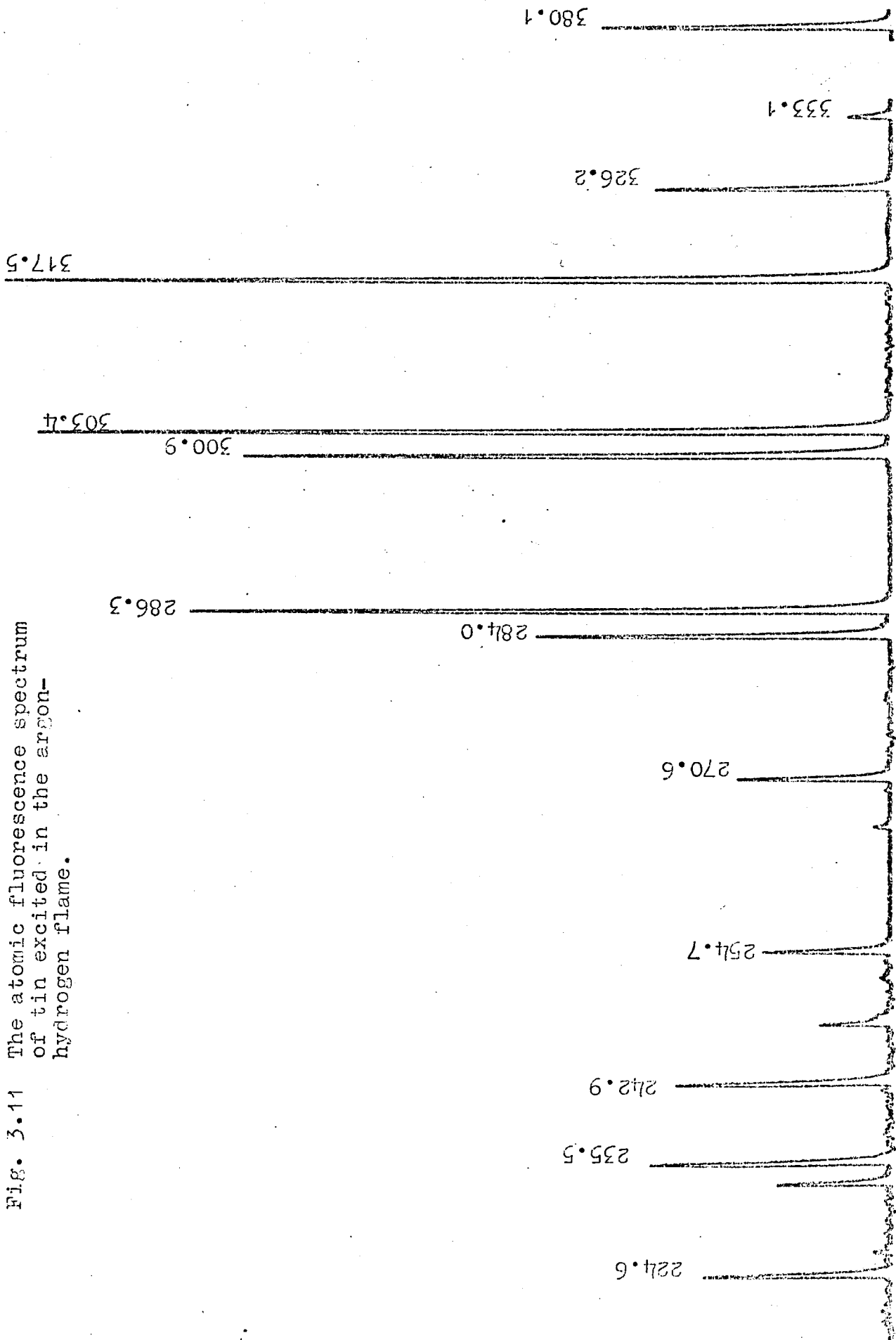


Fig. 3.11 The atomic fluorescence spectrum of tin excited in the argon-hydrogen flame.



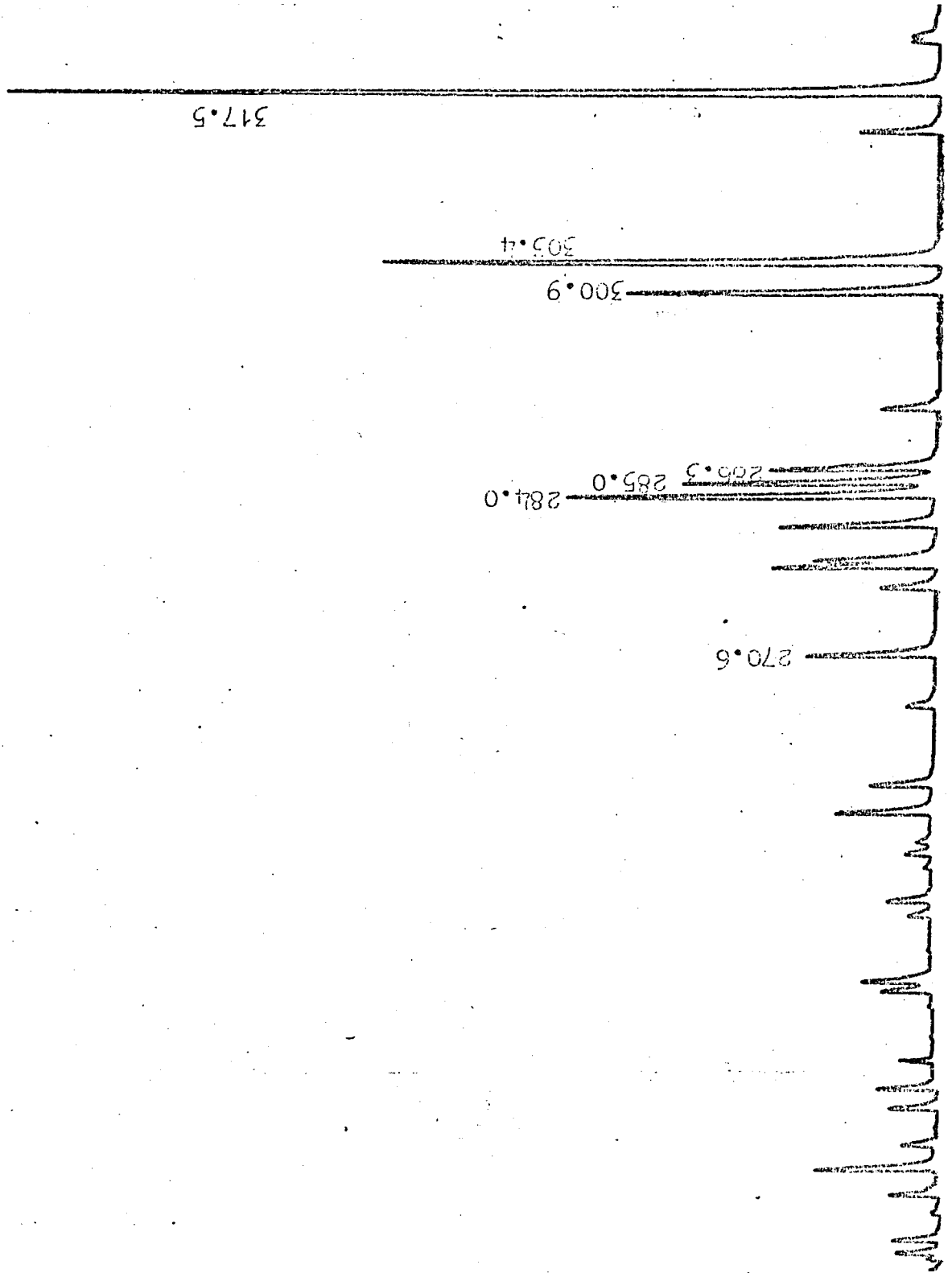
BLE 3.3

INSTRUMENTAL CONDITIONS USED TO OBTAIN ATOMIC FLUORESCENCE  
SPECTRA OF TIN IN FOUR FLAMES

(Gain of photomultiplier tube at 750 volts is approximately 17 times that at 500 volts, and gain at 900 volts is approximately 10 times that at 800 volts)

flame	concentration of solution nebulized (ppm)	Photomultiplier voltage (volts)		Chart recorder		monochromator scan speed nm min <sup>-1</sup>
		below 260nm	above 260nm	full scale deflection (volts)	chart speed (min cm <sup>-1</sup> )	
acetylene	100	900	800	1.0	2.5	2
acetylene	100	900	800	1.0	2.5	2
acetylene	500	900	800	1.0	2.5	2
acetylene	1000	750	500	0.2	2.5	2

Fig. 3.12 The spectrum of the radiant output of the tin EDL.



Browner et al.<sup>9</sup> did not observe the 224.6 nm resonance transition or the 235.5 nm line in the argon-hydrogen flame. These two lines were observed in the present work when using the latter flame. Browner et al. did not give any explanation for not being able to observe the 224.6 or 235.5 nm transitions in the argon-hydrogen flame. They did, however, observe these lines in the Ar/O<sub>2</sub>/H<sub>2</sub> flame and the sensitivity in this flame was significantly better than in the Ar/H<sub>2</sub> flame in their work. As the detection limits obtained in the work presented here (section 3.3.8) are better than an order of ten superior to those limits obtained by Browner et al., it is probable that the latter workers did not observe the two lines in question because of a lack of sensitivity.

In this study the most sensitive lines in each flame were Ar/O<sub>2</sub>/H<sub>2</sub> 303.4 nm; Ar/H<sub>2</sub> 317.5 nm; Air/C<sub>2</sub>H<sub>2</sub> 303.4 nm; and N<sub>2</sub>O/C<sub>2</sub>H<sub>2</sub> 284.0 nm. These are the same wavelengths as found by Browner et al.<sup>9</sup> with the exception of the nitrous-oxide-acetylene flame which they did not study. The sensitivities in the two hydrogen flames were the same whereas Browner et al. reported that the

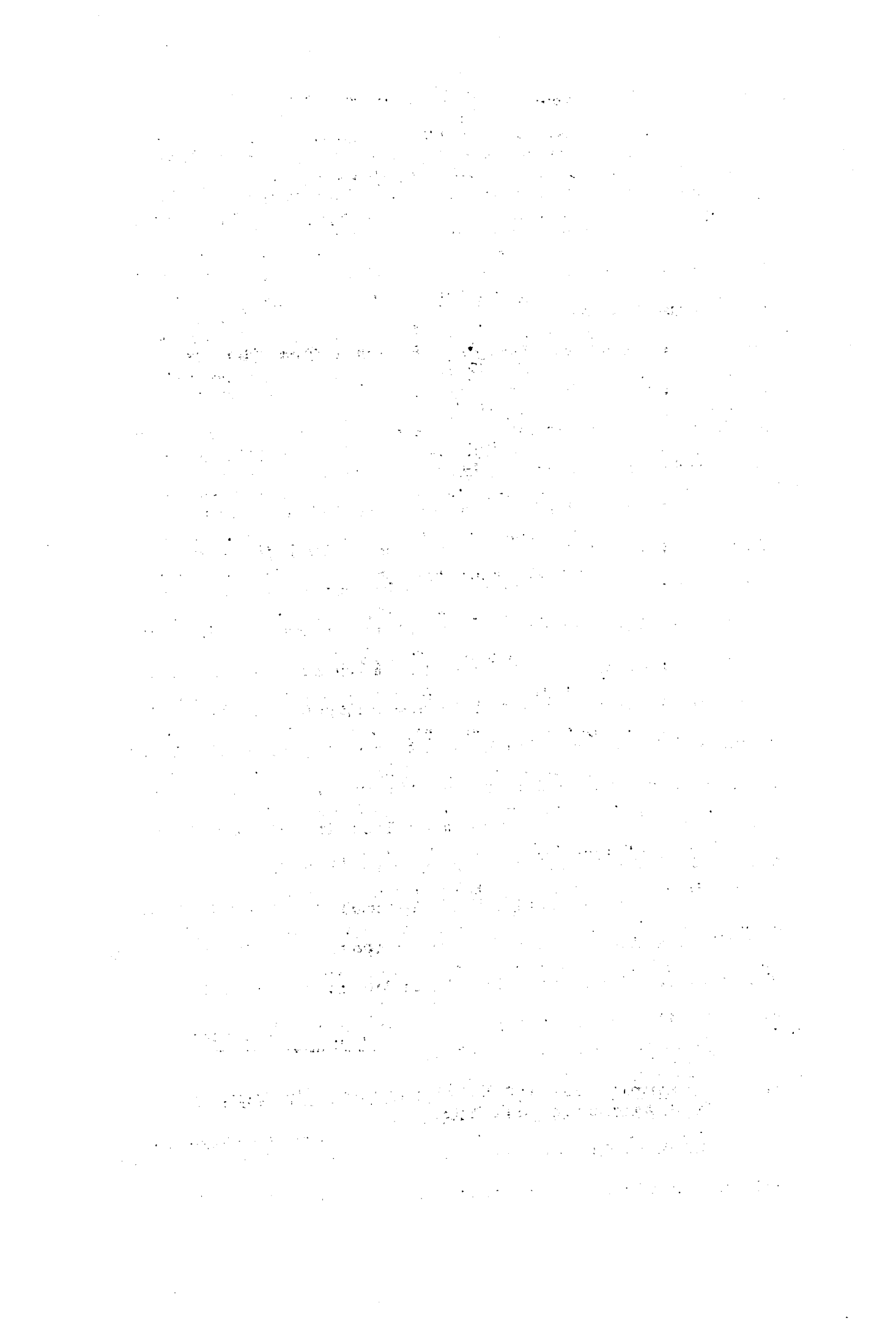
Ar/O<sub>2</sub>/H<sub>2</sub> flame is more sensitive, at the 100 ppm level, by approximately a factor of two. However, fuel flows in the present work were very different to those by Browner et al as mentioned in section 3.2.2. The latter workers used a hydrogen flow of ca 5 l min<sup>-1</sup> implying that their flame was physically larger than the one used in this work. The geometry of the flame may therefore be playing an important part in determining the relative sensitivities in the two hydrogen flames.

Browner and his coworkers carried out filtering studies in order to examine in more detail the fluorescence processes occurring in the hydrogen flames. From their work they conclude that the unexpectedly high ratio of the intensity of the 303.4 to 286.3 nm line implies that the <sup>3</sup>P<sub>1</sub> state (see atomic term diagram Fig 3.13) is populated by a quasi luminescent process, probably involving chemical reduction of the tin salt. In the nitrous-oxide flame this process appears less important although the 303.4 line is still very intense (Fig 3.11).

The most sensitive line in each flame was selected for the detailed work on interferences because preliminary observations indicated that interferences were not significantly different at any of the other wavelengths.

### 3.3 Interferences affecting the determination of tin in aqueous solutions

Kirkbright and West<sup>6</sup> have pointed out that physical and chemical interference effects on atomic fluores-





cence determinations of trace elements are expected to be similar to those found in atomic absorption. Nakahara et al<sup>242</sup> and Juliano and Harrison<sup>243,249</sup> have published the most detailed papers on interferences affecting the atomic absorption determination of tin. The work presented here was designed to investigate the interferences that might occur in the analysis of tin in steels using atomic fluorescence and is compared with the atomic absorption work of Nakahara et al<sup>242</sup>. The papers by Juliano and Harrison<sup>243,249</sup> were more concerned with the effect of flame conditions on interferences on tin atomic absorption in order to elucidate some of the processes taking place in the flame and/or mechanisms of the interferences.

### 3.3.1 The effect of acids

In the argon flames and the air-acetylene flame the effects of five acids on the atomic fluorescence of tin were determined by measuring 10 ppm aqueous tin solutions containing a range of concentrations of the acids. The effects in the three flames are shown in Figs 3.14 to 3.16. A 10 ppm tin solution containing 1% hydrofluoric acid gave 92%, 48% and 26% enhancements of the fluorescence signal in the argon-oxygen-hydrogen, argon-hydrogen, and air-acetylene flames respectively.

Of the three flames studied only the argon-hydrogen flame was studied by Nakahara et al.<sup>242</sup> for atomic absorption.

[The page contains extremely faint and illegible text, likely bleed-through from the reverse side of the paper. The text is too light to transcribe accurately.]

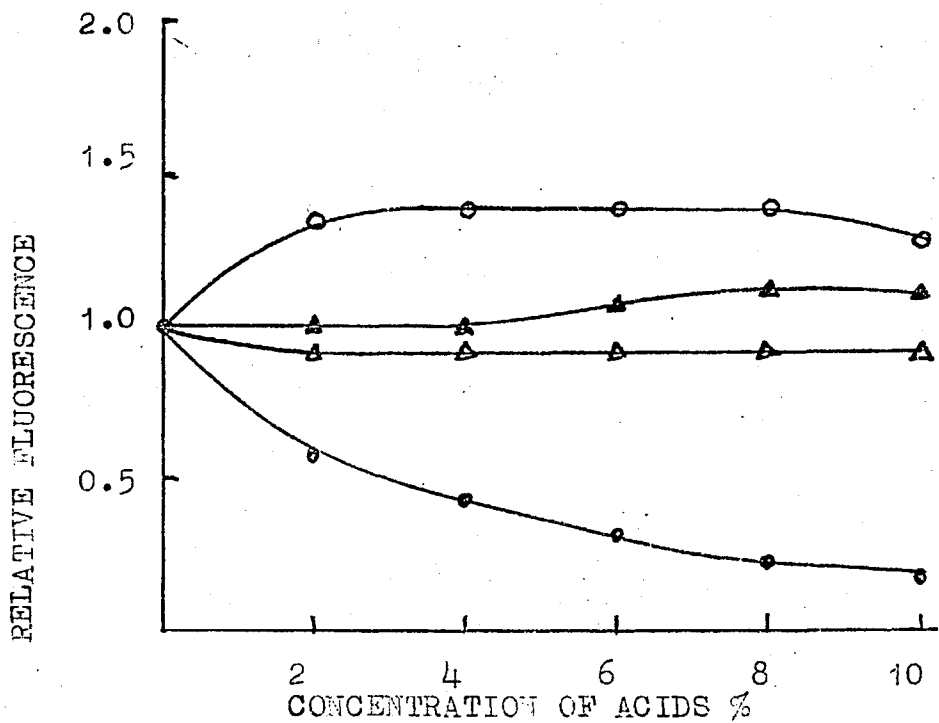


Fig. 3.14 The effect of acids on tin fluorescence in the argon-oxygen-hydrogen flame. 10 ppm tin. (o) - hydrochloric acid; (●) - sulphuric and phosphoric acids; (Δ) - nitric acid; (▲) - perchloric acid.

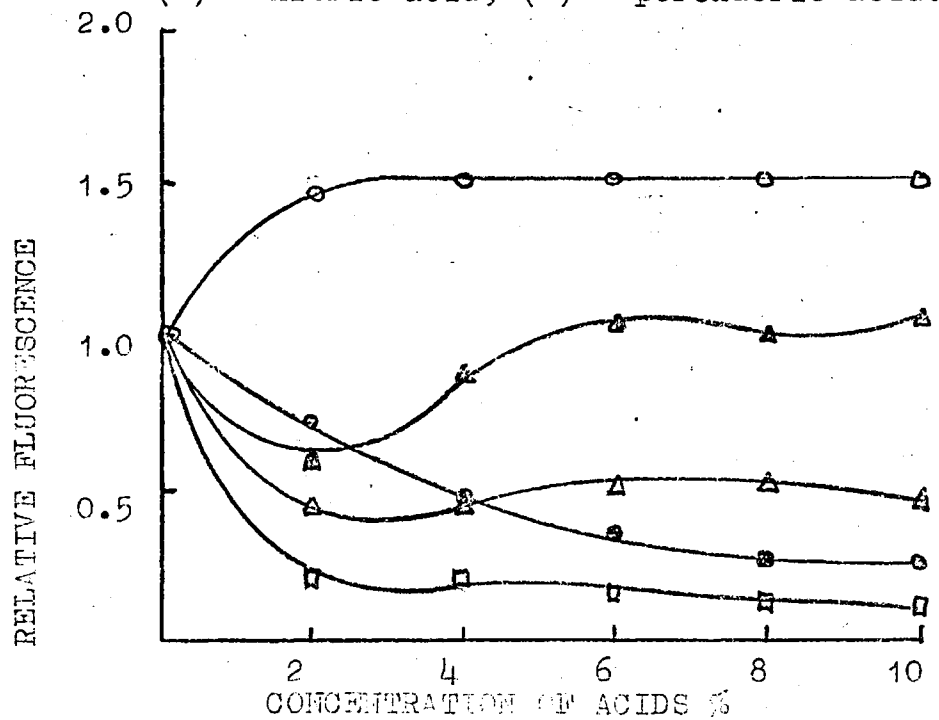


Fig. 3.15 The effect of acids on tin fluorescence in the argon-hydrogen flame. 10ppm tin. (o) - hydrochloric acid; (●) - sulphuric acid; (□) - phosphoric acid; (Δ) - nitric acid; (▲) - perchloric acid. Relative fluorescence is the ratio of the fluorescence of an aqueous tin solution containing acid to the fluorescence of an aqueous tin solution containing no acid.

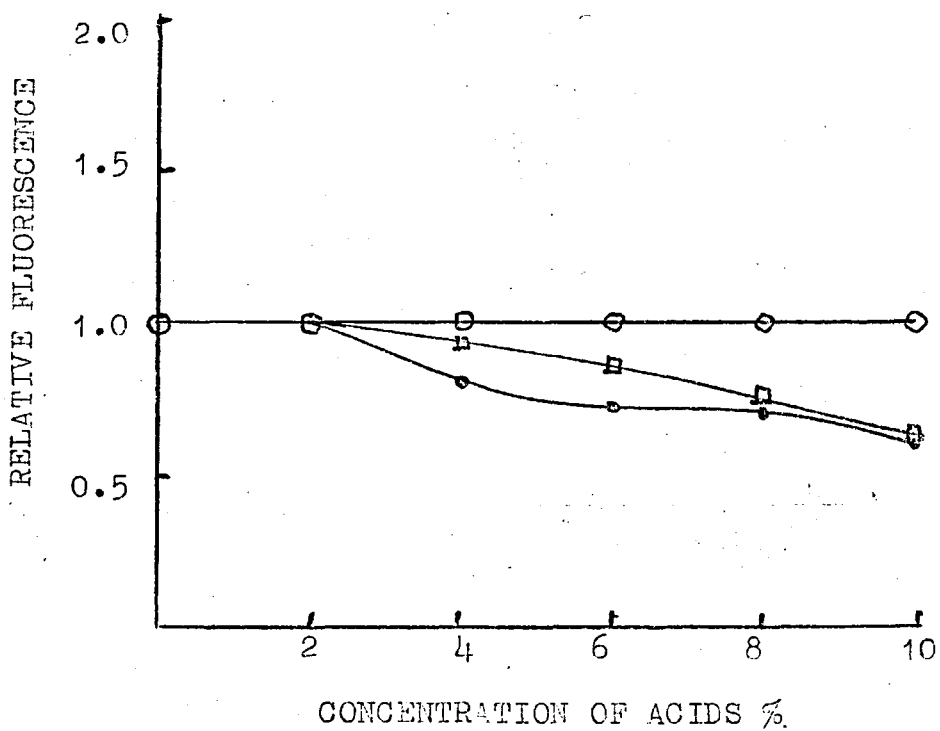


Fig. 3.16 The effect of acids on tin fluorescence in the air-acetylene flame. 10 ppm tin.  
 (o) - hydrochloric, perchloric and nitric acids; (□) - phosphoric acid; (●) - sulphuric acid.

These workers found that hydrochloric and hydrofluoric acids enhanced the absorption signal in this flame and nitric, sulphuric and phosphoric acids depressed the signal. The effect of perchloric acid varied from a depression at low concentrations to an enhancement at higher concentrations. It can be seen from Fig 3.15 that the trends in atomic fluorescence are very similar. The enhancements caused by the halogen containing acids are probably due to the formation of more easily vaporized or dissociated species. The depressions caused by the oxygen-containing acids are most likely to be due to the formation of species which are difficult to vaporize or dissociate in the low-temperature argon-hydrogen flame. The two higher temperature flames show smaller interference effects due to the acids (Figs. 13 and 15).

### 3.3.2 The effect of elements

Nakahara et al.<sup>242</sup> in their atomic absorption study showed that the presence of many elements such as the transition metals caused an extraordinary enhancement in the tin absorption; iron had the greatest effect in this respect. Other metals, such as alkaline earth metals, produced a considerable depressing interference. The interferences from the elements were not linearly related to their concentration.

The interference of twenty-seven elements, including iron, on the atomic fluorescence of tin was studied. The concentration of tin in 0.4M hydrochloric acid was kept constant at 10 ppm and the concentration of fifteen of the twenty-seven elements was varied between 25 and 1000 ppm. The fifteen elements chosen for the more detailed study are those commonly found in steels. The effects of the remaining elements were determined at the ten and hundred-fold excess levels. The magnitudes of all twenty-seven interferences at the ten and hundred-fold excess levels are given in Table 3.4. The interferences of the fifteen elements commonly found in steels were not linear with concentration (Figs. 3.17 to 3.19 illustrate the trends in the argon-hydrogen flame.) Neither the magnitudes nor the nature, i.e. enhancement or depression, of the interferences in the argon-hydrogen flame correlated with those reported by Nakahara et al.<sup>242</sup> for the atomic absorption of tin. The magnitudes of the fluorescence interferences were in general significantly smaller. These observations were not unexpected because the stoichiometry of the argon-hydrogen flame used in this study (Table 3.1) was different from the stoichiometry of the same flame used by Nakahara et al. The gas flows used by the latter workers were: hydrogen  $7.2 \text{ l min}^{-1}$ , argon  $4.5 \text{ l min}^{-1}$ . Browner et al.<sup>9</sup> have shown that flame conditions have a marked effect on interferences with tin

1. The first part of the document discusses the importance of maintaining accurate records of all transactions and activities. It emphasizes the need for transparency and accountability in financial reporting.

2. The second part of the document outlines the various methods and techniques used to collect and analyze data. It includes a detailed description of the experimental procedures and the tools used for data collection.

3. The third part of the document presents the results of the study, including a comparison of the different methods and techniques used. It discusses the strengths and weaknesses of each method and provides a summary of the findings.

4. The fourth part of the document discusses the implications of the study and provides recommendations for future research. It highlights the need for further investigation into the effectiveness of the different methods and techniques used.

5. The fifth part of the document concludes the study and provides a final summary of the findings. It reiterates the importance of maintaining accurate records and the need for transparency and accountability in financial reporting.

6. The sixth part of the document provides a detailed description of the experimental procedures and the tools used for data collection. It includes a list of the equipment and materials used and a description of the experimental setup.

7. The seventh part of the document presents the results of the study, including a comparison of the different methods and techniques used. It discusses the strengths and weaknesses of each method and provides a summary of the findings.

8. The eighth part of the document discusses the implications of the study and provides recommendations for future research. It highlights the need for further investigation into the effectiveness of the different methods and techniques used.

9. The ninth part of the document concludes the study and provides a final summary of the findings. It reiterates the importance of maintaining accurate records and the need for transparency and accountability in financial reporting.

10. The tenth part of the document provides a detailed description of the experimental procedures and the tools used for data collection. It includes a list of the equipment and materials used and a description of the experimental setup.

11. The eleventh part of the document presents the results of the study, including a comparison of the different methods and techniques used. It discusses the strengths and weaknesses of each method and provides a summary of the findings.

12. The twelfth part of the document discusses the implications of the study and provides recommendations for future research. It highlights the need for further investigation into the effectiveness of the different methods and techniques used.

TABLE 3.4

INTERFERENCES ON TIN ATOMIC FLUORESCENCE  
(TEN-FOLD EXCESS)

(10 ppm tin; 100 ppm interfering ion. Results expressed as the ratio of the fluorescence of tin in the presence of the interfering ion to the fluorescence of tin alone. All solutions were made up with 0.4M hydrochloric acid unless the particular salt used was insoluble in acid. In such cases alternative dissolution conditions were used. Measurements were made at the most sensitive wavelength of each flame).

Element	Relative fluorescence			Element	Relative fluorescence		
	Air-C <sub>2</sub> H <sub>2</sub>	Ar-H <sub>2</sub>	Ar-O <sub>2</sub> -H <sub>2</sub>		Air-C <sub>2</sub> H <sub>2</sub>	Ar-H <sub>2</sub>	Ar-O <sub>2</sub> -H <sub>2</sub>
Al <sup>a</sup>	1.19	0.87	1.00	Mn <sup>b</sup>	1.06	1.00	1.00
Al <sup>b</sup>	1.30	0.76	0.95	Mo <sup>e</sup>	1.27	1.02	0.97
As <sup>c</sup>	1.20	0.91	0.96	Nb <sup>f</sup>	1.14	1.00	1.00
Bi <sup>a</sup>	1.15	0.97	1.01	Ni <sup>b</sup>	1.03	0.84	1.00
Ba <sup>d</sup>	1.05	0.98	1.00	Pb <sup>d</sup>	1.00	1.07	1.00
Ca <sup>a</sup>	1.11	0.95	1.00	Rb <sup>a</sup>	1.00	0.74	0.97
Cd <sup>a</sup>	1.00	1.00	1.00	Sb <sup>a</sup>	1.00	1.02	1.05
Ce <sup>d</sup>	1.14	0.88	1.07	Sr <sup>d</sup>	1.04	0.83	1.00
Co <sup>a</sup>	1.00	1.00	1.00	Ti <sup>g</sup>	1.28	1.07	1.13
Cr <sup>d</sup>	1.05	0.85	1.00	Tl <sup>h</sup>	1.00	0.80	0.96
Cu <sup>d</sup>	1.11	1.12	1.00	V <sup>b</sup>	1.06	0.94	0.95
Fe <sup>d</sup>	1.00	1.10	1.00	W <sup>i</sup>	1.00	1.04	1.00
Fe <sup>a</sup>	1.00	1.10	1.00	Zn <sup>d</sup>	1.00	1.02	0.99
La <sup>a</sup>	1.14	0.90	1.03	Zn <sup>b</sup>	1.00	1.05	0.98
Mg <sup>d</sup>	1.04	0.99	1.00	Zr <sup>a</sup>	1.16	0.79	0.93

- a added as chloride  
 b added as sulphate  
 c added as sodium arsenite  
 d added as nitrate  
 e added as ammonium salt  
 f added as pentoxide  
 g added as metal  
 h added as carbonate  
 i added as sodium tungstate

TABLE 3.4 (contd)

INTERFERENCES ON TIN ATOMIC FLUORESCENCE  
(HUNDRED-FOLD EXCESS)

(10 ppm; 1000 ppm interfering ion).

Element	Relative fluorescence			Element	Relative fluorescence		
	Air-C <sub>2</sub> H <sub>2</sub>	Ar-H <sub>2</sub>	Ar-O <sub>2</sub> -H <sub>2</sub>		Air-C <sub>2</sub> H <sub>2</sub>	Ar-H <sub>2</sub>	Ar-O <sub>2</sub> -H <sub>2</sub>
Al <sup>a</sup>	1.86	0.79	1.00	Mn <sup>b</sup>	1.12	1.00	1.00
Al <sup>b</sup>	2.21	0.80	0.79	Mo <sup>e</sup>	1.38	0.91	0.92
As <sup>c</sup>	1.10	0.87	0.98	Nb <sup>f</sup>	1.45	1.00	1.00
Bi <sup>a</sup>	1.22	0.96	1.00	Ni <sup>b</sup>	1.24	0.72	1.00
Ba <sup>d</sup>	1.11	0.98	1.00	Pb <sup>d</sup>	1.00	1.13	1.00
Ca <sup>a</sup>	1.25	1.03	1.00	Rb <sup>a</sup>	1.00	0.85	0.97
Cd <sup>a</sup>	1.00	1.00	1.00	Sb <sup>a</sup>	1.00	1.30	1.28
Ce <sup>d</sup>	1.83	0.93	1.11	Sr <sup>d</sup>	1.09	0.83	1.00
Co <sup>a</sup>	1.00	1.00	1.00	Ti <sup>g</sup>	1.62	0.98	1.18
Cr <sup>d</sup>	1.24	0.73	0.96	Tl <sup>h</sup>	1.00	0.80	0.96
Cu <sup>d</sup>	1.11	1.12	1.00	V <sup>b</sup>	1.44	0.84	0.95
Fe <sup>d</sup>	1.00	1.10	1.00	W <sup>i</sup>	1.00	0.91	1.00
Fe <sup>a</sup>	1.00	1.10	1.00	Zn <sup>d</sup>	1.00	1.02	0.98
La <sup>a</sup>	1.88	0.94	1.12	Zn <sup>b</sup>	1.00	1.05	0.96
Mg <sup>d</sup>	1.22	1.03	0.98	Zr <sup>a</sup>	1.16	0.79	0.96

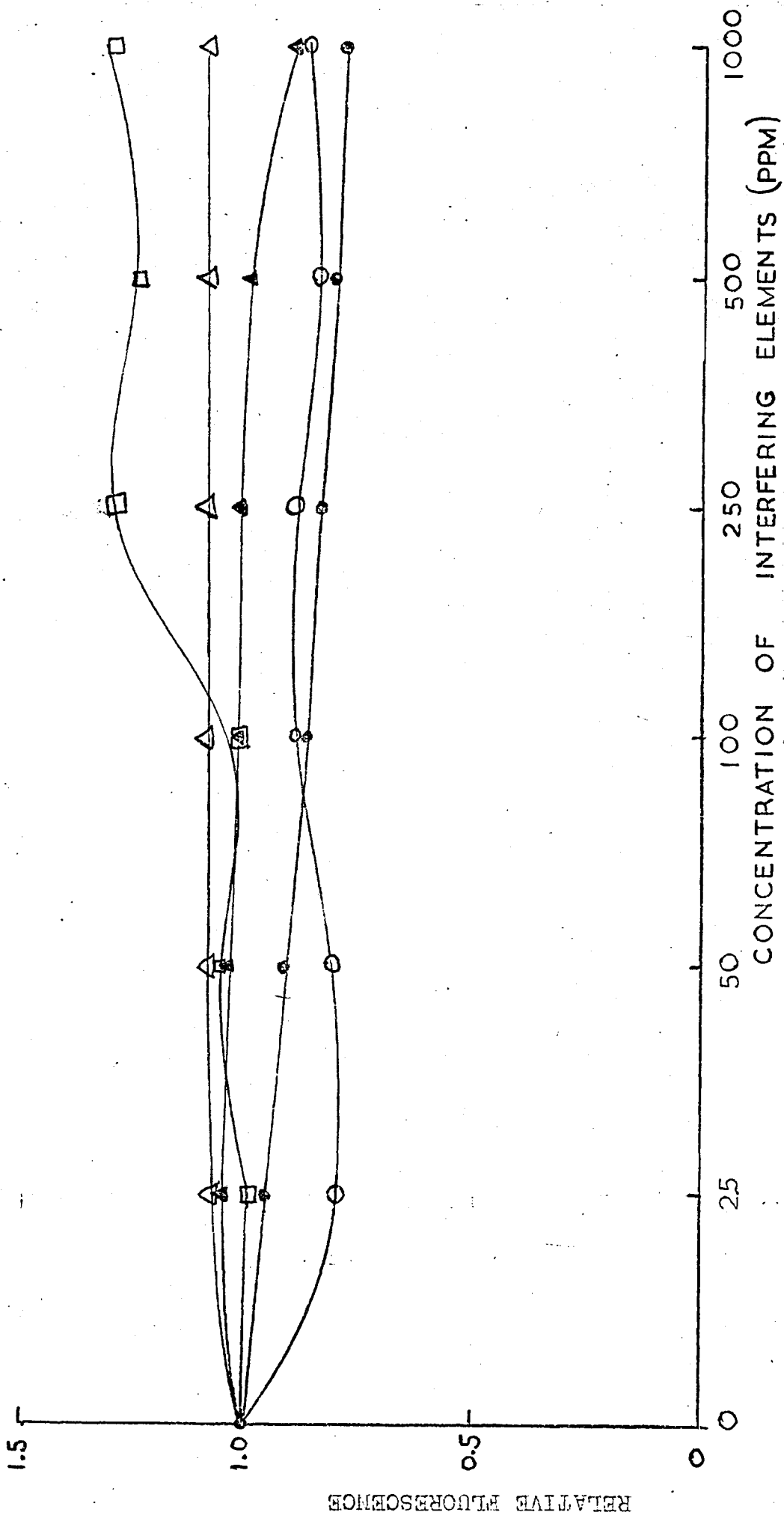


Fig. 3.17 The variation of interference effect with concentration of interfering ion. 10 ppm tin. Results expressed as the ratio of the fluorescence of tin in the presence of interfering ion to the fluorescence of tin alone. Argon-hydrogen flame. (o) - aluminium; (•) - arsenic; (▲) - iron; (●) - molybdenum; (□) - antimony. Solutions 0.4M in hydrochloric acid.

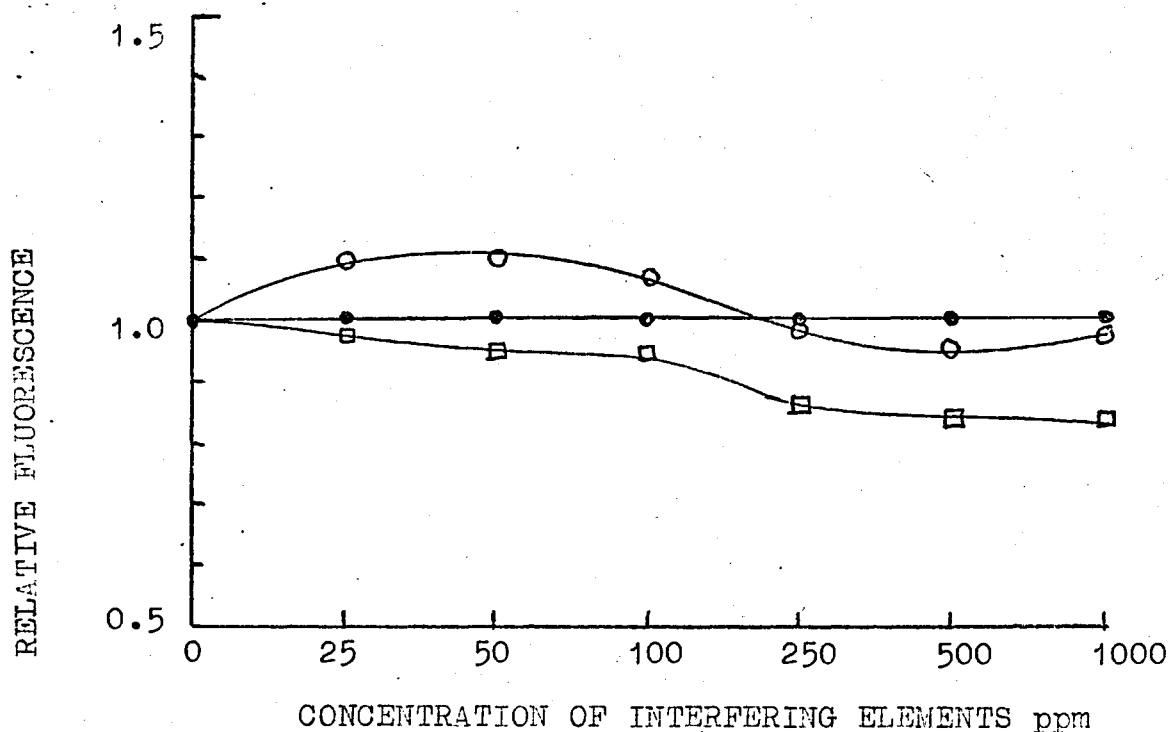


Fig. 3.18 The effect of elements 10 ppm tin. Argon-hydrogen flame. (○) - Titanium ; (●) - Niobium, Manganese and Cobalt ; (◻) - Vanadium.

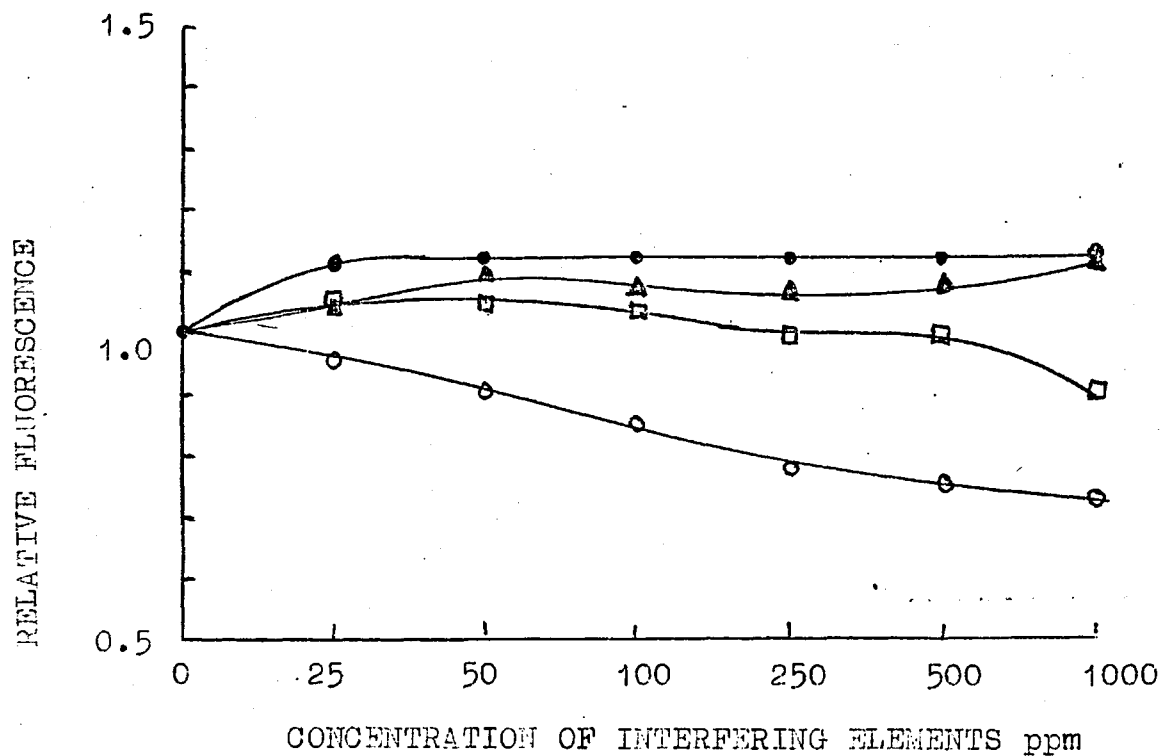


Fig. 3.19 The effect of elements 10 ppm tin. Argon-hydrogen flame. (○) - Chromium and Nickel ; (●) - Copper ; (▲) - Lead ; (◻) - Tungsten.

fluorescence in the argon-oxygen-hydrogen flame and there are of course many other examples of the effect of flame conditions on interferences in flame spectroscopy. Nevertheless the very high levels of interferences found by Nakahara et al were expected to appear in atomic fluorescence. These workers apparently carried out their determinations of interferences on tin atomic absorption in aqueous solution rather than in 0.4M hydrochloric acid. The effects of a few elements on the fluorescence of tin in aqueous solution were therefore studied for comparison with the interferences in 0.4M hydrochloric acid solution. The measurements were taken soon after preparation of the aqueous solutions. Comparison of the results (Table 3.5) with the previous measurements (Table 3.4) indicates that the effect of 0.4M hydrochloric acid is to reduce interferences in general, but for some elements, e.g. chromium, the interference changes from an enhancement in aqueous solution to a depression in 0.4M hydrochloric acid solution. Thus the effect of 0.4M hydrochloric acid could to a large extent explain the lack of correlation between the atomic absorption results of Nakahara et al.<sup>242</sup> and the atomic fluorescence results given here. However, without carrying out atomic absorption measurements on our instrument it is not possible to expect any more than correlation of basic trends in the two techniques, nor is it necessary for the purposes of this work.

TABLE 3.5

INTERFERENCES WITH TIN ATOMIC FLUORESCENCE  
(AQUEOUS SOLUTION)

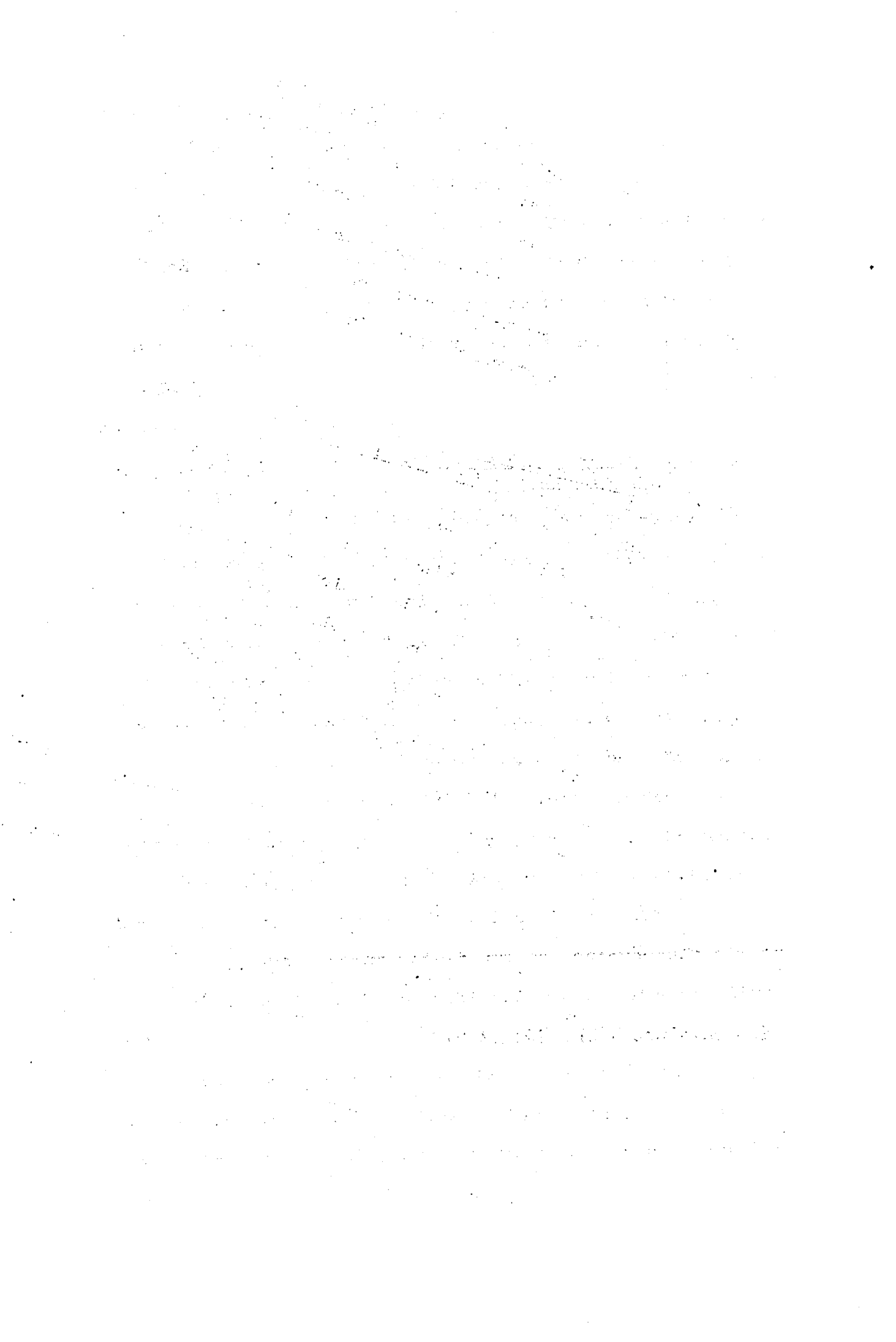
(10 ppm tin; 100 ppm interfering ion; all solutions made up with deionised water; Flame-argon-hydrogen, 317.5 nm; the same metal salts were used as in Table 3.4, superscripts a to i).

Element	Relative fluorescence	Element	Relative fluorescence
Al <sup>a</sup>	1.46	Mo <sup>e</sup>	1.76
As <sup>c</sup>	1.04	Nb <sup>f</sup>	1.26
Co <sup>a</sup>	2.28	Ni <sup>b</sup>	1.12
Cr <sup>d</sup>	1.11	Pb <sup>d</sup>	2.17
Cu <sup>d</sup>	2.04	Ti <sup>g</sup>	1.84
Fe <sup>a</sup>	2.07	V <sup>b</sup>	1.24
Mn <sup>b</sup>	1.52	W <sup>i</sup>	1.44

The general conclusions that can be drawn from these measurements are that there are as many interferences with the atomic fluorescence determination of tin as there are with the atomic absorption method. In the air-acetylene and argon-oxygen-hydrogen flame there are slightly fewer interferences than in the argon-hydrogen flame.

### 3.3.3 The effect of iron on the interferences from other elements

In view of the findings of Nakahara et al<sup>242</sup> that iron III chloride eliminated the interference of most elements in the atomic absorption determination of tin in cool flames it was reasonable to suppose that iron would have a similar effect on the atomic fluorescence of tin. Fig.3.20 shows how the addition of iron affects the interference of chromium on tin fluorescence in the argon-hydrogen flame. The interference of chromium is eliminated in the presence of 1000 ppm iron. Comparison of Fig.3.20 with the results of Nakahara et al shows that the effect of iron in both the atomic absorption and atomic fluorescence of tin is the same. 1000 ppm iron similarly removed the interference from chromium in the air-acetylene flame (Fig.3.21). In all three flames 1000 ppm iron eliminated the interference from most of the other elements studied (Table 3.6). Iron was as effective in removing interferences in the argon-oxygen-



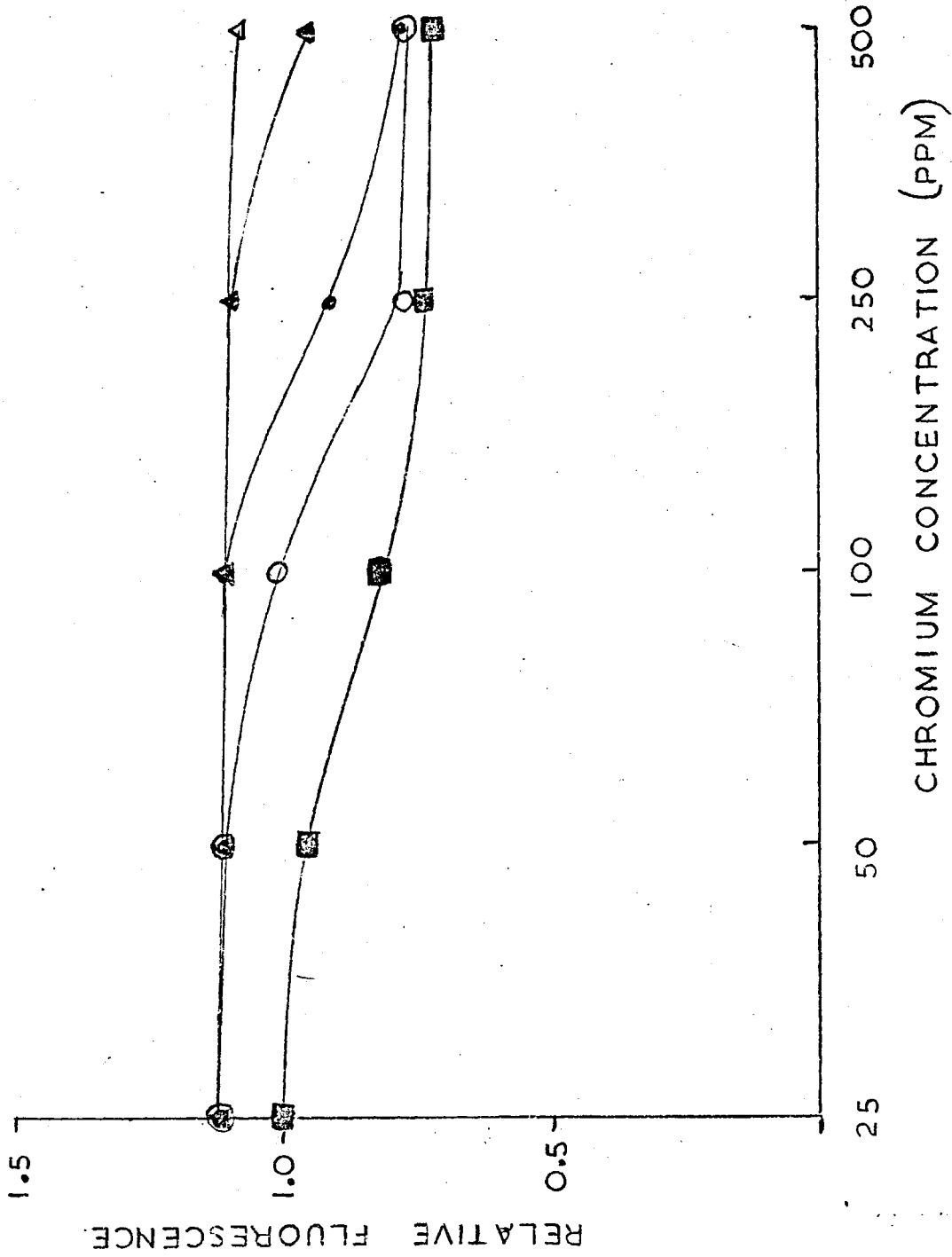


Fig. 3.20 Effect of iron on the interference from chromium. Solutions 0.4 M in hydrochloric acid, 10 ppm tin. Flame - argon-hydrogen. Concentrations of iron added (◻) - 0 ppm ; (○) - 25 ppm ; (◼) - 100 ppm ; (▲) - 500 ppm ; (▼) - 1000 ppm.

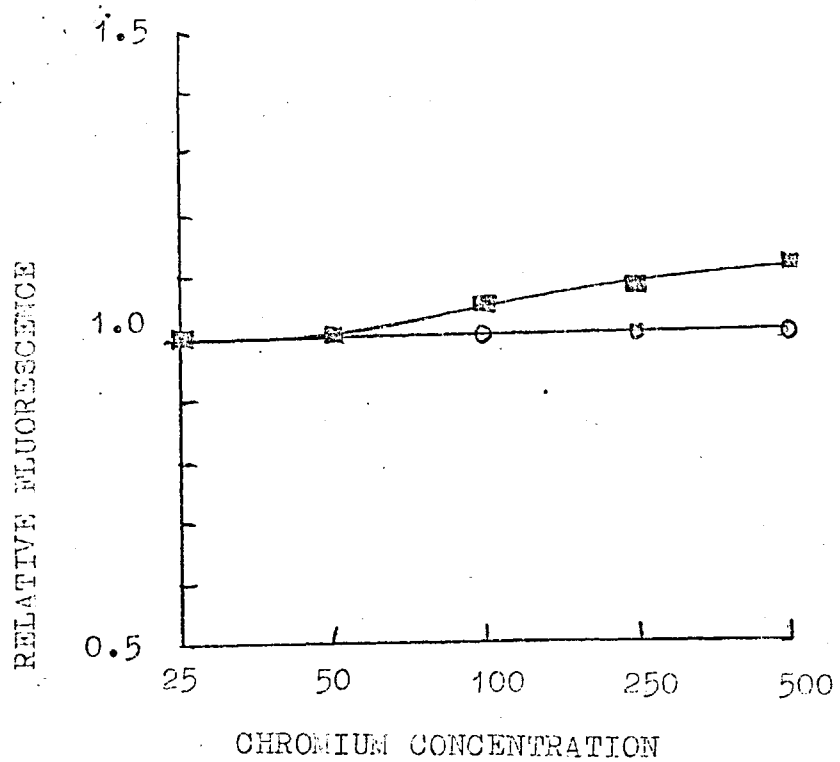


Fig. 3.21 Effect of iron on the interference from chromium. Argon-separated air-acetylene flame. 10 ppm tin. Concentrations of iron added (■) - 0 ppm ; (○) - 25, 100, 500, and 1000 ppm. Relative fluorescence is the ratio of the fluorescence of tin in the presence of iron and chromium to the fluorescence of tin alone.

TABLE 3.6

THE EFFECT OF IRON ON THE INTERFERENCE  
FROM OTHER ELEMENTS

(10 ppm tin; 1000 ppm iron III chloride. Results expressed as the ratio of the fluorescence of tin in the presence of 100 ppm interfering ion and 1000 ppm iron to the fluorescence of tin in the presence of 1000 ppm iron alone. All solutions made up with 0.4M Hydrochloric acid solution, iron added as iron III chloride).

Element	Relative fluorescence			Element	Relative fluorescence		
	Air-C <sub>2</sub> H <sub>2</sub>	Ar-H <sub>2</sub>	Ar-O <sub>2</sub> -H <sub>2</sub>		Air-C <sub>2</sub> H <sub>2</sub>	Ar-H <sub>2</sub>	Ar-O <sub>2</sub> -H <sub>2</sub>
Al <sup>a</sup>	1.00	1.00	1.00	Mn <sup>b</sup>	1.00	1.00	1.00
Al <sup>b</sup>	1.58	0.96	1.00	Mo <sup>e</sup>	1.00	0.90	1.00
As <sup>c</sup>	1.00	1.00	1.07	Nb <sup>f</sup>	1.31	1.02	1.05
Bi <sup>a</sup>	1.00	1.00	1.00	Ni <sup>b</sup>	1.00	0.81	1.00
Ba <sup>d</sup>	1.00	1.02	1.02	Pb <sup>d</sup>	1.00	1.00	1.00
Ca <sup>a</sup>	1.00	1.00	1.00	Rb <sup>a</sup>	1.00	1.00	1.00
Cd <sup>a</sup>	1.00	1.00	1.00	Sb <sup>a</sup>	1.00	0.84	0.89
Ce <sup>d</sup>	1.08	1.00	1.02	Sr <sup>d</sup>	1.00	1.00	1.02
Co <sup>d</sup>	1.00	1.00	1.00	Ti <sup>g</sup>	1.35	1.04	1.02
Cr <sup>d</sup>	1.00	1.00	1.00	V <sup>b</sup>	1.00	0.98	0.94
Cu <sup>d</sup>	1.00	1.00	1.00	W <sup>i</sup>	1.00	1.00	1.00
Fe <sup>d</sup>	1.00	1.00	1.00	Zn <sup>d</sup>	1.00	0.98	1.00
La <sup>a</sup>	1.19	1.00	1.00	Zn <sup>b</sup>	1.00	1.00	1.00
Mg <sup>d</sup>	1.00	0.96	0.96	Zr <sup>a</sup>	1.46	1.00	1.00

hydrogen flame as it was in the argon-hydrogen flame but most effective in the air-acetylene flame.

The interferences not removed in the presence of iron III chloride when using the argon-hydrogen flame were also still present in the comparable atomic absorption results of Nakahara et al (Mo, Ni, Sb) and they correlate both in magnitude and nature. None of these three elements interfered in the air-acetylene flame and only antimony interfered in the argon-oxygen-hydrogen flame. It should be noted that those trace elements which occur in steels and which still interfere in the air-acetylene and argon-oxygen-hydrogen flames in the presence of iron III chloride (Al, Ti, Nb in air-acetylene and As, Sb, V, Nb in argon-oxygen-hydrogen) occur at levels which would not interfere with the determination of tin in steels. (As, Nb, Sb, Al, Ti, V usually occur at less than 0.2% in steel, i.e. 20 ppm if 1g steel is dissolved in 100 ml of solution).

#### 3.3.4 The effect of iron on the interference from acids

In the argon flames 1000 ppm iron failed to remove the interference from the acids studied except hydrochloric acid (Table 3.7). However the enhancement due to iron in the presence of hydrochloric acid is the same as the enhancement due to iron in aqueous 10 ppm tin solutions. (Table 3.7). In the air-acetylene flame only phosphoric,

TABLE 3.7

## THE EFFECT OF IRON ON THE INTERFERENCE FROM ACIDS

(10 ppm tin; all solutions made up with deionised water. Results expressed as the ratio of the fluorescence of tin in the presence of acid and 1000 ppm iron to the fluorescence of the aqueous tin solution containing neither acid nor iron, iron added as iron III chloride)

Acid	concentration of acid %	Relative fluorescence		
		Air-C <sub>2</sub> H <sub>2</sub>	Ar-H <sub>2</sub>	Ar-O <sub>2</sub> -H <sub>2</sub>
hydrochloric	10	1.00	2.08	2.52
phosphoric	10	0.69	0.19	0.22
nitric	10	1.00	1.27	1.31
sulphuric	10	0.47	0.23	0.29
perchloric	10	1.00	1.23	1.27
hydrofluoric	1	1.20	1.96	1.68
0.4M hydrochloric acid - no iron		1.00	1.52	1.36
aqueous tin, no acid, 1000 ppm iron		1.00	2.08	2.52

sulphuric and hydrofluoric acids interfere (Table 3.7).

### 3.3.5 The effect of organic solvents

<sup>252</sup> Gilbert has discussed the effect of acetone, ethyl alcohol and isopropanol on the thermal emission of tin in air-hydrogen flames and quotes enhancements in the emission of up to 75%<sup>254</sup>. Harrison and Juliano<sup>249</sup> found that the addition of a variety of organic solvents depresses the tin atomic absorption in the air-hydrogen flame. Nakahara et al<sup>242</sup> found this was also true of the cooler argon-hydrogen and nitrogen flames. The present author has not been able to find any detailed published information on the effect of organic solvents when the air-acetylene or nitrous oxide-acetylene flames are used for tin atomic absorption methods. However, published solvent extraction methods<sup>240,241,255</sup> do not seem to have suffered any loss in sensitivity due to the use of organic solvents. In this study 10 ppm aqueous tin solutions containing 10% concentrations of a range of organic liquids were nebulized and the fluorescence measured (Table 3.8). In the argon flames acetone, acetic acid, ethanol and methyl-ethyl-ketone all depressed the fluorescence of tin. Acetic acid gave the smallest depression (36.5%), methyl-ethyl-ketone the largest (92.7%). 1000 ppm iron had a releasing effect in all cases but not enough to enhance the signal (Table 3.8). The magnitudes of these

TABLE 3.8

THE EFFECT OF ORGANIC LIQUIDS ON THE ATOMIC  
FLUORESCENCE OF TIN

(10 ppm tin; solutions containing 10% organic liquid and made up with deionised water. Results expressed as the ratio of the fluorecence of tin in the presence of organic liquid to the fluorecence of the aqueous tin solution containing no organic liquid)

Organic liquid	Relative fluorescence		
	Air-C <sub>2</sub> H <sub>2</sub>	Ar-H <sub>2</sub>	Ar-O <sub>2</sub> -H <sub>2</sub>
Acetone	1.05	0.36	0.12
Acetic acid	1.05	0.77	0.63
Ethanol	1.05	0.55	0.24
Methyl ethyl ketone	1.05	0.34	0.07

THE EFFECT OF IRON ON THE INTERFERENCE FROM  
ORGANIC LIQUIDS

(10 ppm tin; solutions containing 10% organic liquid and 1000 ppm iron, added as ferric chloride, and made up with deionised water. Results expressed as the ratio of the fluorecence of tin in the presence of organic liquid and iron to the fluorecence of the aqueous tin solution alone)

Organic liquid	Relative fluorescence		
	Air-C <sub>2</sub> H <sub>2</sub>	Ar-H <sub>2</sub>	Ar-O <sub>2</sub> -H <sub>2</sub>
Acetone	1.05	0.84	0.12
Acetic acid	1.05	0.95	0.93
Ethanol	1.05	0.93	0.34
Methyl ethyl ketone	1.05	0.84	0.13

depressions in the argon flames are similar to those found by Nakahara et al<sup>242</sup> and Juliano and Harrison<sup>249</sup> for the atomic absorption of tin.

In the air-acetylene flame all the organic liquids enhanced the signal by 5%. The addition of 1000 ppm iron had no effect on this enhancement. The enhancement effect in this flame also occurs in atomic absorption as mentioned briefly by Harrison and Juliano<sup>249</sup>. The use of organic solvents often increases nebulization efficiency due to increased uptake rates caused by lower solution viscosities. In the case of tin in any of the flames studied there is a competition between the nebulization effect and the chemical effect.

### 3.3.6 Mechanism of interference elimination

It was indicated (Section 3.3.2) that hydrochloric acid reduces interelement effects on the atomic fluorescence of tin in the argon-hydrogen flame. Further work was carried out using the argon-hydrogen flame which demonstrated that above a hydrochloric acid concentration of 2% the effect of the acid on the fluorescence of tin in the presence of other elements remains constant at the levels listed in Table 3.4. Six elements were tested and the results are plotted in Fig. 3.22. It is therefore important to keep the concentration of hydrochloric acid above 2% to keep interferences constant, and above 0.4M

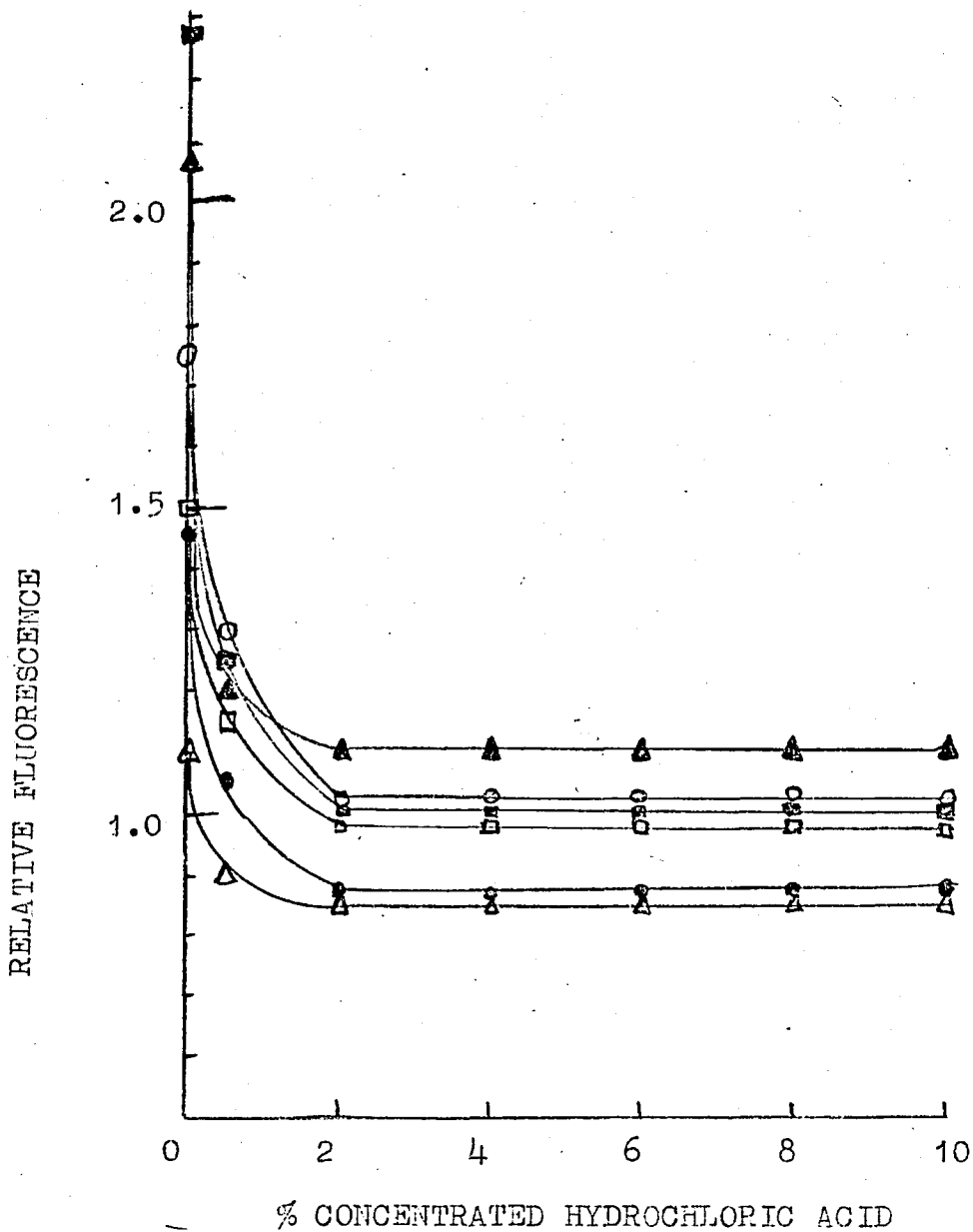
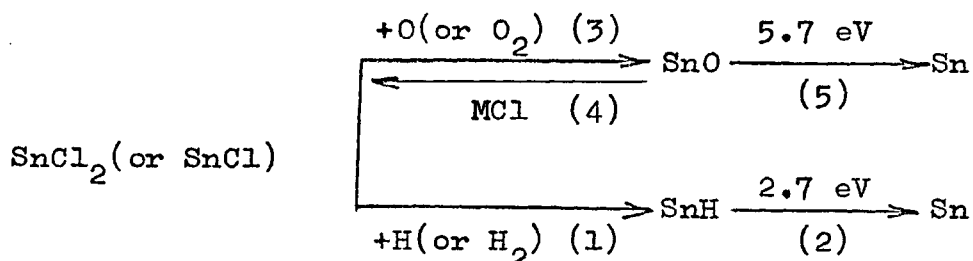


Fig. 3.22 The effect of hydrochloric acid on the fluorescence of tin in the presence of other elements. (●) - aluminium; (■) - cobalt; (Δ) - chromium; (◆) - iron; (□) - manganese; (○) - molybdenum. 100ppm element, 10 ppmtin. Argon-hydrogen flame.

(3.5%, i.e.  $\approx$  pH 1.5) to prevent loss of tin from solution by adsorption.

Interelement effects occurring in the atomic fluorescence determination of tin, using the hydrogen flames, follow the same basic trends as those reported by Nakahara et al.<sup>242</sup> and Harrison and Juliano<sup>249,243</sup> in their work on the atomic absorption of tin. In view of this observation the mechanism for the elimination of interferences by iron III chloride proposed by Nakahara et al, is as acceptable for atomic fluorescence as it is for atomic absorption. The latter authors postulate the following scheme:



where MCl represents hydrogen chloride and/or metallic chloride. Tin is vaporized as  $\text{SnCl}_2$  or  $\text{SnCl}$  and the production of tin atoms is thought to occur through processes (1) and (2), but a larger part of the tin in the flame is present as  $\text{SnO}$ .

Nakahara et al found some enhancing interferences when ammonium halides were present in the solutions used

for atomic absorption analyses in the argon-hydrogen flame. No enhancing effect was observed in the air-hydrogen flame. These observations substantiated the above scheme in that the halide may contribute via step (4) to the formation of species which are stable in cool flame, e.g.  $\text{SnCl}_2$  or  $\text{SnCl}$  and these species may favour the formation of  $\text{SnH}$  which decomposes directly by step (2) to produce tin atoms. Burke and Albright<sup>256</sup> found that interferences were minimised through the use of solutions containing 2% ammonium chloride 5% perchloric acid and hydrochloric acid for atomic absorption analyses for tin in the argon-hydrogen flame. This also indicates that ammonium chloride (or ammonium perchlorate) could act as  $\text{MCl}$  in step (4).

In the above scheme depressing interferences occur through process (3), oxygen atoms or molecules being supplied by air and/or oxygen-containing compounds such as nitrate, sulphate and phosphate. Enhancing interferences occur through process (4), iron III chloride being the most effective as  $\text{MCl}$ . Hydrochloric acid and ammonium halides being less effective than iron chloride.

Harrison and Julian<sup>249</sup> propose that the depressive effect of organic solvents on tin absorption is probably related to the effective removal of active hydrogen atoms which either serve to reduce tin oxide directly to form tin atoms or form a tin hydride species which is more

susceptible to dissociation than the tin oxide. To reach their conclusions these workers studied the effect of organic additives on tin hydride emission at 609.5 nm. Tin hydride showed a sharp decrease in emission intensity as the concentration of the organic species was increased, much like the effect shown for tin absorbance except that a more severe effect was noted on the hydrides.

In the air-acetylene flame a similar mechanism to the schemes above could be postulated. However step (1) could involve a variety of other reducing species which are present in the air-acetylene flame.<sup>257</sup> Harrison and Juliano<sup>249</sup> point out that reduction by carbon species will be favoured energetically because of the more stable C-O bond as compared with the OH bond. That hydrogen does not play a large part in the atomisation of tin in this flame is indicated by the enhancement effect of organic liquids in this fluorescence work as well as in Juliano and Harrison's absorption work, i.e. the removal of active hydrogen is not as significant as it is in the hydrogen flames. Steps (3) and (4) probably still occur in the air-acetylene flame because iron III chloride has the same effect on the fluorescence of tin in the presence of other elements as it does in the hydrogen flames. Juliano and Harrison<sup>243</sup> present a more detailed discussion of the possible mechanisms by which individual elements interfere with tin absorption. They propose various

types of ionisation mechanisms and solute vaporization interferences based on the formation of oxides in the flame.

### 3.3.7 Analytical Curves

The expressions which relate the radiance of fluorescence emission to the concentration of fluorescing atoms are given in appendix I. These expressions highlight the important factors which affect the shape of analytical curves especially at high concentrations of analyte atoms in the flame. At low concentrations the plot of analytical signal vs metal atom concentration has a slope of unity because self-absorption of the emitted fluorescence by ground state analyte atoms is negligible. At high concentrations self-absorption of resonance radiation becomes important. The other factors, related to self-absorption, which affect the shape of analytical curves at high concentrations are mainly concerned with the method of illumination of the flame and the solid angle over which the fluorescence is measured.

The above considerations hold when excitation and fluorescence are taking place at the same wavelength (resonance fluorescence). If the fluorescence is emitted at a different wavelength to the excitation the shape of the analytical curve will be altered. This occurs when a

line source is used and the fluorescence transition terminates in an excited state, (Generalisation 6 Appendix I) an example of such a transition is direct line fluorescence. In these cases the fluorescence radiance at all analyte concentrations becomes independent of the shapes of the absorption and fluorescence bands because ground state analyte atoms will not absorb strongly at the fluorescence wavelength and therefore the self-absorption factor,  $f_s$ , tends to unity (Appendix I). It should be noted however that in flame spectroscopy this excited state should be about 0.5 eV or higher above the ground state for  $f_s$  to approach unity<sup>7</sup>. The consequence of using such non-resonance fluorescence is an analytical curve with a long linear range to higher concentrations than is normally encountered. (see theory, Appendix I).

For the atomic fluorescence of tin in the argon-hydrogen flame, the direct line fluorescence<sup>9</sup> at 317.5 nm is most sensitive (section 3.2.4). In the argon-oxygen-hydrogen and air-acetylene flames the 303.4 nm line is the most sensitive. The latter line is a step-wise transition with a component from a thermally assisted ( $^3P_0$  to  $^3P_1$  see Fig 3.13) resonance fluorescence transition at 303.4 nm<sup>8</sup>. Neither of the fluorescence transitions, 317.5 or 303.4 nm, terminate in an excited state greater than 0.5eV above the ground state (0.210 and 0.425eV respectively<sup>193</sup>) consequently the self-absorption factor,  $f_s$ , cannot be unity. However analytical curves in all three flames were linear

between the detection limit and 250 ppm (Fig. 3.23) a relatively long linear range compared to other elements using resonance lines where such lines give superior detection limits. An example of such an element is manganese which gives calibration graphs, at the 280 nm resonance line, which are linear from 0.0025 to only 10 ppm<sup>12</sup>. Consequently the use of non-resonance transitions for the atomic fluorescence determination of tin has the twofold advantage of extended linear range at high concentrations and superior detection limit. This favourable situation also occurs for other elements, for example lead<sup>14</sup>. In the atomic fluorescence of arsenic (Chapter four) the 235.0 nm thermally-assisted direct-line fluorescence transition gives analytical curves which show less curvature at high concentrations than the resonance line at 189.0 nm. However the 235.0 nm line was found to give poor sensitivity in this work. A choice between linear range to high concentrations and superior detection limits often needs to be made depending upon the application and/or element concerned.

In this work on tin the calibration solutions used to obtain the analytical curves were 0.4M in hydrochloric acid and each contained 1000 ppm iron III chloride. The upper limit of the linear range, 250 ppm, was the same as that obtained by Browner et al<sup>9</sup> in their tin fluorescence studies.

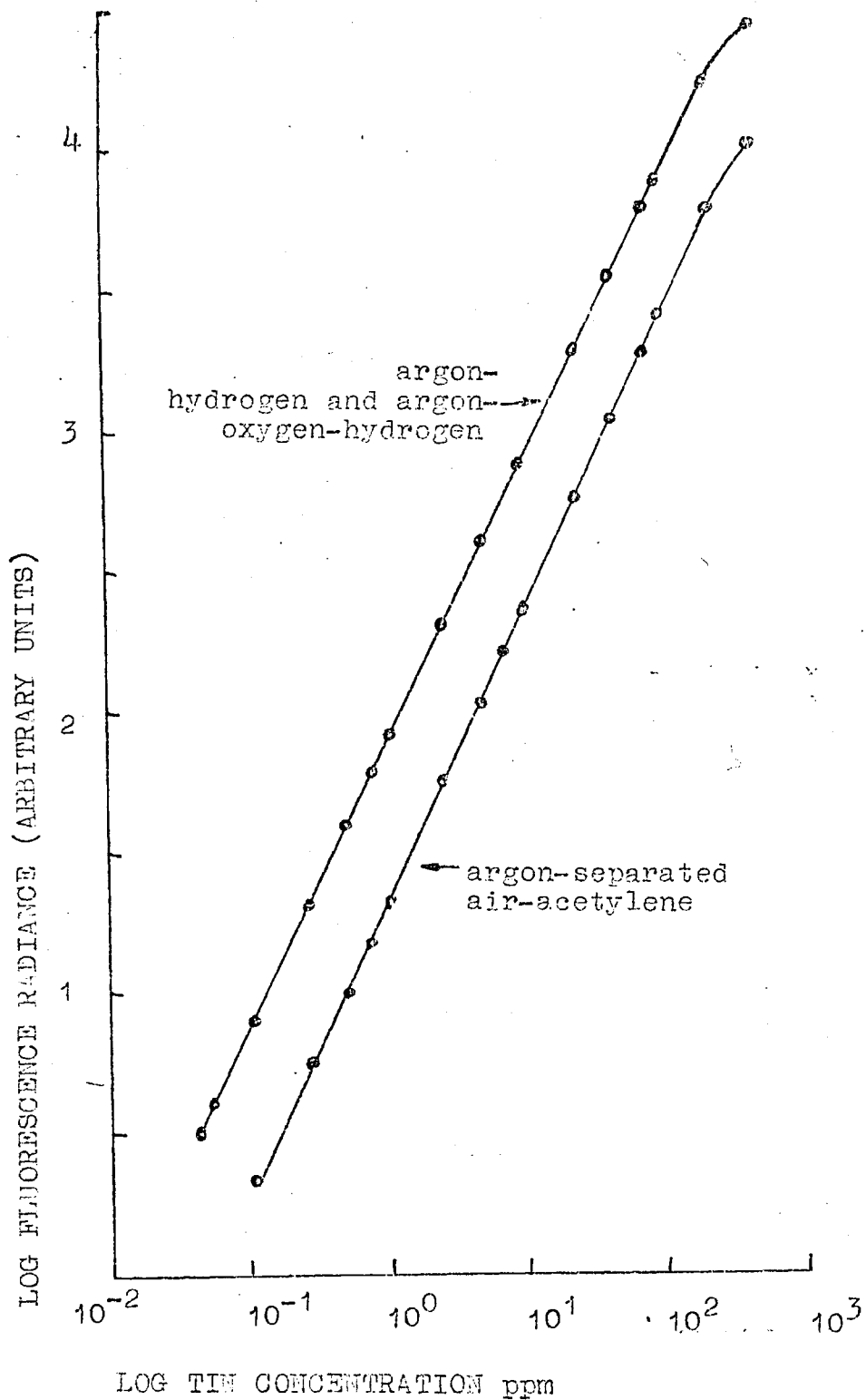


Fig. 3.23 Analytical curves for the determination of tin by atomic fluorescence. All solutions were 0.4 M in hydrochloric acid and contained 1000 ppm iron.

### 3.3.8 Detection Limits

Detection limits in this thesis are defined as that solution containing the analyte which gives a signal-to-noise ratio of two at the readout when using an 18.2s time constant. A full discussion of the factors which affect signal-to-noise ratios is given in chapter two. The procedure and conditions used to measure detection limits are given in appendix 2.

The detection limits obtained for the atomic fluorescence determination of tin were 0.05 ppm in the argon-separated air-acetylene flame, 0.006 ppm in the argon-oxygen-hydrogen and argon-hydrogen flames and 3 ppm in the argon-separated nitrous-oxide acetylene flame. The standard solutions used to measure these limits contained 0.05 ppm tin for air-acetylene, 0.025 ppm tin for the argon flames and 10 ppm for the nitrous-oxide flame. The solutions were also 0.4M in hydrochloric acid and contained 1000 ppm iron (added as iron III chloride).

The magnitude of the signals in the argon-separated nitrous oxide-acetylene flame, argon-separated air-acetylene flame and the argon flames were in the ratio 1:10:30 respectively when using the most sensitive conditions in each flame and the same instrumental conditions. The ratio of the signal in the air-acetylene flame to that in the argon-oxygen-hydrogen flame is approximately the same as that obtained by Browner et al.<sup>9</sup>, if the improvement

due to flame separation is taken into account. (Browner et al did not separate the air-acetylene flame for this measurement).

From a comparison of the above ratios with the detection limits it can be seen that the superior detection limits obtained in the argon flames are a combination of the reduced amount of noise associated with the argon flames and the higher sensitivity in these flames. Whether this larger signal is in fact due solely to the overexcitation phenomenon discussed in section 3.2.2 (which gives a larger atomic population in cool hydrogen flames) or has a contribution due to reduced quenching of fluorescence by flame gas species is not clear from these results. However the fact that the air-acetylene flame is so much more sensitive than the nitrous-oxide-acetylene flame indicates that quenching is appreciable in the latter flame. One would expect the atomic population to be greater in the nitrous-oxide flame because this flame is more sensitive than air-acetylene in atomic absorption.<sup>234</sup> It is interesting to compare these observations with the situation found for the determination of arsenic at 189.0 nm (chapter four).

Comparison of the above atomic fluorescence detection limits with the best atomic absorption limits that we could find (e.g. Winefordner and Elser<sup>5</sup> 0.03 ppm in cool flames) demonstrates the superior limits obtained when using atomic fluorescence for the determination of

tin. The more popular air-acetylene flame gives a detection limit which is comparable with the limits found for atomic absorption in cool flames and further improvements can be obtained by using the cool flames in atomic fluorescence.

### 3.4 The determination of tin in steel samples

Nakahara et al<sup>242</sup> pointed out that the effect of iron III chloride in eliminating interferences facilitates the determination of tin in steels by atomic absorption. These workers successfully determined tin in steel by dissolving 1g of steel in aqua-regia, evaporating to dryness, taking up in 10 ml of 6M hydrochloric acid, diluting to 100 ml in a volumetric flask and measuring the absorption of the resulting solution in the argon-hydrogen flame. In the work reported here the above atomic absorption method was repeated, i.e. calibration curves were obtained using standards containing 1000 ppm iron (added as iron III chloride) and aqua-regia was used to dissolve 1g samples of five B.C.S. standard steels<sup>258</sup>. The resulting solutions were nebulised and the atomic fluorescence measured at the 303.4 nm line. However, all the fluorescence signals from the steel solutions were severely depressed by between 50 and 90% in the argon-hydrogen and argon-oxygen-hydrogen flames and enhanced by up to 40% in the air-acetylene flame (Table 3.9).

TABLE 3.9

THE DETERMINATION OF TIN IN STEEL USING  
CALIBRATION STANDARDS CONTAINING 1000 ppm IRON

(For a discussion of these results and the dissolution method used see text).

British <sup>a</sup> Chemical Standard Steel No.	Description of steel	BCS standardised value %	Tin content %		
			Atomic fluorescence (Duplicate analyses)		
			Air/C <sub>2</sub> H <sub>2</sub>	Ar/H <sub>2</sub>	Ar/O <sub>2</sub> /H <sub>2</sub>
431	plain carbon	0.006	0.007 0.007	b	b
321	mild	0.014	0.019 0.018	b	b
322	mild	0.24	0.30 0.29	0.05 0.07	0.10 0.11
323	mild	0.024	0.032 0.031	b	0.013 0.012
325	mild	0.046	0.055 0.054	0.009 0.010	0.020 0.019

a. The standardised analyses of the steels can be obtained by referring to the list of analysed samples published by the Bureau of Analysed Samples Ltd.<sup>258</sup>

b. Fluorescence signals not detectable.

Norris and West<sup>230</sup> investigating the determination of chromium and manganese in steels using atomic fluorescence spectroscopy found that iron above a 250-fold excess interfered in the determination of chromium causing a depressing effect. They found it necessary to remove most of the iron by extracting it from strong hydrochloric acid-nitric acid solution, immediately after dissolution, with an equal volume of A.R. grade amyl acetate.

Burke and Albright<sup>256</sup> found that 10,000 ppm iron caused a depression of tin atomic absorption signals in the argon-hydrogen flame. This depression was alleviated but not eliminated by the ammonium chloride-perchloric acid system mentioned in section 3.3.6.

The effect of iron (added as iron III chloride) present in the range 0 to 10,000 ppm, on the fluorescence of a 50 ppm tin solution was determined in this work using the two argon flames and the separated air-acetylene flame. The results, plotted in Fig.3.24, show that iron has a depressing effect on the determination of tin in the argon flames. The severe depression caused by iron in the argon-hydrogen flame presents difficulties in the use of this flame for sensitive atomic fluorescence measurements of solutions of steels.

Results of further steel analyses (Table 3.10) using standards containing 8000 ppm iron demonstrated that it

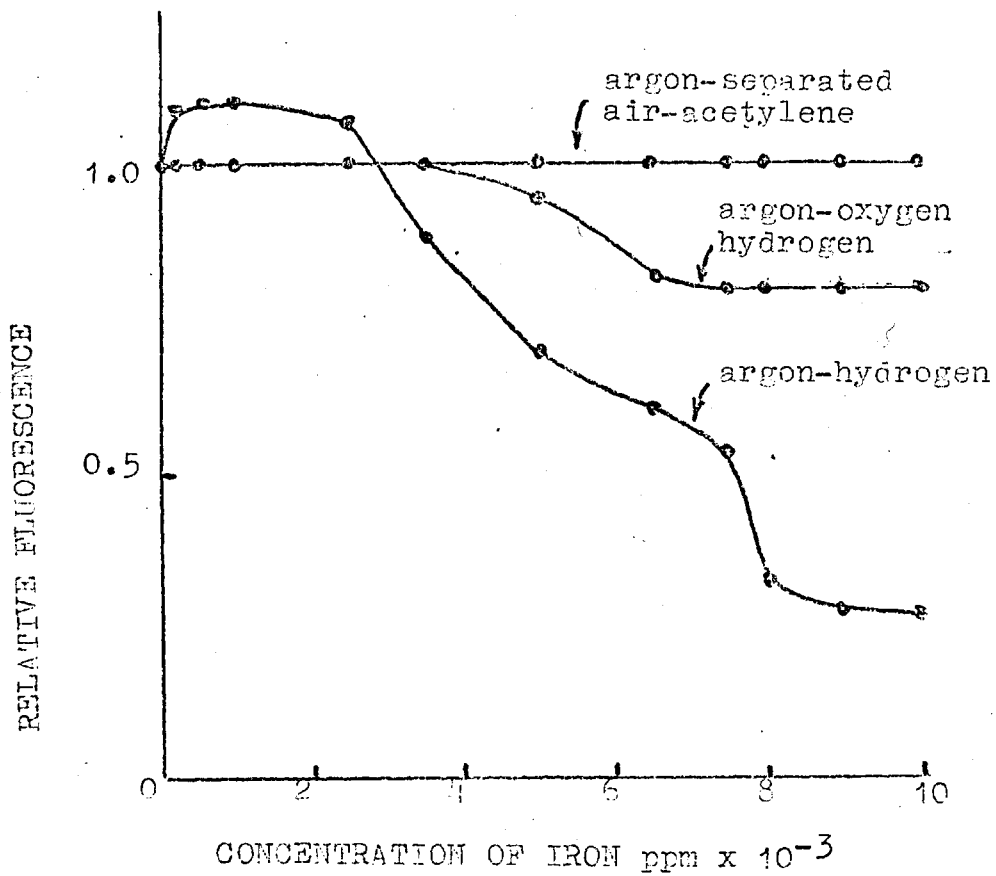


Fig. 3.24 The effect of iron (added as iron (III) chloride) on the atomic fluorescence of tin. Solutions 0.4 M in hydrochloric acid. 50 ppm tin. Relative fluorescence is the ratio of the fluorescence of tin in the presence of iron to the fluorescence of tin alone.

TABLE 3.10

THE DETERMINATION OF TIN IN STEEL USING  
CALIBRATION STANDARDS CONTAINING 8000 ppm IRON

(For a discussion of these results and the dissolution method used see text).

British <sup>a</sup> Chemical Standard No.	Description of steel	Tin content %		
		BCS standardised value %	Atomic fluorescence (Duplicate analyses)	
			Air/C <sub>2</sub> H <sub>2</sub>	Ar/O <sub>2</sub> /H <sub>2</sub>
322	mild	0.24	0.30 0.30	0.14 0.14
323	mild	0.024	0.031 0.030	0.016 0.015
431	plain carbon	0.006	0.007 0.008	b

a. Bureau of Analysed Samples Ltd. <sup>258</sup>

b. Fluorescence signals not detectable.

was not possible to wholly attribute the large depressions in the argon flames to the effect of high concentrations of iron; a ca. 40% depression was still observed in the argon-oxygen-hydrogen flame. Neither could the enhancement in the air-acetylene flame be explained by the effect of iron III chloride on tin fluorescence.

Silicates in solution are well known to cause marked depressions on the atomic absorption determination of a variety of elements; magnesium, calcium and strontium are notable in this respect<sup>117</sup>. Silicon in steel ranges from 0.001 to 5%. The traditional method of minimising the depressive effect of silicates is to filter the steel solution after dissolution. This is effective because gelatinous silica partly precipitates during dissolution techniques which do not include a dehydration step. A method of complete removal of silica is volatilization with hydro fluoric acid during the dissolution process<sup>192,259-260</sup>. The tetra fluoride of silicon is gaseous at ordinary temperatures and therefore easily volatilized from solution. The tin tetrafluoride is an involatile solid which sublimates at 978 K, thus it is unlikely to be volatilized from solution.

The above two methods of removing silicon were applied to the determination of tin in three standard steels from the B.C.S. range<sup>258</sup> (Bureau of Analysed Samples Ltd., Middlesbrough). These two methods of dissolution of the steel sample, both based on the use

of hydrochloric acid/nitric acid mixture, are detailed in Table 3.11 Methods A and B). The calibration curves for these determinations were obtained using standards containing 8000 ppm iron and which were 0.4M in hydrochloric acid, (Fig. 3.25) .

The curves are linear from the detection limit to 250 ppm using both the argon-oxygen-hydrogen and the argon-separated air-acetylene flames. The results of the determinations are given in Table 3.12

The depression in the argon-oxygen-hydrogen flame and the enhancement in the air-acetylene flame are no longer evident. The

enhancement in the air-acetylene flame was probably due to scatter of source radiation by silica particles in the flame.

This was confirmed using the non fluorescing line at 285.0 nm.

This source line was as intense as the 303.4 nm source line

(Fig. 3.12). At 285.0 nm scatter was observed from the unfiltered steel solutions while no signals were observed from standard tin solutions containing 8000 ppm iron or from filtered steel solutions .

Detection limits in the argon-oxygen-hydrogen and argon-separated air-acetylene flames were measured respectively using 0.025 and 0.05 ppm standard tin solutions each containing 8000 ppm iron and which were 0.4M in hydrochloric acid. The detection limit in the air-acetylene flame was 0.05 ppm; the same as for standard tin solutions containing only 1000 ppm iron (section 3.3.8). In the case of the argon-oxygen-hydrogen flame the presence of 8000 ppm iron in the

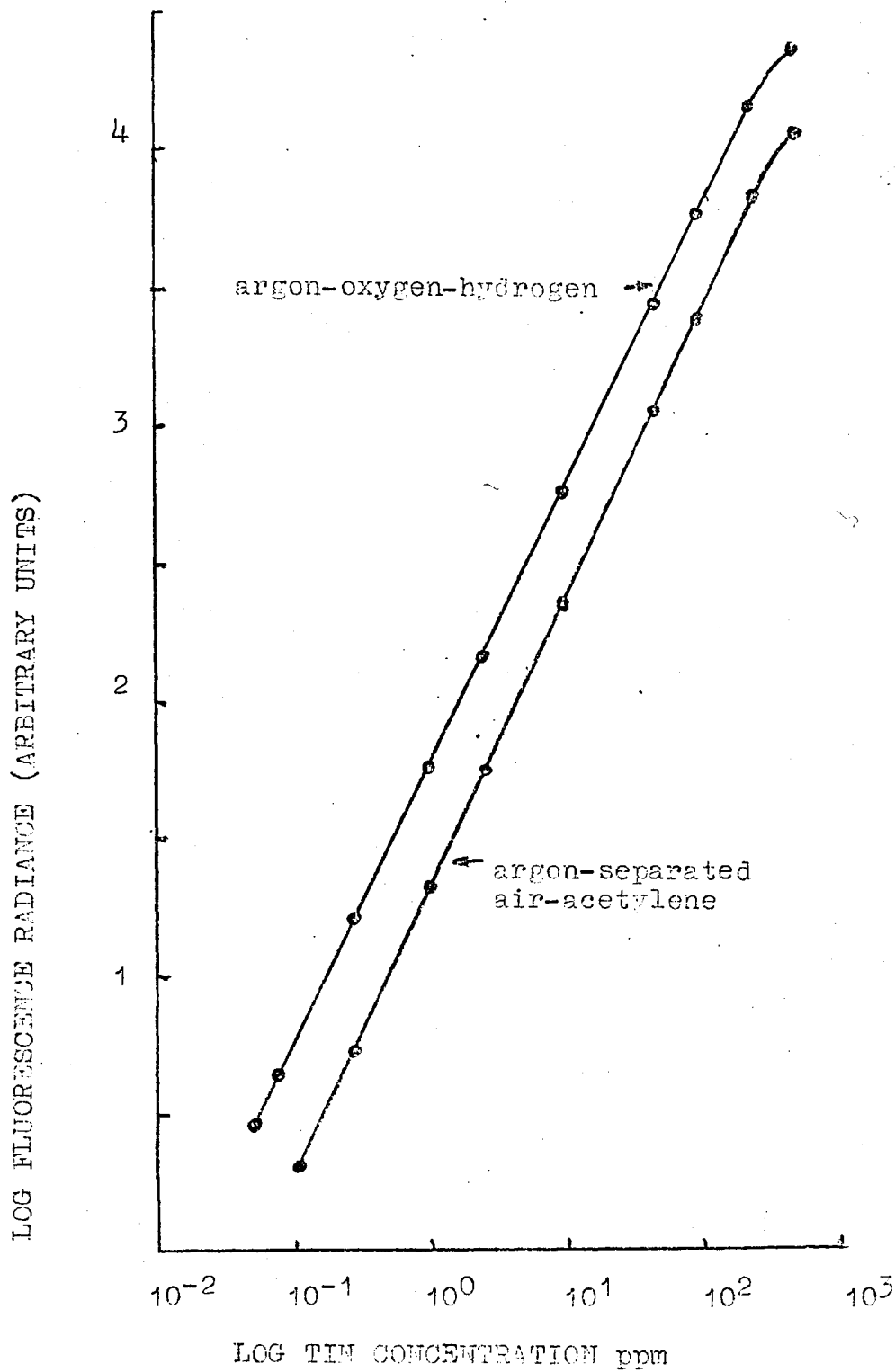


Fig. 3.25 Analytical curves for the determination of tin by atomic fluorescence. All solutions were 0.4 M in hydrochloric acid and contained 8000 ppm iron.

TABLE 3.11

DISSOLUTION METHODS USED FOR THE DETERMINATION OF  
TIN IN STEEL BY ATOMIC FLUORESCENCEMETHOD A.

1g of the steel was dissolved in 7 ml of concentrated hydrochloric acid and 3 ml of concentrated nitric acid and the resulting solution was heated gently until the evolution of brown fumes due to oxides of nitrogen ceased. The solution was then evaporated, almost to dryness, the residue taken up with 10 ml of concentrated hydrochloric acid and filtered through a No.4 sinter crucible. The solution was then transferred to a 100 ml volumetric flask and diluted to the mark.

METHOD B.

1g of the steel was dissolved, in a 100 ml P.T.F.E. beaker with 7 ml of concentrated hydrochloric acid and 3 ml of concentrated nitric acid. The resulting solution was heated gently until the evolution of brown fumes ceased and then 2 ml of hydrofluoric acid was added. The solution was then boiled gently for ten minutes to volatilize the silicon tetrafluoride, evaporated almost to dryness, taken up with 10 ml of hydrochloric acid and diluted to 100 ml in a volumetric flask.

METHOD C.

1g of the steel was dissolved in 7 ml of concentrated hydrochloric acid and 3 ml of concentrated nitric acid. When the reaction had subsided 10 ml of perchloric acid was added and the solution evaporated slowly until fumes of perchloric acid appeared. The solution was then fumed for a further five minutes, cooled, 50 ml of deionised water added, filtered and diluted to 100 ml in a volumetric flask.

TABLE 3.12

THE DETERMINATION OF TIN IN STEEL USING CALIBRATION  
STANDARDS CONTAINING 8000 ppm IRON AND EMPLOYING THE  
REMOVAL OF SILICON DURING DISSOLUTION.

The following trace elements<sup>a</sup> are present in all or most of the steels:  
C, Si, S, P, Mn, Ni, Cr, Mo, Cu, V, W, Ti, As, Al, Sb, Nb. Arsenic, niobium,  
antimony, vanadium, titanium and aluminium are present at levels not  
likely to interfere with the determination (less than 0.2%). The remaining  
elements do not interfere in the presence of iron III chloride.

British <sup>a</sup> Chemical Standard Steel No.	Description of steel	Tin content				
		BCS standardised value %	Atomic fluorescence. (Duplicate analyses)			
			Method A <sup>b</sup>		Method B <sup>b</sup>	
			Air/C <sub>2</sub> H <sub>2</sub>	Ar/O <sub>2</sub> /H <sub>2</sub>	Air/C <sub>2</sub> H <sub>2</sub>	Ar/O <sub>2</sub> /H <sub>2</sub>
322	mild	0.24	0.24	0.23	0.23	0.23
			0.24	0.24	0.24	0.24
323	mild	0.024	0.024	0.023	0.024	0.024
			0.024	0.024	0.023	0.024
431	plain carbon	0.006	0.006	0.005	0.006	0.006
			0.005	0.005	0.006	0.005

a. The standardised analyses of the steels can be obtained by referring to the list of analysed samples published by the Bureau of Analysed Samples Ltd. 258

b. See text and Table 3.11.

standard solutions increased the flame noise as well as depressing the fluorescence signal. This degraded the detection limit from 0.006 ppm to 0.01 ppm.

The precision of Method B (Table 3.11) was investigated for one of the standard steels (B.C.S. No.323, a mild steel). Six samples of this steel were treated using dissolution method B and the average of three atomic fluorescence readings taken for each sample. The relative standard deviation was 3.1% for the air-acetylene flame and 2.3% for the argon-oxygen-hydrogen flame.

A third dissolution method (Method C, Table 3.11) using aqua-regia but followed by oxidation with perchloric acid and a filtration step was used to analyse B.C.S. standard steel No.325 (standardised tin content 0.048%). The atomic fluorescence analysis gave a tin content of 0.049% using the argon-oxygen-hydrogen flame and 0.047% using the argon-separated air-acetylene flame. Calibration was carried out in the same way as for Methods A and B. However if more than 10 ml of perchloric acid was used in the dissolution step large enhancements of the fluorescence signal were observed in either of the above flames. For example, the use of 20 ml of perchloric acid resulted in a tin fluorescence signal corresponding to 0.13% for B.C.S. No.325 (argon-separated air-acetylene flame). Moreover this interference was not reproducible, the enhancement varying between

100 and 400% (three determinations, tin content found: 0.13%, 0.19%, 0.09%, in the air-acetylene flame, and 0.2, 0.24, 0.1 in the argon-oxygen-hydrogen flame). This is probably related to evaporation time during the dissolution step as well as to the volume of perchloric acid added. The effect of the concentration of perchloric acid on the fluorescence of tin in the argon-oxygen-hydrogen flame is not constant below an acid concentration of 10% (Fig.3.14).

In view of the above observations, Method C using perchloric acid could only be considered reliable when using concentrations of perchloric acid accurately controlled below 10%. Price<sup>192</sup> points out that it has been found necessary to take calibration standards through a perchloric acid oxidation step when determining chromium and molybdenum in steels by atomic absorption. This eliminates any problems that may occur due to a difference, probably in oxidation state in the case of chromium, between samples and synthetic standards. This procedure may be necessary for the determination of tin in steel by atomic fluorescence if a perchloric acid dissolution is indicated. For example, if it is desirable to determine a number of trace elements using a single weighing and preparation procedure the use of perchloric acid may be necessary to bring one or more of the elements into solution.

### 3.5 Conclusion

This work has demonstrated that interelement effects in both the atomic absorption and the atomic fluorescence of tin follow the same basic trends. The use of iron III chloride to eliminate interferences has a similar effect in both techniques. The detection limit obtained for tin atomic fluorescence using cool hydrogen based flames is nearly an order of magnitude lower than published figures for the atomic absorption method using the same flames. The air-acetylene flame gives a detection limit which is comparable to the atomic absorption detection limits in the interference prone cool flames.

A method has been developed for the determination of tin in steel using the atomic fluorescence of tin at the 303.4 nm line in the argon-separated air-acetylene flame or the argon-oxygen-hydrogen flame. The effects of interferences were eliminated by the addition of iron (added as ferric chloride) to the calibration standards in about the same amount as found in the sample and the removal of silicon from the sample. The preferred procedure involves the dissolution of the sample in aqua-regia followed by the volatilization of silicon using hydrofluoric acid. Alternatively, the removal of silica by filtration was also found to be satisfactory.

The superior sensitivity of the fluorescence technique has enabled the determination of tin in steels

without preconcentration and moreover the popular air-acetylene flame can be used rather than a cooler flame. If necessary further improvements in sensitivity can be obtained using the argon-oxygen-hydrogen flame.

The application of atomic fluorescence spectrometry to the determination of arsenic in steels.

#### 4.1 Introduction

The fluorescence and analytical characteristics of arsenic have been reported by Dagnall et al.<sup>11,228</sup> and Thompson and Wildy,<sup>179</sup> a detection limit of 0.1 ppm was obtained in both cases. Vickers et al.<sup>60</sup> have determined arsenic using a non-dispersive fluorescence method and Fulton et al.<sup>261</sup> measured the atomic fluorescence of arsenic using a dual-element arsenic-antimony electrodeless discharge lamp as source.

The atomic absorption determination of arsenic has been well characterised<sup>165,192,253,262-269</sup> although two serious problems have been encountered<sup>253</sup>. The first of these is that it is difficult to construct arsenic hollow cathode lamps of high enough quality for routine use.<sup>270</sup> This is because the vapour pressure of arsenic is high and the element is rapidly lost from the cathode of the lamp. Although improvements have been made, arsenic hollow cathode lamps still often have a relatively short operating life. The second problem occurs primarily because the arsenic resonance lines lie below 200 nm and a significant number of atomic absorption instruments perform poorly in that spectral region. Both of these problems have been alleviated in modern instruments by the use of arsenic electrodeless discharge lamps<sup>165</sup> and optical systems which transmit efficiently in the u.v.

Detection limits for arsenic atomic absorption have been reported as low as 0.05 ppm in the argon-hydrogen flame,<sup>262 268</sup> or 0.25 ppm in the air-acetylene flame.<sup>262</sup> Menis and Rains<sup>165</sup> report a limit of 0.1 ppm in the argon-hydrogen flame using an electrodeless discharge lamp as source. Kirkbright et al.<sup>263</sup> quote a detection

limit of 1.2 ppm in the argon-separated air-acetylene flame and improve this slightly to 1.0 ppm using an inert-gas shielded nitrous oxide-acetylene flame<sup>265</sup>.

Interferences affecting the atomic absorption determination of arsenic have been discussed for a variety of applications<sup>263,268,271-273,283</sup>. The sensitive cool flames are so seriously affected by interferences that they have been used very little for the analysis of real samples. The use of the nitrous oxide flame overcomes most of the interferences encountered in either the cool flames or the air-acetylene flame<sup>263-265,273</sup>.

Various emission spectrometric methods for the determination of arsenic have been reported<sup>274,275</sup> which give improved detection limits over the 0.1 ppm figure usually obtained by atomic absorption.

Further improvements in the atomic absorption method have been obtained<sup>276-281</sup> by the chemical conversion of arsenic to arsine and its subsequent introduction into an argon-hydrogen flame<sup>276-278,280,281</sup> or an electrically heated absorption tube<sup>279</sup>. This method is more efficient in introducing arsenic into the flame and consequently an improvement in detection limits of up to two orders of magnitude is obtained. Ando et al.<sup>282</sup> use a long-path Vycor cell to improve atomic absorption sensitivities for arsenic.

The present author has not been able to find any published methods for the determination of arsenic in steels using the atomic fluorescence method. Scholes<sup>8</sup> in 1968 reviewed the analysis of iron and steel by atomic absorption and noted that arsenic was one of the more difficult elements to determine with adequate sensitivity. Hill<sup>283</sup> determined arsenic in steel using atomic absorption after a rapid distillation procedure and Kirkbright et al.<sup>265</sup> used atomic absorption to determine arsenic in steel directly by dissolution of a 2g sample and aspiration into a nitrous oxide flame.

Although the sensitivity obtainable for arsenic determination by atomic absorption has been gradually improved it is still more usual to determine arsenic using spectrophotometric techniques<sup>284</sup> or occasionally an indirect atomic absorption method is used. This usually involves the nebulization of an MIBK extract of arsenomolybdic acid and the determination of molybdenum at 313.3 nm<sup>285-288</sup> (sensitivity 0.01 ppm). Nall<sup>289</sup> reviews some of the existing methods for the determination of arsenic in steel including the British Standard titrimetric method where 1 ml of titrant is equivalent to 0.003% of arsenic on a 5g sample. Nall then describes a simple molybdenum-blue method which is suitable for determinations of arsenic in the range 0.001 to 0.05% in most types of steel.

The stability of dilute standard solutions of arsenic has been investigated by Al-sibaai and Fogg<sup>290</sup>. The solutions, prepared either by dissolving arsenic III oxide in sodium hydroxide solution and then neutralizing with hydrochloric acid, or by dissolving disodium hydrogen arsenate heptahydrate in water, were found to be stable at both the 20 and 4 ppm level.

This chapter describes the interferences which affect the atomic fluorescence determination of arsenic in four different flames and a method for the determination of arsenic in steel by atomic fluorescence. The argon-separated air-acetylene flame is used for the steel determinations and iron is added to the calibration standards. The detection limit in the latter flame is about 20 times better than the best reported atomic absorption detection limits<sup>262,268</sup> known to us for arsenic determinations in the same flame. Cool flames are of no analytical use in atomic fluorescence, as is the case for atomic absorption, because of the large numbers of interferences that occur.

#### 4.2 Optimisation of conditions for measurements of arsenic fluorescence

290

As mentioned above Al-sibaa and Fogg found that arsenic solutions at the 20 and 4 ppm level are stable. The solutions used in this work were therefore prepared using arsenic (III) oxide and sodium hydroxide followed by neutralization with hydrochloric acid. (appendix 2 ). No loss of arsenic from 1000, 400, 10 or 1 ppm solutions was observed over the period of this work, neither was there any loss when the solutions were 4% in hydrochloric acid or when there was 10,000 ppm iron (as ferric chloride) present.

#### 4.2.1. Choice of gas flow rates, flame separation and flame height

The gas flow rates in the premixed nitrous oxide-acetylene, air-acetylene, argon-oxygen-hydrogen and argon-hydrogen flames were optimised by observing the atomic fluorescence signal from 10 ppm arsenic solutions. The fluorescence was measured at 189.0 nm and the monochromator was flushed with nitrogen (see section 4.2.3.). The variations in the arsenic fluorescence with gas flows in each of the flames are shown in Figs. 4.1 to 4.4. The effect of flame separation on the two acetylene flames is also shown. As in the case of tin, argon separation of the argon-oxygen-hydrogen flame was undesirable for the measurement of arsenic fluorescence. The arsenic fluorescence signal from this flame dropped by about 10% upon separation (at a variety of fuel flows) and noise levels were unaffected.

Argon separation of the air-acetylene and nitrous oxide-acetylene flames gave a factor of two and three increase in signal-to-noise ratio respectively. These factors are composed entirely of an increase in signal in going from the largest signal in the unseparated flame to the largest signal in the separated flame, an increase probably caused by decreased flame absorption of source and fluorescence radiations upon separation. Noise levels at the chart readout were not improved upon separation most probably because the noise levels from the flame are already very low at wavelengths below 200 nm. The fuel flows giving the optimal signals in each flame are given in Table 4.1. The variations in the fuel flows are similar to those obtained for the atomic fluorescence of tin, i.e. the critical nature of the oxygen flow in the argon-oxygen-hydrogen flame (Fig. 4.1 cf Fig. 3.4 for tin fluorescence), the decrease in signal with increase in hydrogen flow in both the argon flames (Fig. 4.2 cf Fig. 3.5) and the requirement for reducing conditions in the two acetylene flames.

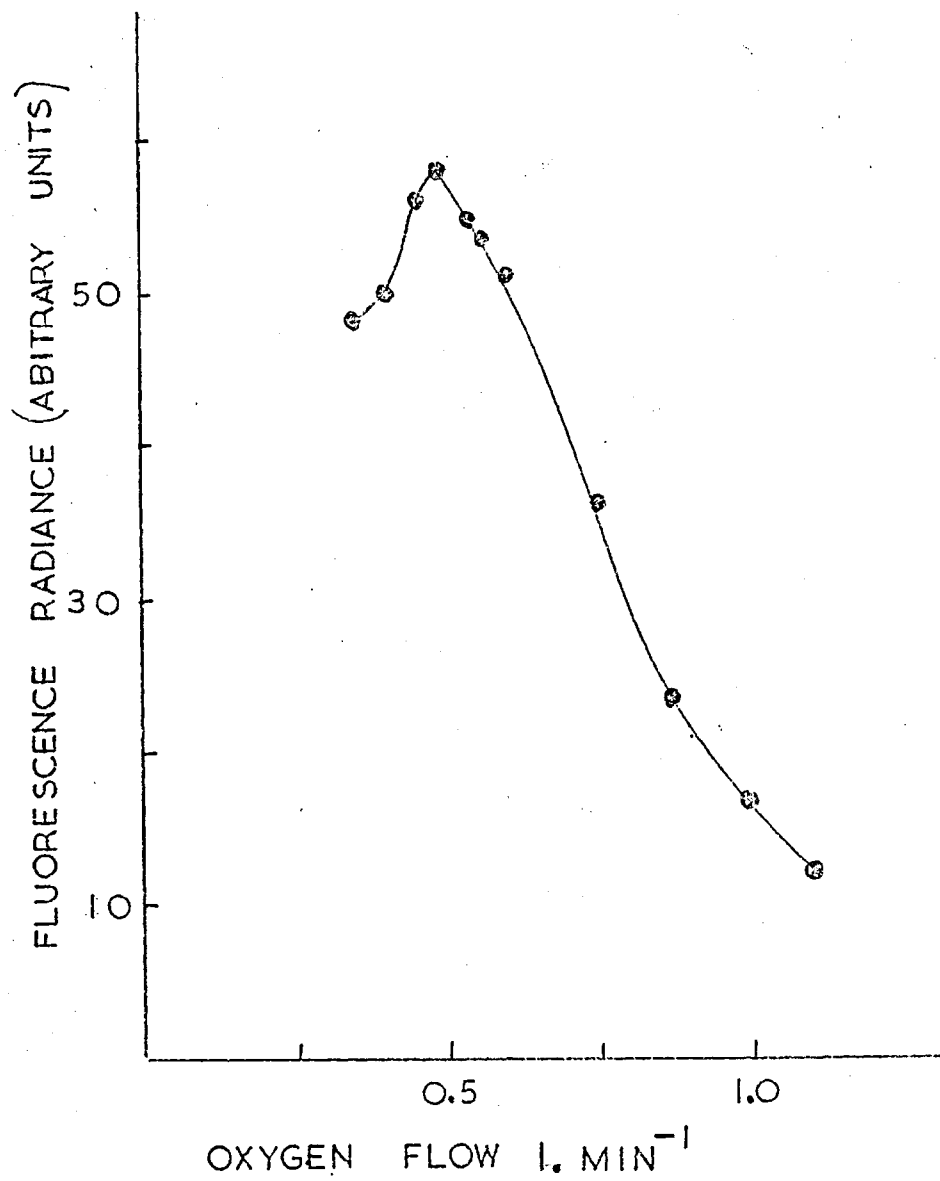


Fig. 4.1 Variation of arsenic fluorescence with oxygen flow in the argon-oxygen-hydrogen flame.  
Argon flow -  $4.8 \text{ l min}^{-1}$   
Hydrogen flow -  $0.72 \text{ l min}^{-1}$

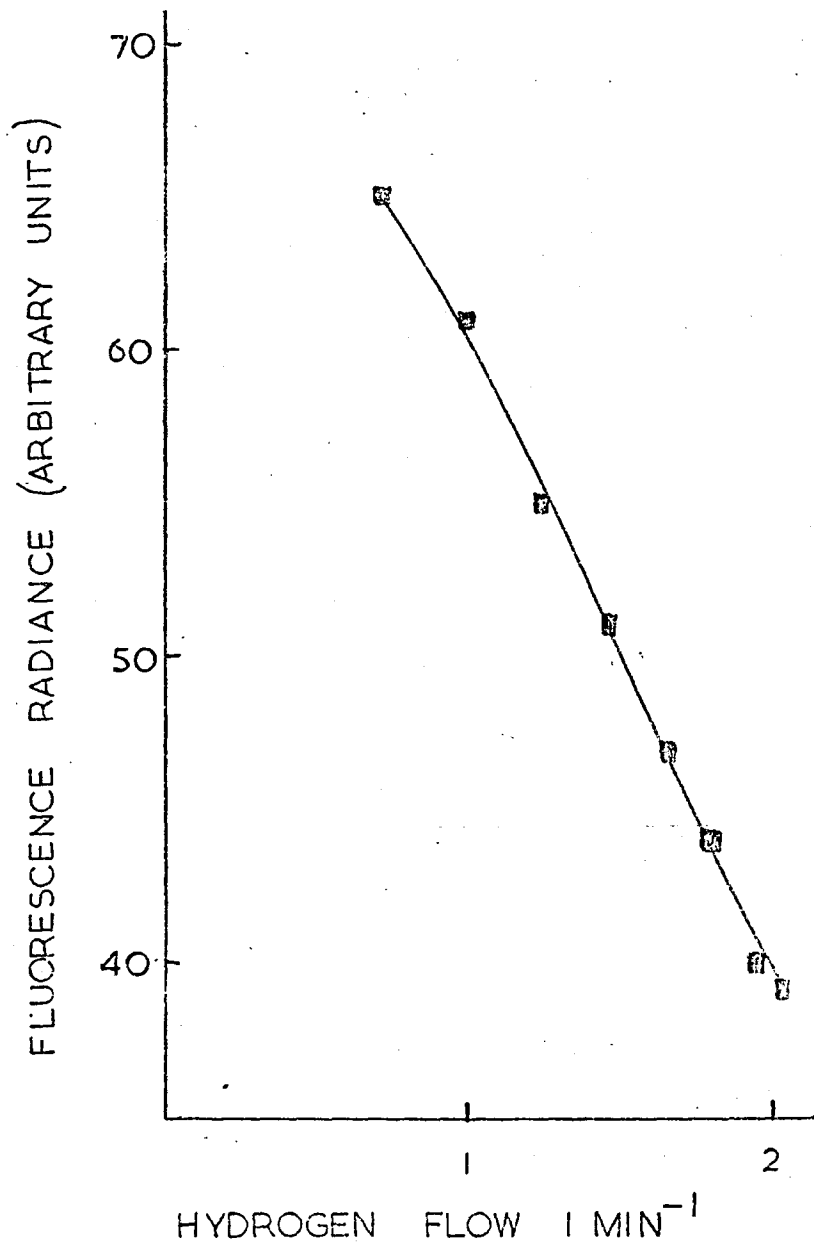


Fig. 4.2 Variation of arsenic fluorescence with fuel flow in the argon-hydrogen and argon-oxygen-hydrogen flames.  
Argon flow - 4.8 l min<sup>-1</sup>  
Oxygen flow - 0.48 l min<sup>-1</sup>

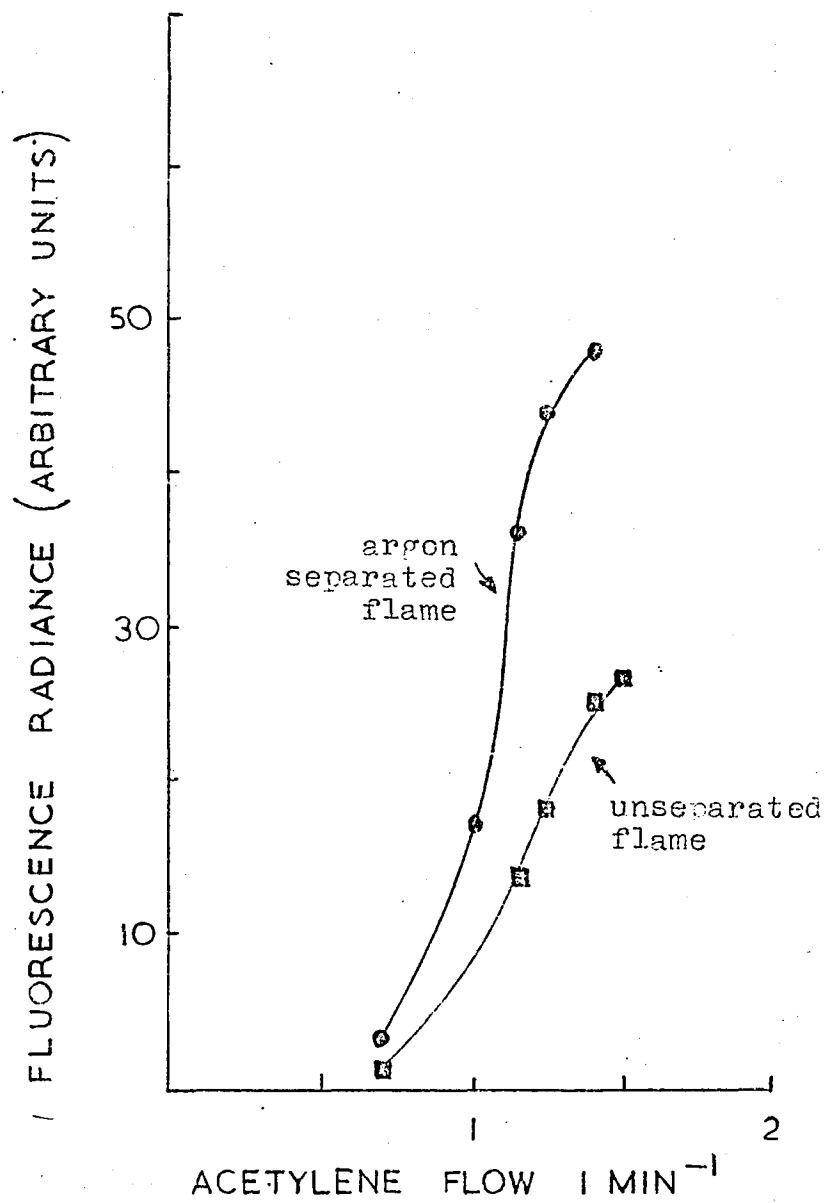


Fig. 4.3 Variation of arsenic fluorescence with fuel flow in the air-acetylene flame. Air flow 4.8 l min<sup>-1</sup>

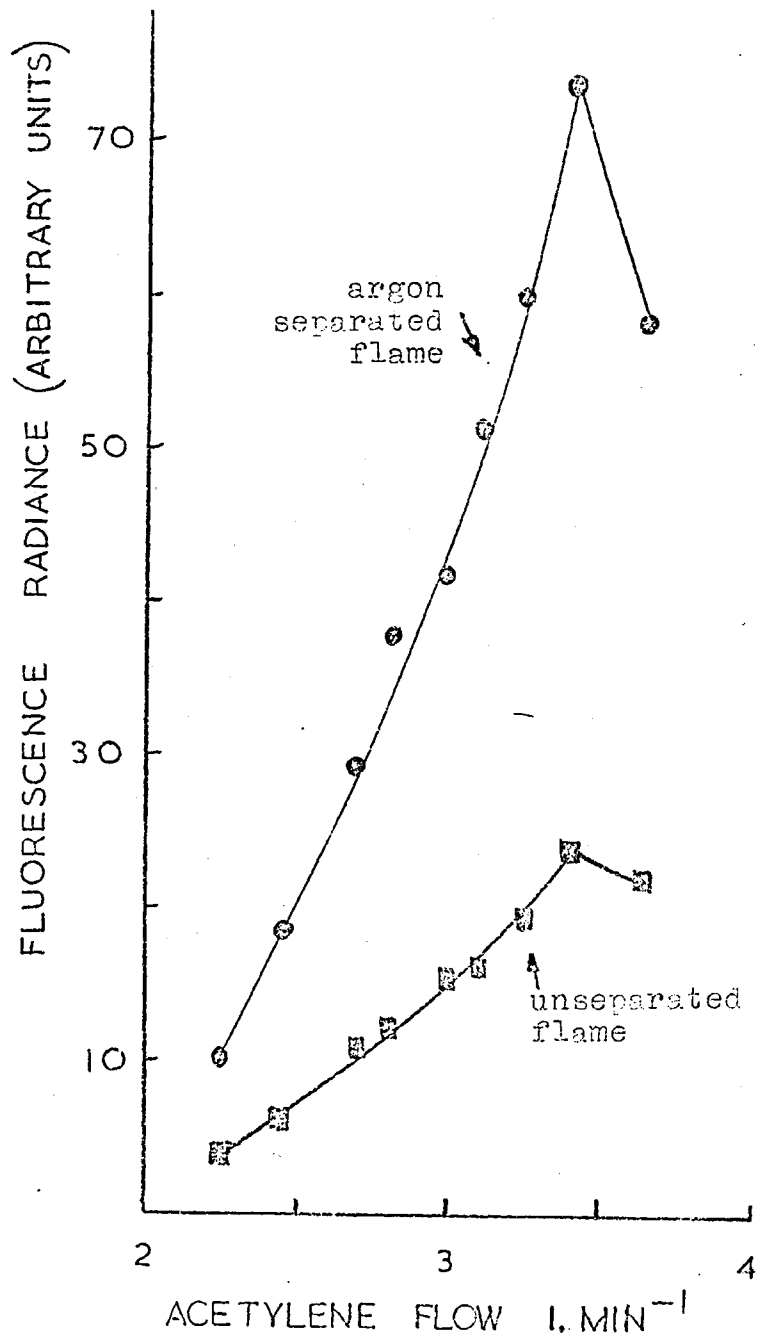


Fig. 4.4 Variation of arsenic fluorescence with fuel flow in the nitrous oxide-acetylene flame. Nitrous oxide flow 4.8 l. min<sup>-1</sup>

TABLE 4.1

## GAS FLOW RATES

(Flow rates giving optimal sensitivity for the determination of arsenic atomic fluorescence at 189.0 nm with various flames)

Flame	Gas flow rates (l min <sup>-1</sup> )	
	unseparated flame	argon separated flame (argon flow 6.0 l min <sup>-1</sup> )
Air	4.8	4.8
Acetylene	1.5	1.4
Argon	4.8	-
Hydrogen	0.72	-
Argon	4.8	-
Oxygen	0.48	-
Hydrogen	0.72	-
Nitrous oxide	4.8	4.8
Acetylene	3.4	3.4

The similarity in trends between the two elements are not unexpected because Mavrodineanu and Boiteux<sup>193</sup> have postulated that high atomic populations of both tin and arsenic are obtained in reducing flames or hydrogen flames as a result of various over-excitation phenomena. (Ref. 193 ch. 22.p.537. )

Various authors discuss chemiexcitation or over-excitation in the book by Dean and Rains<sup>194</sup> and in references 251-253.

The observed optimal fuel flows gave flames which were approximately of the same stoichiometry as the flames used for atomic absorption determinations of arsenic and reported in the literature<sup>117,192,263,264</sup>

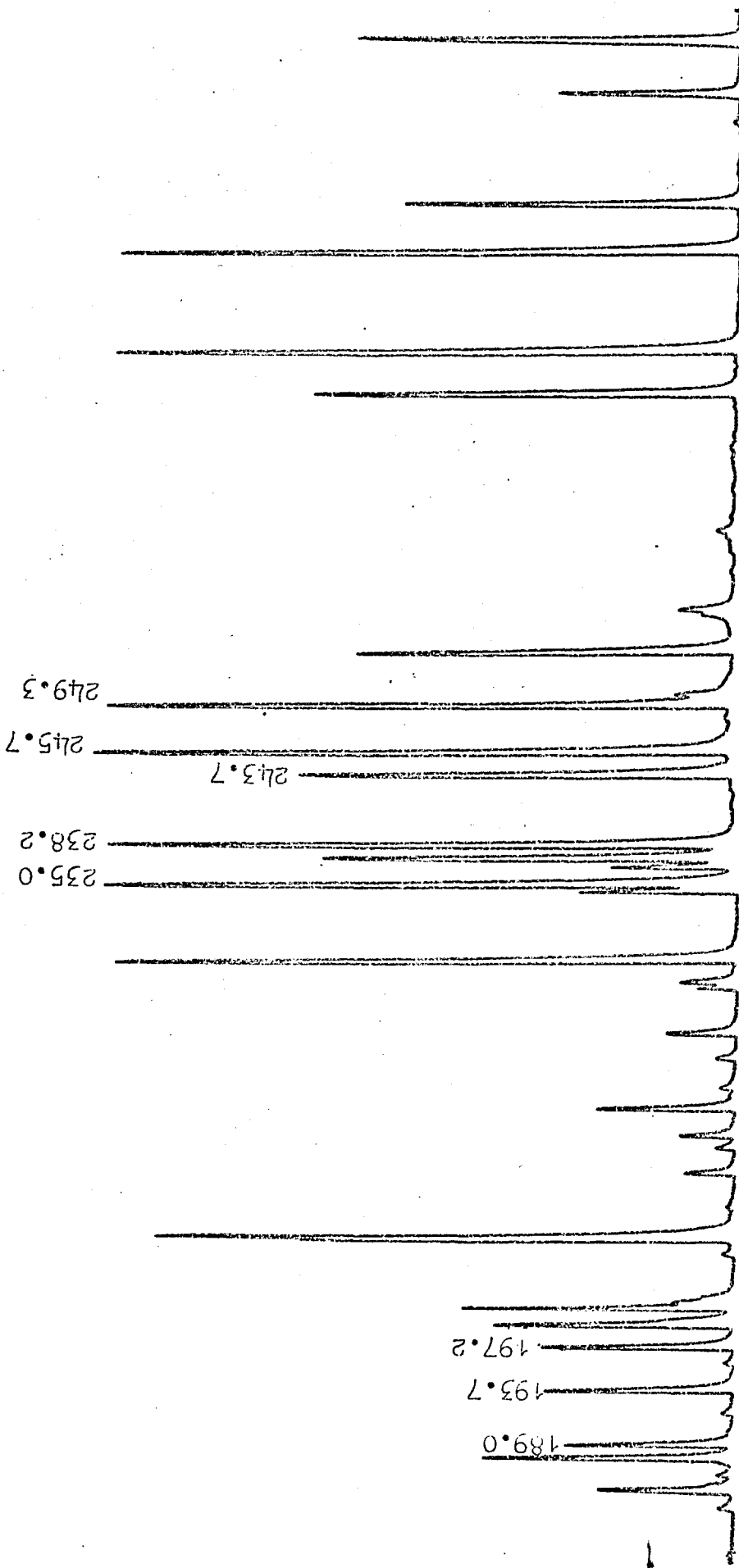
Variation in flame height with respect to the monochromator entrance slit gave very little variation in arsenic fluorescence detected (cf. Tin section 3.2.2.).

#### 4.2.2. Operating conditions for the arsenic electrodeless discharge lamp used as source

Two arsenic lamps were used in this work, both gave the same output radiance and the resulting atomic fluorescence detection limits were also approximately the same. The first lamp lasted about 2 months before a deterioration in the fluorescence signal-to-noise ratio was observed relative to that obtainable using the second lamp (The second lamp was not used extensively in order that this measurement could be made). The deterioration measured was ca. a factor of two. A spectrum of one of the lamps is shown in Fig. 4.5.

The source was modulated at a frequency of 10 KHz<sup>184</sup> and was best operated in a  $\frac{1}{4}$  wave cavity<sup>11,60</sup> using the maximal percentage modulation possible. The lamp was temperature controlled and the operating temperature that gave both the maximal source and fluorescence radiant output at 189.0 nm was 340 K (Fig. 4.6).

Fig. 4.5 The spectrum of the radiant output of an arsenic EDL



The operating temperature used was anywhere between 340 and 360 K because the plateau in the radiance vs temperature plot (Fig. 4.6) allows some latitude in the operating temperature. The lamp was operated at 40 watts incident microwave power. Changes in incident power, made without attempting to compensate for the heating effect of the microwaves at high powers, gave no significant variations in the output radiance of the lamp (Fig. 4.7).

The plateau in the radiance vs incident microwave power plot gives a significant level of stability to the radiant output of the lamp when operated at microwave powers of 40 watts and above (Long period fluctuation over 1 hour was  $\pm 1\%$ ).

#### 4.2.3. Improvements in sensitivity obtained by flushing the monochromator with nitrogen

One of the major difficulties encountered when measuring atomic emission, absorption or fluorescence signals due to arsenic is the absorption of the arsenic resonance radiations by atmospheric oxygen in the light path before the photomultiplier tube. (The resonance lines lie below 200 nm where oxygen absorbs strongly). This situation is further aggravated by strong absorption by the flame gases at wavelengths below 200 nm (section 4.2.4.). In order to reduce the absorption by oxygen in the monochromator nitrogen was passed through the monochromator. The effect of this is illustrated in Fig. 4.8. Spectrum A was obtained before passing nitrogen and spectrum B was obtained after passing nitrogen for half and hour, the time required to fully purge the monochromator of oxygen. It can be seen from Fig. 4.8 that there is a significant increase in transmission of the monochromator when purging with nitrogen. The two spectra were obtained by looking at the lamp output but a proportionate increase in fluorescence signal was not obtained at the 189.0 nm

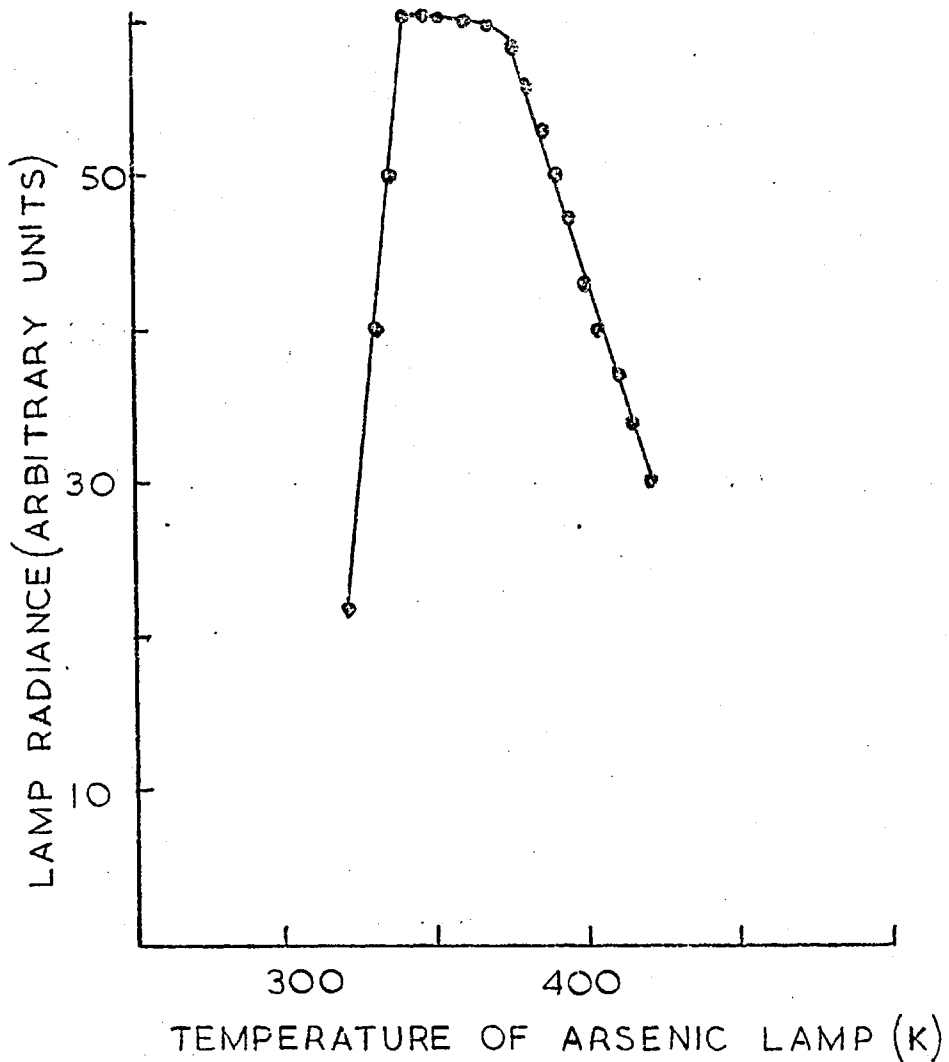


Fig. 4.6 Plot of the radiant output of the arsenic EDL at 189.0 nm vs. temperature of the lamp. Lamp operated at 40 W incident microwave power in the wave cavity and modulated at 10 KHz.

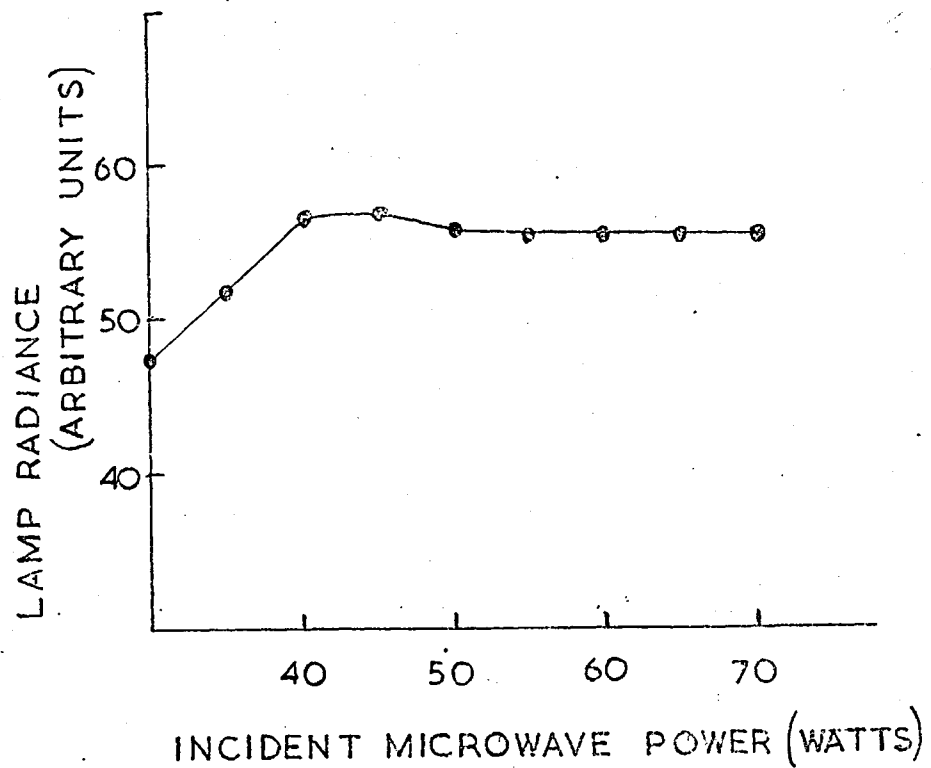


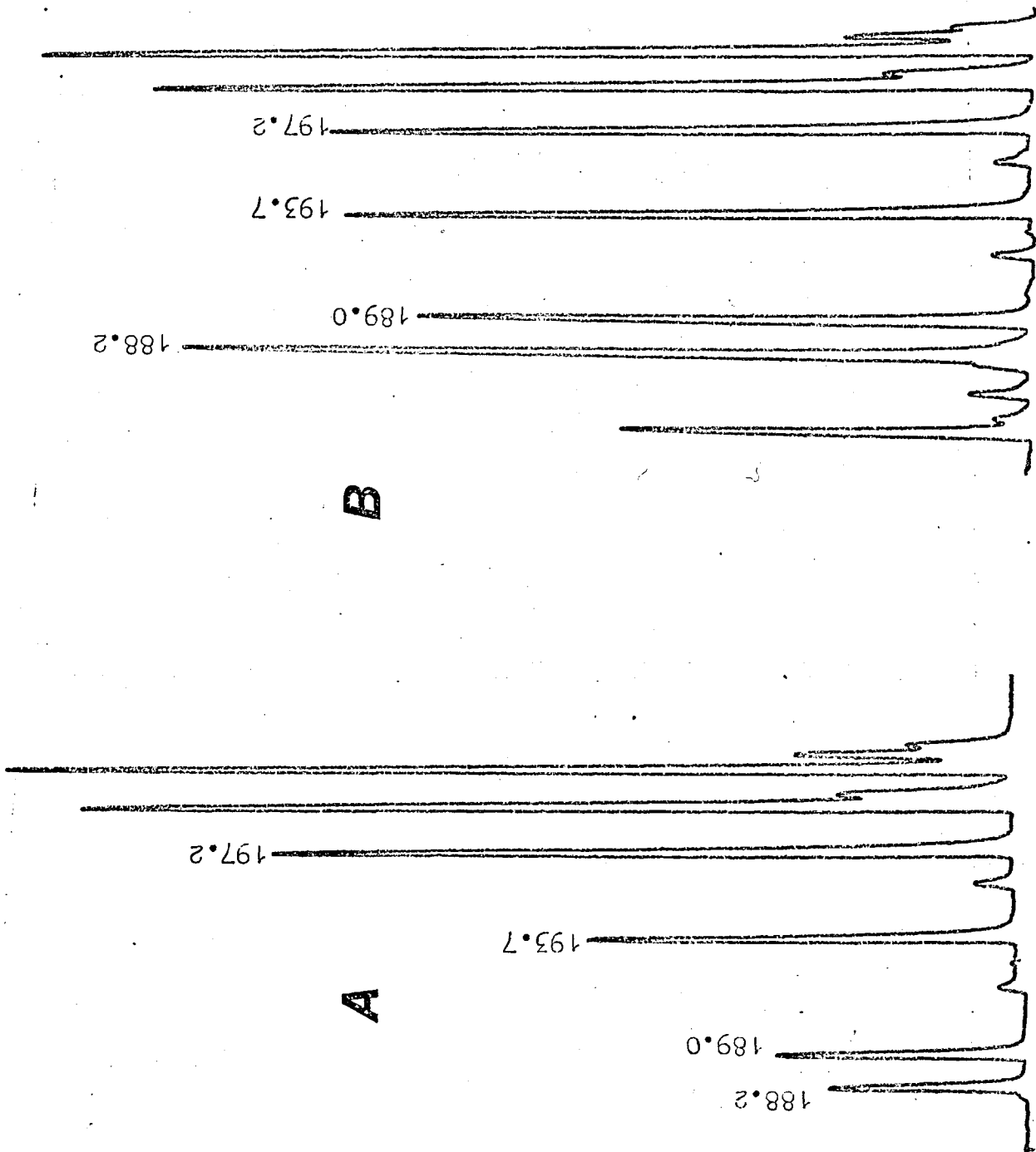
Fig. 4.7 Plot of radiant output of the arsenic EDL at 189.0 nm vs. incident microwave power. (Reflected power ca 10 W) Lamp temperature controlled at 340 K although no compensation was made for the effect of microwave heating. Lamp operated in  $\frac{1}{4}$  wave cavity and modulated at 10 KHz.

Fig. 4.8 Effect of passing nitrogen through the monochromator.

A - Spectrum of As EDL before passing nitrogen

B - Same spectrum after passing nitrogen for half an hour.

Wavelength - nm  
Scan speed -  $1 \text{ nm min}^{-1}$   
Chart speed -  $2.5 \text{ min cm}^{-1}$



line. A factor of 1.9 improvement was obtained when looking at arsenic fluorescence at the 10 ppm level as opposed to a factor of 3.0 when looking at the lamp radiance.

The improvement of almost a factor of two can only just be considered as worthwhile. However as there is work being carried out on the application of atomic absorption to a number of other elements with resonance lines below 200 nm<sup>291-295</sup>, it may be that nitrogen flushed or vacuum monochromators will become commonplace in the near future.

Although there was no fixture on the Jarrell-Ash monochromator for connection of a nitrogen supply it was relatively simple to drill a hole in the cover at the mirror end of the instrument and attach a standard laboratory gas fitting.

#### 4.2.4. Atomic fluorescence spectra of arsenic excited in four flames - Choice of flame

Dagnall et al.<sup>11</sup> studying the atomic fluorescence of arsenic, discussed the choice of flame and analytical wavelength on the basis of sensitivity and linear range of the calibration curves. In the nitrogen-hydrogen and argon-hydrogen flames the 189.0 nm line was the most sensitive resonance line at low concentrations but the analytical curves showed serious curvature above 150 ppm of arsenic. The 197.2 and 193.7 nm lines gave analytical curves which were less curved. The air-acetylene flame gave similar results although the 189.0 nm line was less sensitive than the 193.7 nm line and the 235.0 nm line was most sensitive but the signal-to-noise ratio was unfavourable. The air-acetylene flame gave analytical curves which were of longer linear range than those obtained for the hydrogen flames.

The atomic fluorescence spectra which were obtained in the present work are shown in Figs. 4.9 to 4.12 together with the relative intensities of the four main lines (189.0, 193.7, 197.2

Fig. 4.9

The atomic fluorescence of arsenic in the argon-hydrogen flame. Relative intensities of the lines are as follows:

nm. 189.0:193.7:197.2:235.0  
75 : 70 : 60 : 44

Instrumental conditions used to obtain spectra Figs 4.5, 4.9 - 4.12 are as follows :

chart speed 2.5 min  $\text{cm}^{-1}$   
scan speed 2.0 nm  $\text{min}^{-1}$   
Fluorescence spectra, 100 ppm As.

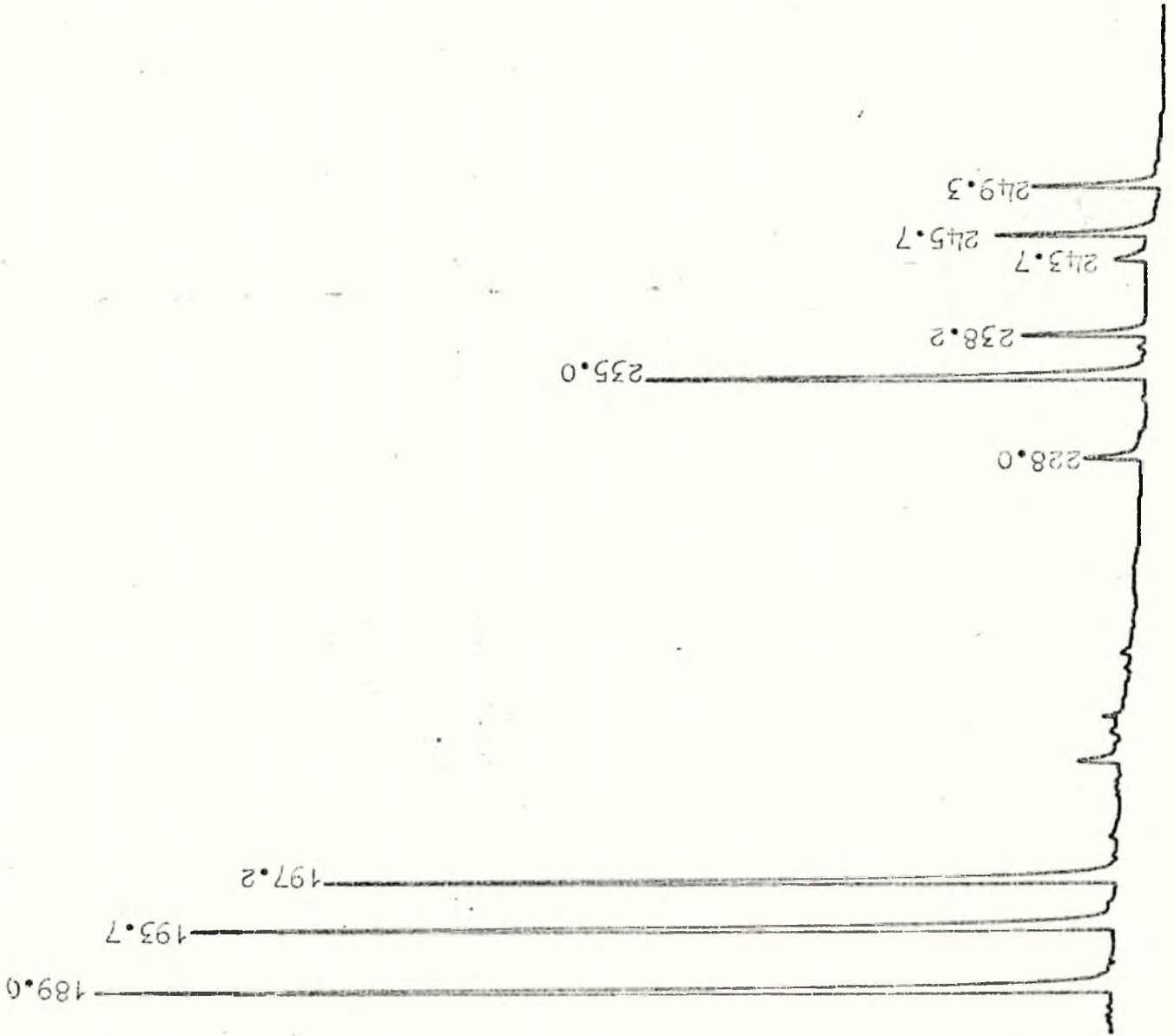


Fig. 4.10 The atomic fluorescence spectrum of arsenic in the argon-oxygen-hydrogen flame. Relative intensities of the lines are as follows:

nm.	189.0	: 193.7	: 197.2	: 235.0
	44	: 43	: 43	: 30

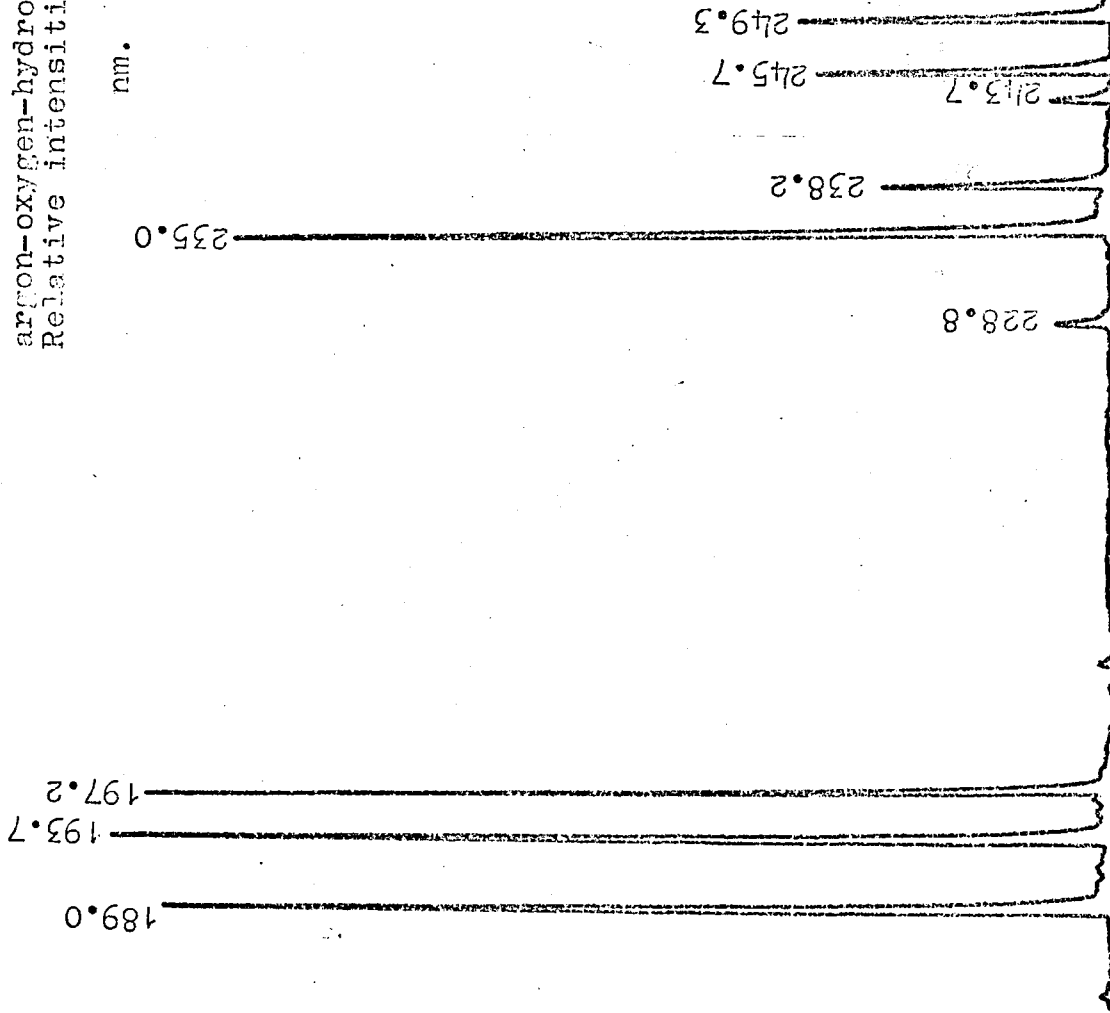


Fig. 4.11 The atomic fluorescence spectrum of arsenic in the argon-separated air-acetylene flame. Relative intensities of the lines are as follows:

nm.	189.0	: 193.7	: 197.2	: 235.0
	85	: 73	: 54	: 45

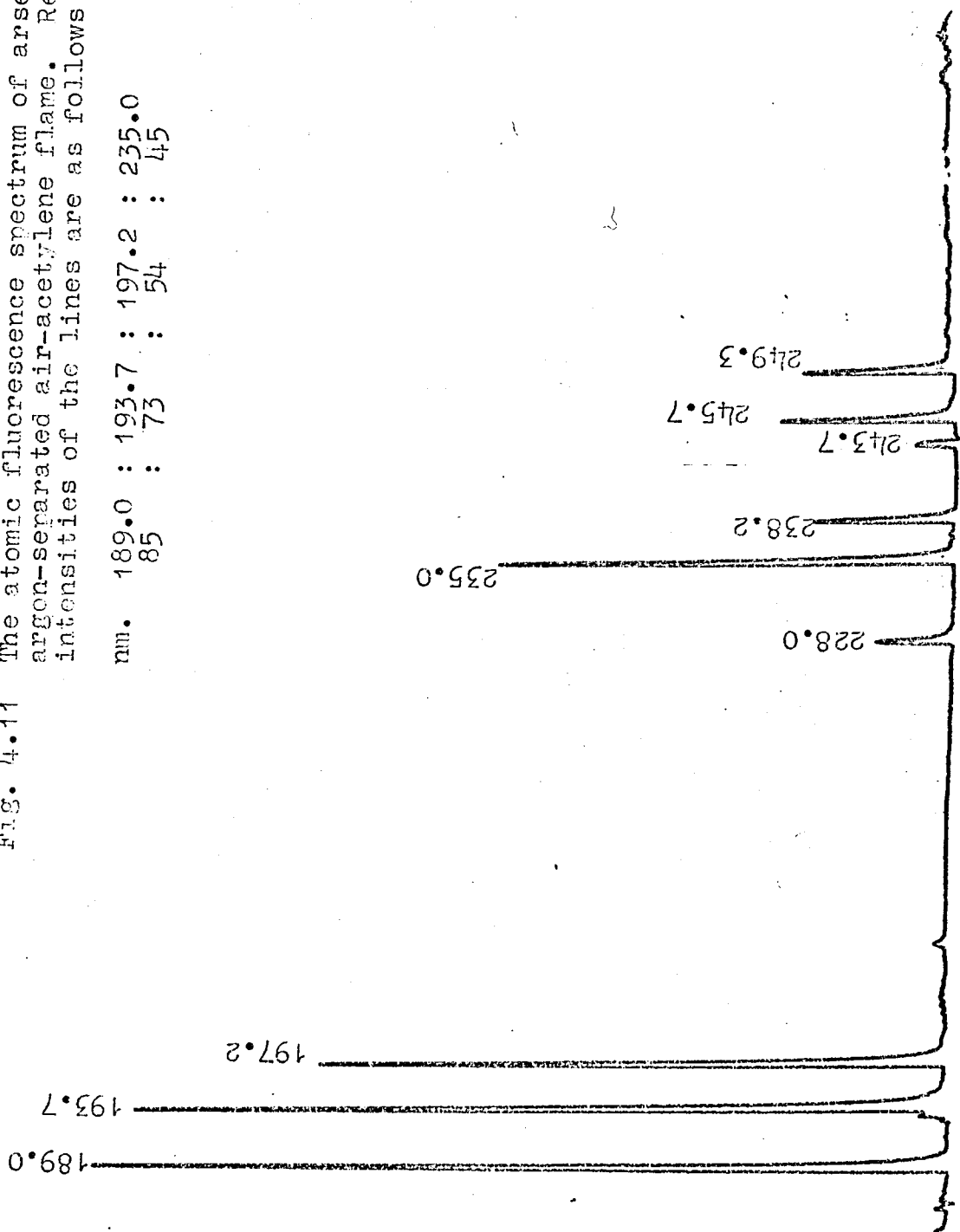
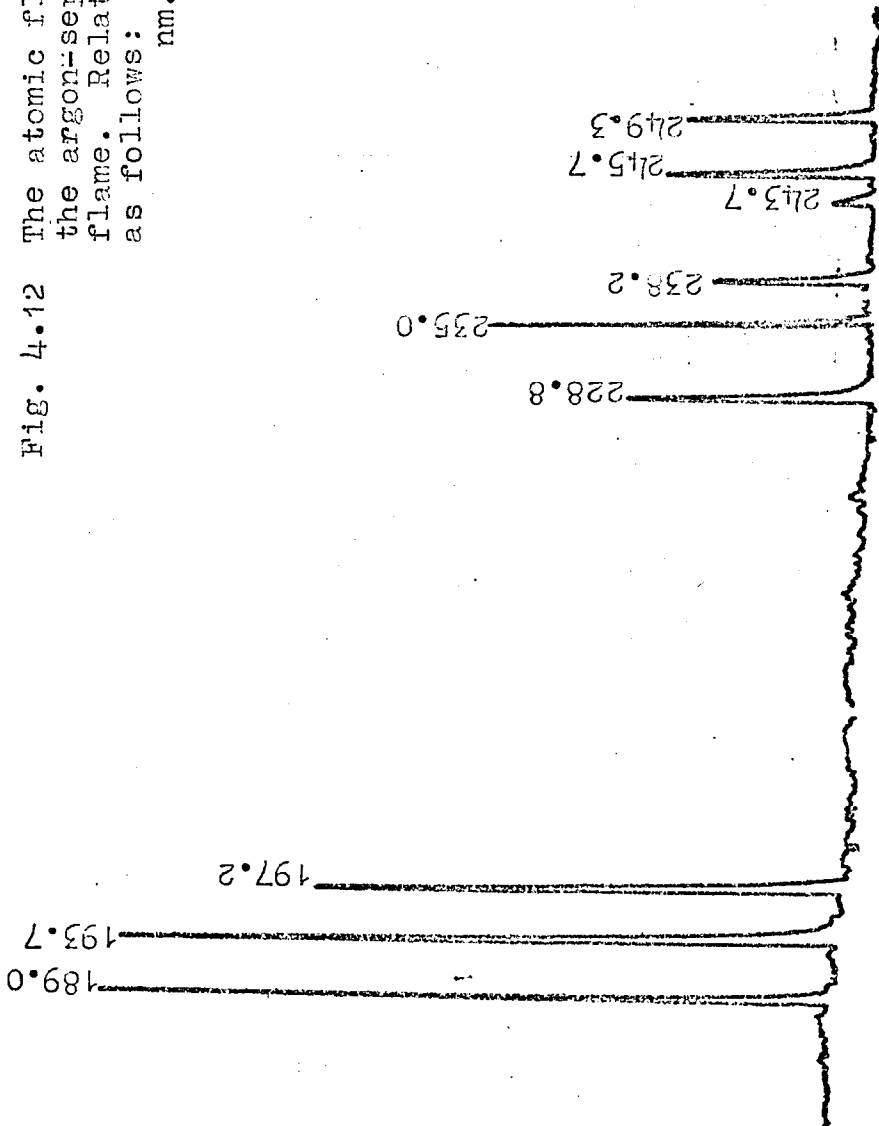


Fig. 4.12 The atomic fluorescence spectrum of arsenic in the argon-separated nitrous oxide-acetylene flame. Relative intensities of the lines are as follows:

nm. 189.0 : 193.7 : 197.2 : 235.0  
 84 : 84 : 60 : 40



and 235.0 nm) at the 100 ppm level. The intensities given are not comparable between flames but they are comparable between the lines emitted from the flame in question. The most significant difference between the relative intensities of the lines as found in this work and the relative intensities as observed by Dagnall et al. is that the 189.0 nm line is always the most sensitive transition in any of the flames. This is probably a result of the superior transmission, below 200 nm, of the nitrogen flushed monochromator. However Dagnall et al. do point out that the photomultiplier (an EMI 9601B) used in their study had very little response at wavelengths below 200 nm. The Hamamatsu R106 used in this study has a better response below 200 nm.

The ratios of the fluorescence intensities at 189.0 nm and at the 10 ppm arsenic level were 50:140:164:132 in the argon-separated nitrous oxide-acetylene, argon-separated air-acetylene, argon-hydrogen and argon-oxygen-hydrogen flames respectively. Measuring the fluorescence signals at 235.0 nm gave the ratios, in the same order 26:75:82:122.

The intensities of the lines below 200 nm relative to the intensities of the lines above 200 nm are influenced by the absorption of the shorter wavelengths by the flame gases and similarly the ratios mentioned above are influenced by the relative absorption characteristics of each flame. Slavin<sup>253</sup> has published flame absorption curves determined by J. E. Allan. These show that air-hydrogen flames are more transparent than air-acetylene flames down to about 195.0 nm, indicating that air-hydrogen would be most convenient for use with the 197.2 nm arsenic line, while air-acetylene is preferable for the 189.0 nm line. The fuels absorb equally at the 193.7 nm line. Although these considerations, discussed by Slavin in the context of atomic absorption, are also important in atomic fluorescence they do not completely explain

the relative intensities of the fluorescence lines in the four flames studied. Indeed Kirkbright and Ranson<sup>264</sup> have shown that the separated nitrous oxide flame is less noisy and absorbs less source radiation at 193.7 nm than the air-acetylene flame. Consequently the atomic absorption detection limit is superior in the former flame despite the sensitivity in the latter flame being superior. This situation does not occur in atomic fluorescence presumably because fluorescence quenching is so much greater in the nitrous oxide flame leading to a further decrease in sensitivity and therefore signal-to-noise ratio. Moreover in the present work the separated nitrous oxide-acetylene flame was found to be slightly more noisy than the separated air-acetylene flame at 189.0 nm (Kirkbright and Ranson made no direct comparison of the two flames when both were separated).

Although over-excitation phenomena<sup>253</sup> may account for the high sensitivity of the cool flames the air-acetylene flame is a high quenching flame relative to the cool flames which gives a further improvement in the relative sensitivity of the cool flames. At 189.0 nm the argon-oxygen-hydrogen flame is less sensitive than the argon-hydrogen flame probably because of absorption of the source and fluorescence radiations by the oxygen added to the flame. Conversely at 235.0 nm the argon-oxygen-hydrogen is the most sensitive probably because the effect of oxygen absorption is not evident at this wavelength and therefore the advantages are revealed of the low quenching characteristics of the flame relative to hotter flames and the increased temperature of the flame relative to argon-hydrogen.

An explanation of the relatively high fluorescence intensity of the 235.0 nm line in any of the flames is given by Dagnall et al.<sup>11</sup> in terms of the energy differences between the atomic states concerned.

The relative sensitivities at the 10 ppm level and at 189.0 nm which are given above and the detection limits given in section 4.4.2 ~~4.3.6.~~ indicate that there is very little advantage in using the cool hydrogen flames rather than the separated air-acetylene flame. The 189.0 line, being the most sensitive line in all flames at low arsenic concentrations, was chosen for the work described here. However it may be advantageous to use the 235.0 nm line for two reasons. Firstly, the instrument in use may perform poorly at wavelengths below 200 nm in which case 235.0 nm would be the most sensitive wavelength. Secondly the linear range of analytical curves in all four flames is greater at 235.0 nm because the latter is a non-resonance fluorescence transition and self-absorption is greatly reduced (See section 4.3.5.).

#### 4.3. Interferences affecting the determination of arsenic

Kirkbright et al.<sup>263</sup> discuss the interferences affecting the determinations of arsenic by atomic absorption in a nitrogen-separated air-acetylene flame and point out that, for the determination of elements whose strongest absorption lines lie below 200 nm, the separated air-acetylene flame combines the advantages of a relatively low background and noise level (comparable with the argon-hydrogen flame) with the less serious interferences obtainable with the hotter flame. Kirkbright and Ranson<sup>264</sup> demonstrate that there are fewer interferences affecting the atomic absorption determination of arsenic in the separated nitrous oxide-acetylene flame than in the air-acetylene flame. In some further work on the same subject Kirkbright et al.<sup>265</sup> compare in more detail the interferences affecting the atomic absorption of arsenic in these two flames and conclude that the argon-separated nitrous oxide-acetylene flame can be used for the determination of arsenic in complex matrices without the need for the addition of the major

constituents of the matrix to the standards. This was not true of the separated air-acetylene flame.

Williams<sup>271</sup> described one of the few applications of the argon-hydrogen flame for the atomic absorption determination of arsenic in a real sample (preserved wood) and obtained an analytical sensitivity of 0.1 ppm. Standards were treated with the same dissolution procedure as the sample and the cations of K, Cu, Cr, Ca, Mg, Na and the anions sulphate and phosphate were shown not to interfere seriously with the determination. Hwang<sup>272</sup> and Sandonato studied interferences affecting the atomic absorption determination in the nitrous oxide-acetylene flame and found them to be insignificant at the concentration levels studied (10 ppm arsenic, 10-fold excess interfering ions).

Dagnall et al.<sup>11</sup> in their atomic fluorescence study found that the air-acetylene flame was less affected by interferences than the cooler flames. They did not study the nitrous oxide flame.

#### 4.3.1. The effect of acids

Using the four flames of interest the effects of five acids on the atomic fluorescence of arsenic were determined by measuring 10 ppm aqueous arsenic solutions containing a range of concentrations of the acids. The effects in the four flames are shown in Figs. 4.13 to 4.16. Except for hydrochloric acid all the acids cause a depression of the fluorescence signals in all four flames. Hydrochloric acid causes enhancements in all four flames, 46%, 7%, 12% and 29% in the Ar/H<sub>2</sub>, Ar/O<sub>2</sub>/H<sub>2</sub>, Air/C<sub>2</sub>H<sub>2</sub> and N<sub>2</sub>O/C<sub>2</sub>H<sub>2</sub> flames respectively. These enhancements are constant at all acid concentrations between 2 and 10% in all but the N<sub>2</sub>O/C<sub>2</sub>H<sub>2</sub> flame. In the latter flame this enhancement varied from 6% at 2% HCl to 29% at 10% HCl. There is also a slight enhancement of the

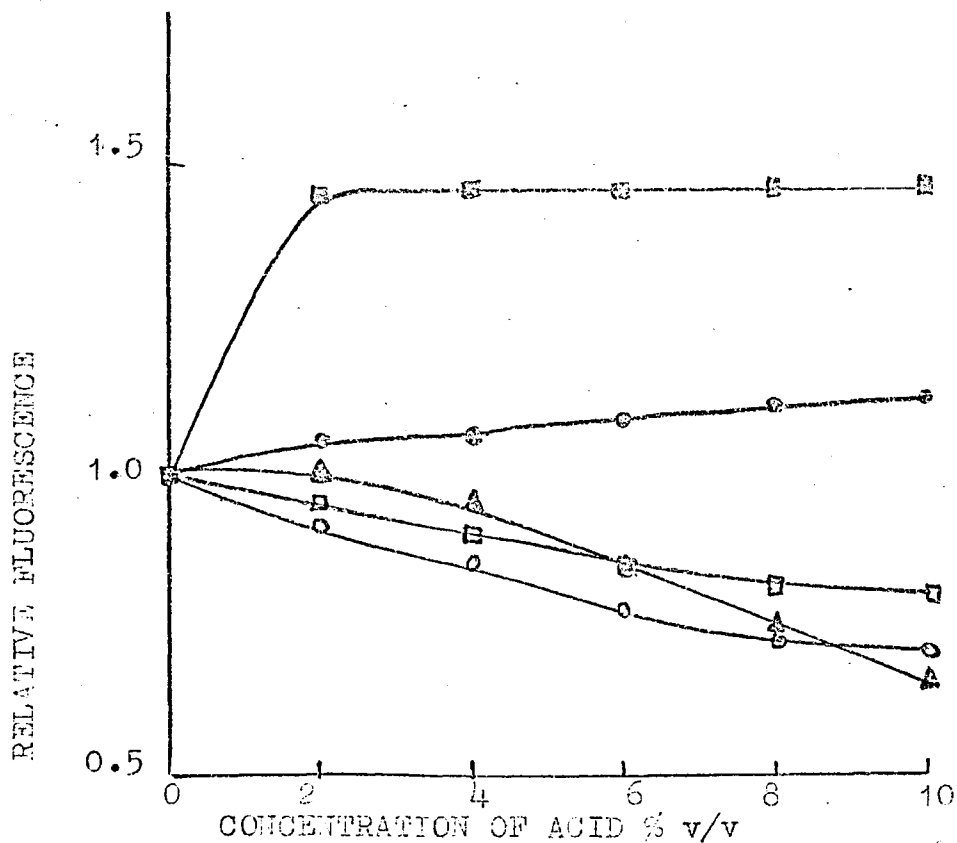


Fig. 4.13 The effects of five acids on arsenic fluorescence in the argon-hydrogen flame. Relative fluorescence is the ratio of the fluorescence of arsenic in the presence of acid to the fluorescence of arsenic alone.

(■) - hydrochloric acid; (⊙) - perchloric acid;  
 (△) - sulphuric acid; (□) - nitric acid;  
 (○) - phosphoric acid.

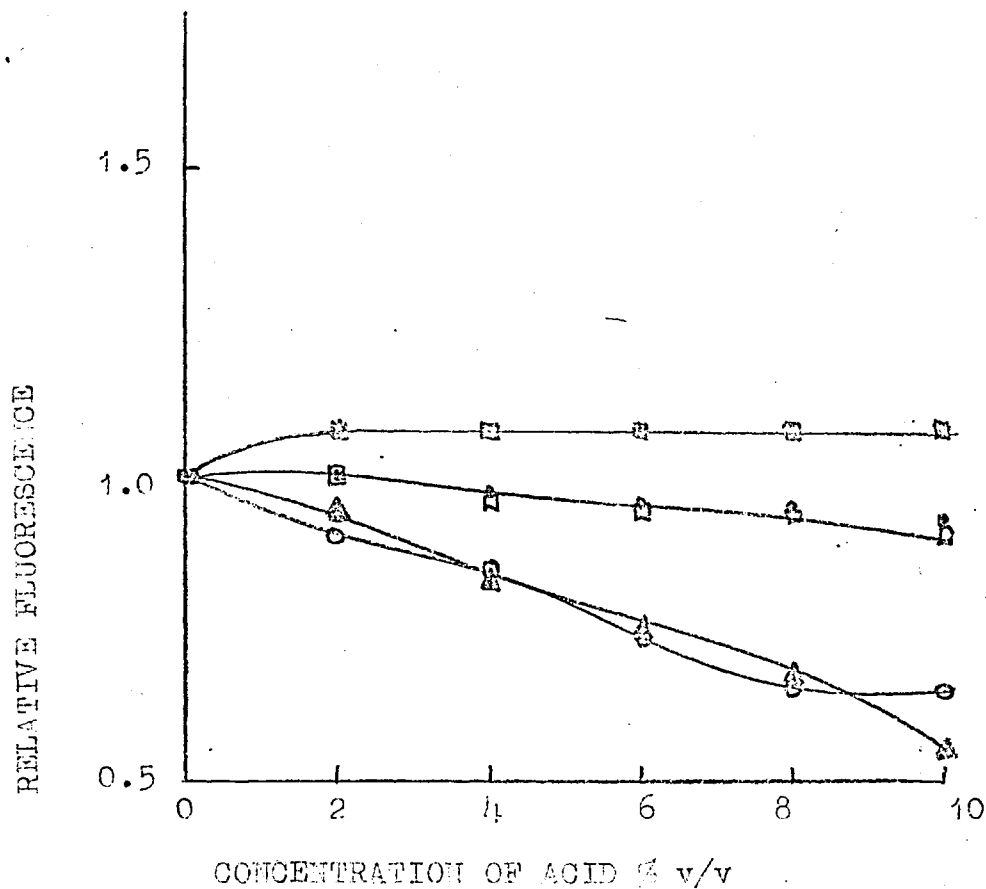


Fig. 4.14 The effects of five acids on arsenic fluorescence in the argon-oxygen-hydrogen flame.

(■) - hydrochloric acid; (e) - perchloric acid;  
 (▲) - sulphuric acid; (□) - nitric acid;  
 (○) - phosphoric acid.

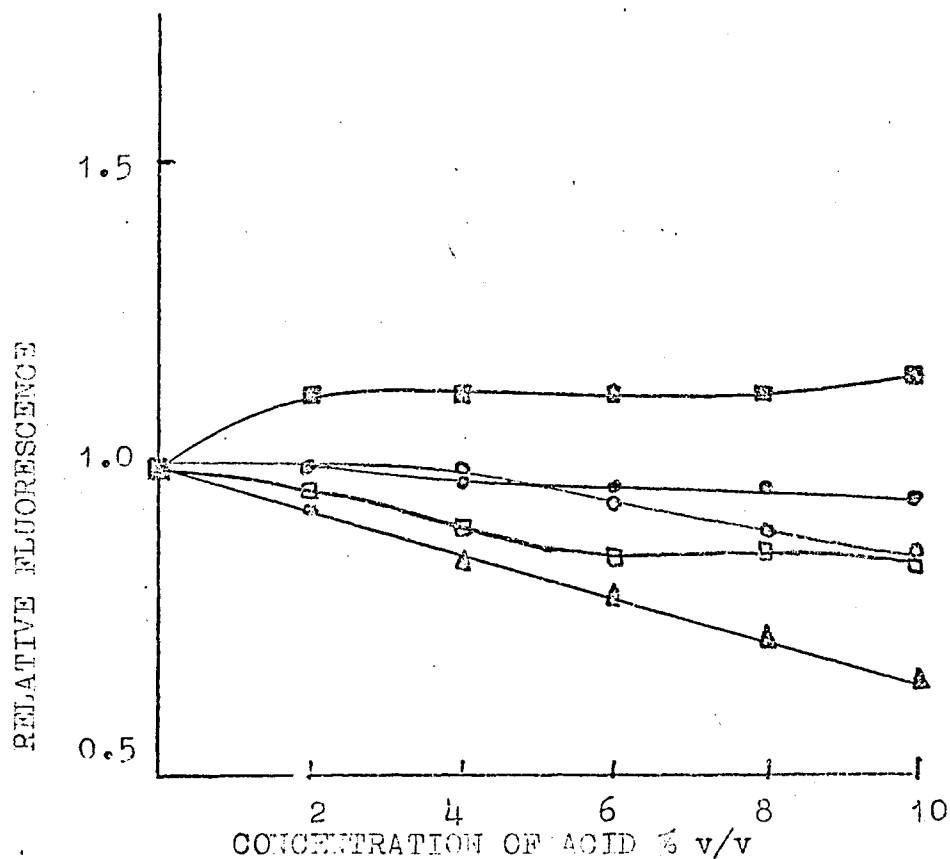


Fig. 4.15 The effects of five acids on arsenic fluorescence in the argon-separated air-acetylene flame.  
 (E) - hydrochloric acid; (⊙) - perchloric acid;  
 (Δ) - sulphuric acid; (□) - nitric acid;  
 (○) - phosphoric acid.

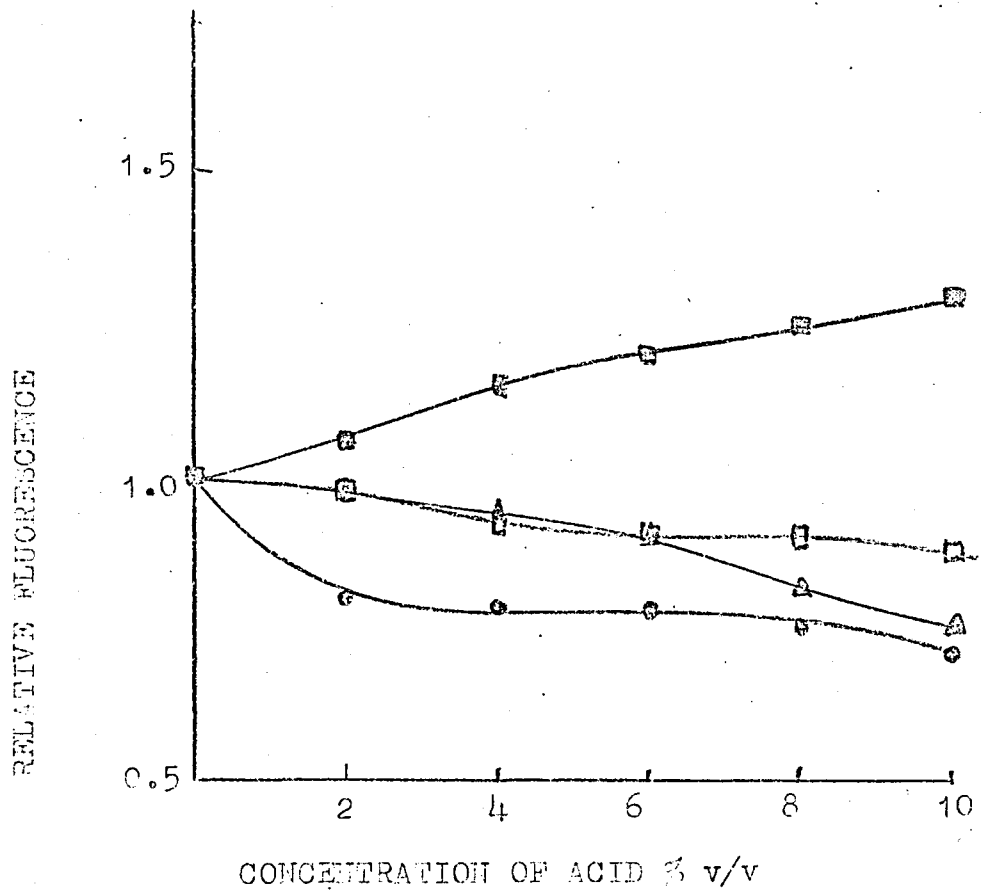


Fig. 4.16 The effects of five acids on arsenic fluorescence in the argon-separated nitrous oxide-acetylene flame.  
 (■) - hydrochloric acid; (●) - perchloric acid;  
 (▲) - sulphuric acid; (□) - nitric acid;  
 Phosphoric acid - flame unstable.

fluorescence signal in the Ar/H<sub>2</sub> flame when perchloric acid is present although the same concentrations of this acid cause depressions in the other flames. The presence of phosphoric acid made all four flames very unstable especially the nitrous oxide flame.

Using the separated air-acetylene flame<sup>263</sup> and the separated nitrous oxide-acetylene flame<sup>264</sup> Kirkbright and his co-workers found no interference with the atomic absorption determination of arsenic from nitric, sulphuric, phosphoric or hydrochloric acids. However these workers were testing for the acid interferences using 100 ppm arsenic solutions containing a 100-fold weight excess of each acid which for any one of the acids results in a solution which contains less than 2% of the acid. Dagnall et al.<sup>11</sup> also found no anion interferences on their arsenic fluorescence signals which is probably explained by the low concentrations of acids used in their study.

The results, shown in Figs. 4.13 to 4.16, at the 2% level of each acid and at the 10 ppm arsenic level show that the fluorescence method is as free from interferences from acids as the atomic absorption method as reported by Kirkbright and his co-workers. Even at acid concentrations of 4% or less in any one of the flames there is no interference greater than 10% and most of the changes in the fluorescence signals are less than 5%.

It is noteworthy that Atushi Ando et al.<sup>282</sup> studied the effect of acids on arsenic atomic absorption using a nitrogen-hydrogen flame and a long-path vycor cell and found similar acid interferences to those found in this atomic fluorescence work, i.e. 18% enhancement due to hydrochloric acid and depressions due to the other acids. They were using 1 ppm arsenic solutions which contained 0.1 to 0.5M concentrations of the acids.

The effects of acids on the fluorescence of arsenic are

similar to those on the fluorescence of tin but the arsenic fluorescence is less severely affected. As in the case of tin the enhancement caused by hydrochloric acid is probably due to the formation of more easily vaporized or dissociated species. The depressions caused by oxygen containing acids are most likely to be due to the formation of species which are difficult to vaporize or dissociate in the four flames.

#### 4.3.2. The effect of elements

In atomic absorption using the air-hydrogen or argon-hydrogen flames most elements have been reported to interfere with arsenic absorption signals <sup>165,264,266</sup> and as mentioned at the beginning of section 4.3 Dagnall et al.<sup>11</sup> report a number of interferences on atomic fluorescence in cool flames although the use of a 75 ppm arsenic test solution probably resulted in the interferences being less apparent than in the present work. Here, the effects were determined of a number of elements on the fluorescence of arsenic in all four flames. (10 ppm arsenic, 100 and 1000 ppm interfering ion most sensitive gas flows in each flame except  $N_2O/C_2H_2$ ). In the argon-hydrogen and argon-oxygen-hydrogen flames the expected large number of interferences were encountered (Table 4.2). None of these interferences were removed in the presence of 10,000 ppm of iron or 4% hydrochloric acid. <sup>282</sup> Atsushi Ando et al. attribute the depressing interferences in the nitrogen-hydrogen flame to the formation of metal arsenides and to test this hypothesis absorption intensity changes of Mg, Ca, Ni and Co were measured in the presence of arsenous acid. The observed decreased absorbance of these metals tended to confirm the formation of arsenides in the flame as the basis of the interference effects. This situation is probably occurring in the atomic fluorescence determination.



TABLE 4.2 (cont.)

## INTERFERENCES ON ARSENIC ATOMIC FLUORESCENCE

Element ppm	argon- separated nitrous oxide- acetylene		argon-separated air-acetylene		argon-oxygen- hydrogen		argon-hydrogen		
	A.C.	HCl	Aq.	HCl	Aq.	HCl	Aq.	HCl	
Cu	1000 100	0.96 1.0	0.95 1.0	1.0 1.0	0.95 1.0	0.96 1.0	0.51 0.69	1.0 1.0	Fe
Fe	10000 1000	0.74 0.91	0.74 0.91	0.96 1.0	0.30 0.99	0.30 0.99	0.60 0.94	0.60 0.94	Fe
K	1000 100	1.55 1.06	1.18 1.00	1.00 1.00	1.38 1.06	1.4 1.05	1.10 1.00	1.24 1.0	1.10 1.0
Mn	1000 100	1.0 1.0	0.83 0.95	1.0 1.0	0.90 1.0	0.91 1.0	1.0 1.0	1.04 1.02	1.0 1.0
Mg	1000 100	1.0 1.0	0.90 0.95	1.0 1.0	1.0 1.0	1.0 1.0	0.58 0.90	0.49 0.77	0.78 0.92
Mo	1000 100	1.0 1.0	1.0 1.0	1.0 1.0	1.0 1.0	1.0 1.0	0.95 1.0	1.0 1.0	1.0 1.0
Na	1000 100	0.84 1.0	0.95 1.0	1.0 1.0	1.0 1.0	1.0 1.0	0.88 0.93	0.86 0.95	0.98 1.0
Ni	1000 100	1.0 1.0	1.0 1.0	1.0 1.0	1.0 1.0	1.0 1.0	0.86 0.89	0.85 0.88	0.91 0.97
Pb	1000 100	0.95 1.0	1.0 1.0	1.0 1.0	0.97 1.0	1.0 1.0	1.0 1.0	1.0 1.0	1.06 1.04
Sn	1000 100	0.98 1.0	1.0 1.0	1.0 1.0	0.96 1.0	1.0 1.0	0.98 1.0	1.0 1.0	0.86 0.89

TABLE 4.2 (cont.)

## INTERFERENCES ON ARSENIC ATOMIC FLUORESCENCE

Element ppm	argon-separated nitrous oxide- acetylene			argon-separated air- acetylene			argon-oxygen- hydrogen			argon-hydrogen		
	Aq	HCl	Fe	Aq	HCl	Fe	Aq	HCl	Fe	Aq	HCl	Fe
Si 1000 100	0.97 1.0	0.96 1.0	0.95 1.0	0.93 1.0	0.97 1.0	1.0 1.0	0.89 0.92	0.91 0.93	0.96 0.97	0.75 0.88	0.79 0.87	0.87 0.91
Sr 1000 100	1.0 1.0	1.0 1.0	1.0 1.0	1.1 1.03	1.13 1.05	1.0 1.0	0.86 0.96	0.85 0.93	1.0 1.0	0.98 0.98	1.0 1.0	1.0 1.0
Ti 1000 100	0.72 0.92	0.95 1.0	1.0 1.0	1.07 1.00	1.0 1.0	1.0 1.0	1.05 1.0	1.03 0.81	1.0 1.0	1.04 1.0	1.0 1.0	0.95 1.0
Tl 1000 100	1.0 1.0	1.0 1.0		1.0 1.0	1.0 1.0		1.0 1.0	1.06 1.0		1.05 1.09	1.3 1.22	
V 1000 100	0.83 1.0	1.0 1.0	1.0 1.0	1.0 1.0	1.0 1.0	1.0 1.0	1.02 1.0	1.0 1.0	1.0 1.0	0.75 0.82	0.85 0.91	0.70 0.79
W 1000 100	1.0 1.0	1.0 1.0		1.0 1.0	1.0 1.0		1.02 1.0	1.0 1.0		0.71 0.82	0.63 1.0	
Zn 1000 100	1.2 1.1	1.18 1.1	1.08 1.05	1.03 1.0	1.08 1.04	1.0 1.0	1.07 1.07	1.11 1.03	1.02 1.0	1.18 1.18	1.15 1.06	1.16 1.09
Zr 1000 100	0.84 0.84	0.73 0.91	0.95 0.97	1.0 1.0	1.0 1.0	1.0 1.0	0.85 0.85	0.8 0.93	0.85 0.88	0.53 0.53	0.77 0.95	0.85 0.89

The addition of oxygen to the argon-hydrogen flame does not significantly alter the interferences encountered in this flame (Table 4.2) consequently it becomes impractical to use either of the cool flames for other than the analysis of relatively pure solutions. The effects of the various metal ions shown in Table 4.2 demonstrate that the fluorescence determination of arsenic in the argon-separated air-acetylene flame is remarkably free from interference. Only potassium gives any change in the fluorescence signal in the presence of 10,000 ppm iron. The cations of Mn, Sr, Ti, Pb, Sn, Si and Zn interfere in pure aqueous solutions but the effects due to all these cations are not significant except at the 1000 ppm level.

The circular slot burner used to support the argon-separated nitrous oxide-acetylene flame had been giving trouble during the determination of the interference effects in Table 4.2. Long use of this burner had gradually produced a sufficiently deformed slot to alter the flow of gases into the flame, consequently, it would not support a flame with a "red feather" greater than 5 mm in height (acetylene flow  $3.1 \text{ l min}^{-1}$ ) without instability occurring. A number of interferences were encountered in this flame (Table 4.2). The burnerhead was subsequently machined to give a slot of more even dimensions and a few interference effects further investigated using a flame with a red feather of about 30 mm (acetylene flow  $3.4 \text{ l min}^{-1}$ ). The results, presented in table 4.3, reveal fewer interferences than is evident with the air-acetylene flame. The lack of interferences occurring in nitrous oxide-acetylene when measuring in the "red feather" zone is normally attributed to the extremely low concentration of oxygen atoms in this region<sup>296,297</sup>.

The interferences with the arsenic fluorescence signals in the various flames tested here follow the same basic trends as has<sup>165,264,266</sup> been reported for arsenic atomic absorption in the cool flames the air-acetylene flame<sup>266,268</sup> and the nitrous oxide-acetylene flame<sup>264</sup>.

TABLE 4.3

INTERFERENCES ON ARSENIC ATOMIC FLUORESCENCE USING A NITROUS  
OXIDE-ACETYLENE FLAME WITH 30 mm "RED FEATHER"

(for conditions see table 4.2)

Element (1000 ppm)	Aq.	Fe
Al	1.0	1.0
Ce	1.0	1.0
Cr	1.0	1.0
Cu	1.0	1.0
Fe	1.0	0.96
K	1.5	1.0
Mg	1.0	1.0
Mn	1.0	1.0
Na	0.9	1.0
Pb	1.0	1.0
Si	1.0	1.0
V	1.0	1.0
Zn	1.0	1.0
Zr	1.0	1.0

The only exception to this observation is in the work of Kirkbright<sup>263,265</sup> et al. who observed the interference of the cations of Mg, Al, Ca, Cr, V, Fe, Co, Ni, Cu, Mo, Hg, Pb and Sn on arsenic atomic absorption in the separated air-acetylene flame using 100-fold weight excesses of the ions and 100 ppm arsenic test solutions.. This large number of interferences is surprising when compared with the few atomic absorption interferences reported by Johns<sup>266</sup> and Smith and Frank<sup>268</sup> when using the air-acetylene flame and further compared with the minor interferences observed by Dagnall and his co-workers<sup>11,261</sup> Thompson and Wildy<sup>179</sup> and the present author for the atomic fluorescence of arsenic in the same flame. Smith and Frank<sup>268</sup> reported the interference of Al, Cr, Mo, Mn, Pb and Sn with arsenic absorption. All these cations except Mn interfered in the similar studies of Kirkbright et al.<sup>263,265</sup> and Mn, Pb and Sn interfered in this fluorescence study. The large number of interferences observed by Kirkbright et al. may be due to the relatively high levels of the ions added (10,000 ppm).

In summary, the separated nitrous oxide-acetylene flame is the most favourable for atomic absorption and fluorescence determinations of arsenic in aqueous solution. However this work has shown that the presence of 10,000 ppm iron eliminates the small number of interferences which affect the fluorescence of arsenic in the separated air-acetylene flame. This phenomenon, often called the "Matrix Dilution" effect, is encountered with the flame spectroscopy of many elements. The presence of the major constituent is said to dilute the salt matrix left after evaporation of the solvent in the flame and hence reduce the effect of small amounts of other elements<sup>298</sup>. The more sensitive air-acetylene flame must not therefore be eliminated as the flame of choice for the atomic absorption or fluorescence of arsenic.

<sup>11</sup>  
Dagnall et al. in their atomic fluorescence study using the

air-acetylene flame found that Na, K and Cu interfered with the determination and attributed these interferences to intense light emission from these easily excited elements. This emission reached the photomultiplier via a light leakage in the Unicam SP900 A monochromator. In the present work the arsenic fluorescence signals in both acetylene based flames were enhanced by potassium but not by copper or sodium. In order to discover why Cu and Na did not interfere an R166 photomultiplier tube was used instead of the R106 tube. The R166 has very little response to wavelengths above 320 nm and would not therefore be expected to respond significantly to any light leakage from strong thermal emissions in the visible region. Using this detector the potassium enhancement remained at exactly the same magnitude (Relative fluorescence 1.5 and 1.4 in the nitrous-oxide-acetylene and air-acetylene flames respectively). At the sodium emission wavelengths, 589.0, 330.2, no signal was observed when aspirating 2500 ppm sodium. Similarly for potassium at 404.4 nm and copper at 327.4 nm. This was the case when either of the two photomultiplier tubes (R106 and R166) were being used. These results demonstrate the absence of a light leakage and emphasize the efficiency with which the combination of high frequency modulation and the lock-in amplifier is able to reject emission from the flame. Without this high rejection light leakage may well be a problem in atomic fluorescence spectroscopy. At least two examples of this have been described in the literature. Barnett and Kahn<sup>36</sup> observed an enhancing interference of sodium on the fluorescence of iron in an air-acetylene flame. The sodium produced no atomic absorption interference (presumably because instrumental gains are not high in atomic absorption). These workers found that when a blank solution containing only sodium and no iron was measured the reading exactly matched the sodium enhancement obtained when measuring iron fluorescence. Thus they

were able to attribute the sodium interference to light leakage.  
<sup>189</sup>  
 Rains et al. were successful in reducing but not eliminating sodium emission signals reaching the photomultiplier by using a R166 photomultiplier tube in conjunction with a lock-in amplifier and 70 Hz modulation. From the latter work it seems that the R166 tube is less effective in reducing light leakage than the use of high-frequency modulation as described in the present work. Further, the complete absence of a light leakage in this work indicates that the potassium enhancement on arsenic signals is probably due to a chemical effect. Dagnall et al.<sup>11</sup> would seem to have been justified therefore in attributing the sodium and copper interferences to a light leakage although the potassium interference was probably only partly attributable to leakage.

#### 4.3.3. The effect of iron on the arsenic fluorescence and on the interferences from other elements

From Table 4.2 it can be seen that the presence of 10,000 ppm iron (as ferric chloride) does minimise the interference from Zn, Mn, Pb, Si, Sn, Ti and Zn in the air-acetylene flame.

The effect of iron (range 0 to 10,000 ppm) on the fluorescence of a 10 ppm arsenic solution was determined using all four flames. The results are tabulated (Table 4.4.) rather than represented graphically because the effects, except for the cool flames, are quite small. The depressions in the cool flames further emphasize that their use for the determination of arsenic is undesirable because of the large number of interferences that occur. The small depressions in the acetylene based flames do not significantly alter the sensitivity of the atomic fluorescence method although they do make it necessary, when carrying out analyses, to add 10,000 ppm of ferric chloride to standard solutions.

In the air-acetylene flame the effect of iron at the 10,000 ppm

TABLE 4.4

## THE EFFECT OF IRON ON ARSENIC FLUORESCENCE

(Solutions contained 10 ppm arsenic, 4% concentrated hydrochloric acid. Iron added as iron (III) chloride. Blank solutions contained iron. Measurements made at 189.0 nm and results expressed as the ratio of the fluorescence of arsenic in the presence of iron to the fluorescence of arsenic alone).

iron ppm	Flame (flow rates for optimal sensitivity)			
	$N_2O/C_2H_2$	Air/ $C_2H_2$	Ar/ $O_2/H_2$	Ar/ $H_2$
10,000	0.90	0.95	0.30	0.63
9,000	0.90	0.95	0.36	0.76
8,000	0.96	0.97	0.39	0.77
7,000	0.96	0.98	0.42	0.77
6,000	0.97	0.98	0.46	0.77
5,000	0.99	0.99	0.63	0.82
4,000	0.98	0.99	0.78	0.85
3,000	0.98	1.0	0.86	0.89
2,000	1.0	1.0	0.91	0.94
1,000	1.0	1.0	0.98	0.95

level causes a depression of similar magnitude to that in the atomic absorption method as reported by Kirkbright et al.<sup>263</sup>

The same workers indicate that it is not necessary to add major constituents of a matrix to standards when determining arsenic absorption in the nitrous oxide-acetylene flame. It does seem however that it is necessary to add iron to standards when measuring fluorescence in this flame. A burner able to cope with a slightly higher solids content than the one used would probably have removed the interference from iron in the nitrous oxide-acetylene flame.

#### 4.3.4. The effect of organic solvents

268

Smith and Frank report that in aqueous acetone, methanol or isopropyl alcohol the absorption of arsenic is considerably enhanced when using an oxy-acetylene flame. Menis and Rains<sup>165</sup> suggest that the interference of CH and C<sub>2</sub> radicals in flame gases in the far ultraviolet region at 193.7 nm precludes the direct burning of organic solutions (These workers used diethylammonium diethyldithiocarbamate, DDDC, to separate the arsenic from interfering cations and after back extraction the atomic absorption detection limit for arsenic in the resulting aqueous medium was 0.1 ppm). Arsenic can be extracted from acid solutions up to pH 6 using APDC and MIBK<sup>192,253</sup> or DDDC<sup>165</sup> to concentrate but the final solution is usually aqueous.

In this study 10 ppm aqueous arsenic solutions containing 10% concentrations of a range of organic liquids were nebulized and the fluorescence measured (Table 4.5). In the argon flames acetone, acetic acid, ethanol and methyl-ethyl-ketone all depressed the fluorescence signals thus demonstrating a further disadvantage of using these two flames for the determination of arsenic. In the two hot flames enhancements of up to 70% are possible when methyl ethyl ketone is added to the analysis solutions. These trends,

THE EFFECT OF ORGANIC LIQUIDS  
ON THE ATOMIC FLUORESCENCE OF ARSENIC

(10 ppm arsenic; solutions containing 10% organic liquid and made up with deionised water. Results expressed as the ratio of the fluorescence of arsenic in the presence of organic liquid to the fluorescence of the aqueous arsenic solution containing no organic liquid).

Organic liquid	Relative fluorescence			
	$N_2O-C_2H_2$	Air- $C_2H_2$	Ar- $O_2-H_2$	Ar- $H_2$
Acetone	1.4	1.20	0.59	0.24
Acetic acid	1.4	1.12	0.15	0.97
Ethanol	1.2	1.12	0.38	0.52
Methyl-Ethyl-Ketone	1.7	1.28	0.15	0.22

THE EFFECT OF IRON ON THE  
INTERFERENCE FROM ORGANIC LIQUIDS

(10 ppm arsenic; solutions containing 10% organic liquids, 10,000 ppm iron and 4% concentrated hydrochloric acid and made up with deionised water. Results expressed as the ratio of the fluorescence of arsenic in the presence of organic liquid, iron and acid to the fluorescence of arsenic in the presence of iron and acid alone).

Organic liquid	Relative fluorescence			
	$N_2O-C_2H_2$	Air- $C_2H_2$	Ar- $O_2-H_2$	Ar- $H_2$
Acetone	1.33	1.05	0.07	0.07
Acetic acid	1.00	1.00	0.27	0.33
Ethanol	1.07	1.00	0.40	0.53
Methyl-Ethyl-Ketone	1.33	1.00	0.07	0.07

being similar to those found for the fluorescence of tin suggest, by analogy, that active hydrogen may be playing a role in the atomization of arsenic in the two cool flames.

Unfortunately when 10,000 ppm of iron is present in solution the enhancements due to the organic liquids are almost halved (Table 4.5). Moreover although these enhancements may be further improved if say a 50% concentration of the organic liquid was used the problems due to the CH and C<sub>2</sub> radicals mentioned by Menis and Rains<sup>165</sup> may reduce the effectiveness of the measure.

#### 4.4. Analytical Curves and detection limits

##### 4.4.1. Analytical Curves

The results obtained by Dagnall and his co-workers<sup>11</sup> when looking at the linear range of analytical curves have been summarized in section 4.2.4. In the present work analytical curves were obtained for solutions containing arsenic alone at the wavelengths 189.0 nm and 235.0 nm and for arsenic solutions containing 10,000 ppm iron at 189.0 nm. All four flames were used and the results compared with those of Dagnall et al.

In Figs. 4.17 to 4.20 the analytical curves obtained are plotted linearly as concentration (ppm) vs fluorescence radiance (arbitrary units). This form of presentation emphasizes the high concentration performance of the curves. It can be seen that the 235.0 nm line yields plots far less curved than the 189.0 nm line. The effect of self-absorption is negligible because the 235.0 nm line is the result of a thermally assisted direct-line fluorescence transition<sup>11</sup>. The 189.0 nm line is a resonance transition and suffers from self-absorption to give the serious curvature observed. In all of the flames it is necessary to use the 189.0 nm line for greatest sensitivity at low concentrations but the 235.0 nm line is preferable when measuring concentrations

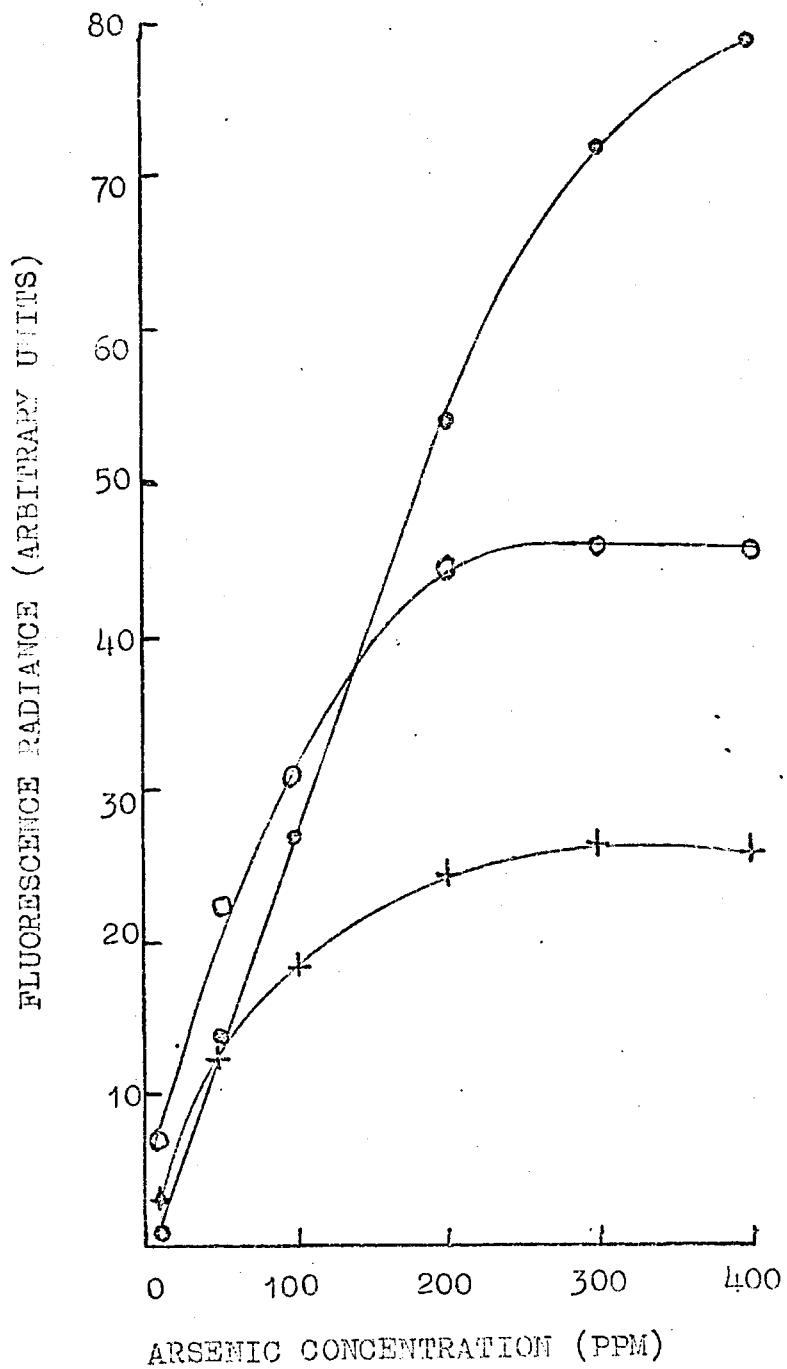


Fig. 4.17 Analytical curves for arsenic in the argon-hydrogen flame. (●) - 235.0 nm; (○) - 189.0 nm; (+) - 189.0 nm, standards contained 10,000 ppm iron and 4% v/v hydrochloric acid.

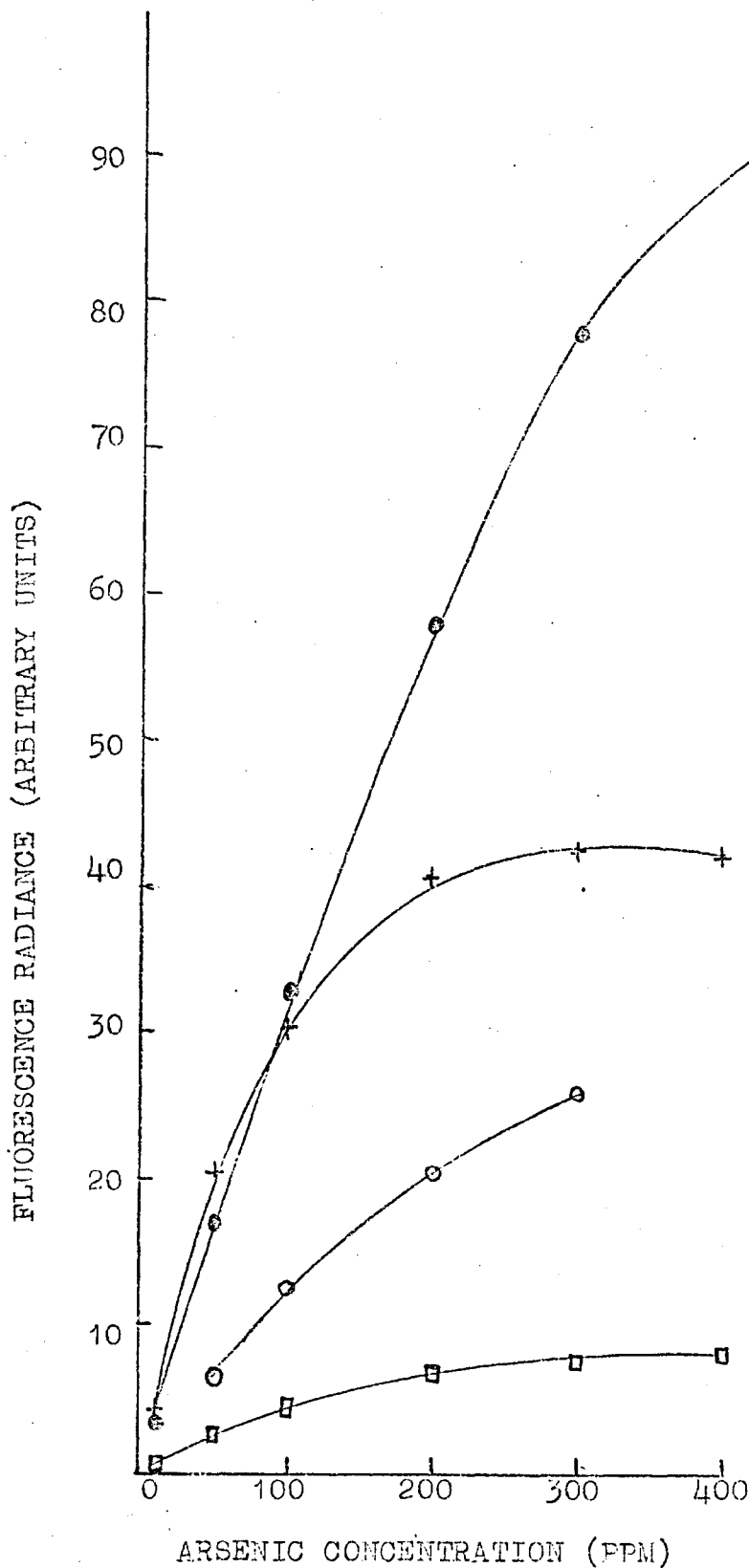


Fig. 4.18 Analytical curves for arsenic in the argon-oxygen-hydrogen flame. (●) - 235.0 nm; (+) - 189.0 nm; (⊖) - 189.0 nm, standards contained 10,000 ppm iron and 4% v/v hydrochloric acid. (□) - mirrors M1 and M3 removed - see text.

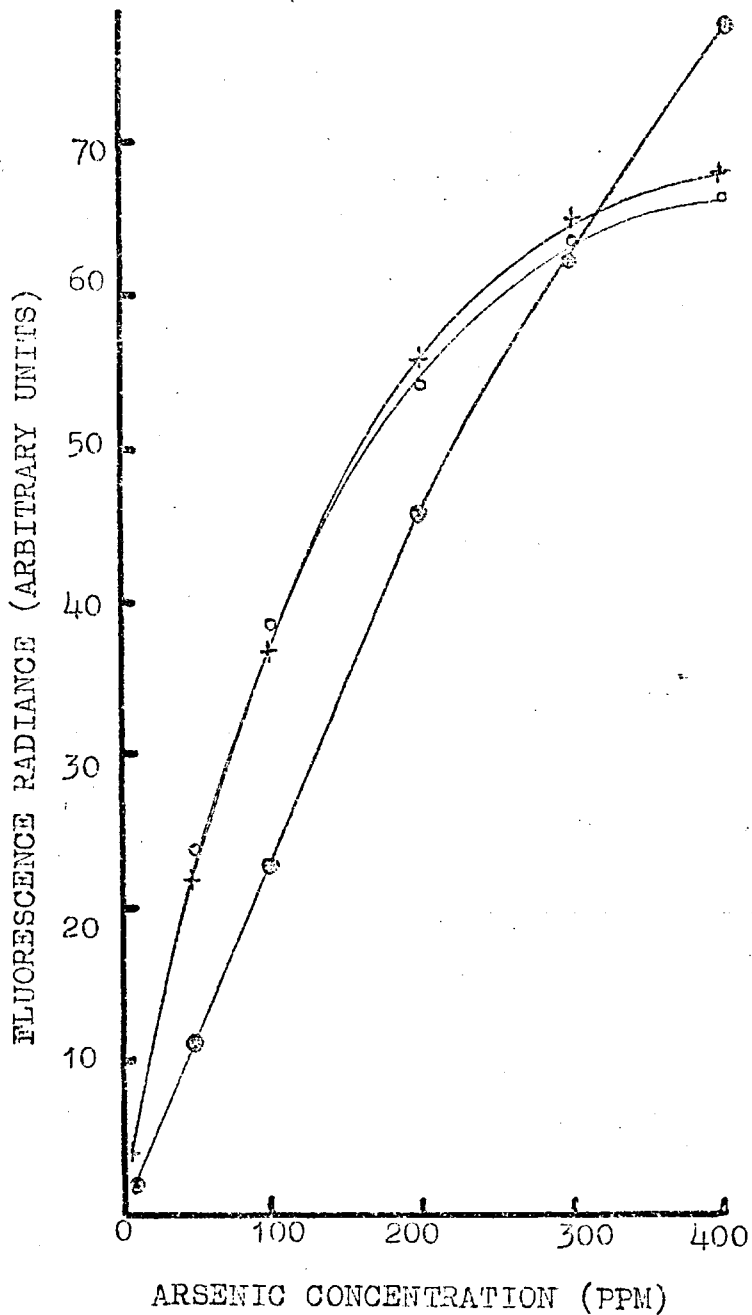


Fig. 4.19 Analytical curves for arsenic in the argon-separated air-acetylene flame; (●) - 235.0 nm; (+) - 189.0 nm; (○) - 189.0 nm, standards contained 10,000 ppm iron and 4% v/v hydrochloric acid.

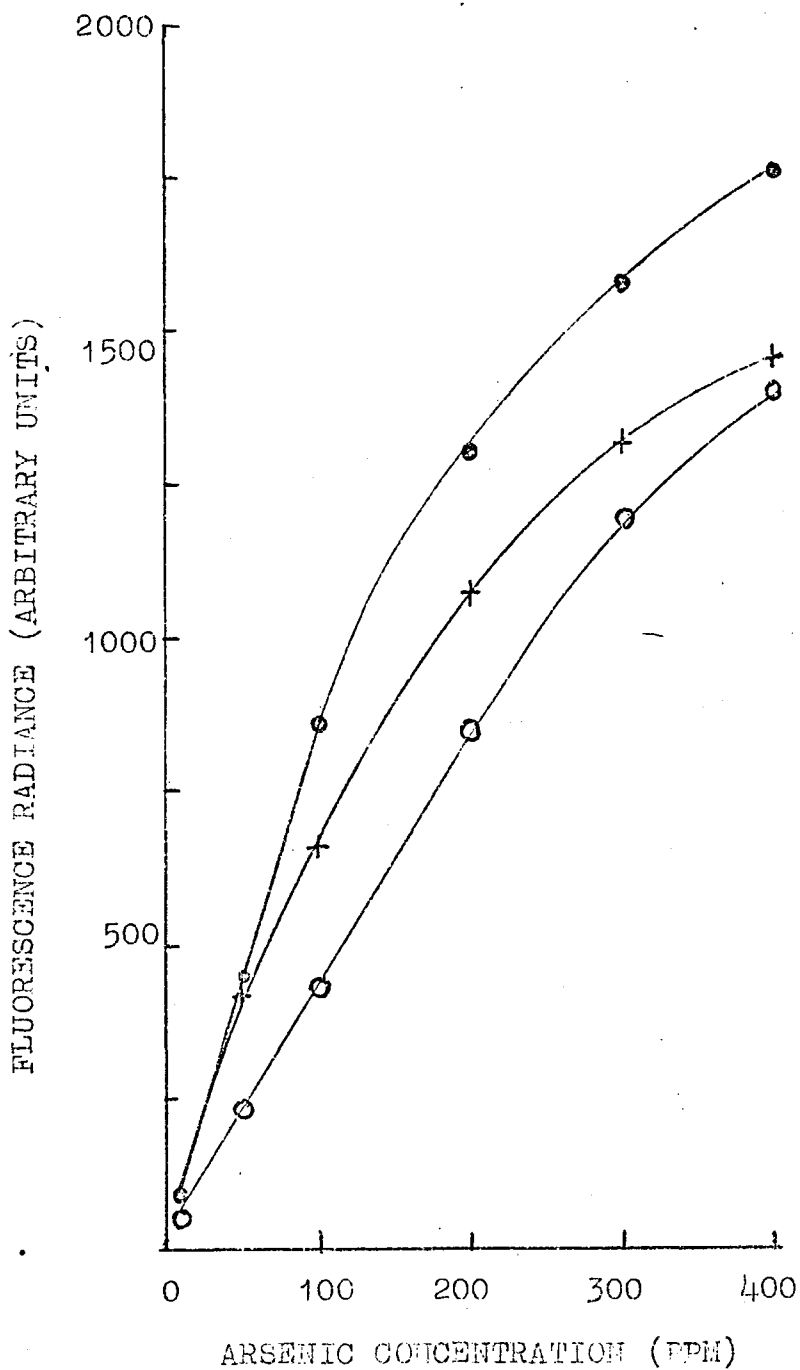


Fig. 4.20 Analytical curves for arsenic in the non-separated nitrous oxide-acetylene flame. (●) - 189.0 nm; (○) - 235.0 nm; (+) - 189.0 nm, standards contained 10,000 ppm iron and 4% v/v hydrochloric acid.

of arsenic greater than 10 to 100 ppm to take advantage of the longer linear range. This is especially obvious in the two cool flames (Figs. 4.17 and 4.18) although, as has been pointed out already, these flames are not analytically useful because firstly, their sensitivity is not significantly better than the air-acetylene flame and secondly too many interferences affect the arsenic determination in these flames.

The nitrous oxide-acetylene flame gives analytical curves which are more linear at high concentrations than either the cool flames or the air-acetylene flame although the total linear range is slightly shorter than the air-acetylene flame because the sensitivity at low concentrations in the latter flame is higher.

The 235 nm line becomes the most sensitive line above 100 ppm in the cool flames and above 300 ppm in the air-acetylene flame but is never more sensitive than the 189.0 nm line in the nitrous oxide-acetylene flame.

The above observations are in general agreement with those of Dagnall et al.<sup>11</sup> except for the comments on the nitrous oxide flame. (This flame was not studied by those workers). The phenomenon of self-absorption is discussed several times elsewhere in this thesis.

The fourth analytical curve in Fig. 4.18 illustrates the effect of removing mirrors M1 and M3 (See Chapter two for the description of the optical arrangement). Self absorption is reduced, because fluorescence is not being reflected through the flame, the linear range is extended and sensitivity is lost as a consequence.

The analytical curves in Figs. 4.17 to 4.20 are replotted on a log-log scale in Figs. 4.21 to 4.24 to emphasize the extent of the useful linear range in the four flames. viz: Just over two orders of magnitude in the argon-hydrogen and nitrous oxide-acetylene

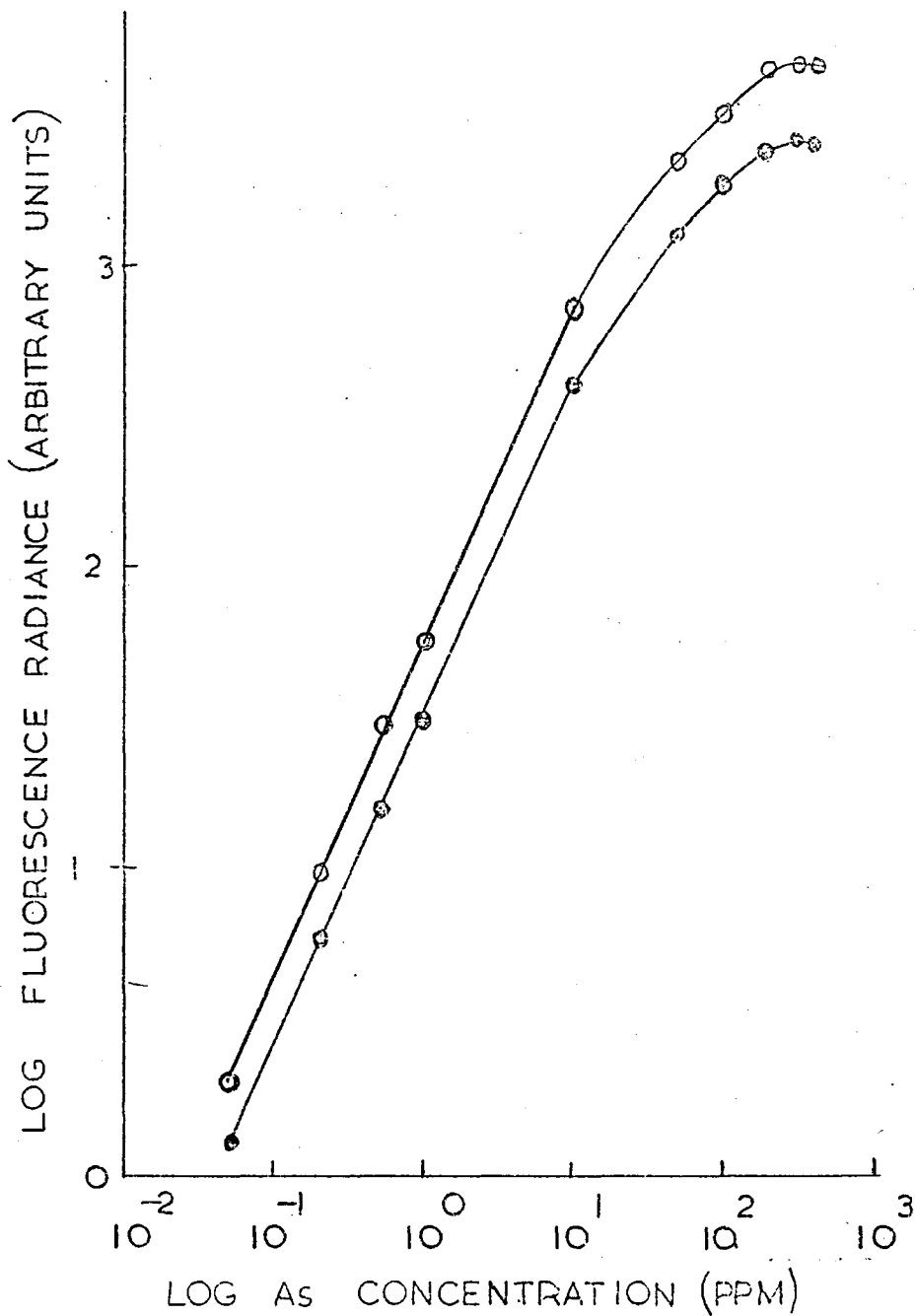


Fig. 4.21 Log plot of arsenic analytical curves in the argon-hydrogen flame. (⊙) - 169.0 nm, standards contained 10,000 ppm iron and 4.5 v/v hydrochloric acid; (○) - 189.0 nm.

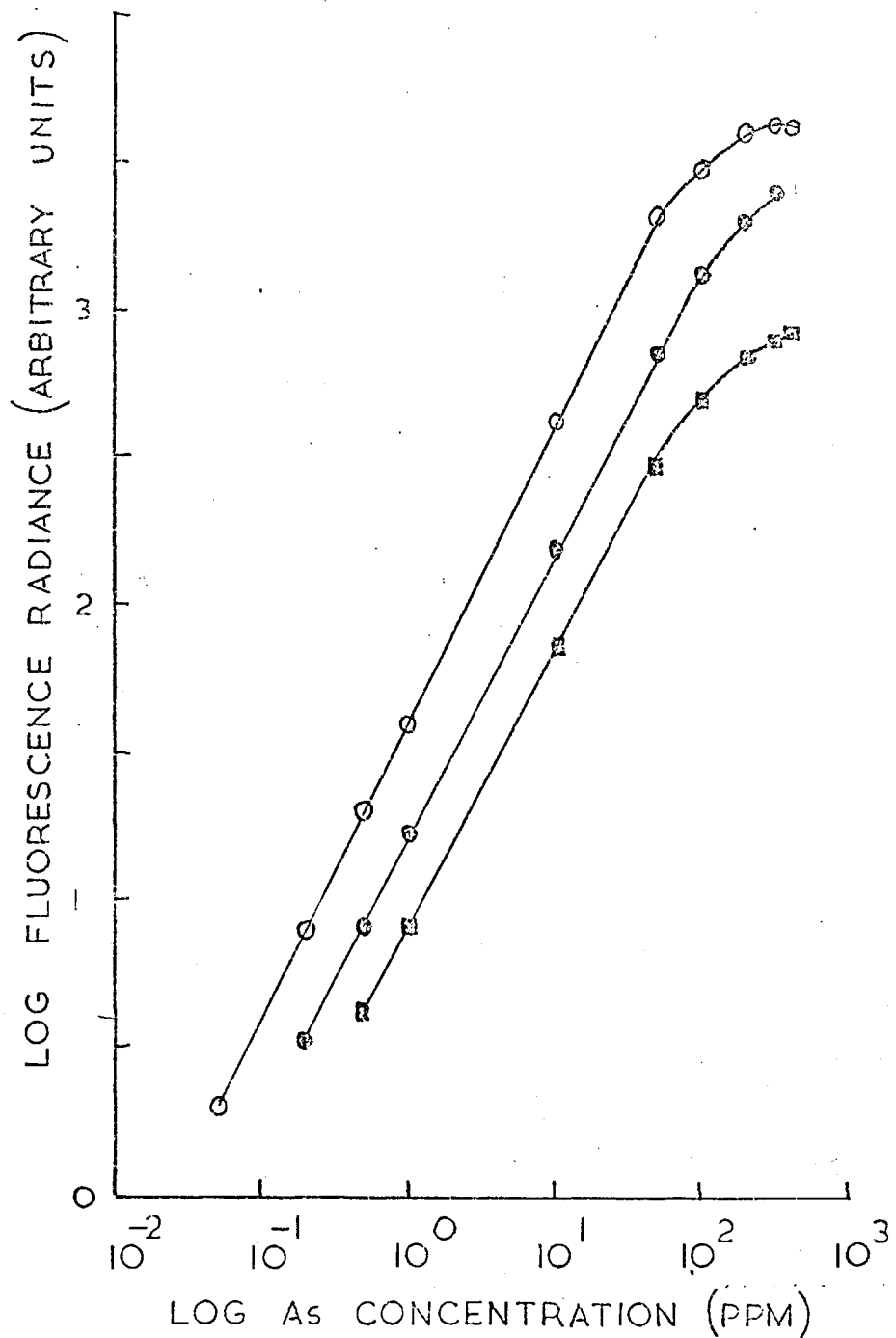


Fig. 4.22 Log plot of arsenic analytical curves in the argon-oxygen-hydrogen flame. (⊙)-189.0 nm, standards contained 10,000 ppm iron and 4% v/v hydrochloric acid; (○)-189.0 nm; (◻) - mirrors M1 & M3 removed, see text.

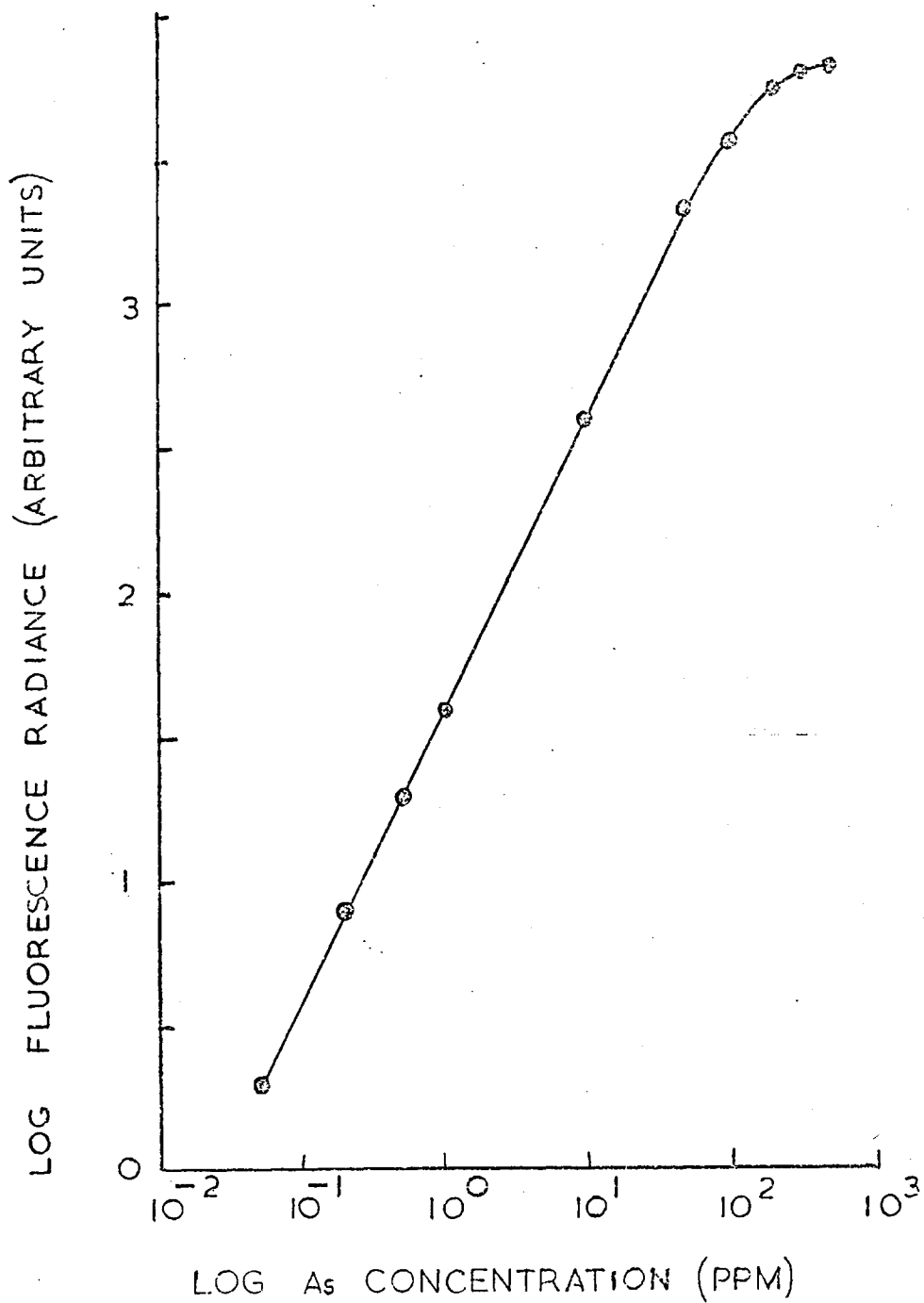


Fig. 4.23 Log plot of arsenic analytical curve in the argon-separated air-acetylene flame. This curve did not change significantly when 10,000 ppm iron was present in the standard solutions. (This was the case in Fig. 4.19)

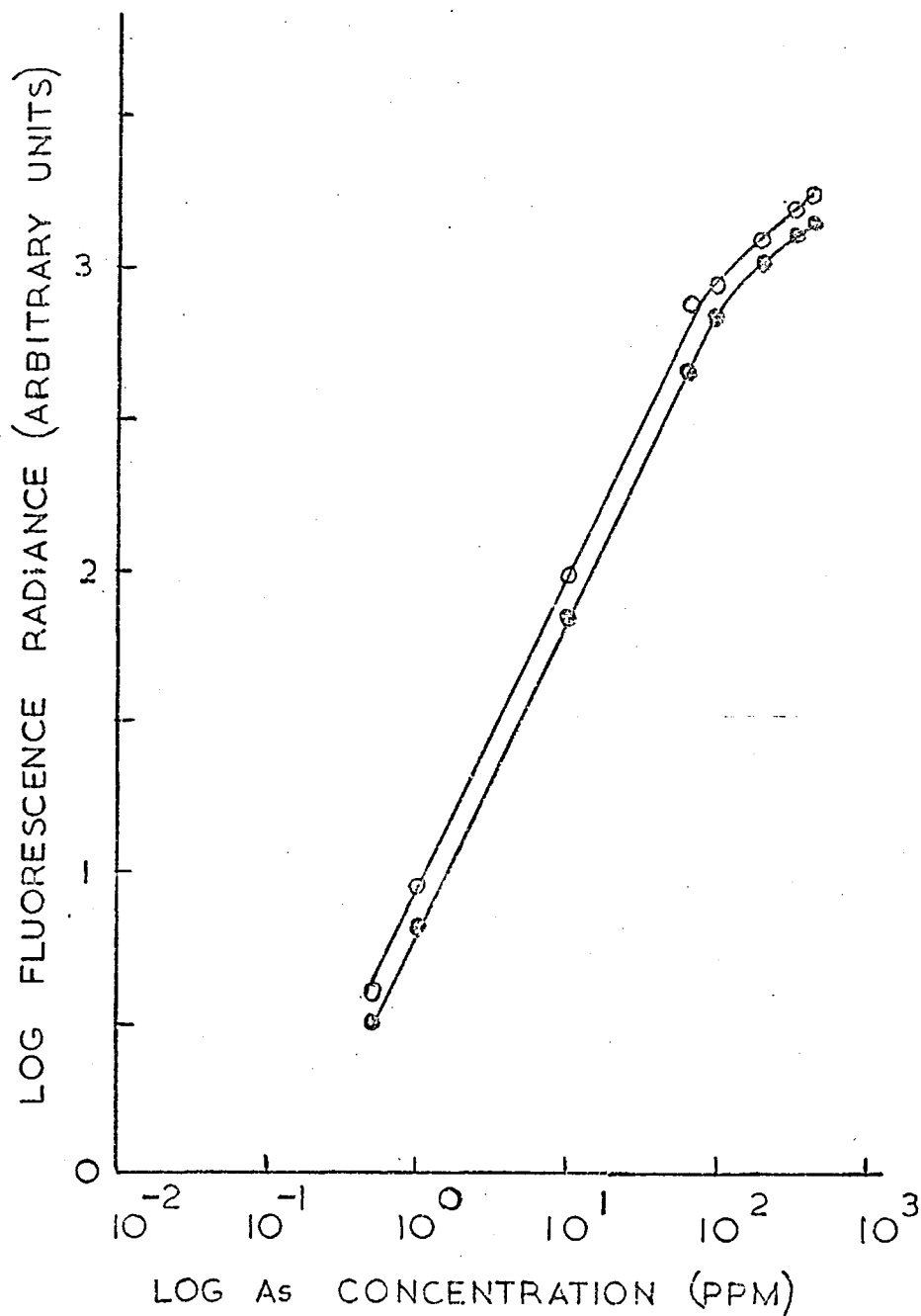


Fig. 4.24 Log plot of arsenic analytical curves in the argon-separated nitrous-oxide acetylene flame.

(●) - 189.0 nm, standards contained 10,000 ppm iron and 4% v/v hydrochloric acid; (○) - 189.0 nm

flames and between three and four orders of magnitude in the air-acetylene and argon-oxygen-hydrogen flames.

The presence of 10,000 ppm of iron (added as ferric chloride) does not affect the linear range or the curvature at high concentrations of any of the analytical curves. The sensitivity is plainly seriously affected in the cool flames, as already shown in section 4.3.3, although in the other two flames the sensitivity is not altered significantly.

Dagnall et al.<sup>11</sup> were able to detect differences in the degree of curvature of the analytical curves at all three resonance lines (189.0, 193.7 and 197.2 nm). This study was not necessary here because if a longer linear range is required, presumably to look at high arsenic levels, the 235.0 nm line is to be preferred to all three resonance lines, as shown by Dagnall et al. and therefore the obvious choice.

#### 4.4.2. Detection limits

At the most sensitive line, 189.0 nm, the relative magnitudes of the signals obtained using the four flames under study were all similar with the exception of the nitrous oxide-acetylene flame which was found to be approximately three times less sensitive than the other flames (Discussed in section 4.2.4.). The noise levels at the output of the lock-in-amplifier were also very similar although the noise from the nitrous oxide flame was approximately a factor of two worse than the noise from the other flames (The two acetylene flames were always used with the separating sheath of argon).

Detection limits (signal-to-noise ratio equal to two, 18.2s time constant) were obtained for pure arsenic solutions and for arsenic solutions containing 10,000 ppm iron. The results are shown in Table 4.6. From these figures it can be seen that the

TABLE 4.6

DETECTION LIMITS FOR THE ATOMIC FLUORESCENCE  
DETERMINATION OF ARSENIC IN FOUR FLAMES

(Measurements made at 189.0 nm using 0.05 ppm arsenic solutions for the hydrogen flames and the air-acetylene flame and 0.5 ppm solutions for the nitrous oxide-acetylene flame. Procedures for measurement of detection limits are detailed in appendix II.)

Detection limits (Signal-to-noise ratio=2 Time constant 18.2s)		
Flame	Aqueous arsenic solutions	Aqueous arsenic solutions containing 10,000 ppm iron and 4% concentrated hydrochloric acid
Argon-hydrogen	0.01	0.025
Argon-oxygen- hydrogen	0.01	0.04
Argon-separated air-acetylene	0.015	0.018
Argon-separated nitrous oxide- acetylene	0.10	0.12

addition of iron to the arsenic solutions has a significant effect only in the cool flames where sensitivity is most affected by such addition. A slight increase in noise occurs in all four flames, when iron is present, resulting in a further deterioration in signal-to-noise ratios.

From the detection limits it can be seen that the cool flames have no advantage over the separated air-acetylene flame especially when iron is present. This is in contrast to the use of the cool flames for the determination of tin by atomic fluorescence where the reduction in sensitivity due to iron is more than compensated for by the increased sensitivity of the argon-oxygen-hydrogen flame relative to the separated air-acetylene flame and by the lower noise levels associated with the cool flame. The arsenic detection limit in the nitrous oxide flame is only about five times worse than the limit in the air-acetylene flame. This again is in contrast with the determination of tin where the noise levels associated with the nitrous oxide acetylene flame at the wavelengths used are relatively high. The cool flames therefore when used for the determination of arsenic suffer from the twofold disadvantage of being firstly, only marginally more sensitive than the argon-separated air-acetylene flame and secondly, at wavelengths below 200 nm all the flames studied have very low noise levels resulting in the cool flames being only marginally less noisy than the two acetylene flames.

Comparison of the arsenic atomic fluorescence detection limits in Table 4.6 with the best atomic absorption limits known to us (examples are given in the introduction to this chapter) reveals that in the air-acetylene flame the atomic fluorescence method can be used to detect arsenic concentrations between ten and twenty times lower than the atomic absorption method in the same flame. In the argon hydrogen flame the detection limits are between five and ten times better than the atomic absorption

determination.

#### 4.5 The determination of arsenic in steel samples

The effects of a number of elements, present as trace levels in steels, on the determination of arsenic in all four flames was described in section 4.3.2. It was shown that in the two argon-separated acetylene based flames there were no significant interferences caused by the elements tested. The effect of 10,000 ppm iron (equivalent to dissolving 1g of steel in 100 ml of solution) has also been described in section 4.3.3. and it was shown that it is desirable to add 10,000 ppm iron to the calibration standards.

It was anticipated that it would be necessary to exercise some care when dissolving the steels because of the relatively low boiling point of the arsenic trichloride (403 K)<sup>299</sup> and the risk of losing arsenic as arsine. The use of an oxidising acid mixture to prevent the latter is quite adequate<sup>289</sup> but it was found necessary to exercise care when evaporating to dryness during the dissolution step. The method used for the dissolution of the standard steels is given in Table 4.7. Four steels were treated in this way and the fluorescence signals in the two acetylene based flames measured. The results are shown in Table 4.8. Calibration curves for these determinations were obtained using standards containing 10,000 ppm iron and 4% concentrated hydrochloric acid (4 ml of concentrated hydrochloric acid were used in the final step of the steel dissolution, Table 4.7). The curves, which covered the range 0 to 5 ppm, were linear, as expected from the results given in section 4.3.5. The curve for the separated air-acetylene flame is given in Fig. 4.2.5.

Some difficulty was found when determining arsenic in standard steel number 321, low results (0.001 and 0.002% in both

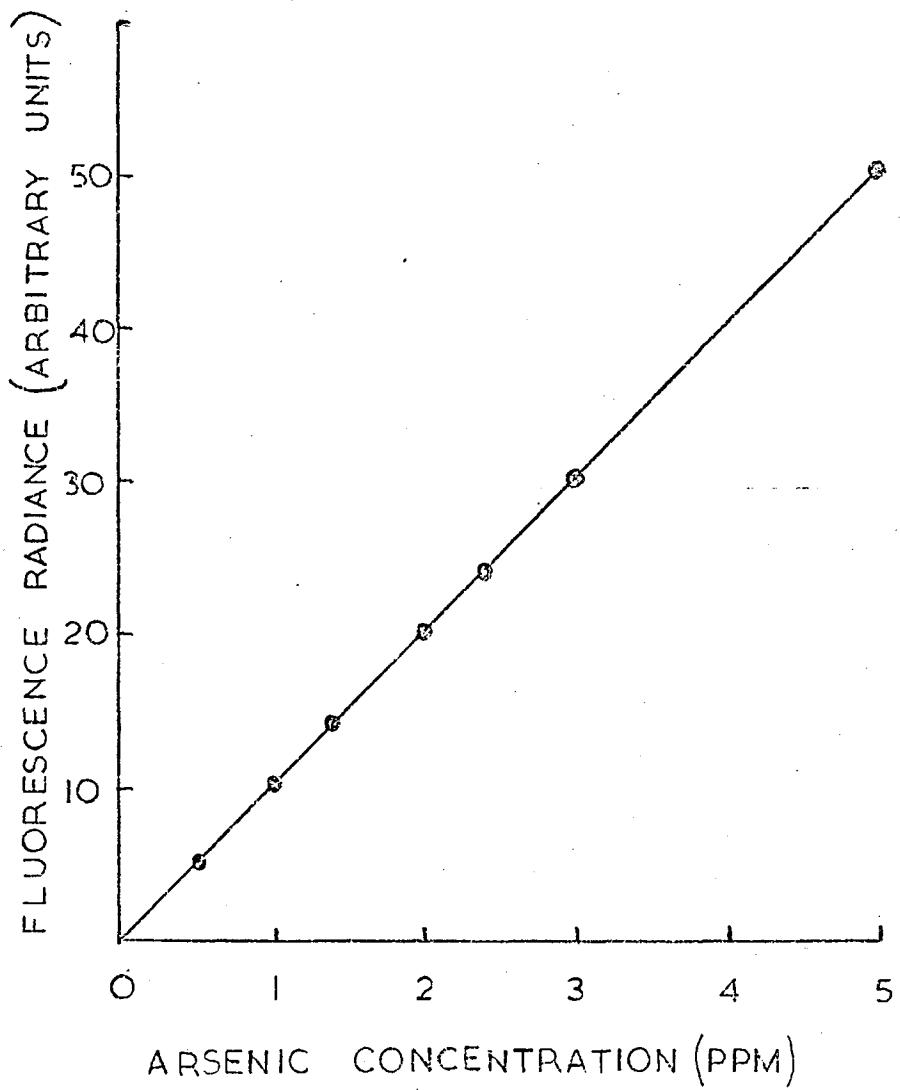


Fig. 4.25 Calibration curve for steel analysis. Argon-separated air-acetylene flame. Standards contained 10,000 ppm iron and 4% v/v hydrochloric acid.

TABLE 4.7

DISSOLUTION METHOD USED FOR THE DETERMINATION  
OF ARSENIC IN STEEL BY ATOMIC FLUORESCENCE

The steel (1 g) was dissolved in 7 ml of concentrated hydrochloric acid and 3 ml of concentrated nitric acid and the resulting solution was heated gently until the evolution of brown fumes due to oxides of nitrogen ceased. The solution was then evaporated almost to dryness with the minimum of heating, the residue taken up with 4 ml of concentrated hydrochloric acid and filtered through a No. 4 sinter crucible. The solution was then transferred to a 100 ml volumetric flask and diluted to the mark.

TABLE 4.8

THE DETERMINATION OF ARSENIC IN STEEL

British Chemical Standard Steel No.	Description of steel	Tin content %			
		BCS standardised value %	Atomic fluorescence (duplicate analyses)		
			Air/C <sub>2</sub> H <sub>2</sub>	N <sub>2</sub> O/C <sub>2</sub> H <sub>2</sub>	
321	mild	0.003	0.003	0.003	detection limit
322	mild	0.012	0.011	0.012	0.011 0.012
323	mild	0.058	0.057	0.058	0.057 0.058
325	mild	0.013	0.013	0.013	0.012 0.013

flames) being obtained with the first two samples. Two further samples of this steel were treated as follows: A 100 ml round-bottomed flask, with a water cooled reflux condenser attached was used during the dissolution until the brown fumes of the oxides of nitrogen were completely expelled. The flask was then cooled, the condenser removed and the sample slowly evaporated almost to dryness with the minimum of heating. The resulting solution was then cooled, taken up with 4 ml concentrated hydrochloric acid and after filtration made up to 100 ml in the normal way. The atomic fluorescence signals obtained showed that the previous low readings were probably due to the loss of arsenic trichloride as a result of the solution becoming too hot at some point during the dissolution procedure. (The results in Table 4.8 are those obtained using the method just described).

To investigate the precision of the method six samples of standard steel number 323 were treated using the dissolution method in Table 4.7 and the fluorescence in the argon-separated air-acetylene flame measured. The average of three atomic fluorescence readings were taken for each sample solution. The relative standard deviation of the measurements was found to be 2.9%.

#### 4.6 Conclusion

A theoretical analysis given by Winefordner<sup>118</sup> indicates that atomic fluorescence with a line source should give similar or lower limits of detection than atomic absorption with a line source for nearly all elements with resonance lines below about 325 nm. On the other hand atomic emission should give lower limits of detection for nearly all elements with resonance lines greater than 325 nm. Dagnall et al.<sup>165</sup> look at the various tabulations of detection limits that are available and come to similar conclusions. Arsenic with its resonance lines below 200 nm

is one of the most favourable elements for atomic fluorescence determination. The arsenic detection limits obtained in this work convincingly demonstrate this because they are at least an order of ten better than arsenic atomic absorption detection limits (In both air-acetylene and cool flames).

The interferences encountered when measuring either arsenic absorption or fluorescence signals are essentially the same. Interferences are minimal in either the argon-separated nitrous oxide-acetylene or argon-separated air-acetylene flames but the cool flames are prone to a large number of interferences. The argon-separated air-acetylene flame gives a detection limit which is not very different from that obtainable in the cool hydrogen flames. The argon-separated air-acetylene flame is therefore the best available flame for the atomic fluorescence determination of arsenic.

The atomic fluorescence method was found to be satisfactory for the determination of arsenic in steel. The fluorescence, excited in the argon-separated air-acetylene flame was measured at 189.0 nm. The monochromator was nitrogen flushed to improve its transmission at this wavelength. It was necessary to add 10,000 ppm iron (as iron (III) chloride) to the calibration standards to compensate for the slight depression of the arsenic fluorescence which is caused by iron (III) chloride. Analytical curves were linear from close to the detection limit (0.018 ppm for solutions containing 10,000 ppm iron) to about 150 ppm.

## CHAPTER FIVE

The application of atomic fluorescence spectrometry to the  
determination of aluminium in steels

5.1. Introduction

Early work on the atomic absorption of aluminium indicated that the element could not be detected in the air-acetylene flame. It was later established experimentally<sup>300</sup> that extremely small concentrations of ground state aluminium atoms are produced when aspirating aqueous solutions (concentration giving 1% absorption > 1000 ppm) into the fuel rich air-acetylene flame. Experiments with oxy-acetylene<sup>301,302</sup> and with the addition of oxygen to an air-acetylene flame<sup>303-305</sup> were more successful, although they involved the risk of explosion. After the nitrous oxide-acetylene flame was introduced<sup>306 - 311</sup> similar high sensitivity was obtained but this sensitivity was accompanied by a greater operating safety because the nitrous oxide based flame has a lower burning velocity than the oxygen based flames. L'vov<sup>97</sup> described the development of the early work (1960-1965) concerning the use of the fuel-rich oxyacetylene, oxyhydrogen and then the nitrous oxide-acetylene flames and less detailed reviews appear in most atomic absorption text books<sup>253</sup>. The oxyhydrogen flame has been shown to be nine times less sensitive than the oxyacetylene flame<sup>301,302</sup> and therefore has not been widely used for aluminium determination. Similarly studies of the premixed nitrous oxide-hydrogen flame<sup>312</sup> have shown poor sensitivity for aluminium in spite of the fact that its temperature is not more than 150° below that of nitrous oxide-acetylene<sup>313-315</sup>. Experiments with an oxygen-shielded air-acetylene flame<sup>211</sup> have shown that although aluminium can be detected (1% absorption 5.7 ppm) the sensitivity is not as good as that obtainable in the nitrous

oxide-acetylene flame (1% absorption 1.0 ppm). The effectiveness of the nitrous oxide-acetylene flame for the determination by atomic spectroscopy of aluminium and several other elements forming refractory oxides has been investigated a great deal in the literature<sup>298,307-311</sup>. It has been shown<sup>297</sup> that the degree of atomisation is not only dependent on temperature but is also critically dependent on the carbon:total oxygen ratio. If this exceeds unity the degree of atomisation is a maximum. The reducing species present in the flame which are most likely helping to maintain this desirable ratio have been shown to be CN and HCN<sup>296,297,316</sup>.

The 309.3 doublet (309.27 and 309.28 nm) is the most sensitive absorbing line for aluminium<sup>306,308</sup>. Other absorption lines have sensitivities in the decreasing order 396.15 nm > > 308.21 nm > 394.40 nm. In atomic emission<sup>10,317,318</sup> and atomic fluorescence<sup>10</sup> determinations of aluminium in the nitrous oxide-acetylene flame the 396.2 nm line is the most sensitive. The best detection limits for aluminium in this flame have been reported by Pickett and Koirtyohann<sup>317</sup> and Boumans and De Boer<sup>318</sup> who obtained values of 0.005 ppm and 0.003 ppm respectively by measuring the atomic emission signals. However Fraser and Winefordner<sup>28</sup> have obtained 0.005 ppm using laser-excited atomic fluorescence. Winefordner and Elser<sup>5</sup> quote a detection limit of 0.04 ppm by atomic absorption (taken from figures published by Varian Techtron for their model AA5 instrument). Dagnall et al.<sup>10</sup> in their paper reporting the atomic fluorescence determination of aluminium, obtained a detection limit of 0.1 ppm by fluorescence. The latter workers obtained a figure of 0.05 ppm for atomic emission in the nitrous oxide-acetylene flame and 0.1 ppm for atomic absorption in the same flame.

The high temperature of the nitrous oxide-acetylene flames

causes some ionization of the aluminium atoms causing a depression in the absorption signal. This particular type of interference can be suppressed by the addition of an easily ionized element which increased the concentration of electrons in the flame<sup>319-321</sup>.

Kornblum and De Galan<sup>322,323</sup> and L'vov<sup>97</sup> have presented quantitative arguments regarding the extent of ionization of elements in the nitrous oxide-acetylene flame. Chemical interferences affecting the determination of aluminium in the nitrous oxide-acetylene flame have been discussed by various workers<sup>298,308,324-326</sup> and interferences that do occur are minimised in the fuel rich flame<sup>298</sup>

Dagnall and his co-workers<sup>10</sup> in reporting the fluorescence characteristics of aluminium looked at a number of interferences caused by anions and cations and compared the results with the same tests carried out on the atomic emission signals obtained using the same instrument.

Methods for the determination of aluminium in steels by atomic absorption are well established<sup>327</sup> and Thomerson and Price<sup>328</sup> Price<sup>192</sup>, and Belcher<sup>259</sup> have included aluminium in their comprehensive schemes for the analysis of a wide range of steels. Aluminium was determined in steel by Amos and Thomas<sup>303</sup> using a nitrogen-oxygen-acetylene flame. König et al<sup>329</sup> described the determination of both soluble and insoluble aluminium. The necessity for this exists because aluminium in steel is present as acid-soluble forms, which include elemental aluminium, and in forms that are insoluble in boiling acid. These acid insoluble forms are corundum,  $\alpha$ -aluminium oxide, and probably aluminium oxide associated with calcium oxide or silicon dioxide or both<sup>330</sup>.

König et al<sup>329</sup> determined the soluble aluminium by dissolving the steel in aqua-regia and siphoning off the insoluble matter before observing the aluminium absorption. To bring the total aluminium into solution they filtered off the insoluble part and, together

with the filter, it is ashed and fused with approximately 1 g of a borax-soda mixture. The melt is dissolved in 5 ml of HCl diluted 1:1, then added to the filtrate and diluted to 100 ml with water (original sample weighed 2 g). Headridge and Sowerbutts<sup>330</sup> described a method for the determination of total aluminium in irons and steels, which does not involve fusion of an oxide residue. The iron or steel was completely dissolved by first subjecting it to conventional treatment with acid in an open beaker and then attack by hydrochloric and hydrofluoric acids in a P.T.F.E.-lined bomb at 200°C. A solvent extraction procedure was then used to isolate the aluminium before aspiration into a nitrous oxide-acetylene flame. The method covers the range 0.001 to 0.14% of total aluminium in the iron or steel. Goto et al.<sup>331</sup> in common with a number of workers used aqua-regia to dissolve iron or steel for subsequent determination of acid-soluble aluminium and for acid-insoluble aluminium the residue from the acid treated sample was fused with  $K_2S_2O_7$  and the melt extracted with water. However after solvent extraction into methyl-isobutyl-ketone these workers determined aluminium by atomic emission at 396.15 nm. The acid concentrations ( 6N  $H_2SO_4$  or  $HNO_3$ ) did not affect the aluminium signals. There was no interference from Mn, Fe, Cu, Mo, Cr or Co (.. 500 ppm) on 2 ppm of aluminium in methanol. The determination of aluminium in iron ores, slags and refractory materials has been reported by a number of researchers, a fusion technique normally being used<sup>329,324</sup>. Samples have been decomposed by fusion with lithium fluoroborate in a few instances<sup>332,333</sup>.

Smith<sup>250</sup> found that aluminium was not stable in aqueous solutions whose pH was greater than 3.5. In the present work however no loss of aluminium seemed to be occurring over the short term (1 to 2 days) therefore interferences were studied

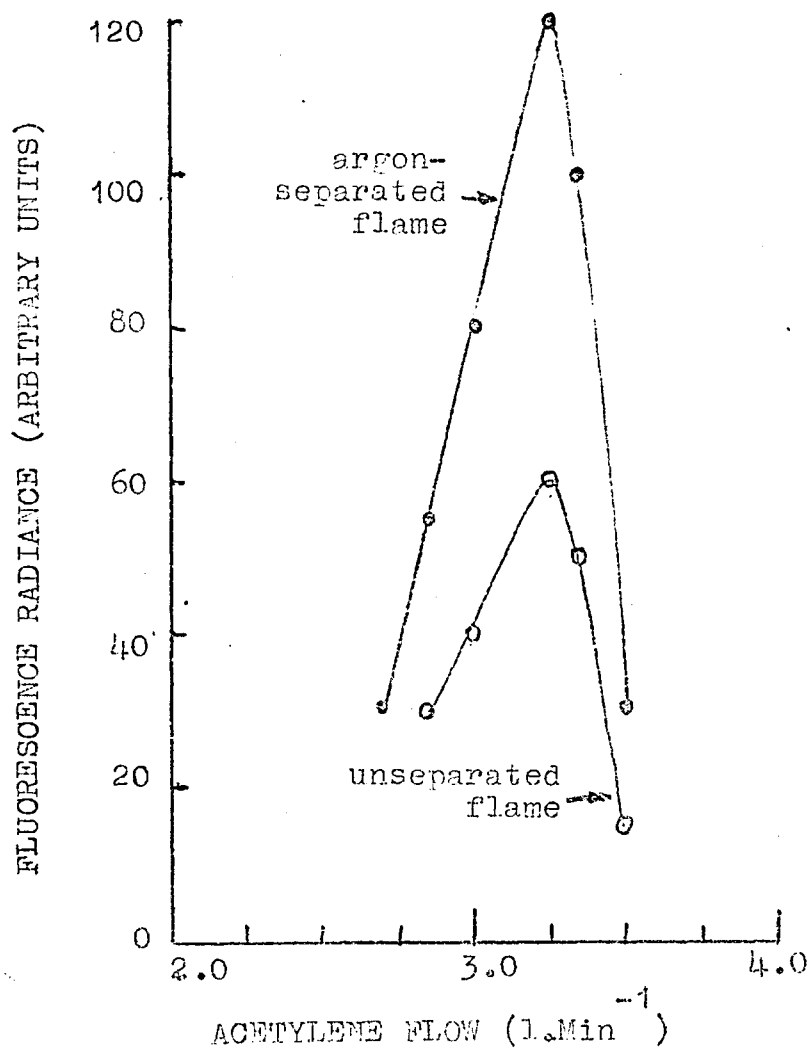


Fig. 5.1 Variation of aluminium fluorescence with fuel flow in the nitrous oxide-acetylene flame. Nitrous oxide flow.  $4.8.1 \text{ min}^{-1}$

in neutral aqueous solution in order that comparisons could be made with interferences reported in the literature. Tests on solutions containing 10,000 ppm iron were carried out in the presence of 4% concentrated hydrochloric acid to ensure the stability of the concentration of aluminium.

In this chapter the interferences affecting both the atomic fluorescence and the atomic emission determination of aluminium are reported and compared to those found by Dagnall et al.<sup>10</sup> when looking at the same techniques. Comparison is also made with the interferences reported in the literature which affect the atomic absorption determination. The use of atomic fluorescence for the determination of acid-soluble aluminium in steels is described.

## 5.2 Optimisation of conditions for measurements of aluminium fluorescence

### 5.2.1. Choice of gas flow rates, flame separation and flame height

The gas flow rates in the premixed nitrous oxide-acetylene flame were optimised by observing the atomic fluorescence signal from 10 ppm aluminium solutions at the most sensitive wavelength, 396.2 nm. The variations in the aluminium fluorescence are shown in Fig. 5.1. The effect of flame separation on the fluorescence signals at the various flow rates are shown in the same figure and it can be seen that there is a factor of two increase in signal in going from the largest signal in the unseparated flame to the largest signal in the separated flame. Noise levels at the chart readout were improved upon separation although not sufficiently to permit accurate measurements. The net improvement in signal-to-noise ratio was therefore better than a factor of two. These measurements were repeated for

the atomic emission signals at the same wavelength. (The Jarrell-Ash amplifier was used for these results). The optimal fuel flows in both the separated and unseparated flames were exactly the same as those found for the atomic fluorescence measurements and the effect of flame separation was also the same, i.e. an increase in the signal of about two times and a slight decrease in noise. Dagnall et al.<sup>10</sup> were able to obtain a similar factor of two improvement in fluorescence signal-to-noise ratio upon argon-separation of the flame but did not report whether there was an improvement or not in the atomic emission determination. The observed optimal fuel flows gave a flame which was of approximately the same stoichiometry as the flames used by Dagnall et al.<sup>10</sup> for atomic emission and fluorescence and by other workers<sup>192,298,322</sup> looking at the atomic absorption of aluminium. (i.e. slightly fuel-rich with a 20-30 mm red "feather"). The optimal fuel flow with the separated flame (Fig. 5.1) was used throughout this study.

Variation in flame height with respect to the monochromator entrance slit gave very little variation in aluminium fluorescence detected.

#### 5.2.2. Operating conditions for the aluminium electrodeless discharge lamp used as source

The lamp was modulated at a frequency of 14 KHz (see chapter two for optimisation of modulation frequency) and would only give an output in a  $\frac{\lambda}{4}$  wave cavity. Maximal percentage modulation was applied and the lamp was temperature controlled at 565 K. The plot of radiant output from the lamp vs. temperature is shown in Fig. 5.2. At temperatures higher than 565 K the discharge in the lamp pinched (i.e. took the form of a thin streamer of visible emission) and eventually self-extinguished.

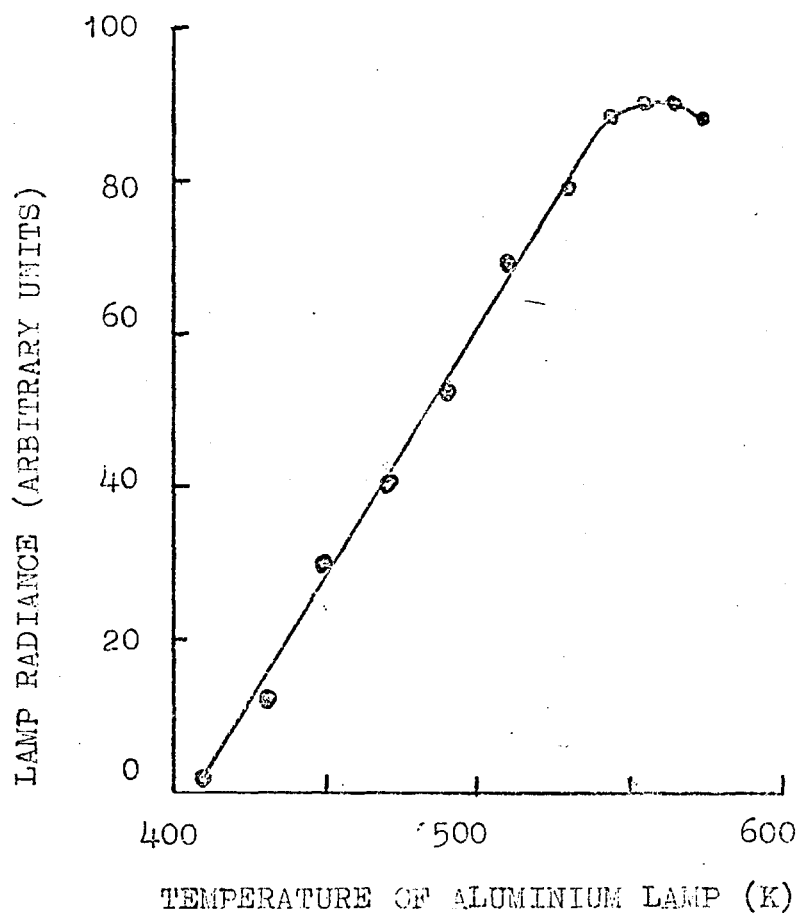


Fig. 5.2 Plot of the radiant output of the aluminium EDL at 396.2 nm vs temperature of the lamp. Lamp operated at 40 W incident microwave power in the  $H_{10}$  wave cavity and modulated at 14 KHz.

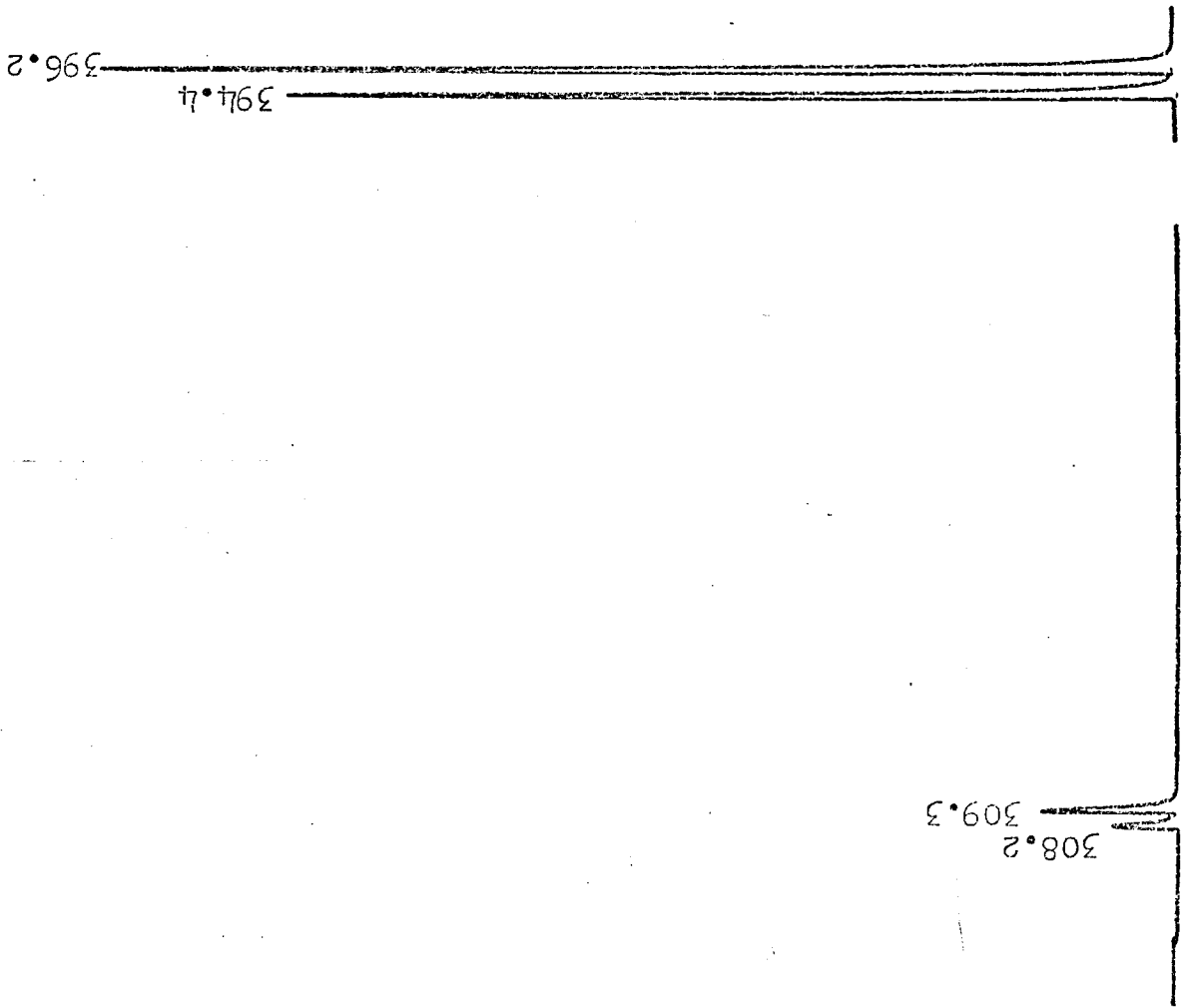
This behaviour indicated that there was too much material in the lamp and gives a possible explanation for the low optimal operating temperature of the lamp. The temperature that gave optimal source radiant output (565 K) also gave optimal fluorescence output. It is interesting that Patel et al.<sup>172</sup> used a compromise temperature of 443 K for a temperature-controlled multiple element lamp containing Al, Ge, Sn and Pb iodides. No other reports of operating temperature for aluminium lamps are known to this author. No significant change in output was obtained at incident microwave powers greater than 40 watts and therefore this was the chosen operating power. The signal became more noisy at powers greater than 65 watts. Under the above optimal conditions the long period fluctuation over 1 hour was  $\pm 2\%$

### 5.2.3. Atomic fluorescence spectrum of aluminium in the argon-separated nitrous-oxide-acetylene flame

The spectrum obtained for aluminium (100 ppm aqueous solution) in the region 300-400 nm consisted of four fluorescence lines 308.2, 309.3, 394.4 and 396.2 nm. The ratios of the intensities of these lines were 6:21:55:100 respectively. The spectrum obtained by looking at the source output also consisted of the same four lines (Fig. 5.3.) The relative atomic emission intensities at the same four wavelengths were also obtained and had intensities of 0:4:56:100. The relative intensities of both the emission and fluorescence signals were similar to those obtained by Dagnall et al.<sup>10</sup>

The spectral details of the most intense fluorescence lines<sup>193</sup> are given below (The 396.2 nm line was chosen for the study of interference effects because this was the most sensitive transition).

Fig. 5.3 The spectrum of the radiant output of the aluminum EDL.  
Chart speed 2.5 min  $\text{cm}^{-1}$   
Scan speed 2.0 nm  $\text{min}^{-1}$



Wave-length nm	Energy Levels				Spectral Term Symbols	
	Lower		Upper		Lower	Upper
	Kaysers	eV	Kaysers	eV		
394.4	0	0	25,348	3.143	$3p^2P_{0\frac{1}{2}}^o$	$4s^2S_{0\frac{1}{2}}$
396.2	112	0.0139	25,348	3.143	$3p^2P_{1\frac{1}{2}}^o$	$4s^2S_{0\frac{1}{2}}$

28

Fraser and Winefordner<sup>334</sup> have looked at the laser-excited atomic fluorescence of aluminium and were able to look not only at the two resonance fluorescence transitions (394.4 nm resonance fluorescence and 396.2 nm excited state resonance fluorescence) but also at Stokes direct line fluorescence at 396.2 nm. The latter is possible because the laser can be tuned to excite the absorption transition at 394.4 nm and the fluorescence transition at 396.2 nm can be separately observed. This is not possible with the line source used in this work because both lines are present in the emission from the lamp. The 396.2 nm line must therefore be a result of both excited state resonance fluorescence and Stokes direct line fluorescence. (A definitive paper on the types of fluorescence transitions possible is given by Omenetto and Winefordner<sup>334</sup>)

### 5.3. Interferences affecting the determination of aluminium

As is usual the extraction of aluminium into an organic phase has previously been used to eliminate interferences with atomic absorption and emission methods as well as using the extraction as a concentration step. The most commonly used method seems to be the extraction of an aluminium chelate into methyl isobutyl ketone or butyl acetate<sup>301,331,335</sup>. However a large number of authors have used the direct method for determination

of aluminium which necessitated a study of interferences.

Amos and Willis<sup>304</sup>, with the nitrous oxide-acetylene flame, could detect no effect of hydrochloric acid (0.5N) on aluminium absorption, while iron, added as either chloride or sulphate, had a slight enhancing effect at the 10,000-30,000 ppm level. The enhancing effect of iron has been reported by a number of researchers<sup>298,328</sup> although König et al.<sup>329</sup> observed enhancement up to approximately 15,000 ppm and depression thereafter. Most workers tested for interference up to 5000<sup>298</sup> or 10,000<sup>328</sup> ppm iron. Cobb and Harrison<sup>324</sup> detected no interference due to iron but found an inhibiting effect due to 30% w/w amounts of silica on 20 ppm aluminium. (These workers tested for large amounts of silica because they were analysing slags and refractory materials). At the 100 ppm level of silicon Ferris et al.<sup>325</sup> noted a slight depression of aluminium absorption. Ramakrishna et al.<sup>308</sup> looked at the effect of 200 ppm amounts of 32 cations and 19 anions on the absorption of 20 ppm aluminium solutions and found no interferences except for an enhancement of 25% due to Ti(IV) and 10% due to acetic acid. They found no effect due to silicate, calcium, iron or chloride. It has been pointed out<sup>194,298,308</sup> that it is probable that refractory metals compete with one another for oxide formation which results in the production of a greater number of atoms of those metals which have a tendency to form less stable oxides. The greater stability of the titanium oxide has been put forward as the reason for the interference on the aluminium absorption and enhancement by aluminium has been reported for titanium<sup>336,337</sup>. The red feather zone has an extremely low concentration of oxygen atoms<sup>296,297,316</sup> and a further depletion of oxygen atoms by addition of even small concentrations of other refractory elements has been said to be able to affect the atomic population of the analyte<sup>194</sup>. However

338

arguments have since been presented which indicate that there cannot be any such competition for oxygen. Sachdev and co-workers<sup>339</sup> observed an enhancement for vanadium upon addition of aluminium or titanium. This was not due to suppression of ionization of vanadium because the enhancement attainable with alkali metals was only half the value found for aluminium and titanium.

340

Koirtzyohann and Pickett<sup>340</sup> reported in 1968 the interferences of a number of acids on both the atomic emission and atomic absorption of a group of elements in the nitrous oxide acetylene flame. Their results indicated that the acids tested were giving an initial enhancement in signal, when the long axis of the slot burner was parallel to the optical axis, followed by a suppression at higher concentrations. The suppression was attributed to solution uptake interference. The enhancement was greatly reduced or eliminated when the slot was perpendicular to the optical axis. The authors concluded by proposing a new type of interference, called lateral diffusion interference and caused by the spatial distribution of the sample within the flame. Fassel and co-workers<sup>338</sup> reported apparent confirmation of the existence of lateral diffusion interference in 1973.

(In particular the effects of Co, Mo and W on aluminium atomic absorption and emission). This type of interference can account for the reports<sup>298,307,308,310,311,336,339,340</sup> of enhancement effects that

could not be attributed to ionization suppression. All these enhancements were observed in nitrous oxide-acetylene flames formed on linear slot burners. (Fassel et al.<sup>338</sup> pointed out that Dagnall et al.<sup>10</sup> have reported the enhancement effects of various concomitant on the emission signals of Al, Mo, Ti, V and Zr using a circular rather than a linear slot burner. However they stress that they were unable to confirm the more prominent

enhancements observed by Dagnall et al.). Fassel et al. show experimentally that enhancements occur at the center of a linear slot flame and depression at the edges and that a major part of each large centre enhancement was due, not to an increase in the total free atom population in the flame, but to an increase in the number density or concentration of analyte at the centre of the flame. The postulate put forward was that: a) slower atomization in the presence of concomitant delays the production of free atoms; b) the atoms then have a shorter time for lateral diffusion before entering the optical path; c) they will have diffused a shorter distance and will be concentrated at the centre of the flame, accounting for an enhancement at the centre and a depression at the edges. Lateral diffusion would be the primary cause of enhancements and ionization suppression and other possible effects (e.g. competition for oxygen) would be of secondary importance. Marks and Welcher<sup>298</sup> found that Ni, Co, Fe, Mn, Cr, V and Ti at the 5000 ppm level enhanced the absorbances of 100 ppm aluminium solutions by about 10%. The measurements were made using a nitrous oxide-acetylene flame with a 7 mm high red feather. The interferences from chromium and titanium were reduced as the flame became more fuel rich. (They did not test for this effect with Co, Ni, Fe, Mn and V). All the measurements were made at the flame height giving maximum sensitivity and as the flame was made more fuel rich this absorbance maximum shifted to higher positions in the flame where vaporization is nearer completion and salt vaporization effects are nearly eliminated. These workers could not find evidence for lateral diffusion interference to explain the observed enhancements but Fassel et al.<sup>338</sup> were able to suggest why Marks and Welcher were not able to observe such evidence. The latter researchers in fact concluded that competition for oxygen may account for some of the

enhancement effects observed between refractory elements because in particular aluminium monoxide emission intensity showed a decrease in the presence of titanium.

Dagnall et al.<sup>10</sup> tested for the interference of 22 ions on the fluorescence determination of aluminium, and none were found to interfere (including K and Na but they did not test for Ti). Eleven of the ions interfered with the emission signals.

### 5.3.1. The effect of acids

The use of a fuel-rich flame to minimise interferences was recommended by Marks and Welcher<sup>298</sup> for the absorption determination of aluminium. All interferences in this aluminium study were therefore looked at using the fuel-rich flame giving the most sensitive conditions (Fig. 5.1).

The effects of five acids on the atomic fluorescence and atomic emission of aluminium were determined by measuring 10 ppm aqueous aluminium solutions containing a range of concentrations of the acids. The results are shown in Fig. 5.4. and 5.5. The depressions due to phosphoric, sulphuric and perchloric acids occur in both fluorescence and emission with similar magnitudes. Hydrochloric and nitric acids only interfere at the highest concentrations (> 6% acid). The interferences are not significant when the acids are present at levels below 4%.

In atomic absorption Ramakrishna et al.<sup>308</sup> found no interference from hydrochloric, sulphuric, nitric and perchloric acids, all at the 5% level with 20 ppm aluminium. Depressions at the higher levels have been reported in atomic emission by Koiryohann and Pickett<sup>340</sup> and attributed to reduced nebulizer efficiency. Dagnall et al.<sup>10</sup> studied  $\text{Cl}^-$ ,  $\text{NO}_3^-$  and  $\text{PO}_4^-$  at 100-fold weight excess level over 20 ppm aluminium. The fluorescence and emission signals were unaffected but the concentrations of these anions were fairly low (less than 2%) compared to the concentrations

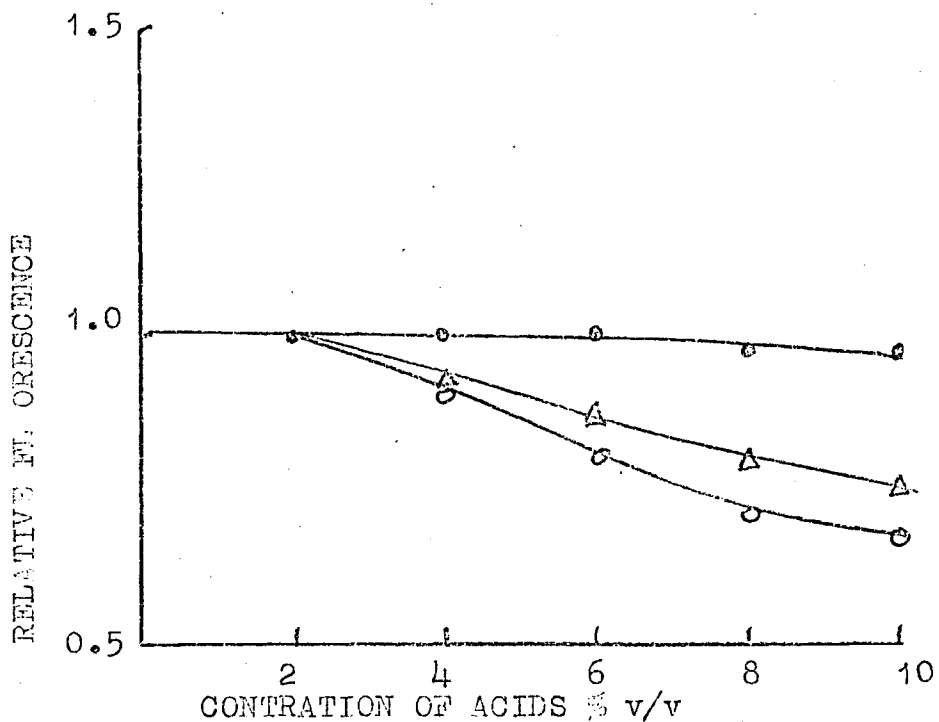


Fig. 5.4 The effect of acids on aluminium fluorescence  
 (●) - nitric and hydrochloric acids  
 (○) - sulphuric and perchloric acids  
 (Δ) - phosphoric acid

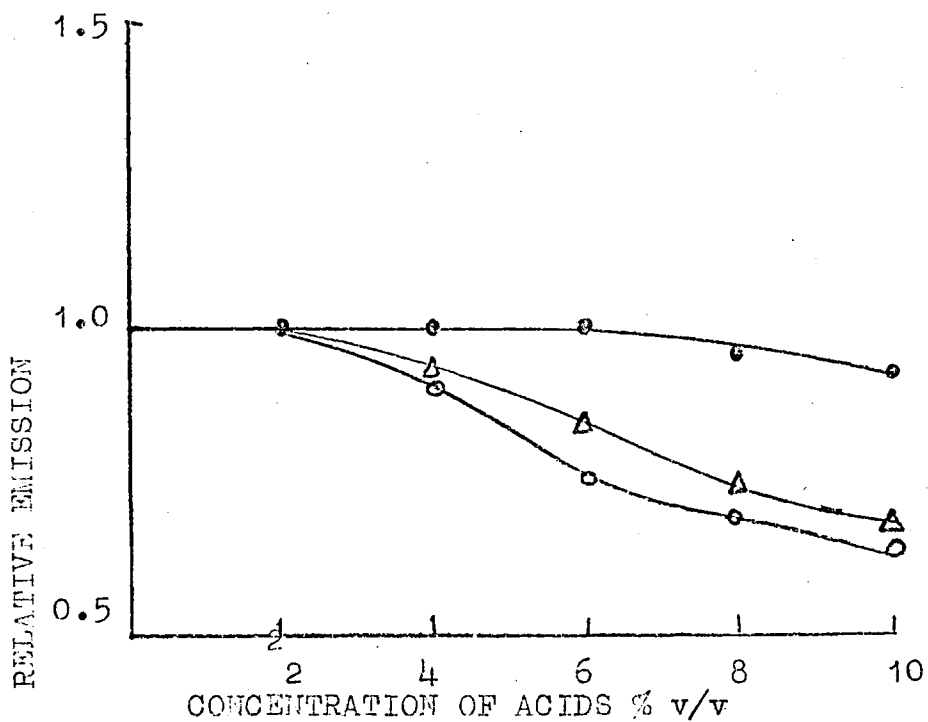


Fig. 5.5 The effect of acids on aluminium atomic emission  
 (●) nitric and hydrochloric acids  
 (○) sulphuric and perchloric acids  
 (Δ) phosphoric acid

used in this study.

The above observations indicate that interferences due to acids in the fluorescence of aluminium only occur at high acid concentrations (above 4%) and follow similar trends to those found in atomic absorption and atomic emission.

### 5.3.2. The effect of elements

The effects were determined of a number of elements on the fluorescence and emission of aluminium in the argon-separated nitrous oxide-acetylene flame. (10 ppm aluminium, 100 and 1000 ppm interfering ion). The results given in Table 5.1. can be compared with the results obtained by Dagnall et al.<sup>10</sup> who found that the fluorescence signals were unaffected by the elements tested. Table 5.2. facilitates comparison of the two sets of results because only the points of difference are tabulated.

The results of West, Knisely and Fassel<sup>326,338</sup> are included because they also compared their work to that of Dagnall et al.<sup>10</sup> Referring to Table 5.2, K, Na and Sr interfered in the present work. They would be expected to suppress the ionization of aluminium because all three elements are nearly completely ionized in the nitrous oxide-acetylene flame<sup>322</sup>. (Ionization energies (eV) of Al, K, Na and Sr are respectively 5.98, 4.34, 5.14 and 5.69).

Enhancements caused by K and Na on aluminium atomic absorption are well known<sup>319-321,342</sup> and such ionization interference would be expected to appear in atomic fluorescence. It cannot therefore be explained why Dagnall et al.<sup>10</sup> did not observe enhancement due to K or Na unless they had added another easily ionisable element such as caesium to suppress ionization. This was not mentioned in their paper.

In their study of lateral diffusion interference Fassel et al.<sup>338</sup> emphasise the primary importance of the type of burner used. Lateral diffusion interferences should be most prominent

TABLE 5.1.

INTERFERENCES ON ALUMINIUM ATOMIC EMISSION AND  
ATOMIC FLUORESCENCE AT 396.2 nm WITH THE  
ARGON-SEPARATED NITROUS OXIDE-ACETYLENE FLAME

(10 ppm aluminium, 100 and 1000 ppm interfering ion. Results expressed as the ratio of the fluorescence of aluminium in the presence of interfering ion to the fluorescence of aluminium alone. All solutions were made up with deionised water unless a particular salt was insoluble in water. In such cases alternative dissolution conditions were used. The metal salts were those detailed in appendix 2 ).

Element	Results			
	Atomic fluorescence		Atomic Emission	
	1000 ppm ion	100 ppm ion	1000 ppm ion	100 ppm ion
As	1.0	1.0	1.0	1.0
Bi	1.0	1.0	1.0	1.0
Cd	1.0	1.0	1.0	1.0
Co	1.0	1.0	1.0	1.0
Cr	1.0	1.0	1.1	1.07
Cu	1.0	1.0	1.0	1.0
Fe	1.0	1.0	1.0	1.0
K	1.15	1.1	1.07	1.03
Mn	1.0	1.0	1.0	1.0
Mg	1.0	1.0	1.0	1.0
Mo	1.0	1.0	1.1	1.03
Na	1.15	1.05	1.13	1.1
Ni	1.0	1.0	1.0	1.0
Pb	1.0	1.0	1.0	1.0
Sn	1.0	1.0	1.0	1.0
Si	1.0	1.0	1.1	1.0
Sr	1.13	1.07	1.07	1.03
Ti	1.13	1.06	1.15	1.05
V	1.0	1.0	1.03	1.0
W	1.0	1.0	1.0	1.0
Zn	1.0	1.0	1.0	1.0
Zr	1.0	1.0	1.0	1.0

TABLE 5.2.

THE EFFECT OF VARIOUS IONS ON ALUMINIUM ATOMIC  
FLUORESCENCE AND ATOMIC EMISSION AT 396.2 nm WITH  
THE ARGON-SEPARATED NITROUS OXIDE-ACETYLENE FLAME

Concomitant	This work		Dagnall et al. <sup>10</sup>		Fassel et al. <sup>326</sup>
	AFS	AES	AFS	AES	AES
W	NI	NI	NI	+22%	NI
Mo	NI	+10%	NI	+11%	+10%
Ti	+13%	+15%	-	-	-
Sr	+13%	+ 7%	-	-	-
Na	+15%	+13%	NI	+ 9%	-
K	+15%	+ 7%	NI	+11%	-
Mg	NI	NI	NI	+ 9%	-

AFS: Atomic fluorescence spectroscopy

AES: Atomic emission spectroscopy

NI: No interference

+: enhancement interference.

THIS STUDY - 1000 ppm ion, 10 ppm aluminium

Dagnall et al.<sup>10</sup> - 100 fold weight excess of ion, 20 ppm aluminium

Fassel et al.<sup>326</sup> - 2500 ppm ion, 25 ppm aluminium.

(and perhaps occur only) with linear slot burners, because only such burners viewed lengthwise permit observation of the centre of the flame with virtual exclusion of the edges. As a circular slot burner was being used in the work presented here this type of interference should not be immediately obvious and indeed no enhancements, only depressions, due to acids were observed for both fluorescence and emission. Further no enhancing interference was found for Ni, Co, Fe, Mg, Cr, V, Mo and W in fluorescence or (except for Cr, Mo, V see below) emission. These elements have all been reported to give atomic absorption enhancements of varying magnitudes (depending probably on instrumentation and choice of experimental variables). Enhancement due to titanium was found in both fluorescence and emission. Titanium has been usually either the only element reported to give serious enhancement of aluminium absorption or the element that gives the most serious enhancement relative to other enhancing concomitants. It seems unlikely that titanium produces a lateral diffusion interference to enhance signals obtained using a circular slot burner<sup>338</sup>. Alternatively competition for oxygen may be important<sup>298</sup> but with the reservations as already noted<sup>338</sup>.

Referring back to Table 5.1, the cations of Cr, Si, Mo, V, Th and Ta interfered with the emission signals of Dagnall et al.<sup>10</sup> and the existence of some spectral contribution to interference was experimentally confirmed. In the present work the cations of Cr, Si, Mo and V were tested and found to interfere with the emission signals but not with the fluorescence signals. This is in accord with the work of Dagnall et al.<sup>10</sup>. Spectral interferences have not been expected<sup>6</sup> nor encountered in atomic fluorescence.

It appears therefore that interferences with aluminium fluorescence are fewer than those found in atomic absorption

probably because the use of a circular slot burner minimises lateral diffusion.

### 5.3.3. The effect of iron and of easily ionizable elements

Iron, present as iron (III) chloride, was found to have no effect on either the fluorescence or emission of 10 ppm aluminium solutions. The concentration of iron was varied from 0 to 10,000 ppm. Addition of 4% of concentrated hydrochloric acid had no effect when iron was present. In atomic absorption and emission using linear slot burners iron usually causes an enhancement effect. The possible explanations for the different situation reported here for fluorescence have been discussed in section 5.3.2., i.e. lateral diffusion interferences and their relative effect when using a circular slot burner.

Ionization in the nitrous oxide-acetylene flame causes lower sensitivity, concave analytical curves <sup>304</sup> and ionization interferences if the sample accidentally contains an ionization suppressor. To overcome these problems excess of an alkali metal is normally added to stabilize the degree of ionization of aluminium in the flame. Kornblum and De Galan <sup>322,323</sup> in their study of ionization interferences in the nitrous oxide-acetylene flame concluded that aluminium requires 2000 ppm caesium or potassium for ionization suppression. Table 5.3a shows the effect on the atomic emission and fluorescence signals of adding 2000 ppm Na, K and Sr to 10 ppm aluminium solutions. The signals are enhanced equally in all three cases. (KCl and KNO<sub>3</sub> each behaved in exactly the same way for all the results reported in Table 5.3.). Table 5.3b demonstrates that the addition of 10,000 ppm iron (added as iron (III) chloride) removes the enhancing effect of the three elements. The addition of 4% concentrated hydrochloric acid to the 10 ppm aluminium solutions had the same effect (Table 5.3c). The removal of free electrons

TABLE 5.3

THE EFFECTS OF Na, K, Sr ON THE ATOMIC  
EMISSION AND FLUORESCENCE OF ALUMINIUM

(10 ppm aluminium, 2000 ppm Na, K or Sr, 10,000 ppm Fe, added as iron (III) chloride. Results expressed as the ratio of the fluorescence of aluminium in the presence of interfering ions to the fluorescence of aluminium alone).

Solution	Results	
	fluorescence	emission
a) Al + K	1.19	1.17
Al + Na	1.18	1.19
Al + Sr	1.19	1.20
b) Al + K + Fe	1.0	1.0
Al + Na + Fe	1.0	1.0
Al + Sr + Fe	1.0	1.0
c) Al + K + 4% conc. HCl	1.0	1.0
Al + Na + 4% conc. HCl	1.0	1.0
Al + Sr + 4% conc. HCl	1.0	1.0

by  $\text{Cl}^-$  formation which occurs when chlorine is present in large concentrations<sup>343</sup> probably explains the removal of the ionization suppression effects of potassium, sodium and strontium by the presence of ferric chloride or hydrochloric acid.

Potassium had the expected ionization suppression effect on 10 ppm aluminium solutions over the range 0 to 4000 ppm. (Fig. 5.6). When 10,000 ppm iron was present potassium did not enhance the emission or fluorescence signals at any point in the range, i.e. it appears that the effect of easily ionisable elements is stabilized by the presence of ferric chloride. This is also true in atomic absorption. For example Scholes<sup>342</sup> reports the results of a co-operative study which covered the effects of iron and sodium on aluminium atomic absorption. The investigation involved found that the presence of iron and sodium stabilizes the interference caused by sodium and iron respectively, i.e. essentially the same results as reported here for fluorescence except Scholes reports that iron did cause the usual atomic absorption enhancement.

#### 5.3.4. The effect of organic solvents

Ramakrishna<sup>308</sup> found that the increases in absorption sensitivity obtained in the presence of glycols were not great (30% increase in the presence of 5% of a glycol). Other examples of the enhancing effects of organic liquids are common. Marks and Welcher<sup>298</sup> showed that acetone has little effect on the magnitude of interferences, although it does increase the absorption sensitivity for aluminium. Acetic acid (5% glacial) has been shown to increase aluminium absorption signals by a number of workers<sup>308</sup>.

Acetic acid (5% glacial) had no effect on the 10 ppm aluminium fluorescence signals observed in this work. 10% concentrations of ethanol, acetone and ethyl-methyl-ketone all

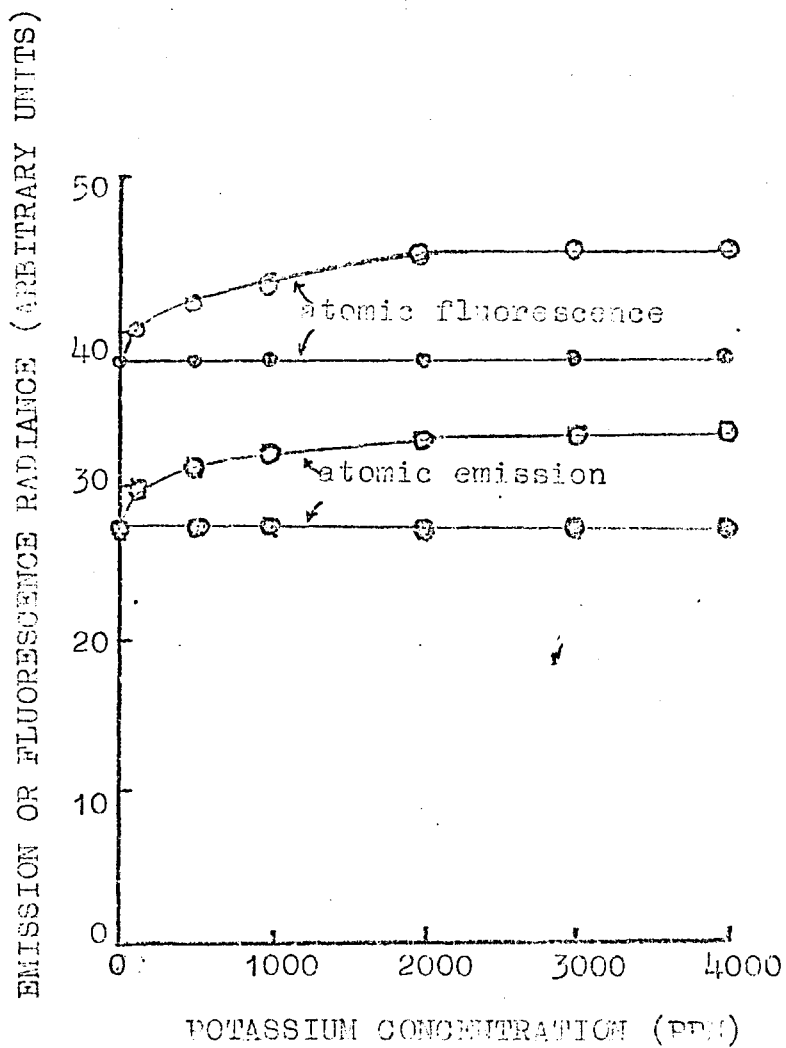


Fig. 5.6 The effect of potassium on aluminium fluorescence.

- (○) - solutions contained 10,000 ppm iron
- (□) - solutions contained aluminium and potassium only.

enhanced the signals by 10%. The addition of 10,000 ppm iron had no effect on the enhancements caused by the presence of the organic liquids.

#### 5.4. Analytical Curves and Detection limit

##### 5.4.1. Analytical Curves

At 396.2 and 394.4 nm analytical curves were obtained using solutions containing aluminium alone (Fig. 5.7). These curves were essentially linear to approximately 150 ppm and became parallel to the concentration axis at about 500 ppm.

Dagnall et al.<sup>10</sup> found the range of linearity to be 1 to 250 ppm with slight curvature toward the concentration axis between 250 and 500 ppm and appreciable curvature at concentrations between 500 and 1000 ppm. The slightly greater curvature found in the present work was probably due to the optical system. When 10,000 ppm iron and 4% concentrated hydrochloric acid were added to the calibration solutions no significant difference in the analytical signals was observed. The resulting curves were the same as those shown in Fig. 5.7. Slight bending of the curves away from the concentration axis was observed in the range 0-100 ppm (Fig. 5.8). This is symptomatic of ionization taking place and has been observed in atomic absorption for a number of elements which are significantly ionized in the nitrous oxide-acetylene flame, notably calcium<sup>304</sup>. Addition of 2000 ppm potassium nitrate to the standards removed the slight bending and gave the increase in signal associated with ionization suppression (Fig. 5.8). It has already been shown that potassium does not suppress ionization in the presence of 10,000 ppm iron (Section 5.3.3.). The curve shown in Fig. 5.9 was obtained using solutions containing aluminium, 10,000 ppm iron (added as iron (III) chloride) and 4% concentrated hydrochloric acid. This

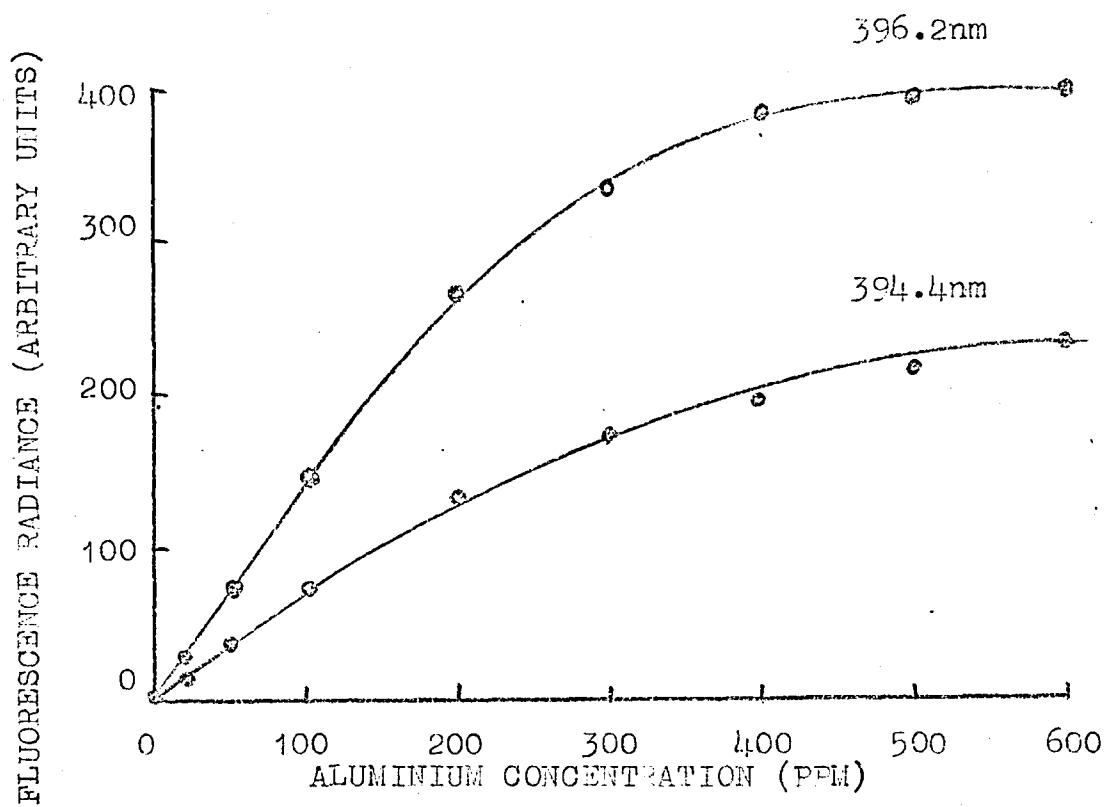


Fig. 5.7 Analytical curves for aluminium fluorescence in the argon-separated nitrous-oxide acetylene flame. Solutions contained aluminium alone.

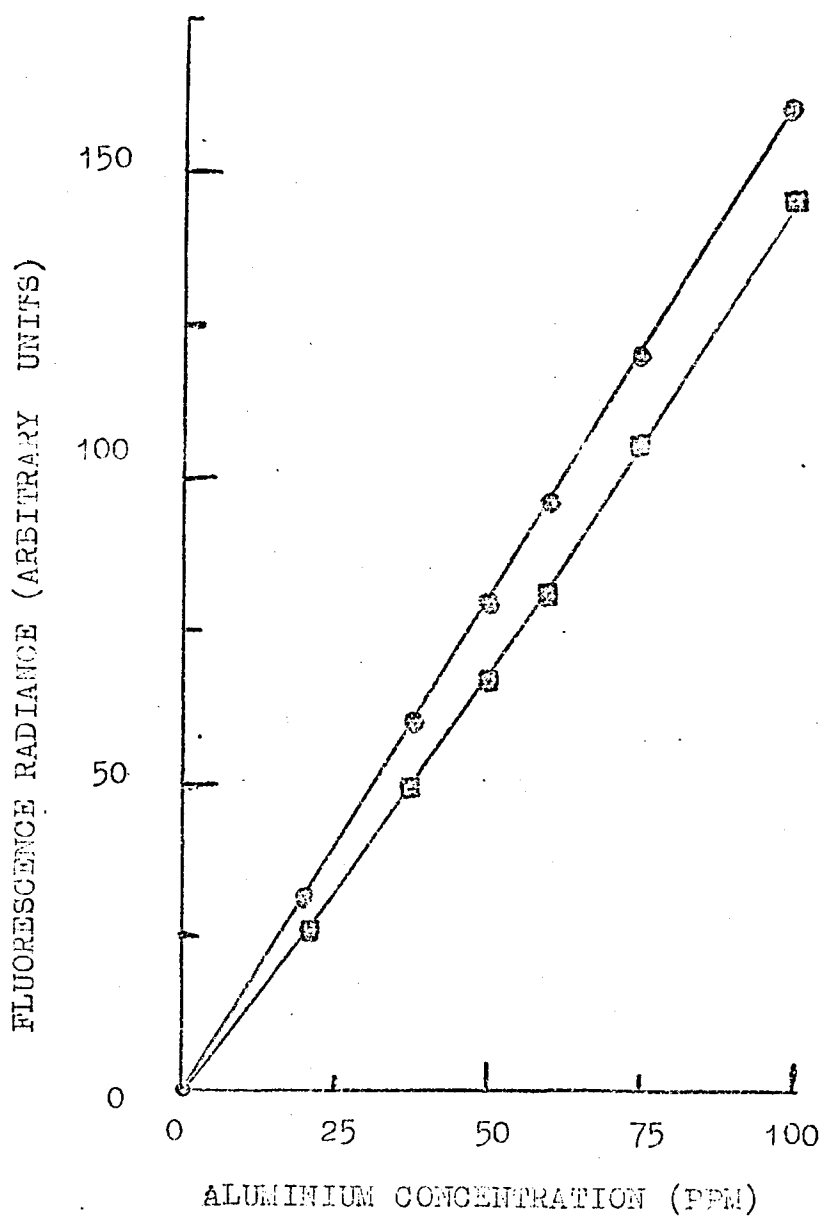


Fig. 5.8 Analytical curves for aluminium which illustrate (■) slight bending due to ionization and (●) the effect of adding 2000 ppm potassium to the standard solutions.

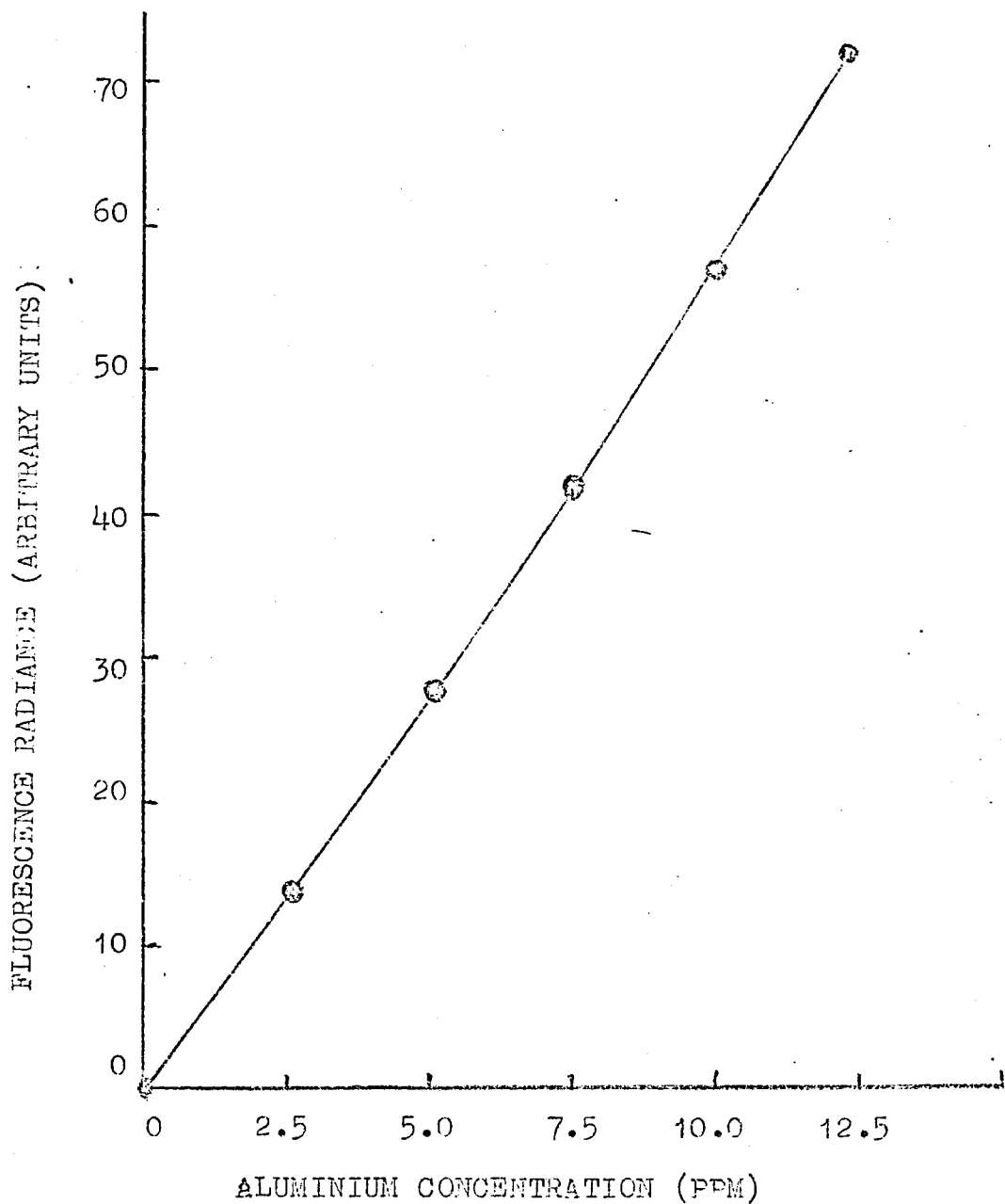


Fig. 5.9 Analytical curve for aluminium in the argon-separated nitrous oxide-acetylene flame. Standards contained 10,000 ppm iron and 4% v/v hydrochloric acid. This curve was used in the steel analyses - section 5.5

plot was used to determine aluminium in steel samples (Section 5.5) and is slightly curved due to ionization.

#### 5.4.2. Detection limit

Aluminium detection limits were measured in two ways. Firstly the criterion of a signal-to-noise ratio of two was applied. A 0.1 ppm aqueous aluminium solution containing 2000 ppm potassium (added as nitrate) was used to measure signal-to-noise ratios. The resulting detection limits were 0.07 ppm and 0.025 ppm using the 4.7s and 18.2s time constants respectively. Secondly the criterion of the detection limit being equal to twice the standard deviation on a low level signal was used. Using the 18.2s time constant and the same 0.1 ppm solution ten successive readings had a relative standard deviation from the mean of 12%, i.e. a standard deviation of 0.012 ppm. The detection limit was therefore 0.024 ppm.

The relative standard deviation of a 0.1 ppm aluminium solution containing 10,000 ppm iron and 4% concentrated hydrochloric acid was found to be 21% (18.2s time constant, ten results) i.e. a standard deviation of 0.021 ppm and therefore a detection limit of 0.04 ppm.

An atomic emission detection limit of 0.014 ppm was obtained using the Jarrell-Ash instrument (i.e. the same optics, flame, monochromator and photomultiplier tube as for the fluorescence measurements but with the Jarrell-Ash amplifier rather than the lock-in amplifier). The detection limit was calculated on the basis of the standard deviation of a 0.05 ppm solution containing 2000 ppm potassium. A time constant of 5s was used.

Comparison of the atomic fluorescence detection limit (0.07 ppm 4.7s time constant) with the atomic emission detection limit (0.014 ppm 5s time constant) reveals a significant superiority of the atomic emission technique by a factor of five.

The best reported detection limits in atomic absorption (see introduction to this chapter) have usually been about the same as the atomic fluorescence figures obtained here.

#### 5.5. The determination of aluminium in steel samples

The choice of dissolution methods for determination of aluminium in steels by atomic absorption depends upon whether both the acid soluble and acid insoluble aluminium content or just the acid soluble content is required. As the procedures for determination of total aluminium by flame spectroscopy are well established (see introduction to this chapter) a simple method of dissolution with aqua-regia was used here to determine acid soluble aluminium.

The effects of concomitant elements on the aluminium determination in the nitrous oxide-acetylene flame have been described in section 5.3. The presence of 10,000 ppm iron (corresponding to 1 g of steel dissolved in 100 ml of solution) was shown to stabilise the effect of ionization interferences due to K, Na and Sr. Other interferences commonly found in atomic absorption (notably enhancing interferences due to lateral diffusion effects) were not observed in the fluorescence determination. The only element which did interfere was titanium, 100 ppm of which caused a 6% enhancement of the 10 ppm aluminium signal. However the relative standard deviation for the steel analysis (see below) was found to be 3.2%. The titanium interference can therefore be considered to be not significant at the 10 ppm titanium level.

The method used for dissolution of the steel samples is given in Table 5.4. A similar method for the determination of acid soluble aluminium has been used by a number of workers<sup>329,331</sup> although others use perchloric acid as well as aqua-regia<sup>304,328</sup>

TABLE 5.4.

DISSOLUTION METHOD USED FOR THE DETERMINATION  
OF ALUMINIUM IN STEEL BY ATOMIC FLUORESCENCE

1 g of the steel was dissolved in 7 ml of concentrated hydrochloric acid and 3 ml of concentrated nitric acid and the resulting solution was heated gently until the evolution of brown fumes due to oxides of nitrogen ceased. The solution was then evaporated, almost to dryness, the residue taken up with 4 ml concentrated hydrochloric acid and filtered through a No. 4 sinter crucible. The solution was then transferred to a 100 ml volumetric flask and diluted to the mark with deionised water.

TABLE 5.5.

RESULTS OF DETERMINATIONS OF ACID  
SOLUBLE ALUMINIUM IN STANDARD STEELS

British Chemical Standard Steel No.	Descrip- tion of steel	BCS Al standardised value %		Found		
		acid soluble	total	Atomic fluorescence (duplicate analyses)	Ref 328 (acid soluble)	Ref 330 (total)
321	mild	-	0.12	0.123 0.128	0.13	0.135
322	mild	0.087	0.093	0.091 0.089	-	0.0939
329	mild	0.053	0.058	0.061 0.053	0.06	0.058

and less oxidising conditions are also used, for example the steel may be dissolved in 10-15% sulphuric acid or in dilute hydrochloric acid.

The results of the atomic fluorescence analysis of three mild steels are given in Table 5.5. The results reported in the literature for the atomic absorption determination of the same steels for soluble<sup>328</sup> and total<sup>330</sup> aluminium are also given for comparison. It can be seen that the atomic fluorescence method is as accurate as the atomic absorption method. (The certificate values quoted were taken from certificates attached to the B.C.S. samples. These same values were also quoted in the two references<sup>328</sup> and<sup>330</sup>). Due to the fairly oxidising dissolution conditions used it may be that some so-called acid insoluble aluminium will have gone into solution. This could explain the slightly high acid-soluble aluminium content obtained for samples 322 and 329 (i.e. the two results 0.091% and 0.061% respectively). It is noteworthy that Thomerson and Price<sup>328</sup> also obtained a high value for the acid soluble content of steel no. 329. These authors were using the even more strongly oxidising system involving perchloric acid.

The calibration curve used to obtain the above results is given in Fig. 5.9. The standard solutions contained 10,000 ppm iron (added as iron (III) chloride) to stabilise ionization effects and 4% concentrated hydrochloric acid to ensure stability of the concentration of aluminium.

To obtain precision values six samples of standard steel number 322 were treated using the dissolution method in Table 5.4 and the average of three atomic fluorescence readings taken for each sample solution. The relative standard deviations of the measurement was found to be 3.2%.

## 5.6. Conclusion

The most outstanding feature of this work on the fluorescence of aluminium is the apparent lack of interferences affecting the determination. This same observation was made by Dagnall et al.<sup>10</sup> but thrown into some doubt by Fassel et al.<sup>326,338</sup> who could not reproduce some of the surprisingly large interferences found by Dagnall et al. for the flame emission determinations of Al, V and Mo (reported in the same paper<sup>10</sup> as the fluorescence work). The present study appears to have reinforced the conclusions of Dagnall et al. that the atomic fluorescence determination of aluminium is relatively free from interferences.

In order to achieve a favourable aluminium atomic absorption sensitivity and detection limit it is necessary to use a linear slot burner. However Fassel et al.<sup>338</sup> have confirmed the existence of lateral diffusion interferences when using this type of burner for atomic absorption measurements. They argue that the use of a circular slot burner would minimise the effects of lateral diffusion interference and indeed this does appear to be the case with the atomic fluorescence determination of aluminium using the circular slot burner. Moreover it is possible to achieve the same detection limit by atomic fluorescence using a circular slot burner as is obtainable by atomic absorption with a linear slot burner. This situation clearly represents an advantage of atomic fluorescence over atomic absorption determinations of aluminium.

The atomic fluorescence method was found to be satisfactory for the determination of acid-soluble aluminium in steel. The aluminium fluorescence was measured at 396.2 nm using an argon-separated nitrous oxide-acetylene flame. The presence of 10,000 ppm iron (as iron (III) chloride) in samples and standards was found to stabilise ionization interferences from various easily

ionizable metals. Concentrated hydrochloric acid (4 ml acid in 100 ml steel solution) was added to the steel solutions to minimise loss of aluminium.

## CHAPTER SIX

## Conclusions

Since atomic fluorescence was first introduced in 1964 a number of researchers have used various improvements in instrumentation which have increased the signal-to-noise ratio of the atomic fluorescence measurement. However this author was not able to find any publications which report the combined use of most of the more simple instrumental modifications which are possible on a typical atomic absorption instrument.

The instrumentation described in Chapter Two combined the use of a lock-in amplifier with temperature controlled, high-frequency modulated electrodeless discharge lamps, inert gas flame separation and an efficient optical system. All these modifications gave improvements in signal-to-noise ratio sufficient to realise detection limits for the determination of tin and arsenic fluorescence in cool hydrogen flames which were between ten and twenty times superior to reported atomic absorption and fluorescence detection limits using the same flames. Further, for both elements the argon-separated air-acetylene flame could be used to minimise interferences whilst still retaining a sensitivity which was superior to that obtainable in atomic absorption. For the determination of aluminium in the argon-separated nitrous oxide-acetylene flame a detection limit was obtained which was equal to the best reported atomic absorption detection limits for aluminium in this flame. Not only were these sensitivities obtained using pure aqueous solutions but also, when looking at the fluorescence signals obtained using steel solutions, it was found that the presence of 10,000 ppm

iron had little effect except in the cool hydrogen flames where interferences often have been shown to be serious, both here and elsewhere<sup>344</sup>.

Winefordner<sup>20,118</sup> has argued that atomic fluorescence should give better detection limits than atomic absorption because the limiting noise in atomic absorption is due to the source as well as the flame. In atomic fluorescence the source noise is not the limiting factor, only flame noise. However these observations are only true if the source in atomic fluorescence gives sufficient radiant output. In 1969<sup>118</sup> this was only true of a few EDL sources for example Ag, Cd, Hg and Zn and marginally true for such elements as Sn and As. However the more recent advances with thermostatted EDL's may lead to improvements in the radiant output of other more difficult element EDL's. Work of this type has, to this authors knowledge, not yet been reported. Arsenic and tin EDL's would therefore be considered 'easy' lamps and this partly explains why satisfactory results were obtained in the work reported here. The use of temperature control and optimisation of modulation frequency helped to ensure that these lamps were giving of their best in terms of radiant output and stability. In the case of aluminium temperature control ensured the highest radiant output possible without the necessity for the use of high microwave powers to give the correct operating temperature. For all three lamps, however, it is likely that preparative procedures designed for operation under temperature controlled conditions would have improved the attainable outputs considerably. For example the amount of material in the lamps seemed excessive as shown by the 'pinching' of the discharges near the optimal operating temperature. All three lamps were obtained from commercial manufacturers.

Winefordner<sup>118</sup> also indicated that atomic fluorescence is more likely to give superior detection limits, relative to atomic absorption and emission, for elements which have their resonance lines below ca. 325 nm. Above this wavelength atomic emission will give superior detection limits because for analytical flames (2000-3000K) the black body spectral radiance corresponding to the flame temperature is greater than the line spectral radiance of available sources. Reported tabulations of flame spectroscopic detection limits<sup>5,6,10,118</sup> have tended to confirm this wavelength dependence. The results obtained in the present work and the work of others<sup>345</sup> also conform to this trend i.e. arsenic (189.0 nm), detection limits are superior to those in atomic absorption; aluminium (396.2 nm) detection limits are similar to atomic absorption but inferior to atomic emission; tin lay in between these extremes at 303.4 nm. The volatile elements do tend to have their resonance lines in the 190 to 300 nm region and these volatile elements usually make the better EDL's. Moreover flames are also generally less noisy at wavelengths below 300 nm and especially below 230 nm. These latter two factors improve signal-to-noise ratios below 300 nm and therefore contribute significantly towards the observed wavelength dependence.

The work reported in this thesis demonstrates that the potential of atomic fluorescence flame spectroscopy as a more sensitive technique than atomic absorption can be realised by simple modifications to a conventional atomic absorption flame instrument provided that a good EDL is available. The table below compares detection limits obtained in this work with detection limits claimed for the Jarrell-Ash model 840 two channel, double beam atomic absorption instrument<sup>357</sup>. This

is probably a good example of 'state-of-the-art' atomic absorption  
(This was not the instrument used in the work for this thesis.)

Element	Flame	Detection Limits ppm	
		This work	Model 810
Aluminium	$N_2O/C_2H_2$	0.025	0.05
Tin	$C_2H_2/Air$	0.05	-
	cool hydrogen flames	0.006	0.05
Arsenic	$C_2H_2/Air$	0.015	-
	$C_2H_2/N_2O$	0.10	-
	cool hydrogen flames	0.01	0.2

The favourable fluorescence signal-to-noise performance reported here was particularly useful when attempting sensitive determinations of the three test elements in steel. This was because the acetylene based flames could be used and advantage taken of their relative freedom from interferences. In atomic absorption the use of the hot flames would have entailed an unacceptable loss in sensitivity.

One of the interesting features of this work was the observed lack of interferences affecting the fluorescence of aluminium in the nitrous oxide-acetylene flame. The use of a circular slot burner for the atomic fluorescence measurements apparently minimised the effect of lateral diffusion interferences. This type of interference has been confirmed in atomic absorption using linear slot burners. This situation clearly represents a further advantage of atomic fluorescence over atomic absorption

for a number of elements particularly those forming refractory oxides which are usually determined in the nitrous oxide-acetylene flame. The linear slot burner is necessary in atomic absorption to give sensitive measurements but possesses no advantages for atomic fluorescence where a circular burner is optimal.

With the exception of the lateral diffusion interference situation the work reported here indicates that interferences in atomic fluorescence follow the same basic trends as have been demonstrated in atomic absorption. Such studies of fluorescence interferences are necessary for the future development of the technique and may lead to further insight to the nature of flame interferences in general as well as revealing any further differences between the interferences that affect the three flame atomic spectroscopic techniques.

The limitation in atomic fluorescence is the availability of high radiance sources for a number of elements. Hollow cathode lamps are available for most elements and therefore atomic absorption is possible for elements such as Nb and W whereas high radiance EDL's suitable for atomic fluorescence are not available for elements such as Nb and W. However the use of a turnable dye laser has been reported to have considerable potential as discussed in appendix I and may for some applications be a solution to the source problem despite the expense involved.

Unfortunately, on the basis of sensitivity, instrument manufacturers do not seem to have, at present, any reason to justify the marketing of specially designed flame atomic fluorescence instrumentation to compete with the well established atomic absorption instruments. These are at the moment being extensively used with non-flame cells which can give very high absolute sensitivities. It is therefore likely that atomic fluorescence

will in the future take a different path to the one followed by atomic absorption. Some such possible paths are a) high sensitivity determination of a wide range of elements using a laser source and a flame or non-flame cell and b) multielement analysis<sup>352</sup> where there is the greater optical freedom, relative to atomic absorption, in being able to arrange a number of element line sources around a flame. This can be utilised for both non-dispersive and dispersive instruments and for simultaneous or sequential recording of analytical results. Some areas in which research is being carried out to further multielement atomic fluorescence and indeed atomic emission<sup>352,358</sup> are the use of multielement EDL's<sup>230,261,348-351</sup>, image vidicon detectors<sup>346,347</sup> and non-dispersive instrumentation<sup>35,54</sup>.

Published applications of atomic fluorescence to real analyses have so far been relatively rare but those that have been reported<sup>354-356</sup> and the work presented here have all demonstrated the sensitivity and selectivity that has been predicted for the technique.

The work reported here for the determination of three elements in steel has shown that more detailed work is needed on interferences in atomic fluorescence. A particular area is the lateral diffusion interference situation. Future work, within the framework of the present instrumentation can also be directed at further improving the performance of EDL's and the development of the use of non-flame cells or a better burner such as has been reported in the atomic fluorescence literature. Other future possibilities are mechanical modulation of EDL's or alternatively a look at other types of source such as the high radiant output and demountable hollow cathode lamps. Any other suggestions for instrumental development would necessarily

be expensive. For example sophisticated electronic processing of fluorescence signals buried in noise and the use of lasers to improve signal-to-noise ratios both add versatility to the technique.

This work has indicated that atomic fluorescence flame spectroscopy is particularly suited to steel analysis. The technique retains the freedom from interferences which is characteristic of atomic absorption. However the superior sensitivity of the fluorescence technique ensures that preconcentration using solvent extraction procedures need not be used as often as it is in flame atomic absorption.

Flame atomic absorption methods have been applied to the analysis of the steel samples which are used to standardize automatic emission or x-ray instruments. The more sensitive flame atomic fluorescence could be even more useful in the same application.

Contamination and vaporization problems with the non-flame systems currently being developed are more likely with samples with a high solids content such as steel solutions. If non-flame cells are applied to steel analysis the sensitive and selective flame atomic fluorescence method will be a useful standardization technique.

Future work directed at applying flame atomic fluorescence to the measurement of low levels of elements in steel must involve not only instrumentation but also attention to the details of dissolution conditions and measurement procedure which give the most accurate and precise analyses. For example it is often desirable to carry out an analysis for a number of trace elements using a single weighing and preparation procedure. To ensure that all the elements of interest are in solution it is

necessary to choose appropriate dissolution conditions. A particular problem was encountered in this work when using perchloric acid in the dissolution of steels. This acid is useful for bringing a number of elements into solution. It became clear however that if tin was to be determined in the presence of perchloric acid careful control of the acid concentration was necessary to ensure accuracy and precision. Other examples of considerations that affect dissolution procedure were also encountered in this work. In particular, the volatility of the arsenic chloride and the discrimination between acid soluble and acid insoluble forms of aluminium both affect the choice of dissolution conditions. Measurement procedure is particularly important when considering the effect of iron on the fluorescence signals. It is usually convenient to keep the iron in solution and spray the steel solution directly into the flame. If iron interferes its effect must be minimised by proper standardization procedure and also by the use of a good nebulizer-burner system. The latter will minimise 'clogging' of the burner with solids and optimize nebulizer efficiency. The choice of dissolution conditions is just one of the many compromises necessary when attempting multielement analysis. However a particular versatility of flame atomic fluorescence is its suitability for development as a multielement technique which has many of the virtues of both atomic absorption and atomic emission in flames.

## Appendix I

## THEORY OF ATOMIC FLUORESCENCE

The types of atomic fluorescence (resonance, normal direct line, thermally assisted direct line, normal stepwise line and thermally assisted stepwise line) have been described in several reviews<sup>5,6,7,334,359,360</sup> Resonance fluorescence has been most used for analytical studies.

The summary below shows the main steps in the derivation of the radiance (intensity) of atomic fluorescence,  $B_F$ . The treatment that follows the summary was adapted from the review by Winefordner and Elser<sup>5</sup> and the textbook by Winefordner et al.<sup>7</sup> For a more thorough discussion see Alkemade<sup>361</sup>, Hooymayers<sup>122</sup> and Winefordner et al.<sup>123</sup> as well as the above two publications<sup>5,7</sup>.

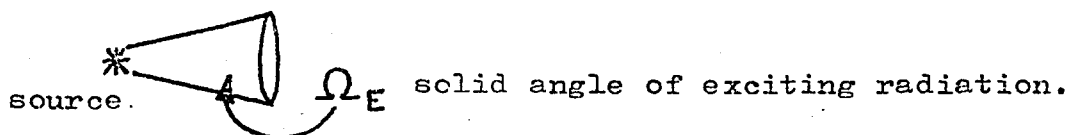
The following assumptions were made by Winefordner et al.<sup>7</sup> in deriving the expressions: the sample cell (a parallelepiped, see below) is completely illuminated and the fluorescence emitted at right angles to the exciting beam is measured. (If the cell is incompletely illuminated and if all the emitted fluorescence is not measured then correction factors must be included<sup>122,359</sup>.) The source area ( $L \times l'$ ) is larger than the absorption area ( $L \times l'$ ) of the cell; the exciting radiation reaching the cell is collimated and the measured fluorescence radiation is also a collimated beam at right angles to the exciting beam; and the atomic concentration,  $n_0$ , and temperature of the atomiser are constant across atomiser.

DERIVATION OF THE RADIANCE (INTENSITY) OF ATOMIC FLUORESCENCE

$B_F$ . (ERGS OF FLUORESCENCE PER SECOND PER UNIT AREA OF THE CELL PER UNIT SOLID ANGLE)

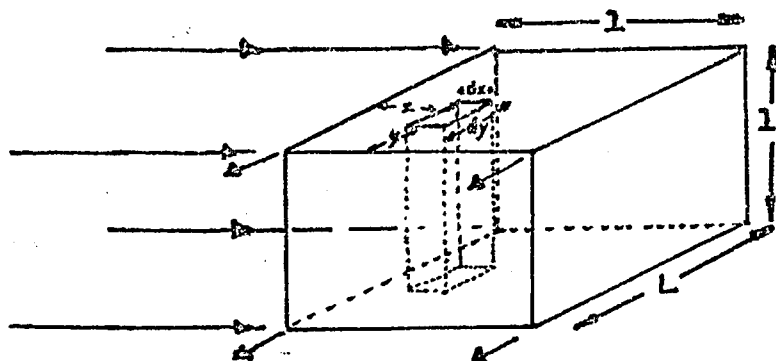
## SUMMARY

I Source spectral radiance,  $B_{s\lambda}^{\circ}$



II Source spectral radiance flux  $\phi_{s\lambda}^{\circ}$

exciting radiation imaged on the cross-sectional area  $dy \text{ l' cm}^2$  of volume element  $dy \text{ dx l' cm}^3$



Perspective view of volume element  $dy \text{ dx l'}$  in the atom cell.

- fluorescent radiation, (observed perpendicular to exciting radiation).

III Radiant flux absorbed  $d\phi_{s\lambda}$



absorbed by a small volume element of path length  $dx$

IV Conversion of flux absorbed by volume element to

radiant flux fluoresced,  $d\phi_{F\lambda}$ , by same volume element



- V Conversion of flux fluoresced to radiance fluoresced,  
 $dB_F$ , by same volume element
- ↓
- VI Integration to give  $B_F$
- ↓
- VII Evaluation of integrals in VI
- a) Self-absorption integral,  $f_s$ .
- b) Absorbed radiance integral,  $E_A$ , - solved using  
 two limiting cases 1. continuum source and  
 2. line source.
- ↓
- VIII Final fluorescence radiance expressions
- ↓
- IX Generalizations made from the radiance expressions

## DERIVATION

- I Source Spectral Radiance  $B_{s\lambda}^o$   
 (erg sec<sup>-1</sup> cm<sup>-2</sup> sr<sup>-1</sup> nm<sup>-1</sup>)

The solid angle, in steradians, of light collected by a lens from a point source is  $\Omega_E = A_l / F_c^2$  where  $A_l$  is the area of the lens (cm<sup>2</sup>) and  $F_c$  is its focal length (cm). This favours a large diameter and short focal length of lens and a similar expression would also apply to concave mirrors.

- II Source spectral radiance flux  $\phi_{s\lambda}^o$  (erg sec<sup>-1</sup> nm<sup>-1</sup>)
- The flux incident on cross-sectional area  $dy$  l' cm<sup>2</sup> of volume element  $dx$  l' cm<sup>3</sup> is

$$\phi_{s\lambda}^{\circ} = B_s \lambda^{\circ} \Omega_E [dy \ l'] \frac{1}{M_L M_H} [T_E] \quad (1)$$

where  $M_L$  and  $M_H$  are the source image magnification at the cell surface in the longitudinal and horizontal directions respectively,  $T_E$  is a factor to account for absorption and reflection losses due to optical components between source and absorption cell.  $\Omega_E$  is the solid angle of exciting radiation collected by the optical arrangement and imaged on the volume element.

### III Radiant flux absorbed

According to the Lambert absorption law, the spectral radiant flux at any distance  $x$  from the front surface of the cell  $\phi_{s\lambda}(x)$  ( $\text{erg sec}^{-1} \text{ nm}^{-1}$ ) is given by:-

$$\phi_{s\lambda}(x) = \phi_{s\lambda}^{\circ} [\exp -K_{\lambda} x] \quad (2)$$

where  $K_{\lambda}$  = absorption coefficient of the analyte at the excitation wavelength (i.e. the fraction absorbed). Therefore the radiant flux absorbed at wavelength  $\lambda$ , per unit wavelength interval, by the small volume element of path length  $dx$  is given by:-

$$d\phi_{s\lambda} = \phi_{s\lambda}^{\circ} K_{\lambda} [\exp -K_{\lambda} x] dx \quad (3)$$

### IV Fluorescence radiance $B_F$

Conversion of radiant flux absorbed by volume element  $dx \ dy \ l'$  to radiant flux fluoresced by the same volume element.

Fluorescence spectral power yield  $Y_{\lambda}(\lambda')$  given by

$$Y_{\lambda}(\lambda') = Y_p f(\lambda') \quad (4)$$

where  $Y_p$  = power yield of fluorescence =

$$\frac{\text{fluoresced radiant flux}}{\text{absorbed radiant flux}}$$

(and is dependent on the excitation wavelength  $\lambda$ )

$f(\lambda')$  = spectral distribution of fluorescence and is dependent only on the fluorescence wavelength  $\lambda'$ .

The product  $f(\lambda')d\lambda'$  represents the probability that an emitted photon has a wavelength between  $\lambda'$  and  $\lambda' + d\lambda'$ ; i.e.

$$\int_0^{\infty} f(\lambda') d\lambda' = 1$$

Therefore  $f(\lambda')$  represents the normalized shape of the fluorescence line or band and is given by:-

$$f(\lambda') = \frac{K\lambda'}{\int_0^{\infty} K\lambda' d\lambda'} \quad (5)$$

where the emission coefficient for the fluorescence process  $K\lambda'$  is identical to the absorption coefficient  $K\lambda$ .

The fluorescence spectral radiant flux,  $d\phi_{F\lambda'}$ , from the small volume element  $dx dy l'$  is .'. given by

$$d\phi_{F\lambda'} = \underbrace{d\phi_{s\lambda'}}_{\text{flux absorbed}} \cdot Y_{\lambda}(\lambda') \cdot \underbrace{[\exp - K\lambda'y]}_{\text{factor to account for loss of fluorescence due to self-absorption}} dy \quad (6)$$

spectral power  
yield

V The spectral radiance of fluorescence from the volume element

The spectral radiant flux of fluorescence can be converted to the spectral radiance of fluorescence by dividing  $d\phi_{F\lambda'}$  by  $4\pi$ , by the area  $dAs$  of the 6 surfaces of the volume element and by  $n^2$ . (There are  $4\pi$  sr in a sphere of isotropic fluorescence and  $n$  is the refractive index of the flame (usually))

$$\therefore dB_{F\lambda'} = d\phi_{F\lambda'} \left[ \frac{1}{4\pi n^2} \right] \left[ \frac{1}{dAs} \right] \quad (7)$$

the fluorescence radiance  $dB_F$  ( $\text{erg sec}^{-1} \text{cm}^{-2} \text{sr}^{-1}$ ) from the volume element  $dx dy l'$  is therefore given by:-

$$dB_F(\lambda') = \left[ \frac{\Omega E}{4\pi} \right] \left[ \frac{l' dx dy}{dAs} \right] \left[ \frac{T_E}{n^2 M_L M_H} \right] \left[ \frac{1}{\int_0^\infty K \lambda' d\lambda'} \right] \cdot \left( \int_0^\infty \phi_s \lambda^\circ K \lambda [\exp -K \lambda x] d\lambda \right) \cdot \left[ \int_0^\infty Y_p K \lambda' [\exp -K \lambda' y] d\lambda' \right] \quad (8)$$

VI If equation (8) is integrated w.r.t.  $x$  and  $y$  between the limits of 0 and  $l$  for  $x$  and 0 and  $L$  for  $y$ , then the fluorescence radiance  $B_F$  is given by:-

$$B_F = \left[ \frac{\Omega E}{4\pi} \right] \left[ \frac{LL'}{2Ll' + 2lL' + 2Ll} \right] \left[ \frac{T_E}{n^2 M_L M_H} \right] Y_p \cdot \left[ \int_0^\infty B_s \lambda^\circ (1 - [\exp -K \lambda l]) d\lambda \right] \left[ \frac{\int_0^\infty (1 - \exp -K \lambda' L) d\lambda'}{\int_0^\infty L K \lambda' d\lambda'} \right] \quad (9)$$

Absorbed radiance,  $E_A$ .

Self-absorption factor,  $f_s$ , accounts for reabsorption of fluorescence by analyte species.

VII Evaluation of integrals in equation (9)

a) The self-absorption integral,  $f_s$

$f_s$  is unity or near unity for:-

(A) Atomic fluorescence involving dilute atomic gas and transitions terminating in the ground or any excited state.

(B) Atomic fluorescence involving any concentration of atoms for transitions terminating in states above the ground state.

(The hotter the gas the higher the level must be above the ground state for  $f_s$  to be unity).

However, for atomic fluorescence of concentrated gases and for transitions terminating in the ground or near ground states, the  $f_s$  factor is less than unity and is given by:-

$$f_s = \frac{\int_0^{\infty} (1 - \exp(-K\lambda'L)) d\lambda'}{\int_0^{\infty} LK\lambda' d\lambda'}$$

$$= \frac{2\sqrt{a'}}{\sqrt{\pi} K_0' L} \quad (10)$$

where  $k_0'$  is the peak atomic absorption coefficient for pure doppler broadening for the fluorescence line.

$a'$  is the damping constant for the fluorescence line, and is given by  $a' = \sqrt{\ln 2} \frac{\Delta\lambda'_C}{\Delta\lambda'_D}$  for the fluorescence

process and  $a = \sqrt{\ln 2} \frac{\Delta\lambda_C}{\Delta\lambda_D}$  for the absorption process.

$\Delta\lambda'_C$  is the collisional half width of the fluorescence line and  $\Delta\lambda'_D$  is the doppler half width of the fluorescence line.

For resonance fluorescence  $a = a'$ . For non-resonance fluorescence  $a \neq a'$ . In (10)  $a'$  must be used.

b) Absorbed radiance integral,  $E_A$

This integral is solved by defining limiting but nevertheless analytically useful cases:-

1. Continuum Source Case

In this case the source of excitation has a constant spectral radiance over the entire absorption line and therefore:-

$$\int_0^{\infty} B_S \lambda^0 (1 - \exp(-K_\lambda l)) d\lambda = B_C^0 \lambda_0 \int_0^{\infty} (1 - \exp(-K_\lambda l)) d\lambda \quad (11)$$

where  $B_C^0 \lambda_0$  is the spectral radiance of the continuum source at the peak absorption wavelength.

This condition thus simplifies integration by making  $B_S \lambda^0$  a constant. The resulting integral is easily solved for absorption lines having a Voigt profile and which result from either very low or very high concentrations of absorbers.

For low concentrations of atomic absorbers collisional (Lorentzian) broadening is assumed to be negligible and by substituting an equation for  $K_\lambda$ , which describes the absorption profile of a line broadened by only pure Gaussian, doppler, effects, the integral in equation (11) becomes:-

$$\int_0^{\infty} (1 - \exp(-K_\lambda l)) d\lambda = \int_0^{\infty} K_\lambda l d\lambda = \frac{\sqrt{\pi} K_0 \Delta \lambda_G l}{2 \sqrt{\ln 2}} \quad (12)$$

where  $\Delta \lambda_G$  is the Gaussian half width and  $K_0$  is the absorption coefficient at absorption line center for pure Gaussian broadening.

At high concentrations of absorbers collisional broadening becomes significant and the damping constant "a" is again introduced to account for the further broadening.

The integral becomes:-

$$(1 - \exp - K_{\lambda} l) d\lambda = \Delta \lambda_G \sqrt{\left( \frac{\sqrt{\pi} K_0 l a}{\ln 2} \right)} \quad (13)$$

## 2. Line source case

In this case the source of excitation is a narrow line source, i.e. the half width of the source line is less than the half width of the absorption line.

Hence:-

$$\begin{aligned} B_{s\lambda}^0 (1 - \exp - K_{\lambda} l) d\lambda &= (1 - \exp - \bar{K} l) \int_0^{\infty} B_{s\lambda}^0 d\lambda \\ &= (1 - \exp - \bar{K} l) B_N^0 \end{aligned} \quad (14)$$

where  $\bar{K}$  is the effective or average absorption coefficient over the source line half width and where  $B_N^0$  is the source integrated spectral radiance (integrated over the exciting line), i.e. the source radiance in  $\text{erg sec}^{-1} \text{cm}^{-2} \text{sr}^{-1}$ .

For a low concentration of absorbers the coefficient  $\bar{K}$  is directly proportional to the concentration of absorbers and

$$1 - \exp - \bar{K} l = \bar{K} l \quad (15)$$

$$\text{For high concentrations} \quad 1 - \exp - \bar{K} l = 1 \quad (16)$$

## VIII FINAL FLUORESCENCE RADIANCE EXPRESSIONS

1. Continuum Source - Low concentration of Analyte - from eqns (11), (12) with (9) and  $f_s = 1$ .

$$B_F = \left[ \frac{\Omega E}{4\pi} \right] \left[ \frac{Ll1'}{2Ll1'+2ll1'+2Ll1} \right] \left[ \frac{T_E}{n^2 M_L M_H} \right] Y_P B_{c\lambda}^{\circ} \left[ \frac{\sqrt{\pi} K_o \Delta \lambda G}{2 \ln 2} \right]$$

2. Continuum Source - Atomic fluorescence terminating in ground or near ground state - High concentration of analyte - from (10), (11) and (13) with (9)

$$B_F = \left[ \frac{\Omega E}{4\pi} \right] \left[ \frac{Ll1'}{2Ll1'+2ll1'+2Ll1} \right] \left[ \frac{T_E}{n^2 M_L M_H} \right] Y_P B_{c\lambda}^{\circ} \left[ \frac{K_{olaa'}}{K_o' L \ln 2} \right]^{\frac{1}{2}} \Delta \lambda G$$

3. Continuum Source - Atomic fluorescence terminating in excited state - High concentration of Analyte - from (11) and (13) with (9)  $f_s = 1$

$$B_F = \left[ \frac{\Omega E}{4\pi} \right] \left[ \frac{Ll1'}{2Ll1'+2ll1'+2Ll1} \right] \left[ \frac{T_E}{n^2 M_L M_H} \right] Y_P B_{c\lambda}^{\circ} \left[ \frac{\sqrt{\pi} K_{ola}}{\ln 2} \right]^{\frac{1}{2}} \Delta \lambda G$$

4. Line Source - Low concentration of analyte - from (14) and (15) with (9)  $f_s = 1$ .

$$B_F = \left[ \frac{\Omega E}{4\pi} \right] \left[ \frac{Ll1'}{2Ll1'+2ll1'+2Ll1} \right] \left[ \frac{T_E}{n^2 M_L M_H} \right] Y_P B_N^{\circ} \bar{K}$$

5. Line source - atomic fluorescence terminating in ground or near ground state - High concentration of analyte - from (11), (14) and (16) with (9)

$$B_F = \left[ \frac{\Omega E}{4\pi} \right] \left[ \frac{Ll1'}{2Ll1'+2ll1'+2Ll1} \right] \left[ \frac{T_E}{n^2 M_L M_H} \right] Y_P B_N^{\circ} \left[ 2 \frac{a'}{\sqrt{\pi} K_o' L} \right]^{\frac{1}{2}}$$

6. Line source - atomic fluorescence terminating in excited state - High concentration of analyte - from (14) and (16) with (9)  $f_s = 1$ .

$$B_F = \left[ \frac{\Omega E}{4\pi} \right] \left[ \frac{Ll1'}{2Ll1'+2ll1'+2Ll1} \right] \left[ \frac{T_E}{n^2 M_L M_H} \right] Y_P B_N^{\circ}$$

IX Generalizations made from radiance expressions

1.  $B_F \propto$  conc of analyte for any type of atomic fluorescence only as long as the concentration is low. (NB  $K_o$ ,  $K_o'$  and  $\bar{K}$  are directly proportional to concentration. See chapter two and references 7, 97, 117 )
2.  $B_F$  dependent only on cell volume (not cell shape) as long as concentration is low and as long as the entrance optics allow the entire cell cross section  $l l'$   $\text{cm}^3$  to be fully illuminated and the entire fluorescence of  $l l'$   $\text{cm}^2$  is measured - holds for any type of atomic fluorescence.
3.  $B_F \propto$  spectral radiance of continuum source  $B_o^\circ \lambda_o$  or integrated spectral radiance of line source  $B_N^\circ$  for all concentrations.
4.  $B_F \propto$  fluorescence power yield  $Y_p$  for either type of source and all concentrations.
5.  $B_F \propto$  solid angle of radiation collected from source  $\Omega_E$  for either type of source and for all concentrations.
6.  $B_F$  independent of concentration for high concentrations of absorbers for continuum source and transitions terminating in the ground or near ground state.  
 $B_F$  independent of concentration for high concentration of absorbers for line source when transitions terminate in excited state.
7.  $B_F$  independent of shapes of absorption and fluorescence bands as long as concentration is low and when a continuum source is used. - Also true for line source, especially if line source is very narrow compared to absorption band - if

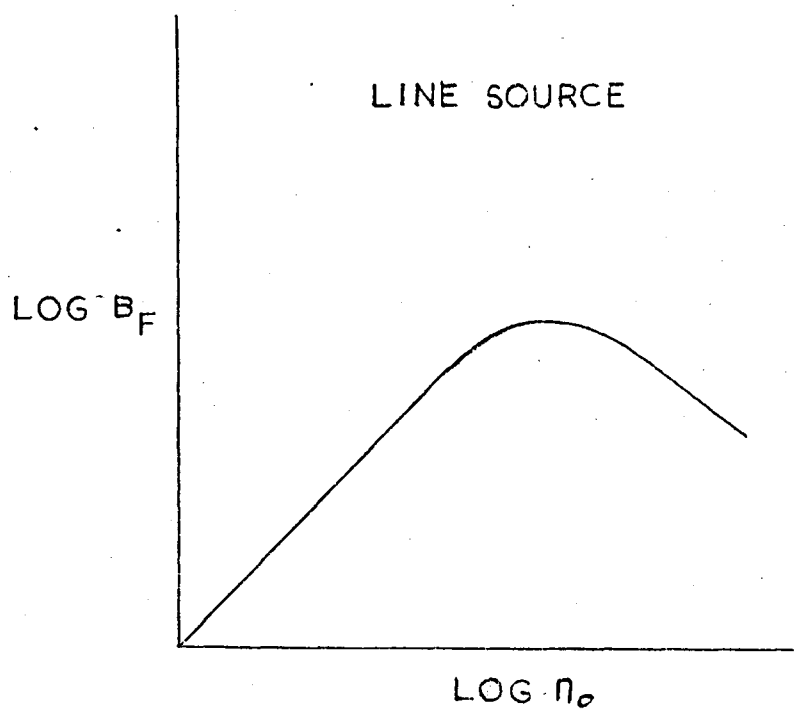
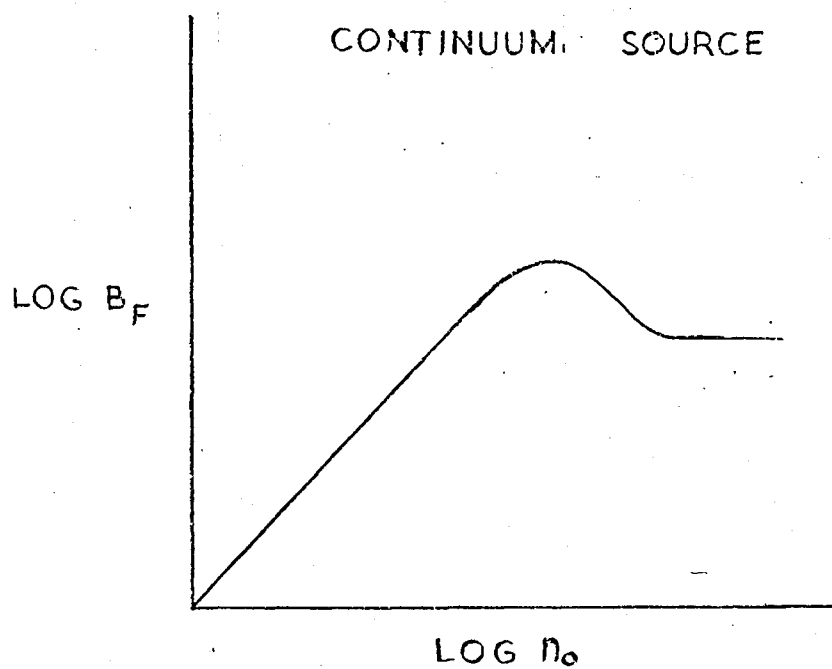


FIGURE A1.1. GROWTH CURVES (THEORETICAL)

line source width  $\approx$  width of absorption band then there is a complex dependence of  $B_F$  on the shapes of absorption and fluorescence bands.

8.  $B_F$  independent of shapes of absorption and fluorescence bands if absorber concentration is high and if line source is used and transitions terminate in an excited state.
9.  $B_F \propto \sqrt{\text{conc.}}$  for atomic fluorescence transitions terminating in an excited state if a continuum source is used and if absorber concentration is high.
10.  $B_F \propto 1/\sqrt{\text{conc}}$  for transitions terminating in the ground or near ground state, if line source is used and if absorber concentration is high.

The first set of conclusions that can be drawn from the above generalisations are that the fluorescence radiance,  $B_F$ , is proportionately related to the concentration,  $n_0$ , at all except high concentrations. At high  $n_0$ ,  $B_F \propto 1/\sqrt{n_0}$  when a line source is used and  $B_F$  is independent of  $n_0$  if a continuum source is used. These conclusions indicate the main features of the shape of growth curves ( $\lg B_F$  vs  $\lg n_0$  - Fig.A1.1) which in turn can be compared with curves obtained in the real analytical situation (analytical curves). Note that  $a$ , the damping constant determines the shape of growth curves. This constant is introduced in the theory (equation 13) to account for collisional broadening at high concentrations of absorbers.

This parameter does not depend on concentration or flame temperature but is related to atom type and flame composition<sup>7,359</sup>. The shape of analytical curves deviates from the shape of growth curves at low concentrations because of ionisation of analyte atoms and at high concentrations because of decreased sample introduction rates into the atomiser, reduced solute vaporisation rate and reduced aspirator yield. Note also that if the assumptions concerning complete illumination of the cell and measurement of all the emitted fluorescence are not made then the growth curves will be affected by pre-filter and postfilter effects<sup>5,7</sup>. (Incomplete illumination of flame cell causes reabsorption in the cell volume of fluorescence of atoms which are not being illuminated by excitation radiation - postfilter effect, and the fluorescence radiance is decreased if the fluorescence in the portion of the flame cell nearest the source is not measured - pre-filter effect). These effects only have a significant effect on growth curves at high concentrations of analyte atoms. For a comparison of theoretical and experimental analytical curves for magnesium see Zeegers and Winefordner<sup>124</sup> and for further treatments of the theory of analytical curves see Hooymeyers<sup>122</sup> and Alkamade<sup>361</sup> as well as references 5,7,123,359.

The second set of conclusions that can be drawn from the generalisations are that the fluorescence radiance  $B_F$  is directly proportional to the power yield  $Y_p$  (which affects the choice of flame) and the effective source radi-

ance (which has led to the many published studies of high irradiance sources). These considerations are discussed in detail in Chapter two of this thesis but recent developments in the theory and analytical use of lasers in atomic fluorescence spectroscopy have considerable interest.

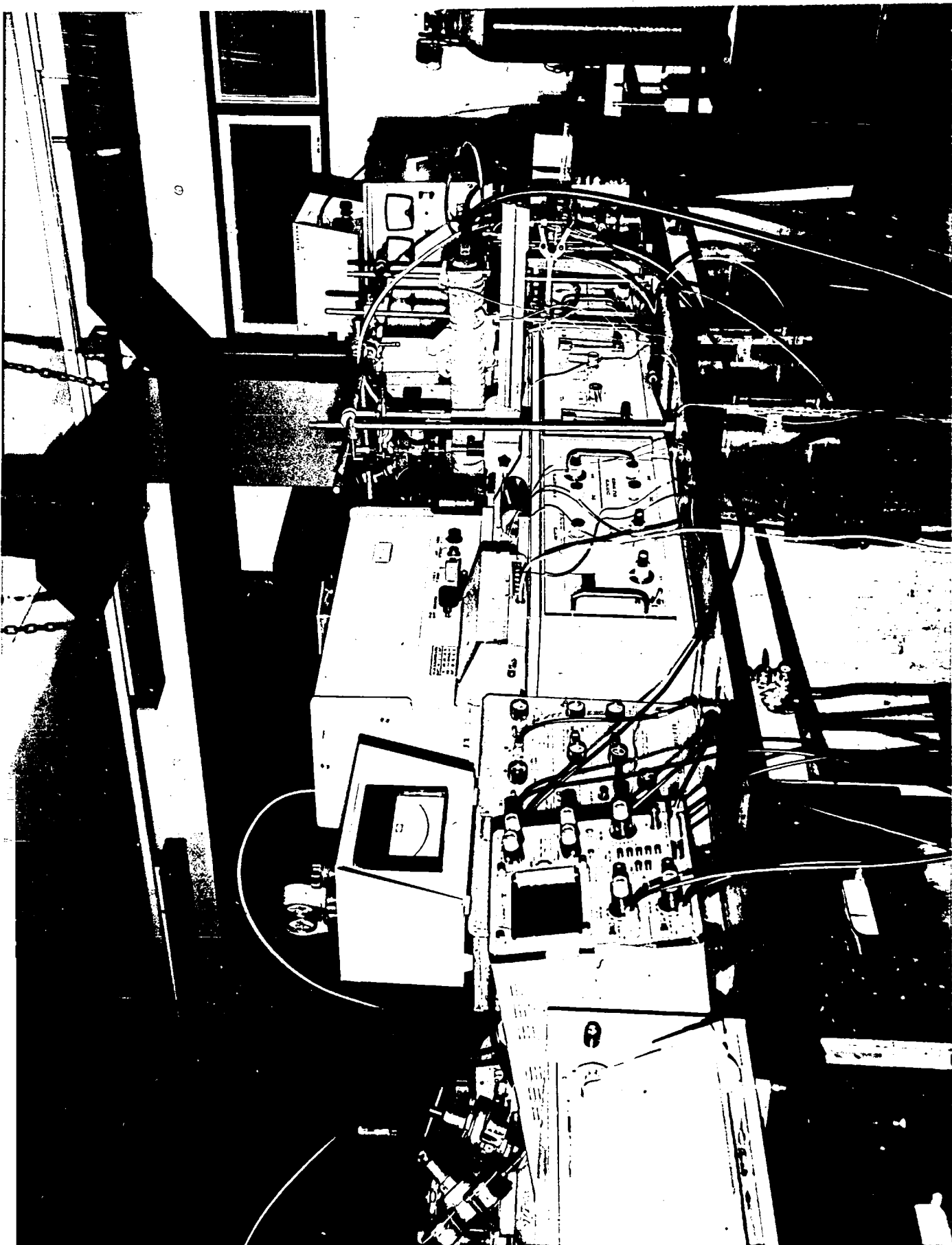
Winefordner and his coworkers have been developing the use of a pulsed, tunable dye laser as a source in atomic fluorescence flame spectrometry<sup>27,28,362-365</sup>. Piepmeir<sup>366</sup> has considered the theory of laser saturated atomic resonance fluorescence and Webb<sup>367</sup> has described tunable organic dye lasers.

Piepmeir<sup>366</sup> pointed out that it is theoretically possible to saturate the excited atom population in flames using sources of very high irradiance such as lasers. The saturated atomic population should then give a high fluorescence output which is almost independent of changes in the source irradiance. Winefordner and his coworkers<sup>364,365</sup> have presented theoretical and experimental results concerned with saturated atomic fluorescence using a tunable dye laser as the high irradiance source. Assuming a simple two level situation these workers show that as the source irradiance is increased and saturation approaches the fluorescence radiance no longer increases linearly. There is a limit to the fluorescence radiance that can be achieved. This is because although at low source irradiances the population of the lower level is not significantly changed upon excitation and therefore the effect of the source irradiance on the absorption behaviour of the atomic population can be

neglected, at high source irradiances there is a relationship between the spectral irradiance of the source and the integrated absorption coefficient. (Note that the laser is treated as a quasi-continuum source). As saturation approaches, the system becomes practically transparent to a further increase in source irradiance and the two levels become equally populated as the integrated absorption coefficient approaches zero. The linear relationship between atomic concentration and source irradiance is still retained as indicated by the theoretical equations developed by Winefordner and his coworkers<sup>364</sup>. These workers verified Piepmeir's predictions that under saturation conditions the fluorescence radiance is almost independent of source irradiance and quenching collisions. Analytically this is important because the stability of the source is no longer as critical as with low irradiance sources (e.g. electrodeless discharge tubes). Furthermore the dependence of the fluorescence radiance on the quantum efficiency which is observed at low source irradiance is removed under saturation conditions, i.e. the fluorescence radiance is not expected to be greater in the cool, low quenching flames than in the hot flames. Thus the more efficient atomisation properties of the hot flames can be utilized to better advantage. One disadvantage of the above observations is that the amount of scattered light continues to increase with increase in source irradiance while the fluorescence radiance is levelling out, thus degrading signal-to-noise ratios. Therefore a compromise has to be reached between

scattering and signal stability.

The effect of the above considerations on the shape of growth curves and analytical curves has also been considered by Winefordner et al<sup>365</sup>. Because under saturation conditions, the system is transparent, self-absorption cannot take place nor can the source irradiance be a function of the distance along the absorption path. Consequently growth curves will have unity slope even at high concentrations of absorbers. Any deviation from linearity will depend on the source irradiance. The above workers demonstrated experimentally that decrease in source irradiance does decrease the linear range of analytical curves. They stress however that bending of the curves could occur if any pre-filter and/or post-filter effects are present. Experimental conditions must be chosen to minimise these filter effects.



## EXPERIMENTAL

A.2.1. ApparatusSources

Electrodeless discharge lamps, tin, arsenic (EDT Supplies Ltd., London) and aluminium (EMI Ltd., Hayes, Middlesex) were operated in either a  $\frac{3}{4}$  wave Broida or a  $\frac{1}{4}$  wave Evenson, resonant cavity and powered by one of two microwave generators in conjunction with either, a 400 Hz modulator modified to give 200 Hz to 40 KHz modulation, or a 50/100 Hz modulator (all from Electromedical Supplies Ltd., Greenham). Reflected microwave power was monitored using either a separate meter (EDT Supplies Ltd.) or the meter built into one of the generators. (The 400 Hz modulator and the microwave generator with the 'built in' Reflected Power meter were on loan to the Polytechnic Department of Chemistry and Biology from BISRA, the Corporate Laboratories of the British Steel Corporation).

Lamp temperature was controlled by passing air from an air-compressor (Binks-Bullows PR303E, portable, Mk V) through a heated tube and upwards around the lamp in either of the cavities. (See Chapter two, section 2.3.2.B and Fig. 2.2.2.). External heating for the tube was provided by 20 ft of heating tape. The power to this tape (500 watts maximum) was provided by a 0-260 volt variac. Internal heating for the tube was provided by 5 yards of nichrome wire with a resistance of  $4.2\Omega$  per yard. The power to this heater (480 watts maximum) was provided by a 0-100 volt variac.

A photograph of the instrument is shown opposite. The thermostating system can be seen in the centre of the picture.

### Burners and nebulizer

The burners and nebulizer have been described in chapter two, section 2.3.3.A

Calibrated manometric flowmeters (Gallenkamp, London, type FL-420) with interchangeable jets were used to control flow rates. Each flowmeter jet was calibrated by the manufacturers.

Air when required as a support gas was supplied by a Binks-Bullows PR303E portable rotary air-compressor Mk V.

### Optical Components

The mirrors and lens have been adequately described in Chapter two, section 2.3.4. Fig. 2.27.

### Basic Spectrometer

A Jarrell-Ash Maximum Versatility atomic absorption/atomic emission spectrometer model 82-529.

### Monochromator

Jarrell-Ash  $\frac{1}{2}$ -m Ebert grating, 52x52 mm with 1180 lines per mm blazed at 300 nm. Fixed slits were provided. (Two 25  $\mu$ m, one 100  $\mu$ m and one 150  $\mu$ m). Throughout this study the 100  $\mu$ m slit was used at the monochromator entrance and 150  $\mu$ m at the exit.

### Detector

Hamamatsu T.V. R106 photomultiplier tube operated using the Jarrell-Ash stabilized power supply of the 82-529 spectrometer (variable from 270 to 1100 V).

### Amplifiers

Homebuilt pre-amplifier and lock-in amplifier as described in Chapter two, section 2.3.1.D (For atomic fluorescence work) or the Jarrell-Ash a.c. 50 Hz tuned amplifier. (For atomic emission work).

### Recorder

Honeywell Elektronik 194, chart recorder.

### Signal Generator

Sine-square oscillator Type LFM2 (Farnell Instruments Ltd.) This was used to test and calibrate the lock-in amplifier and later to drive the modulation system with variable frequency from 200 Hz to 40 KHz. The oscillator itself could supply frequencies variable, continuously, from 5 Hz to 1 MHz.

### Oscilloscope

Tequipment, D54, portable dual-trace.

This was used to monitor the signals at Test point 1 to 4 on the lock-in amplifier. These test points can be seen on the circuit diagrams of the lock-in amplifier, chapter two, Figs. 2.12 to 2.14.

### A.2.2. Reagents

The reagents used in this study were all of 'Analytical-Reagent' grade. Stock solutions were stored in stoppered glass bottles and deionised water was used for making up all the solutions. The details of the solutions used in the interference studies are given in Table A2.1. The tin, arsenic and aluminium stock solutions used for pure solution studies were 1000 ppm in the metal. Their details are given in Table A2.2 Concentrated hydrochloric, nitric, perchloric, phosphoric and sulphuric acids

TABLE A2.1

## STOCK METAL SOLUTIONS USED FOR STUDYING INTERFERENCE EFFECTS

Two sets of stock metal solutions were prepared. The first set was used for the tin study and were 0.4M in hydrochloric acid unless the particular salt was insoluble in acid. In such cases alternative dissolution conditions were used. The second set were made up in deionised water and were used for the aluminium and arsenic studies. The final metal concentration was 2500 ppm at all times.

Solution	Metal	Weight used g diluted to 250 mLs
Aluminium sulphate	Al	6.945
Aluminium chloride	Al	3.089
Arsenic trioxide	As <sup>a</sup>	0.825
Bismuth trichloride	Bi <sup>b</sup>	0.943
Barium nitrate	Ba	1.189
Calcium chloride	Ca	3.418
Cadmium chloride	Cd	1.270
Cerous nitrate	Ce	1.937
Cobaltous chloride	Co	2.523
Chromic nitrate	Cr	4.810
Copper nitrate	Cu	2.376
Ferric nitrate	Fe	4.521
Ferric chloride	Fe	3.05
Lanthanum chloride	La	1.67
Magnesium nitrate	Mg	3.813
Manganese sulphate	Mn	2.538
Ammonium molybdate	Mo <sup>c</sup>	1.150
Niobium pentoxide	Nb <sup>c</sup>	0.894
Nickel sulphate	Ni <sup>d</sup>	2.854
Lead nitrate	Pb <sup>d</sup>	0.999
Rubidium chloride	Rb <sup>e</sup>	0.884
Antimony metal	Sb <sup>f</sup>	0.625
Sodium silicate	Si	4.750
Tin metal	Sn <sup>g</sup>	0.625
Strontium nitrate	Sr	1.50
Potassium titanium oxalate	Ti <sup>d</sup>	4.620
Thallos carbonate	Tl <sup>d</sup>	1.434
Vanadyl sulphate	V	2.442
Sodium tungstate	W	0.999
Zinc sulphate	Zn	2.749
Zinc nitrate	Zn	2.844
Zirconyl chloride	Zr	1.597

- a Dissolved in 10 ml 5% w/v sodium hydroxide solution and neutralized with concentrated hydrochloric acid.
- b Dissolved in 10 ml concentrated hydrochloric acid and diluted to 250 ml with 0.4M hydrochloric acid
- c Dissolved in 10 ml 40% hydrofluoric acid and diluted to 250 ml with deionised water
- d Insoluble in 0.4M acid. Dissolved in deionised water

TABLE A2.1 (continued)

- e Dissolved in 10 ml concentrated hydrochloric acid and diluted to 250 ml in the same acid
- f Dissolved in 10 ml concentrated hydrochloric acid plus a few drops concentrated nitric acid plus 6 g tartaric acid
- g Dissolved in 5 ml concentrated hydrochloric acid plus 1 ml concentrated nitric acid.

TABLE A2.2

## TIN, ARSENIC AND ALUMINIUM 1000 ppm STOCK SOLUTIONS

Tin metal, 1.000 g dissolved in 50 ml concentrated hydrochloric acid and 3 ml concentrated nitric acid. Then diluted to one litre with deionised water.

Arsenic trioxide, 1.320g dissolved in 20 ml 5% w/v sodium hydroxide, neutralized with concentrated hydrochloric acid and diluted to one litre with deionised water.

Aluminium metal, 1.000 g dissolved in 10 ml hydrochloric acid with a few drops of concentrated nitric acid added and diluted to one litre with deionised water.

and the organic liquids acetone, ethanol, methyl ethyl ketone and acetic acid were all supplied by British Drug Houses Ltd.

#### A.2.3. Measurement procedure

The usual precautions were taken when measuring the fluorescence signals. i.e. All measurements were repeated three times with a spraying of a blank solution between each measurement. If 10,000 ppm iron solutions were being nebulized then it was necessary to spray deionised water between each sample, standard or blank in order to prevent solids accumulating in the orifices of the burner. This was particularly true of the circular slot burner used for the nitrous oxide-acetylene flame. Measurement order for steel analyses was, series of standards, series of sample steel solutions, standards, sample solutions and standards.

#### Detection limit measurement procedure

The theoretical considerations of detection limit have already been discussed in chapter two, section 2.2.3. To measure a detection limit by the criterion of a signal-to-noise ratio of two the noise and signal were measured separately in the following manner. The system was set for maximum sensitivity with the 18.2s time constant and the detection limit estimated using a standard solution with a concentration between 0.1 and 1 ppm. A convenient standard solution concentration was then chosen which was a factor of three or five times the detection limit. Six measurements of the fluorescence obtained with this solution were then recorded and the results averaged. The noise under these conditions was then estimated by setting the chart speed at the slowest possible, 5 min  $\text{cm}^{-1}$ , aspirating the chosen standard solution for fifteen minutes and measuring the resulting average peak-to-peak noise. All the signals

on the chart were measured to the nearest millimeter with a ruler and the signal-to-noise ratio and hence the detection limit calculated.

Detection limits were measured using optimised instrumental conditions, i.e. the optical system was checked for optimal alignment using a tungsten filament lamp (see chapter two, section 2.3.4.) The nebulizer was adjusted to give maximal signals and the burner-nebulizer system checked for cleanliness. The source was optimised to give maximal radiant output and stability by using the correct operating temperature and microwave power. The optimal flame conditions, analytical line etc. were used.

#### A.2.4. Some practical instrumental considerations

##### Use of the lock-in amplifier

a. Use of the output low pass filters (Chapter two, Figs. 2.15 and 2,16)

Output filter 1, Fig. 2.15 has a fixed time constant of 4.7s and is most convenient for routine analyses. Output filter 2, Fig. 2.16, has switchable time constants of 18.2s, 51.7s and 103.4s. The 18.2s time constant is the best compromise between time and signal-to-noise ratio. The necessity of increasing the time constant to reduce noise implies a necessity for an increase in gain. Thus in selecting output 2 rather than output 1 the noise at the readout in fact is the same but the gain is increased by nearly three times (Table 2.4, chapter two) and the time for the signal to reach its maximum value is also increased.

##### b. Continuous use of the oscilloscope

The double beam oscilloscope is useful from two points of view. Firstly the output from the tuned section of the

amplifier can be monitored at Test point 1, Fig. 2.12. At this point the modulated signal from the lamp can be observed and this can be very convenient when optimising radiant output. When measuring fluorescence signals the noise levels can be observed at Test point 1. This means that it is possible to tell if the amplifiers are saturated by too much noise (or signal) in which case the photomultiplier voltage needs to be reduced or the load resistor lowered in value, whichever gives the best compromise insofar as the requirements for sensitivity are concerned. It is also interesting that the reduction in noise upon flame separation can be observed at this point. Similarly the relative noise levels in different flames and the dependence of noise upon wavelength can also be monitored.

Secondly the oscilloscope can be used to monitor at Test point 4 (Fig. 2.14, chapter two) where the signal and reference come together at the output of the p.s.d. and before being rectified. This is a convenient point to observe the effects of the phase shift control and hence bring the signal accurately in phase with the reference. It is convenient to do this at Test point 4 rather than at the chart recorder because the former is not affected by the output time constant while the chart recorder output will be sluggish because of the time constant.

The reference signal can be monitored at Test point 2 (Fig. 2.13, chapter two) and the squared reference signal can be checked at Test point 3 (Fig. 2.13). These two points really only need to be checked occasionally if the amplifier is being used at a set frequency. If the frequency of modulation is being varied it is essential that a good square wave is obtained at Test point 3 in order to ensure that the p.s.d. is operating

correctly.

### Choice of photomultiplier tube

The R106 photomultiplier gave a better signal-to-noise ratio over the 200 to 500 nm range than the R213 which was available. This was especially true below 250 nm. The R213 was therefore never used. The R166 solar blind photomultiplier has its peak response in the 200 to 300 nm range and very little response above 300 nm. It is unfortunately less sensitive than the R106 over 200-300 nm. However because the noise levels are lower than the R106 the operating voltage can be increased to give higher sensitivity. However this gives no advantage because the R166 signal to noise ratio cannot as a result be improved to better than the R106. However at 189.0 nm, the arsenic wavelength, the two tubes gave equivalent results but the R166 was being operated at an unacceptably high voltage (1100 volts). The solar blind photomultiplier has been used most often in the non-dispersive applications which have been reported in the literature. This is because a non-dispersive system views a large part of the light spectrum and its lack of response above 300 nm can then give improvements in signal-to-noise ratio below 300 nm.

### Optics

Once the optics have been set up using the tungsten filament lamp it is not usually necessary to make further adjustments to burner position, burner height, position of mirrors etc. Only small changes in sensitivity, relative to the system without mirrors, will result after such adjustments because the mirrors reflect a large solid angle of radiation from

the flame to the entrance slit thus making selection of particular areas of the flame unlikely. It is an interesting point that this same property of the optical system also probably averages interference effects.

A.2.5. Significance of the magnitude of quoted results for interference effects

There are a number of criteria in the literature which are used to decide whether or not an interference is significant. One common criterion is that an interference is significant if it changes the analyte signal by more than twice the standard deviation of the measurement. In this study this criterion was used to evaluate whether any observed interference was likely to affect the steel analysis. However the tables of interferences in chapters three to five quote results which may be apparently insignificant. For example an enhancement interference of +5% may not be significant if the standard deviation is 3% but if such a change was apparently reproducibly observed it was recorded. Such interferences at the 1000 ppm level of concomitant may become significant at the 10,000 ppm level and may prove a useful guide in any future reference to the interferences observed in this work.

## Appendix 3

### DATA FOR ELECTRONIC COMPONENTS

The data in this section is included as a guide to future users of the lock-in amplifier both to help identify components if any failure occurs and to provide more complete information about the circuits of the amplifier.



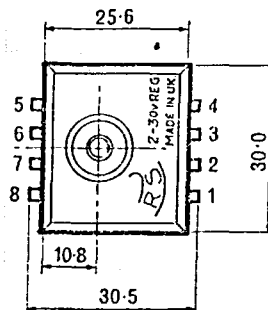
# 2-30V REG

## 2-30V 0.7A REGULATED D.C. POWER SUPPLY

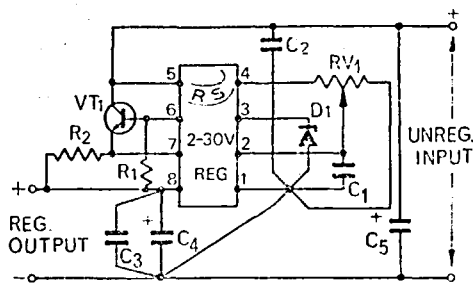
General purpose encapsulated series regulator incorporating over current protection. Provides regulated d.c. output from an unregulated d.c. source. Voltage and current capabilities of basic unit can be extended by the addition of external components.

### SPECIFICATION

Voltage Range	Output Current Max.	Output Impedance	Ripple Voltage P-P
2-30V	1A	0.15Ω	25mV
2-20V	1.5A	0.15Ω	25mV
2-13V	2A	0.15Ω	25mV
2-6.5V	2.5A	0.15Ω	25mV
2-30V	50mA	0.5Ω	10mV
2-20V	75mA	0.5Ω	10mV
2-13V	100mA	0.5Ω	10mV
2-6.5V	140mA	0.5Ω	10mV



## BASIC REGULATED D.C. SUPPLY > 1A WITH EXTERNAL TRANSISTOR

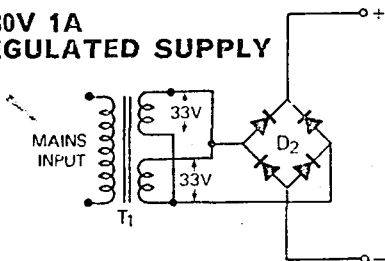


### COMPONENTS

- R<sub>1</sub> 470Ω ½ W Resistor
- R<sub>2</sub> 47Ω 1W W/W Resistor
- C<sub>1</sub>, C<sub>2</sub>, C<sub>3</sub> 1μF 250V Polyester
- C<sub>4</sub> 100μF 50V Tube
- C<sub>5</sub> 3300μF 63V H-R Electro
- D<sub>1</sub> BZY88 8.2V
- 2-30V Regulator
- RV<sub>1</sub> 5kΩ Midget Lin:
- VT<sub>1</sub> 2N3055

Heat Sink for VT<sub>1</sub>  
 (Mount with smear of silicone grease)  
 Keep wires as short as possible and wire as shown to minimise hum.  
 Heat Sink for 2-30V Regulator:—  
 Size 50 mm × 50 mm × 18 s.w.g.  
 Bright Aluminium.

## 2-30V 1A REGULATED SUPPLY



### SPECIFICATION

- Output Current, 1A max.
- Short Circuit Current, 1.5A
- Output Impedance, 0.15Ω
- Output Ripple Voltage (P-P), 25mV.
- Mains Input Variation, ±5% from nom.

### COMPONENTS

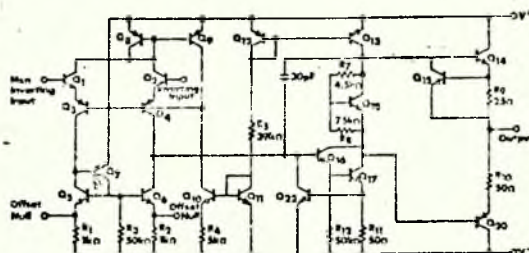
- T<sub>1</sub> Universal Rec. Trans. D<sub>2</sub> Rec 41A
- Plus Components for Basic Regulator with external transistor.

# SN72741 HIGH PERFORMANCE OPERATIONAL AMPLIFIER

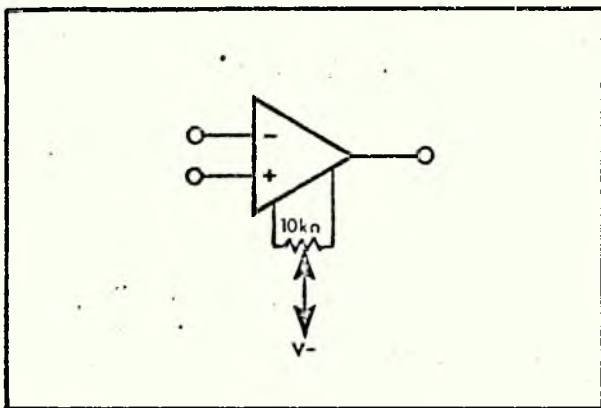
## DESCRIPTION

The SN72741 is a high performance operational amplifier characterised over the 0-70°C temperature range.

The high common mode input voltage range and the absence of latch up make the SN72741 ideal for voltage follower applications. The device is short circuit protected and the internal frequency compensation ensures stability without external components.

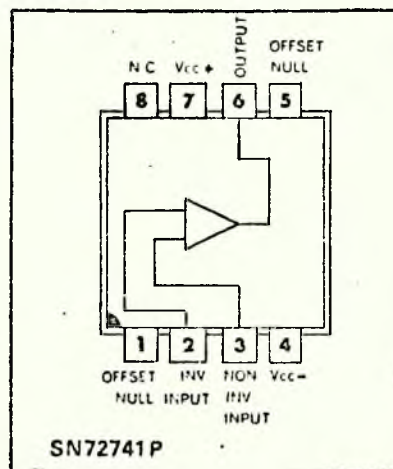


## Voltage Offset Null Circuit



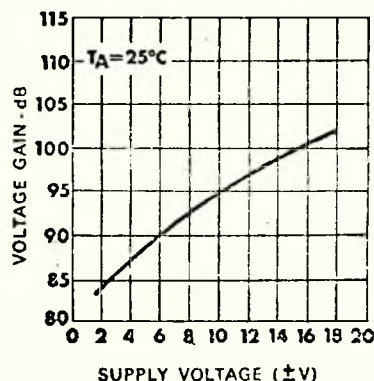
## TERMINAL ASSIGNMENTS

P. Pack

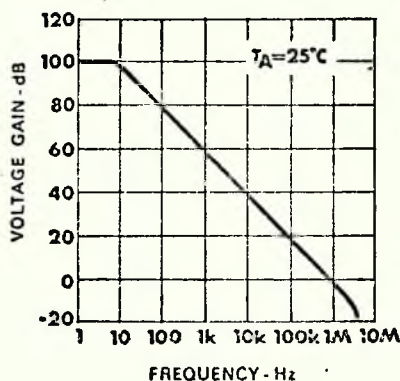


## TYPICAL PERFORMANCE CURVES

Open Loop Voltage Gain



Open Loop Frequency Response



## HIGH PERFORMANCE OPERATIONAL AMPLIFIER (Cont.)

PARAMETER	CONDITIONS	VALUE	UNITS
	$(T_A = +25^\circ\text{C}, V_S = \pm 15\text{ V})$		
Input Offset Voltage	$R_S \leq 10\text{ k}\Omega$	1.0	mV
Input Offset Current		30	nA
Input Bias Current		200	nA
Input Resistance		1000	k $\Omega$
Large Signal Voltage Gain	$R_L \geq 2\text{ k}\Omega, V_{\text{OUT}} = \pm 10\text{ V}$	200,000	
Output Voltage Swing	$R_L \geq 10\text{ k}\Omega$	$\pm 14$	V
	$R_L \geq 2\text{ k}\Omega$	$\pm 13$	V
Input Voltage Range		$\pm 13$	V
Common Mode Rejection Ratio	$R_S \leq 10\text{ k}\Omega$	90	dB
Supply Voltage Rejection Ratio	$R_S \leq 10\text{ k}\Omega$	30	$\mu\text{V/V}$
Power Consumption		50	mW
Transient Response (unity gain)	$V_{\text{IN}} = 20\text{ mV}, R_L = 2\text{ k}\Omega$		
	$C_L \leq 100\text{ pF}$		
Risetime		0.3	$\mu\text{Sec}$
Overshoot		5.0	%
Slew Rate (unity gain)	$R_L \geq 2\text{ k}\Omega$	0.5	V/ $\mu\text{Sec}$

**Inverting Amplifier**

The inverting amplifier, as shown in Fig 2.8a is one of the most suitable connections where high accuracy and low distortion are required. This is because the amplifier does not see any large signal swings at its input. It is also the most suitable configuration for summing applications as the summing junction is a virtual earth, giving good isolation between the inputs. However, the input resistance is low compared to the non-inverting configuration, being approximately equal to  $R_{\text{in}}$ .

A summary of the performance is given below.

Gain	$R_{\text{IN}}$	$R_f$	Typical Bandwidth	Input Resistance
1	10 k $\Omega$	10 k $\Omega$	1 MHz	10 k $\Omega$
10	1 k $\Omega$	10 k $\Omega$	100 kHz	1 k $\Omega$
100	1 k $\Omega$	100 k $\Omega$	10 kHz	1 k $\Omega$
1000	100 $\Omega$	100 k $\Omega$	1 kHz	100 $\Omega$

**Non-Inverting Amplifier**

The non-inverting configuration, as shown in Fig 2.8b is particularly useful in applications where high input impedances are required. For closed loop gains of less than about 50 dB, the input impedance is dominated by the common mode input impedance, which is typically 200 M $\Omega$ . Common mode input impedance is defined as the parallel sum of the impedances from each input to earth. In the voltage follower mode, only one of these impedances is seen, hence the 400 M $\Omega$  in the table below. A summary of the performance is given below:

Gain	$R_{\text{IN}}$	$R_f$	Typical Bandwidth	Input Impedance
1	$\infty$	0	1 MHz	400 M $\Omega$
10	1 k $\Omega$	9 k $\Omega$	100 kHz	400 M $\Omega$
100	100 $\Omega$	9.9 k $\Omega$	10 kHz	280 M $\Omega$
1000	100 $\Omega$	100 k $\Omega$	1 kHz	80 M $\Omega$

SN72702 /  $\mu$ A702

# Wide band operational amplifier

## GENERAL DESCRIPTION

The  $\mu$ A702 is a complete DC amplifier constructed on a single silicon chip. It may be used in high speed analogue computers, as a precision instrumentation amplifier, or in other applications requiring a feedback amplifier useful from DC to 20 MHz.

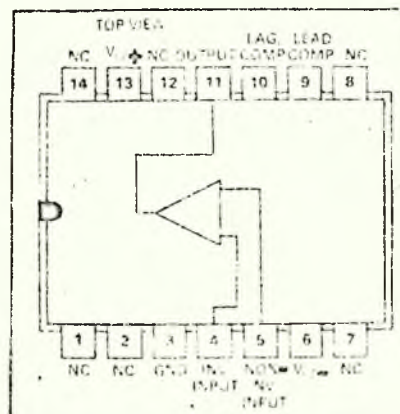
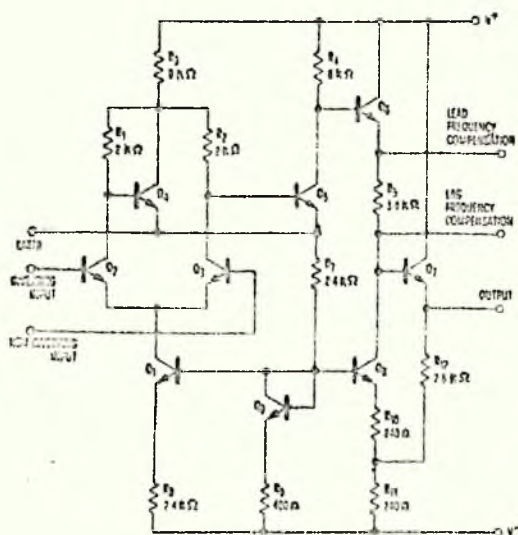
## FEATURES:

- WIDE BANDWIDTH
- HIGH GAIN
- HIGH COMMON MODE REJECTION RATIO
- HIGH SUPPLY REJECTION RATIO
- LOW INPUT OFFSET VOLTAGE

## ABSOLUTE MAXIMUM RATINGS

Total supply voltage between $V^+$ and $V^-$ terminals	21 V
Peak load current	50 mA
Power dissipation (Note 1)	300 mW
Storage temperature range	$-65^\circ\text{C}$ to $150^\circ\text{C}$
Operating temperature range	$0^\circ\text{C}$ to $70^\circ\text{C}$
Differential input voltage	$\pm 15$ V
Input voltage, either input	1.5 V to $-6$ V
Lead temperature (soldering, 60 sec. time limit)	$300^\circ\text{C}$

## CIRCUIT DIAGRAM



Typical Performance of the  $\mu$ A702A Integrated  
Operational Amplifier (cont.)

All data for 25°C ambient temperature unless otherwise indicated

	$V^+ = 12\text{ V}$ $V^- = -6\text{ V}$	$V^+ = 6\text{ V}$ $V^- = -3\text{ V}$
Input Offset Voltage	0.5 mV	0.7 mV
Input Offset Current	0.18 $\mu\text{A}$	0.12 $\mu\text{A}$
Input Bias Current	2 $\mu\text{A}$	1.2 $\mu\text{A}$
Input Resistance	40 k $\Omega$	67 k $\Omega$
Temperature Coefficient of Input Offset Voltage		
— 55°C $\leq T_A \leq$ 125°C $R_s = 50\ \Omega$	2.5 $\mu\text{V}/^\circ\text{C}$	3.5 $\mu\text{V}/^\circ\text{C}$
Common-mode Rejection Ratio	95 dB	95 dB
Large-Signal Voltage Gain	3600	900
Output Resistance	200 $\Omega$	300 $\Omega$
Output Voltage Swing	$\pm 5.3\text{ V}$	$\pm 2.7\text{ V}$
Power Consumption	80 mW	17 mW
Supply Voltage Rejection Ratio	75 $\mu\text{V}/\text{V}$	75 $\mu\text{V}/\text{V}$

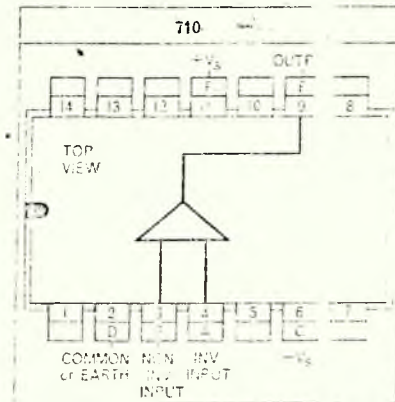
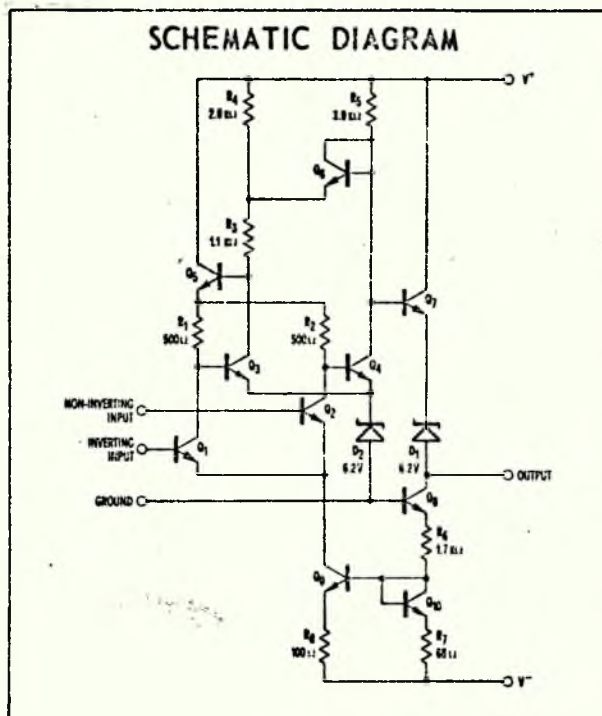
$\mu$ A710

## HIGH SPEED DIFFERENTIAL COMPARATOR

**GENERAL DESCRIPTION** - The  $\mu$ A710 is a differential voltage comparator intended for applications requiring high accuracy and fast response times. It is constructed on a single silicon chip using the Fairchild Planar epitaxial process. The device is useful as a variable threshold Schmitt trigger, a pulse height discriminator, a voltage comparator in high-speed A-D converters, a memory sense amplifier or a high-noise immunity line receiver. The output of the comparator is compatible with all integrated logic forms.

**ABSOLUTE MAXIMUM RATINGS**

Positive Supply Voltage	+ 14 V
Negative Supply Voltage	- 7 V
Peak Output Current	10 mA
Differential Input Voltage	$\pm$ 5 V
Input Voltage	$\pm$ 7 V



Typical Conditions;  $T_A = 25^\circ\text{C}$ ,  $V^+ = 12\text{ V}$ ,  $V^- = -6\text{ V}$

Input Offset Voltage	0.6 mV
Input Offset Current	0.75 $\mu\text{A}$
Input Bias Current	13 $\mu\text{A}$
Temperature Coefficient of Input Offset Voltage	3.5 $\mu\text{V}/^\circ\text{C}$
Input Voltage Range	$\pm$ 5 V
Differential Input Voltage Range	$\pm$ 5 V
Response Time for 5 mV Overdrive	40 ns
Voltage Gain	1700
Output Resistance	200 $\Omega$
Positive Output Level	+ 3.2 V
Negative Output Level	- 0.5 V
Power Consumption	90 mW

# RCA MOS FIELD-EFFECT TRANSISTOR

## For Critical Chopper Applications & Multiplex Service

RCA-3N138‡ is a silicon, insulated-gate field-effect transistor of the N-channel depletion type, utilizing the MOS\* construction. It is intended primarily for critical chopper and multiplex applications up to 60MHz.

This transistor features a New Terminal Arrangement in which the gate and source connections are interchanged to provide maximum isolation between the output (drain) and the input (gate) terminals. Although this new basing configuration does not appreciably change the measured device feedback capacitance, it permits the use of external inter-terminal shields to reduce the feedback due to external capacitances, particularly on printed circuit boards. This feature makes it possible to minimize feedthrough capacitance.

The insulated gate provides a very high value of input resistance ( $10^{14}$  ohms typ.) which is relatively insensitive to temperature and is independent of gate-bias conditions (positive, negative, or zero bias). The 3N138 also features extremely low feedthrough capacitance (0.18pF typ.) and zero inherent offset voltage.

The 3N138 is hermetically sealed in the JEDEC TO-72 package and features a gate metallization that covers the entire source-to-drain channel.

‡ Formerly Dev. No. TA7032.

\* Metal-Oxide-Semiconductor.

### Maximum Ratings, Absolute-Maximum Values:

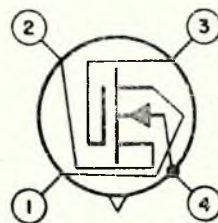
(Substrate connected to source unless otherwise specified)

DRAIN-TO-SOURCE		
VOLTAGE, $V_{DS}$	+35 max.	V
DRAIN-TO-SUBSTRATE		
VOLTAGE, $V_{DB}$	+35, -0.3 max.	V
SOURCE-TO-SUBSTRATE		
VOLTAGE, $V_{SB}$	+35, -0.3 max.	V
DC GATE-TO-SOURCE		
VOLTAGE, $V_{GS}$	±10 max.	V
PEAK GATE-TO-SOURCE		
VOLTAGE, $V_{GS}$	±14 max.	V
PEAK VOLTAGE, GATE-TO-ALL OTHER TERMINALS: $V_{GS}$ , $V_{GD}$ , $V_{GB}$ , non-repetitive		
	±45 max.	V
DRAIN CURRENT, $I_D$ (Pulse duration 20 ms, duty factor ≤ 0.10)		
	50 max.	mA
TRANSISTOR DISSIPATION, $P_T$ :		
At ambient temperatures from -65 to +125°C		
	150 max.	mW
AMBIENT TEMPERATURE RANGE:		
Storage	-65 to +150	°C
Operating	-65 to +125	°C
LEAD TEMPERATURE (During Soldering):		
At distances ≥ 1/32" to seating sur- face for 10 seconds max.		
	265 max.	°C

The flexible leads of the 3N138 are usually soldered to the circuit elements. As in the case of any high-frequency semiconductor device, the tips of soldering irons should be grounded, and appropriate precautions should be taken to protect the device against high electric fields.

This device should not be connected into or disconnected from circuits with the power on because high transient voltages may cause permanent damage to the device.

## 3N138



- 1 - Drain
- 2 - Source
- 3 - Insulated Gate
- 4 - Bulk (Substrate) and Case

## SGS-FAIRCHILD LINEAR INTEGRATED CIRCUIT $\mu$ A727B

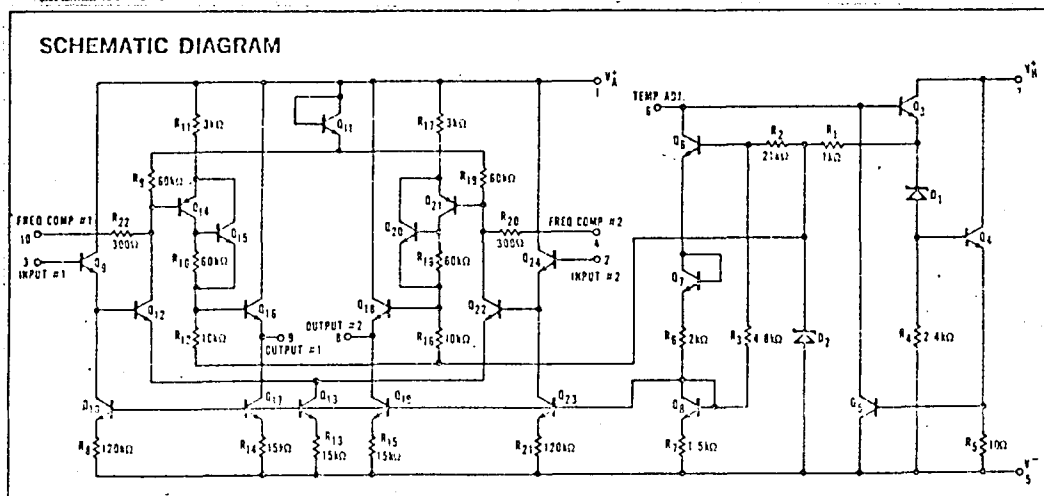
### FEATURES

- VERY LOW OFFSET DRIFTS
- HIGH INPUT IMPEDANCE
- WIDE COMMON MODE RANGE

**GENERAL DESCRIPTION** — The  $\mu$ A727B is a monolithic, fixed gain, differential-input differential-output amplifier, constructed with the Fairchild Planar<sup>®</sup> epitaxial process, mounted in a high thermal-resistance package, and held at constant temperature by active regulator circuitry. The high gain and low standby dissipation of the regulator circuit give tight temperature control over a wide ambient temperature range. The device is intended for use as a self-contained input stage in very low-drift DC amplifiers, replacing complex chopper-stabilized amplifiers in such applications as thermo-couple bridges, strain gage transducers, and A to D converters. For full temperature range operation ( $-55^{\circ}\text{C}$  to  $+125^{\circ}\text{C}$ ) see  $\mu$ A727 data sheet.

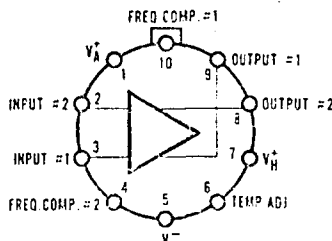
### ABSOLUTE MAXIMUM RATINGS

Operating Temperature Range	-20°C to +85°C
Storage Temperature Range	-65°C to +150°C
Lead Temperature (Soldering, 60 second time limit)	300°C
Supply Voltage (Amplifier and Heater)	± 18 V
Differential Input Voltage	± 10 V
Common Mode Input Voltage	± 15 V



### CONNECTION DIAGRAM

(top view)

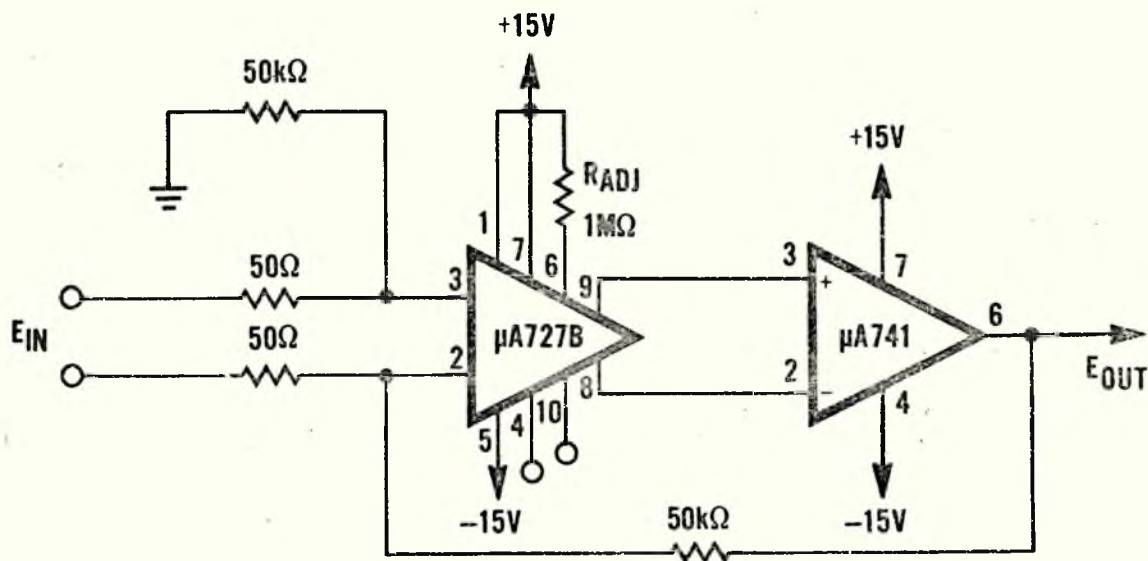


## FAIRCHILD LINEAR INTEGRATED CIRCUITS $\mu$ A727B (CONT.)

**ELECTRICAL CHARACTERISTICS** ( $-20^{\circ}\text{C} \leq T_A \leq +85^{\circ}\text{C}$ ,  $V_{H+} = V_A' = +15\text{V}$ ,  $V = -15\text{V}$ ,  $R_{ADJ} = 1\text{M}\Omega$ , unless otherwise specified)

PARAMETER	CONDITIONS	TYP.	MAX.	UNITS
Input Offset Voltage	$R_S \leq 50\ \Omega$	2.0		mV
Input Offset Current		2.5		nA
Input Bias Current		12		nA
Input Offset Voltage Drift	$R_S \leq 50\ \Omega$	0.6		$\mu\text{V}/^{\circ}\text{C}$
Input Offset Current Drift		2.0		$\text{pA}/^{\circ}\text{C}$
Input Bias Current Drift		15		$\text{pA}/^{\circ}\text{C}$
Differential Input Resistance		300		$\text{M}\Omega$
Common Mode Input Resistance		1000		$\text{M}\Omega$
Input Voltage Range		$\pm 13$		V
Supply Voltage Rejection Ratio	$R_S \leq 100\ \text{k}\Omega$	80		$\mu\text{V}/\text{V}$
Common Mode Rejection Ratio	$R_S \leq 100\ \text{k}\Omega$	100		dB
Output Resistance		1.0		$\text{k}\Omega$
Output Common Mode Voltage		-5.0		V
Differential Output Voltage Swing		$\pm 7.0$		V
Output Sink Current		30		$\mu\text{A}$
Differential Load Rejection		5.0		$\mu\text{V}/\mu\text{A}$
Differential Voltage Gain		100		
Low Frequency Noise	$\text{BW} = 10\ \text{Hz to } 500\ \text{Hz}$ , $R_S \leq 50\ \Omega$	3.0		$\mu\text{V}_{\text{rms}}$
Long Term Drift	$R_S \leq 50\ \Omega$	5.0		$\mu\text{V}/\text{week}$
Amplifier Supply Current	$T_A = +25^{\circ}\text{C}$	1.0		mA
Heater Supply Current	$T_A = +25^{\circ}\text{C}$	10		mA

**TYPICAL X1000 CIRCUIT**



## REFERENCES

1. J.D.Winefordner and T.J.Vickers, *Anal. Chem.*, 36 (1964) 161.
2. J.D.Winefordner and R.A.Staab, *Anal. Chem.*, 36 (1964) 165.
3. J.D.Winefordner and R.A.Staab, *Anal. Chem.*, 36 (1964) 1367.
4. A. Walsh, *Spectrochim. Acta.*, 7 (1955) 108.
5. J.D.Winefordner and R.C.Elser, *Anal. Chem.*, 43 (1971) No.4, 24A.
6. G.F.Kirkbright and T.S.West, *Chem. Br.*, 8 (1972) 428.
7. J.D.Winefordner, S.G.Schulman and T.C.O'Haver, *Luminescence Spectrometry in Analytical Chemistry*, Vol.38 in *Chemical Analysis*, Wiley - Interscience, New York, 1972.
8. P.H.Scholes, *Analyst*, 93 (1968) 197.
9. R.F.Browner, R.M.Dagnall and T.S.West, *Anal. Chim. Acta.*, 46 (1969) 207.
10. R.M.Dagnall, G.F.Kirkbright, T.S.West and R.Wood, *Anal. Chem.*, 42 (1970) 1029.
11. R.M.Dagnall, K.C.Thompson and T.S.West, *Talanta*, 15 (1968) 677.
12. L.Ebdon, G.F.Kirkbright and T.S.West, *Talanta*, 17 (1970) 965.
13. R.S.Hobbs, G.F.Kirkbright and T.S.West, *Talanta*, 18 (1971) 859.
14. V.Sychra and J.Matoušek, *Talanta*, 17 (1970) 363.
15. D.N.Hingle, G.F.Kirkbright and T.S.West, *Analyst*, 93 (1968) 522.
16. R.M.Dagnall, G.F.Kirkbright, T.S.West and R.Wood, *Anal. Chim. Acta.*, 47 (1969) 407.
17. J. Matoušek and V.Sychra, *Anal. Chim. Acta*, 49 (1970) 175.
18. R.F.Browner and D.C.Manning, *Anal. Chem.*, 44 (1972) 843.
19. N.V.Mossholder, V.A.Fassel and R.N.Kniseley, *Anal. Chem.*, 45 (1973) 1614.
20. J.D.Winefordner, V.Svoboda and L.Cline, *C.R.C. Crit. Rev. Anal. Chem.*, 1 (1970) 233.
21. M.P.Bratzel, Jr., R.M.Dagnall and J.D.Winefordner, *Anal. Chim. Acta*, 52 (1970) 157.

22. M.S.Cresser and T.S.West, *Spectrochim. Acta*, 25B (1970) 61.
23. W.K.Fowler, D.O.Knapp and J.D.Winefordner, *Anal. Chem.*, 46 (1974) 601.
24. R.C.Elser and J.D.Winefordner, *Anal. Chem.*, 44 (1972) 698.
25. G.J.Nitis, V.Svoboda and J.D.Winefordner, *Spectrochim. Acta*, 27B (1972) 345.
26. C.Veillon and P.Merchant, Jr., *Appl. Spectrosc.*, 27 (1973) 361.
27. L.M.Fraser and J.D.Winefordner, *Anal. Chem.*, 43 (1971) 1693.
28. L.M.Fraser and J.D.Winefordner, *Anal. Chem.*, 44 (1972) 1444.
29. S. Neumann and M.Kriese, *Spectrochimica Acta*, 29B (1974) 127.
30. E.P.Krivchikova and N.M.Vasil'eva, *Zh.Analit.Khim.*, 28 (1973) 928 (in Russian) Referat. Anal. Abstr. May 1974 No. 2043.
31. J.B.Dawson and D.J.Ellis, *Spectrochim. Acta*, 23A (1967) 565.
32. J.O.Weide and M.L.Parsons, *Analyt. Lett.*, 5 (1972) 363.
33. M.Prugger, R.Grosskopf and R.Torge, *Spectrochim. Acta*, 26B (1971) 191.
34. D.G.Mitchell and A.Johansson, *Spectrochim. Acta.*, 25B (1970) 175.
35. D.G.Mitchell and A. Johansson, *Spectrochim. Acta.*, 26B (1971) 677.
36. W.B.Barnett and H.L.Kahn, *Anal. Chem.*, 44 (1972) 935.
37. J.O.Weide and M.L.Parsons, *Anal. Chem.*, 45 (1973) 2417.
38. G.M.Hieftje, B.E.Holder, A.S.Maddux, Jr., and R.Lim, *Anal. Chem.*, 45 (1973) 238.
39. E. Cordos and H.V.Malmstadt, *Anal. Chem.*, 44(1972) 2277.
40. E.Cordos and H.V.Malmstadt, *Anal. Chem.*, 44 (1972) 2407.
41. E.Cordos and H.V.Malmstadt, *Anal. Chem.*, 45 (1973) 27.
42. J.V.Sullivan and A.Walsh, *Spectrochim. Acta.*, 21(1965)721.
43. Z.van Gelder, *Appl. Spectry* 22 (1968) 581.
44. R.M.Lowe, *Spectrochim. Acta*, 26B (1971) 201.
45. H.G.C.Human, *Spectrochim. Acta.*, 27B (1972) 301.

46. H.G.C.Human, P.J.Th. Zeegers and J.A.Van Elst, Spectro. Chim. Acta., 29B (1974) 111.
47. G.Rossi and N.Omenetto, Appl. Spec., 21 (1967) 329.
48. A.A.Woodriff, G.V.Wheeler and W.A.Ryden, Appl. Spec., 22 (1968) 348.
49. J.I.Dinnin and A.W.Helz, Anal. Chem., 39 (1967) 1489.
50. G.Rossi and N.Omenetto, Talanta, 16 (1969) 263.
51. T.S.West and X.K.Williams, Anal. Chim. Acta, 42 (1968) 29.
52. W.E.Rippetoe, V.I.Muscat, and T.J.Vickers, Anal. Chem., 46 (1974) 796.
53. D.Kolihova and V.Sychra, Anal. Chim. Acta, 63 (1973) 479.
54. R.M.Dagnall, G.F.Kirkbright, T.S.West and R.Wood, Analyst, 97 (1972) 245.
55. T.S.West and X.K.Williams, Anal. Chem., 40 (1968) 335.
56. J.Matoušek and V.Sychra, Anal. Chem., 41 (1969) 518.
57. J.W.Robinson and C.J.Hsu, Anal. Chim. Acta, 43 (1968) 109.
58. R.Smith, R.C.Elser and J.D.Winefordner, Anal. Chim. Acta, 48 (1969) 35.
59. D.R.Jenkins, Spectrochimica Acta, 23B (1967) 167.
60. T.J.Vickers, P.J.Slevin, V.I.Muscat and L.T.Farias, Anal. Chem., 44 (1972) 930.
61. P.L.Larkins, Spectrochim. Acta, 26B (1971) 477
62. P.L.Larkins and J.B.Willis, Spectrochim Acta, 26B (1971) 491.
63. P.D.Warr, Talanta, 18 (1971) 234.
64. P.D.Warr, Talanta, 17 (1970) 543.
65. P.L.Larkins, R.M.Lowe, J.V.Sullivan and A.Walsh, Spectrochim. Acta, 24B (1969) 187.
66. T.J.Vickers and R.M.Vaught, Anal. Chem., 41 (1969) 1476.

67. A.Walsh, Paper presented at the International Atomic Absorption Spectroscopy Conference, Sheffield, England, 1969.
68. M.Jones, G.F.Kirkbright, L.Ranson and T.S.West, Anal. Chim. Acta, 63 (1973) 210.
69. E.F.Palermo and S.R.Crouch, Anal. Chem., 45 (1973) 1594.
70. T.S.West and X.K.Williams, Anal. Chim. Acta, 45 (1969) 27.
71. R.G.Anderson, I.S.<sup>M</sup>aines and T.S.West, Anal. Chim. Acta, 51 (1970) 355.
72. J.F.Alder and T.S.West, Anal. Chim. Acta, 51 (1970) 365.
73. J.Aggett and T.S.West, Anal. Chim. Acta, 55 (1971) 349.
74. J.Aggett and T.S.West, Anal. Chim. Acta, 57 (1971) 15.
75. D.Alger, R.G.Anderson, I.S.Maines and T.S.West, Anal. Chim. Acta, 57 (1971) 271.
76. R.G.Anderson, H.N.Johnson and T.S.West, Anal. Chim. Acta, 57 (1971) 281.
77. L.Ebdon, G.F.Kirkbright and T.S.West, Anal. Chim. Acta, 58 (1972) 39.
78. J.F.Alder and T.S.West, Anal. Chim. Acta, 58 (1972) 331.
79. K.W.Jackson and T.S.West, Anal. Chim. Acta, 59 (1972) 187.
80. L.Ebdon, G.F.Kirkbright and T.S.West, Anal. Chim. Acta, 61 (1972) 15.
81. J.F.Alder and T.S.West, Anal. Chim. Acta, 61 (1972) 132.
82. G.L.Everett, T.S.West and R.W.Williams, Anal. Chim. Acta, 66 (1973) 301.
83. G.L.Everett, T.S.West and R.W.Williams, Anal. Chim. Acta, 70 (1974) 291.
84. T.W.Steele and B.D.Guerin, Analyst, Lond., 97 (1972) 77.
85. S.Dipierro and G.Tessari, Talanta, 18 (1971) 707.
86. M.P.Bratzel, Jr., and C.L.Chakrabarti, Anal. Chim. Acta, 61, (1972) 25.

87. R.B.Baird, Soloukid Pourian and S.M.Gabrielian, *Anal. Chem.*, 44 (1972) 1887.
88. R.D.Reeves, C.J.Molnar, M.T.Glenn, J.R.Ahlstrom and J.D.Winefordner, *Anal. Chem.*, 44 (1972) 2205.
89. L.Ebdon, G.F.Kirkbright and T.S.West, *Talanta*, 19 (1972) 1301.
90. K.G.Brodie and J.P.Matoušek, *Anal. Chem.*, 43 (1971) 1557.
91. M.D.Amos, P.A.Bennett, K.G.Brodie, P.W.Y.Lung and J.P.Matoušek, 43 (1971) 211.
92. B.M.Patel and J.D.Winefordner, *Anal. Chim. Acta*, 64 (1973) 135.
93. R.D.Reeves, B.M.Patel, C.J.Molnar and J.D.Winefordner, *Anal. Chem.*, 45 (1973) 246.
94. K.W.Jackson and T.S.West, *Anal. Chem.*, 45 (1973) 249.
95. H.Massmann, *Spectrochim. Acta*, 23B (1968) 215.
96. B.V. L'vov, *Spectrochim. Acta*, 17 (1961) 761.
97. B.V. L'vov, *Atomic Absorption Spectrochemical Analysis*, Hilger, London, 1970.
98. J.Y.Hwang, C.J.Mokeler and P.A.Ullucci, *Anal. Chem.*, 44 (1972) 2018.
99. T.Takeuchi and M.Yanagisawa, *Talanta*, 19 (1972) 465.
100. J.Y.Hwang, P.A.Ullucci, S.B.Smith and A.L. Malenfant, *Anal. Chem.*, 43 (1971) 1319.
101. M.P.Bratzel, Jr., R.M.Dagnall and J.D.Winefordner, *Anal. Chim. Acta*, 48 (1969) 197.
102. J.B.Headridge and D.R.Smith, *Talanta*, 19 (1972) 833.
103. Y.Talmi and G.H.Morrison, *Anal. Chem.*, 44 (1972) 1455.
104. D.A.Segar and J.G.Gonzalez, *Anal. Chim. Acta*, 58 (1972) 7.
105. C.J.Pickford and G.Rossi, *Analyst*, 97 (1972) 647.
106. J.W.Robinson, P.J.Slevin, G.D.Hindman and D.K.Wolcott, *Anal. Chim. Acta*, 61 (1972) 431.

107. W.W.Harrison and N.J.Prakash, *Anal. Chim. Acta*, 49 (1970) 151.
108. D.S.Gough, P.Hannaford and A.Walsh, *Spectrochim. Acta*,  
28B (1973) 197.
109. G.F.Kirkbright, *Analyst, Lond.*, 96 (1971) 609.
110. K.M.Aldous, D.G.Mitchell and F.J.Ryan, *Anal. Chem.*, 45  
(1973) 1990.
111. J.D.Winefordner, M.L.Parsons, J.M.Mansfield and W.J.McCarthy,  
*Anal. Chem.*, 39 (1967) 436.
112. T.C.O'Haver and J.D.Winefordner, *Fluorescence News*, 6 (5)  
(1972) 1.
113. G.M.Hieftje, *Anal. Chem.*, 44 (6) (1972) 81A and 44 (7)  
(1972) 69A.
114. J.D.Winefordner, W.J.McCarthy and P.A.St. John, *J. Chem. Ed.*  
44 (1967) 80.
115. J.D.Winefordner and T.J.Vickers, *Anal. Chem.*, 36 (1964) 1939.
116. J.D.Winefordner and T.J.Vickers, *Anal. Chem.*, 36 (1964) 1947.
117. J.Ramirez-Munoz, *Atomic Absorption Spectroscopy*. Elsevier  
Publishing Company, New York, 1968.
118. J.D.Winefordner, Paper presented at the international Atomic  
Absorption Spectroscopy Conference, Sheffield, England.
119. P.A.St. John, W.J.McCarthy and J.D.Winefordner, *Anal.*  
*Chem.*, 38 (1966) 1828.
120. J.M.Mansfield, Jr., M.P.Bratzel, Jr., H.O.Norgordon, D.O.Knapp,  
K.E.Zacha and J.D.Winefordner, *Spectrochim. Acta*, 23B (1968)  
389.
121. V.Svoboda, R.F.Browner and J.D.Winefordner, *Appl. Spectrosc.*,  
26 (1972) 505
122. H.Hooymayers, *Spectrochimica Acta*, 23B (1968) 567.
123. J.D. Winefordner, M.L.Parsons, J.M.Mansfield, and W.J.McCarthy,  
*Spectrochimica Acta*, 23B (1967) 37.

124. P.J.Th.Zeegers and J.D.Winefordner, *Spectrochim Acta*, 26B  
(1971) 161.
125. C.Th.J.Alkemade, Paper presented at the International Atomic  
Absorption Spectroscopy Conference, Sheffield, England. 1969.
126. G.M.Hieftje, R.I.Bystroff and R.Lim, *Anal. Chem.*, 45 (1973) 253.
127. T.C.O'Haver, *J.Chem. Educ.*, 49 (1972) No. 3 A131 and No. 4 A211.
128. C.D.Flint, *Chem. Brit.*, 7 (1971) 4.
129. H.V.Malmstadt, M.L.Franklin and G.Horlick, *Anal. Chem.*,  
44 (8) (1972) 63A.
130. D.Alger, R.M.Dagnall, B.L.Sharp and T.S.West, *Anal. Chim.*  
*Acta*, 57 (1971) 1.
131. R.M.Dagnall, B.L.Sharp and T.S.West, *Talanta*, 19 (1972) 1442.
132. J.D.Winefordner and T.J.Vickers, *Anal. Chem.*, 42 (1970) 206R.
133. M.K.Murphy, S.A.Clyburn and C.Veillon, *Anal. Chem.*, 45  
(1973) 1468.
134. J.D.Ingle, Jr., and S.R.Crouch, *Anal. Chem.*, 44 (1972) 785.
135. S.A.Miller, *Rev. Scient. Instrum.*, 39 (1968) 1923.
136. J.D.Ingle, Jr., and S.R.Crouch, *Anal. Chem.*, 44 (1972) 777.
137. K.C.Ash and E.H.Piepmeier, *Anal. Chem.*, 43 (1971) 26.
138. J.D.Ingle, Jr., and S.R.Crouch, *Anal. Chem.*, 43 (1971) 1331.
139. R.E.Santini, *Anal. Chem.*, 44 (1972) 1708.
140. J.D.Ingle, Jr., and S.R.Crouch, *Anal. Chem.*, 44 (1972) 1711.
141. Shardanand, *Rev. Sci. Instrum.*, 43 (1972) 641.
142. L.C.Caplan and R.Stern, *Rev. Sci. Instrum.*, 42 (1971) 689.
143. J.B.Grimbleby and D.W.Harding, *J. Phys. E., Scient., Instrum.*,  
4 (1971) 944.
144. E.D.Morris, Jr., and H.S.Johnston, *Rev. Scient. Instrum.*,  
59 (1968) 620.
145. G.W.Ewing, *J.Chem. Ed.*, 49(1972) A333.

146. H.Nishita, R.Farmer and S.Peterson, Anal. Chim. Acta, 58 (1972) 1.
147. W.W.<sup>H</sup>arrison and F.E.Berry, Anal. Chim. Acta, 47 (1969) 415.
148. S.R.<sup>P</sup>areles, Anal. Chem., 45 (1973) 998.
149. M.P.Bratzel, Jr., R.M.Dagnall and J.D.Winefordner, Anal. Chem., 41 (1969) 713.
150. M.E.Hofton and D.P.Hubbard, Anal. Chim. Acta, 62 (1972) 311.
151. M.E.Hofton, Ph.D. Thesis, Sheffield Polytechnic, Feb. 1973.
152. P.G.Cath, Analytical Flame Spectroscopy (Selected Topics), Chapter 4, R.Mavrodineanu (Editor) Macmillan, London, 1970
153. J.Keen (Editor), The Application of Linear Microcircuits, Vols. 1 and 2, SES (UK) Ltd. 1971.
154. J.J.Brophy, Basic Electronics for Scientists, McGraw-Hill Kogakusha, Tokyo, 1966.
155. V.I.Muscat, T.J.Vickers and Anders Andren, Anal. Chem., 44 (1972) 218.
156. K.C.Thompson and G.D.Reynolds, Analyst, Lond., 86 (1971) 771.
157. V.I.Muscat and T.J.Vickers, Anal. Chim. Acta, 57 (1971) 23.
158. R.M.Dagnall, M.R.G.Taylor and T.S.West, Spectrosc. Lett., 1 (12) (1968) 397.
159. K.E.Zacha, M.P.Bratzel, Jr., J.D.Winefordner and J.M.Mansfield, Jr. Anal. Chem., 40 (1968) 1733.
160. T.S.West, Pure Appl. Chem., 26 (1971) 47.
161. T.S.West, Pure Appl. Chem., 23 (1970) 99.
162. R.M.Dagnall and T.S.West, Appl. Opt. 7 (1968) 1287.
163. R.F.Browner, R.M.Dagnall and T.S.West, Anal. Chim. Acta, 45 (1969) 163.
164. D.O.<sup>C</sup>ooke, R.M.Dagnall and T.S.West, Talanta, 19 (1972) 1309.
165. O.Menis and T.C.Rains, Anal. Chem., 41 (1969) 952.

166. J.P.S.Haarsma, G.J.De Jong and J.Agterdenbos, *Spectrochim. Acta*, 29B (1974) 1.
167. F.C.Fehsenfeld, K.M.Evenson and H.P.Broida, *Rev. Sci. Instrum.*, 36 (1965) 294.
168. D.O.Cooke, R.M.Dagnall and T.S.West, *Anal. Chim. Acta*, 54 (1971) 381.
169. D.O.Cooke, R.M.Dagnall and T.S.West, *Anal. Chim. Acta*, 56 (1971) 17.
170. B.McCarroll, *Rev. Sci. Instrum.*, 40 (1969) 279.
171. R.F.Browner and J.D.Winefordner, *Spectrochim. Acta*, 28B (1973) 263.
172. B.M.Patel, R.F.Browner and J.D.Winefordner, *Anal. Chem.*, 44 (1972) 2272.
173. R.F.Browner, B.M.Patel, T.H.Glenn, M.E.Rietta and J.D.Winefordner *Spectry. Lett.*, 5 (1972) 311.
174. R.F.Browner, M.E.Rietta, T.H.Glenn and J.D.Winefordner, *Pittsburgh Conference on Analytical Chemistry and Applied Spectroscopy*, Cleveland, Ohio (1972).
175. R.M.Dagnall, M.D.Silvester and T.S.West, *Colloq. Spectrosc. Internat. XVI Heidelberg* (1971).
176. D.Alger, R.M.Dagnall, M.D.Silvester and T.S.West, *Anal. Chem.*, 44 (1972) 2255.
177. K.M.Aldous, D.Alger, R.M.Dagnall and T.S.West, *Lab. Pract.* 19 (1970) 587.
178. L.Ebdon, G.F.Kirkbright and T.S.West, *Anal. Chim. Acta*, 47 (1969) 568.
179. K.C.Thompson and P.C.Wildy, *Analyst*, 95 (1970) 776.
180. P.C.Wildy and K.C.Thompson, *Analyst*, 95 (1970) 562.
181. L.F.Phillips, *Rev. Sci. Instrum.*, 42 (1971) 1078.

182. K.L.Smith, Rev, Sci. Instrum., 44 (1973) 1108.
183. J.A.Goleb, J.P.Bobis and F.R.George, U.S. Patent Number 3,600,091 Aug. 17, (1971).
184. R.M.Dagnall, M.D.Silvester and T.S.West, Talanta, 18 (1971) 1103.
185. C.Th.J.Alkemade, H.P.Hooymayers, P.L.Lijnse and T.J.M.J. Vierbergen Spectrochim. Acta, 27B (1972) 149.
186. G.Mossotti and I.N.Abercrombie, Colloq. Spectrosc. Internat. XVI Heidelberg (1971).
187. J.Brandenberger, Rev. Sci. Instrum., 42 (1971) 1535.
188. T.C.Rains, The 1st Annual Reports on Analytical Atomic spectroscopy symposium, 3rd Jan. (1974) Sheffield.
189. T.C.Rains, M.S.Epstein and O.Menis, Anal. Chem., 46 (1974) 207.
190. J.J.Ball, Rev. Sci. Instrum., 44 (1973) 1141.
191. R.M.Dagnall and M.D.Silvester, Anal. Chem., 44 (1972) 204.
192. W.J.Price, Analytical Atomic Absorption Spectrometry. Heydon and Son Ltd., London, 1972.
193. R. Mavrodineau and H.Boiteaux, Flame Spectroscopy, John Wiley & Sons, Inc., New York, 1965.
194. J.A.Dean and T.C.Rains, Flame Emission and Atomic Absorption Spectrometry. Vol. 1 - Theory. Marcel Dekker, inc. New York, 1969.
195. D.R.Jenkins, Spectrochim. Acta 25B (1970) 47.
196. D.N.Armentrout, Anal. Chem., 38 (1966) 1235.
197. J.M.Mansfield, J.D.Winefordner and C.Veillon, Anal. Chem., 37 (1965) 1049.
198. T.L.Marlin, R.M.Hamm, P.B.Zeeman, Anal. Chim Acta., 53 (1971) 437.
199. P.J.Slevin, V.I.Muscat and T.J.Vickers, Appl. Spectrosc., 26 (1972) 296.

200. R.M.Dagnall, G.F.Kirkbright, T.S.West and R.Wood, *Analyst*,  
Lond., 95 (1970) 425.
201. J.H.Fionna, R.N.Kniseley and V.A.Fassel, *Spectrochim. Acta*,  
23B (1968) 413.
202. K.M.Aldous, B.W.Bailey and J.M.Rankin, *Anal. Chem.*, 44 (1972)  
191.
203. K.M.Aldous, R.F.Browner, R.M.Dagnall and T.S.West, *Anal.*  
*Chem.*, 42 (1970) 939.
204. M.B.Denton and D.B.Swartz, *Rev. Sci. Instrum.*, 45 (1974) 81.
205. M.B.Denton and H.V.Malmstadt, *Anal. Chem.*, 44 (1972) 241.
206. M.B.Denton and H.V.Malmstadt, *Anal. Chem.*, 44 (1972) 1813,
207. T.R.Copeland, K.W.Olson and R.K.Skoogerboe, *Anal. Chem.*,  
44 (1972) 1471.
208. N.E.Korte, J.L.Moyers and M.B.Denton, *Anal. Chem.*, 45 (1973)  
530.
209. R.Bouckaert, J.D'Olieslager and S.De Jaegere, *Anal. Chim.*  
*Acta*, 58 (1972) 347.
210. D.J.Nicolas, *J. Phys. E. Sci. Instrum.*, 4 (1971) 69.
211. R.Stephens, *Talanta*, 20 (1973) 765.
212. H.G.C.Human and A.Strasheim, *Spectrochim. Acta*, 27B (1972) 503.
213. G.F.Kirkbright, A.Semb and T.S.West, *Talanta*, 15 (1968) 441.
214. D.N.Hingle, G.F.Kirkbright and T.S.West, *Talanta*, 15 (1968) 199.
215. G.F.Kirkbright, A.Semb and T.S.West, *Talanta*, 14 (1967) 1011.
216. K.M.Aldous, R.F.Browner, D.Clark, R.M.Dagnall and T.S.West,  
*Talanta*, 19 (1972) 927.
217. R.S.Hobbs, G.F.Kirkbright and T.S.West, *Analyst*, London.,  
94 (1969) 554.
218. R.S.Hobbs, G.F.Kirkbright, M.Sargent and T.S.West, *Talanta*,  
15 (1968) 997.

219. G.F.Kirkbright, M.Sargent and T.S.West, *Talanta*, 16 (1969) 245.
220. G.F.Kirkbright, M.Sargent and T.S.West, *Talanta*, 16 (1969) 1467.
221. G.F.Kirkbright and S.Vetter, *Spectrochim. Acta*, 26B (1971) 505.
222. T.S.West, Paper presented at the International Atomic Absorption Spectroscopy Conference, Sheffield, England 1969.
223. D.W.Ellis and D.R.Demers, *Anal. Chem.*, 13 (1966) 1943.
224. N.Omenetto and G.Rossi, *Anal. Chim. Acta*, 40 (1968) 195.
225. P.Benetti, N.Omenetto and G.Rossi, *Applied Spectroscopy*, 25 (1971) 57.
226. R.F.Browner, R.M.Dagnall and T.S.West, *Anal. Chim. Acta*, 50 (1970) 375.
227. N.Omenetto, L.P.Hart and J.D.Winefordner, *Appl. Spectrosc.*, 26 (1972) 612.
228. R.M.Dagnall, M.R.G.Taylor and T.S.West, *Lab. Pract.*, 20 (1971) 209.
229. G.F.Kirkbright, A.P.Rao and T.S.West, *Analyt. Lett.*, 2 (1969) 465.
230. J.D.Norris and T.S.West, *Anal. Chim. Acta*, 59 (1972) 474.
231. J.D.Norris and T.S.West, *Anal. Chim. Acta*, 55 (1971) 359.
232. B.B.Hundy, *Spec. Rep. Iron Steel Inst.*, No. 81 (1963) 75.
233. J.M.Capus, *Iron Steel, Lond.*, (1965) 594.
234. J.A. Bowman, *Anal. Chim. Acta*, 42 (1968) 285.
235. B.Moldan, I.Rubeška, M.Mikšovsky and M.Huka, *Anal. Chim. Acta*, 52 (1970) 91.
236. L.Capacho-Delgado and D.C.Manning, *Spectrochim. Acta*, 22 (1966) 1505.
237. I.Rubeška and M.Mikšovsky, *Atomic Absorption Newsletter*, 11 (1972) 57.

238. T.M.Quarrell, R.J.W.Powell and H.J.Cluley, *Analyst*, 98  
(1973) 443.
239. J.U.Gouin, J.L.Holt and R.E.Miller, *Anal. Chem.*, 44  
(1972) 1042.
240. K.E.Burke, *Analyst*, 97 (1972) 19.
241. J.B.Headridge and A.Sowerbutts, *Analyst*, 97 (1972) 442.
242. Taketoshi Nakahara, Makoto Munemori and Soichiro Musha,  
*Anal. Chim. Acta*, 62 (1972) 267.
243. P.O.Juliano and W.W.Harrison, *Anal. Chem.* 42 (1970) 84.
244. J.R.Levine, S.G.Moore and S.L.Levine, *Anal. Chem.*, 42  
(1970) 412.
245. A.E.Smith, *Analyst*, 98 (1973) 209.
246. Ase Engberg, *Analyst*, 98 (1973) 137.
247. H.Kahn, *Advan. Chem. Ser.* , 73 (1968) 183.
248. Detection limits for model AAS Atomic Absorption Spectro-  
photometry, Varian Techtron, Walnut Creek, Calif.
249. W.W.Harrison and P.O.Juliano, *Anal. Chem.*, 41 (1969) 1016.
250. A.E.Smith, *Analyst*, 98 (1973) 65.
251. O.Menis and T.C.Rains, *Analytical Flame Spectroscopy*,  
(Selected topics), Chapter two, R.Mavrodineanu (Editor),  
Macmillan, London, 1970.
252. P.T.Gilbert, *Analytical Flame Spectroscopy (Selected Topics)*,  
Chapter Five, R.Mavrodineanu (Editor), Macmillan, London 1970.
253. W.Slavin, *Atomic Absorption Spectroscopy*, Interscience,  
New York, 1968.
254. J.H.Gibson, W.E.L.Grossman and W.D.Cooke, *Anal. Chem.*,  
35 (1963) 266.
255. J.E.Schallis and H.L.Kahn, *Atomic Absorption Newsletter*, 7  
(1968) 84.

256. K.E.Burke and C.H.Albright, Developments in Applied Spectroscopy, Volume 8, Editor E.L.Grove, Plenum press, London, 1970.
257. D.T.Coker and J.M.Ottaway, Nature Physical Science, 230 (1971) 156.
258. British Chemical Standards and Spectroscopic Standards prepared and issued by the Bureau of Analysed Samples Ltd., Newham Hall, Newby, Middlesbrough, Teesside, England TS8 9EA.
259. C.B.Belcher, The preparation of ferrous alloys for analysis by atomic absorption spectroscopy. Varian Techtron PTY. Ltd. Australia, 1971.
260. W.T.Rees, Analyst, 87 (1962) 202.
261. A.Fulton, K.C.Thompson and T.S.West, Anal. Chim. Acta, 51 (1970) 373.
262. H.L.Kahn and J.E.Schallis, Atomic Absorption Newsletter, 7 (1968) 5.
263. G.F.Kirkbright, M.Sargent and T.S.West, Atomic Absorption Newsletter, 8 (1969) 34.
264. G.F.Kirkbright and L.Ranson, Anal. Chem., 43 (1971) 1238.
265. G.F.Kirkbright, L.Ranson and T.S.West, Spectrosc. Lett., 5 (1972) 25.
266. P.Johns, Spectrovision. Number 24, (1970) 6.
267. J.Ramirez-Munoz and M.E.Roth, Flame Notes, 4 (1969) 21.
268. K.E.Smith and C.W.Frank, Appl. Spectrosc., 22 (1968) 765.
269. J.Ramirez-Munoz, Revta Soc. quim. Mex., 12 (1968) 25B (in Spanish). Anal. Abstr. June 1969, No. 2972.
270. W.Slavin, C.Sebens and S.Sprague, Atomic Absorption Newsletter, 4 (1965) 341.
271. A.I.Williams, Analyst (Lond.) 97 (1972) 104.

272. J.Y.Hwang and L.M.Sandonato, *Anal. Chem.*, 42 (1970) 744.
273. B.Gandrud and J.C.Marshall, *Appl. Spectrosc.*, 24 (1970) 367.
274. R.S.Braman, L.L.Justen and C.C.Foreback, *Anal. Chem.*, 44  
(1972) 2195.
275. F.E.Lichte and R.K.Skogerboe, *Anal. Chem.*, 44 (1972) 1480.
276. W.Holak, *Anal. Chem.*, 41 (1969) 1712.
277. E.E.Dalton and A.J.Malonoski, *Atomic Absorption Newsletter*,  
10 (1971) 92.
278. F.J.Fernandez and D.C.Manning, *Atomic Absorption Newsletter*,  
10 (1971) 86.
279. R.C.Chu, G.P.Barron and P.A.W.Baumgarner, *Anal. Chem.*,  
44 (1972) 1476.
280. D.C.Manning, *Atomic Absorption Newsletter*, 10 (1971) 123.
281. Kwok-Tai Kan, *Analyt. Lett.*, 6 (7) (1973) 603.
282. A.Ando, M.Suzuki, F.Fuwa and B.L.Vallee, *Anal. Chem.*,  
41 (1969) 1974.
283. U.T.Hill, *Spec. tech. Publs. Am. Soc Test. Mater.*, No. 443,  
(1969) 83. *Referat Anal. Abstr. July, 1970 No. 249.*
284. P.Pakalns, *Anal. Chim. Acta*, 47 (1969) 225.
285. G.F.Kirkbright and H.N.Johnson, *Talanta*, 20 (1973) 433.
286. Y.Yamamoto, T.Kumamaru, Y.Hayashi, M.Kanke and A.Matsui,  
*Talanta*, 19 (1972) 1633.
287. S.P.Singhal, *Microchem. J.*, 18 (1973) 178.
288. V.Ramakrishna, J.W.Robinson and P.W.West, *Anal. Chim. Acta*,  
45 (1969) 43.
289. W.R.Nall, *Analyst*, 96 (1971) 398.
290. A.A.Al-Sibaai and A.G.Fogg, *Analyst*, 98 (1973) 732.
291. R.M.Dagnall, J.M.Manfield, M.D.Silvester and T.S.West,  
*Spectrosc. Lett.*, 6 (1973) 183.

292. G.F.Kirkbright and M.Marshall, Anal. Chem., 44 (1972) 1288.
293. G.F.Kirkbright, T.S.West and P.J.Wilson, Anal. Chim. Acta, 66 (1973) 130.
294. G.F.Kirkbright, T.S.West and P.J.Wilson, Analyst, Lond., 98 (1973) 49.
295. G.F.Kirkbright, M.Marshall and T.S.West, Anal. Chem., 44 (1972) 2379.
296. G.F.Kirkbright, M.K.Peters, M.Sargent and T.S.West, Talanta, 15 (1968) 663.
297. J.E.Chester, R.M.Dagnall and M.R.G.Taylor, Anal. Chim. Acta, 51 (1970) 95.
298. J.Y.Marks and G.G.Welcher, Anal. Chem., 42 (1970) 1033.
299. P.C.L.Thorne and E.R.Roberts, Inorganic Chemistry, Gurney and Jackson, London, Fifth Edition - revised 1949.
300. B.M.Gatehouse and J.B.Willis, Spectrochim. Acta, 17 (1961) 710.
301. C.L.Chakrabarti, Anal. Chim. Acta, 29 (1963) 489.
302. S.Shibata, Anal. Chim. Acta, 28 (1963) 392.
303. M.D.Amos and P.E.Thomas, Anal. Chim. Acta, 32 (1965) 139.
304. M.D.Amos and J.B.Willis, Spectrochim. Acta, 22 (1966) 1325.
305. J.F.Chapman and L.S.Dale, Analyst, Lond., 94 (1969) 563.
306. J.B.Willis, Nature, No. 207 (1965) 715.
307. J.A.Bowman and J.B.Willis, Anal. Chem., 39 (1967) 1211.
308. T.V.Ramakrishna, P.W.West and J.W.Robinson, Anal. Chim. Acta, 39 (1967) 81.
309. R.J.Jaworowski, R.P.Weberling and D.J.Bracco, Anal. Chim. Acta, 37 (1967) 284.
310. L.Capacho-Delgado and D.C.Manning, Analyst, Lond., 92 (1967) 553.
311. H.D.Fleming, Spectrochim. Acta, 23B (1967) 207.

312. R.M.Dagnall, K.C.Thompson and T.S.West, *Analyst*, Lond.,  
93 (1968) 153.
313. J.B.Willis, V.A.Fassel and J.A.Fiorino, *Spectrochim. Acta*,  
24B (1969) 157.
314. J.E.Chester, R.M.Dagnall and M.R.G.Taylor, *Anal. Chim.*  
*Acta*, 55 (1971) 47.
315. J.E.Chester, R.M.Dagnall and M.R.G.Taylor, *Analyst*, Lond.,  
95 (1970) 702.
316. G.F.Kirkbright, M.K.Peters and T.S.West, *Talanta*, 14 (1967) 789.
317. E.E.Pickett and S.R.Koirttyohann, *Spectrochim. Acta*,  
24B (1969) 325.
318. P.W.J.M.Boumans and F.J.de Boer, *Spectrochim. Acta*,  
27B (1972) 391.
319. D.C.Manning, *Atomic Absorption Newsletter*, 5 (1966) 127.
320. P.E.Paus, *Anal. Chim. Acta*, 54 (1971) 164.
321. D.C.Manning and L.Capacho-Delgado, *Anal. Chim. Acta*, 36 (1966)  
312.
322. G.R.Kornblum and L.De Galan, *Spectrochim. Acta*, 28B (1973) 139.
323. G.R.Kornblum and L. De Galan, *Colloq. Spectrosc. Internat.*,  
XVI Heidelberg (1971).
324. W.D.Cobb and T.S.Harrison, *Analyst*, (Lond.) 96 (1971) 764.
325. A.P.Ferris, W.B.Jepson and R.C.Shapland, *Analyst*, (Lond.)  
95 (1970) 574.
326. A.C.West, R.N.Knisely and V.A.Fassel, *Anal. Chem.*, 45 (1973)  
815.
327. J.L.Jimenez Seco and A.G.Coedo, *Revta. Metal*, 6 (1970) 64  
(in Spanish) *Referat Anal. Abstr.*, vol. 20 No. 1669.
328. D.R.Thomerson and W.J.Price, *Analyst*, 96 (1971) 825.
329. P.Konig, K.H.Schimitz and E.Thiemann, *Atomic Absorption*  
*Newsletter*, 9 (1970) 103.

330. J.B.Headridge and A Sowerbutts, *Analyst*, 98 (1973) 57.
331. H.Goto, Y.Kakita and M.Namiki, *Japan Analyst*, 19 (1970) 1211  
(in Japanese) *Referat Anal. Abstr.* April 1972, No. 2289.
332. P.L.Boar and L.K.Ingram, *Analyst, Lond.*, 95 (1970) 124.
333. S.Abbey, *Geol. Surv. Pap. Can.*, No. 72-73, 1970, 20 pp-  
*Referat Anal. Abstr.*, Feb. 1971 No. 1049.
334. N.Omenetto and J.D.Winefordner, *Appl. Spectrosc.*, 26 (1972)  
555.
335. B.H.Smith, *Lab. Pract.* Feb. 1973, pp.100-102.
336. J.B.Headridge and D.P.Hubbard, *Anal. Chim. Acta*, 37 (1967) 151.
337. V.K.Panday, *Anal. Chim. Acta*, 57 (1971) 31.
338. A.C.West, V.A.Fassel and R.N.Knisely, *Anal. Chem.*, 45 (1973)  
1586.
339. S.L.Sachdev, J.W.Robinson and P.W.West, *Anal. Chim. Acta*,  
37 (1967) 12.
340. S.R.Koirtyohann and E.E.Pickett, *Anal. Chem.*, 40  
(1968) 2068.
341. E.E.Pickett and S.R.Koirtyohann, *Spectrochim. Acta*, 23B (1968)  
235.
342. P.H.Scholes, Second Report of the working party on the  
application of the atomic absorption spectroscopic technique:  
A collaborative study on inter-element interference effects.  
CDL/CAC/117/73 Superseding CAC/82/73. Corporate  
Development Laboratory, British Steel Corporation, Hoyle  
Street, Sheffield S3 7EY.
343. J.A.Dean and T.C.Rains, Editors, *Flame Emission and Atomic  
Absorption Spectrometry*, Marcel Dekker, New York, 1969.  
Vol. I (Theory) page 135.
344. R.Smith, C.M.Stafford and J.D.Winefordner, *Anal. Chim.  
Acta*, 42 (1968) 523.

345. J.R.Dawson and B.D.Tucker, Proc. Colloq. Spectrosc. Internat. XVI (1971) Heidelberg.
346. D.O.Knapp, N.Omenetto, L.P.Hart, F.W.Plankey and J.D.Winefordner Anal. Chim. Acta, 69 (1974) 455.
347. D.G.Mitchell, K.W.Jackson and K.M.Aldous, Anal. Chem., 45 (1973) 1215A.
348. J.D.Norris and T.S.West, Anal. Chim. Acta, 55 (1971) 359.
349. M.S.Cresser and T.S.West, Anal. Chim. Acta, 51 (1970) 530.
350. J.D.Norris and T.S.West, Anal. Chem., 45 (1973) 226.
351. G.B.Marshall and T.S.West, Anal. Chim. Acta, 51 (1970) 179.
352. K.W.Busch and G.H.Morrison, Anal. Chem., 45 (1973) 713A.
353. P.Murugaiyan, S.Natarajan and Ch. Venkateswarlu, Anal. Chim. Acta, 69 (1974) 451.
354. P.Murugaiyan, S.Natarajan and Ch. Venkateswarlu, Anal. Chim. Acta, 64 (1973) 132.
355. J.W.Robinson and Y.E.Araktingi, Anal Chim. Acta, 63 (1973) 29.
356. G.B.Marshall and A.C.Smith, Analyst, Lond., 97 (1972) 447.
357. The Jarrell-Ash Model 810, Fisher Scientific Company, Analytical Instrument Division. British agent, V.A.Howe and Company Limited, Peterborough Road, London.
358. D.O.Cooke, R.M.Dagnall, H.N.Johnson, G.F.Kirkbright, and T.S.West, Lab. Pract., 21 (1972) 171.
359. J.D.Winefordner, Accounts of Chemical Research, 4 (1971) 259.
360. J.D.Winefordner and J.M.Mansfield, Jr., Applied Spectroscopy Reviews, 1 (1967) 1-27.
361. C.Th.J.Alkemade, Plenary lectures presented at the IUPAC International Atomic Absorption Spectroscopy Conference, Sheffield (1969).

362. N.Omenetto, N.H.Hatch, L.M.Fraser, and J.D.Winefordner,  
Anal. Chem., 45 (1973) 195.
363. N.Omenetto, N.N.Hatch, L.M.Fraser and J.D.Winefordner,  
Spectrochimica Acta, 28B (1973) 65.
364. N.Omenetto, P.Benetti, L.P.Hart, J.D.Winefordner, and  
C.Th.J.Alkamade, Spectrochim. Acta, 28B (1973) 289.
365. N.Omenetto, L.P.Hart, P.Benetti and J.D.Winefordner,  
Spectrochim. Acta, 28B (1973) 301.
366. E.H.Piepmeyer, Spectrochim. Acta, 27B (1972) 431.
367. J.P.Webb. Anal. Chem., 44 (1972) No. 6. 30A.

## PUBLICATIONS

The work on the instrumentation was published in Analytica Chimica Acta 67 (1973) 55-67. This publication was entitled "STUDIES IN ATOMIC FLUORESCENCE SPECTROMETRY. PART 1.

INEXTENSIVE METHODS OF IMPROVING SIGNALS-TO-NOISE RATIOS".

The work on the determination of tin by atomic fluorescence has been accepted for publication by Analytica Chimica Acta and takes the form of two papers which continue the series "STUDIES IN ATOMIC FLUORESCENCE SPECTROMETRY". The two papers are entitled "PART 2 - INTERFERENCE EFFECTS OCCURRING WHEN USING VARIOUS PREMIXED FLAMES FOR THE DETERMINATION OF TIN" and "PART 3 - THE DETERMINATION OF TIN IN STEELS". Publication will probably be in Autumn 1974.